



**IDENTIFICATION AND
CHARACTERISATION OF A PUTATIVE
OSTEOPROTEGERIN RECEPTOR ON
PULMONARY ARTERIAL SMOOTH
MUSCLE CELLS**

Sarah Helen Dawson

**Pulmonary Vascular Research Group
Department of Cardiovascular Science
University of Sheffield**

Thesis submitted for the degree of Doctor of Philosophy

October 2014

ACKNOWLEDGMENTS

I would first like to thank my supervisor, Dr Allan Lawrie, for without his intellectual guidance, help and support throughout the entirety of my PhD, this thesis would not have been possible. His patience while I was learning and encouragement to persevere when things didn't go right were greatly appreciated. I am also very grateful for the time he dedicated to reading this thesis, from the first drafts, right through to the final version and for all the valuable feedback and advice about all aspects of my PhD.

I would also like to thank my second supervisor and the head of department, Professor Sheila Francis, for her support and encouragement, especially after the DRIP meetings, her feedback on my thesis and for making me feel a part of such a friendly and welcoming department.

There are a number of people I would also like to thank, for without their technical and moral support, this thesis would not have been possible. I would like to thank Josephine Pickworth for her very kind and continued support in the lab and for teaching me how to do western blotting and cell culture. Thank you to James Iremonger and Dr Alex Rothman for all of their help with the RNA microarrays that are discussed in this thesis. Thank you to Nadine Arnold for helping me with the immunohistochemistry discussed in this thesis. A big thank you to everyone in the PVRG for your friendship, encouragement and for always putting a smile on my face. I will miss our group bonding sessions and trips to conferences in that far off place called London.

I would like to thank Mark Southwood and Nicholas Morrell from the Department of Medicine, University of Cambridge School of Clinical Medicine, Addenbrooke's and Papworth Hospital, Cambridge for kindly providing the IPAH patient cells and tissues. I would like to thank the Medical Research Council and The University of Sheffield for funding this research.

Finally, I would like to thank all my friends and family for their continued support throughout my PhD, especially Ismael who has had to live through my frustration and stress when things haven't gone right. Thank you for enduring repeat after repeat of my favourite TV programmes and for providing the constant supply of tea throughout the years. Thank you to my parents for the Saturday night take-away's, which provided an escape from the clutches of thesis writing every once in a while. Without your continued support, completion of this thesis would not have been possible.

TABLE OF CONTENTS

ACKNOWLEDGMENTS	II
LIST OF FIGURES	VII
LIST OF TABLES	VIII
ABBREVIATIONS	IX
SUMMARY	XII
1. INTRODUCTION	13
1.1 THE NORMAL PULMONARY CIRCULATION AND RIGHT VENTRICLE	13
1.2 PULMONARY HYPERTENSION	13
1.2.1 Historical Classification of Pulmonary Hypertension	14
1.3 PULMONARY ARTERIAL HYPERTENSION	17
1.3.1 Clinical Presentation and Diagnosis	18
1.3.2 PAH and the Right Heart	19
1.4 THE PATHOGENESIS OF PULMONARY ARTERIAL HYPERTENSION	19
1.4.1 Endothelial Cell Apoptosis	20
1.4.2 Endothelial Cell Proliferation	21
1.4.3 Pulmonary Vasoconstriction	22
1.4.3.1 Endothelin 1	22
1.4.3.2 Serotonin	23
1.4.4 Pulmonary Arterial Smooth Muscle Cell Proliferation	23
1.4.5 Fibroblast Activation and Proliferation	25
1.4.6 Inflammation	26
1.4.7 Genetics of Pulmonary Arterial Hypertension	28
1.4.7.1 Bone Morphogenetic Protein Receptor 2 Mutations	28
1.4.7.2 Activin Receptor-Like Kinase 1 and Endoglin Mutations	29
1.4.7.3 SMAD9	30
1.4.7.4 Caveolin-1	30
1.4.7.5 KCNK3	31
1.5 TRAIL IN PULMONARY ARTERIAL HYPERTENSION	32
1.6 CURRENT TREATMENTS FOR PAH	33
1.7 OSTEOPROTEGERIN	34
1.7.1 The OPG/RANKL/RANK Axis in Bone Biology	36
1.7.2 OPG in Tumour Cell Biology	37
1.7.3 OPG and Calcification	38
1.7.4 OPG and Vascular Cell Proliferation	39
1.7.5 OPG in Cardiovascular Disease	39
1.7.6 Osteoprotegerin in Pulmonary Arterial Hypertension	41
1.8 HYPOTHESIS AND AIMS	43
2. GENERAL METHODS	45
2.1 CELL CULTURE	45
2.1.1 Human Pulmonary Arterial Smooth Muscle Cells (HPA-SMC)	45
2.1.1.1 HPA-SMC Culture and Passage	45
2.1.1.2 HPA-SMC Haemocytometer Counts	46
2.1.1.3 HPA-SMC Synchronization	46
2.2 PIERCE™ 660 NM PROTEIN ASSAY	47
2.2.1 Preparation of Bovine Serum Albumin (BSA) Standards	47
2.2.2 Microplate Procedure for Protein Assay	48
2.3 WESTERN BLOTTING	48
2.3.1 General Protocol	48
2.3.1.1 Sample Preparation	48

2.3.1.2	Electrophoresis System Set-up and Sample Loading	49
2.3.1.3	Gel Electrophoresis	49
2.3.1.4	Protein Wet Transfer	49
2.3.1.5	Membrane Blockade.....	50
2.3.1.6	Primary Antibody Incubation	50
2.3.1.7	Secondary Antibody Incubation	51
2.3.1.8	Membrane Scanning	51
2.3.1.9	Membrane Stripping.....	52
2.4	RETROGENIX CELL MICROARRAY	52
2.4.1	Pre-Screen.....	52
2.4.2	Primary Screen.....	53
2.4.3	Confirmation Screen	53
2.5	CO-IMMUNOPRECIPITATION.....	53
2.5.1	Preparation of CHAPS Lysis Buffer	54
2.5.2	Preparation of HPA-SMC lysate.....	54
2.5.3	Preparation of Co-IP Reactions	54
2.5.4	Precipitation of Immune Complexes.....	56
2.5.5	Dissociation of Immune Complexes	56
2.5.6	Analysis of Immune Complexes	56
2.6	IMMUNOHISTOCHEMISTRY.....	57
2.7	KINEX ANTIBODY MICROARRAY	58
2.8	DAVID (THE DATABASE FOR ANNOTATION, VISUALIZATION AND INTEGRATED DISCOVERY) ANALYSIS OF KINEX ANTIBODY MICROARRAY RESULTS	58
2.9	KINEX ANTIBODY MICROARRAY VALIDATION	59
2.9.1	In-Cell Western Assay	59
2.9.1.1	HPA-SMC Stimulation	59
2.9.1.2	HPA-SMC Fixing and Permeabilization	59
2.9.1.3	Cell Blockade	59
2.9.1.4	Primary Antibody Incubation	59
2.9.1.5	Secondary Antibody and Nuclear Staining.....	60
2.9.1.6	Plate Analysis.....	60
2.9.2	Western Blotting.....	61
2.9.2.1	HPA-SMC Stimulation	61
2.9.2.2	HPA-SMC Lysis	62
2.9.2.2.1	Sodium Orthovanadate Lysis.....	62
2.9.2.2.2	Triton X-100 Lysis.....	62
2.9.2.3	Primary Antibody Incubation	63
2.9.2.4	Secondary Antibody Incubation	63
2.9.2.5	Membrane Scanning.....	63
2.10	AGILENT RNA MICROARRAY.....	63
2.10.1	HPA-SMC Stimulation.....	64
2.10.2	HPA-SMC RNA Isolation	64
2.10.3	Bioanalyzer Analysis of RNA Quality	65
2.10.4	Agilent RNA Microarray	65
2.10.5	Agilent RNA Microarray Analysis.....	65
2.10.6	Heat Map Generation.....	66
2.10.7	DAVID (The Database for Annotation, Visualization and Integrated Discovery) Analysis of Agilent RNA Microarray	66
2.11	TAQMAN® REAL-TIME QUANTITATIVE POLYMERASE CHAIN REACTION.....	66
2.11.1	HPA-SMC stimulation	67
2.11.2	DirectZol RNA Extraction	67
2.11.2.1	Preparation of DNase I Cocktail.....	67
2.11.2.2	RNA Extraction	68
2.11.2.3	Nanodrop 1000 Spectrophotometer	68
2.11.3	Reverse Transcription of Isolated RNA	69
2.11.4	TaqMan RT-qPCR Reaction Set-up	69
2.11.5	TaqMan 7900HT Fast Real Time PCR System Set-up	70
2.11.6	TaqMan data analysis.....	70

2.12	FAS AND TRAIL NEUTRALIZATION TO ASSESS OPG-INDUCED PROLIFERATION OF HPA-SMC	70
2.12.1	HPA-SMC Pre-Incubation with Antibodies.....	70
2.12.2	HPA-SMC Stimulation.....	71
2.12.3	CellTiter-Glo® Measurement of HPA-SMC Proliferation	71
2.12.3.1	CellTiter-Glo® Assay.....	71
2.13	FAS NEUTRALIZATION TO ASSESS RNA EXPRESSION IN HPA-SMCs	72
3.	IDENTIFICATION OF NOVEL OPG BINDING PARTNERS	73
3.1	INTRODUCTION	73
3.2	AIMS	75
3.3	METHODS.....	75
3.3.1	Retrogenix Cell Microarray.....	75
3.3.2	TaqMan RT-qPCR.....	75
3.3.3	Co-Immunoprecipitation	76
3.3.4	Immunohistochemistry.....	76
3.3.5	Statistical Analysis.....	76
3.4	RESULTS.....	77
3.4.1	Identification of OPG Binding Partners.....	77
3.4.2	Fas, IL1RAcP and Gap43 RNA Expression in PA-SMCs.....	84
3.4.3	Validating the Interaction of OPG with Endogenous Fas and IL1RAcP in PA-SMC Lysates.....	85
3.4.4	OPG, Fas and IL1RAcP Expression in Human IPAH Tissues.....	87
3.5	DISCUSSION	90
4.	IDENTIFICATION OF OPG REGULATED PROTEIN AND RNA EXPRESSION IN PULMONARY ARTERIAL SMOOTH MUSCLE CELLS.....	98
4.1	INTRODUCTION	98
4.2	AIMS	99
4.3	METHODS.....	99
4.3.1	Kinex Antibody Microarray	99
4.3.2	In-Cell Western Assay (primary validation of the KAM)	99
4.3.3	Western Blotting (secondary validation of the KAM).....	100
4.3.4	Agilent 8-plex single colour RNA microarray.....	100
4.3.5	Real-time TaqMan qPCR Validation	100
4.3.6	Statistical analysis.....	100
4.4	RESULTS.....	101
4.4.1	Kinex Antibody Microarray	101
4.4.2	In-Cell Western Validation of OPG-induced Protein Expression and Phosphorylation	107
4.4.3	Western blot validation of OPG-induced protein expression and phosphorylation.....	109
4.4.3.1	Effect of OPG on ERK1/2 and HSP27 Phosphorylation.....	109
4.4.3.2	Effect of OPG on CDK4 Phosphorylation and CDK5 Expression.....	111
4.4.3.3	Effect of OPG on Daxx and FADD Expression	112
4.4.3.4	Investigating the Effect of OPG on mTOR Phosphorylation, Atg13, Atg7 and GβL Expression in PA-SMCs	115
4.4.4	Microarray Analysis of OPG-induced Changes in Gene Expression in HPA-SMCs	120
4.4.5	TaqMan Validation of the mRNA Microarray	124
4.5	DISCUSSION	126
4.5.1	The Effects of OPG on PA-SMC Proliferation	127
5.	INVESTIGATING THE EFFECT OF BLOCKING THE OPG-FAS INTERACTION ON HUMAN PA-SMC PHENOTYPE	140
5.1	INTRODUCTION	140
5.2	AIM	140

5.3	METHODS.....	141
5.3.1	Real-time TaqMan qPCR	141
5.3.2	HPA-SMC Proliferation	141
5.3.2.1	Statistics	141
5.4	RESULTS.....	142
5.4.1	The Effect of Blocking the OPG-Fas Interaction on OPG-induced PAH-associated Gene Expression	142
5.4.2	Investigating the Effect of Blocking the OPG-Fas Interaction on OPG-induced PA-SMC Proliferation	143
5.5	DISCUSSION	147
6.	GENERAL DISCUSSION	154
6.1	SUMMARY OF KEY FINDINGS	154
6.2	OPG, PAH AND THE CANCER HYPOTHESIS.....	156
6.3	THE OPG-FAS INTERACTION AS A POTENTIAL THERAPEUTIC TARGET.....	159
6.4	LIMITATIONS.....	160
6.5	FUTURE DIRECTIONS.....	161
7.	APPENDIX.....	165
7.1	PRODUCT SUPPLIERS	165
7.1.1	General Reagents.....	165
7.1.2	Cell Culture Reagents	166
7.1.3	Co-Immunoprecipitation Reagents	166
7.1.4	In-Cell Western Assay Reagents	166
7.1.5	Pierce 660 nm Protein Assay	167
7.1.6	Primary Antibody Suppliers	167
7.1.7	Proliferation Assay Reagents	168
7.1.8	Recombinant Proteins.....	169
7.1.9	RNA Extraction and RT-qPCR.....	169
7.1.10	Secondary Antibody Suppliers	169
7.1.11	TaqMan Probes	170
7.1.12	Western Blotting Reagents	170
7.2	PREPARATION OF SOLUTIONS	171
7.2.1	General Solutions	171
7.2.2	Cell Culture Solutions.....	172
7.2.3	Pierce 660 nm Protein Assay Bovine Serum Albumin Standards Preparation 173	
7.2.4	Western Blotting Solutions	173
7.2.5	Co-Immunoprecipitation Solutions	174
7.2.6	Cell Assay Solutions	175
7.2.7	RNA Isolation, Reverse Transcription and TaqMan RT-qPCR.....	175
7.2.8	Preparation of Recombinant Proteins.....	176
7.2.9	Preparation of Primary Antibodies	177
7.2.10	Preparation of Secondary Antibodies.....	179
7.3	ANTIBODIES SCREENED IN THE KINEX ANTIBODY MICROARRAY	180
7.4	BIOANALYSER RESULTS	207
7.5	PAH-ASSOCIATED GENES.....	208
8.	BIBLIOGRAPHY.....	218

LIST OF FIGURES

FIGURE 1.1- UPDATED CLINICAL CLASSIFICATION OF PULMONARY HYPERTENSION, NICE, FRANCE 2013 (FIFTH WHO SYMPOSIUM).....	16
FIGURE 1.2- THE STRUCTURE OF FULL LENGTH OPG AND THE SYNTHESISED OPG-FC PROTEIN.....	35
FIGURE 1.3- GENETIC DELETION OF OPG PREVENTS DISEASE DEVELOPMENT IN THE SuHx MOUSE MODEL AND ANTIBODY BLOCKADE OF OPG REVERSES DISEASE IN THE PAIGEN FED ApoE ^{-/-} MOUSE MODEL OF PH.....	42
FIGURE 1.4- AIMS TO BE ADDRESSED IN THIS THESIS.....	44
FIGURE 2.1- WET TRANSFER SET-UP.....	50
FIGURE 2.2- ICW ASSAY PROTOCOL.....	61
FIGURE 3.1- PRE-SCREEN TO DETERMINE BACKGROUND LEVELS AND BINDING.....	78
FIGURE 3.2- CONFIRMATION SCREEN RESULTS.....	82
FIGURE 3.3- RETROGENIX TRANSFECTION CONFIRMATION (ZSGREEN1 FLUORESCENCE).....	83
FIGURE 3.4- FAS, IL1RACp AND GAP43 RNA EXPRESSION LEVELS IN QUIESCED AND OPG-STIMULATED PA-SMCs.....	84
FIGURE 3.5- CO-IMMUNOPRECIPITATION OF OPG FROM PA-SMC LYSATES AND RECOMBINANT HUMAN PROTEINS.....	86
FIGURE 3.6- IMMUNOHISTOCHEMICAL STAINING OF FAS, IL1RACp AND OPG IN THE PULMONARY ARTERY AND RIGHT VENTRICLE.....	88
FIGURE 3.7- FAS RNA EXPRESSION IN IPAH PATIENT LUNGS.....	89
FIGURE 3.8- SCHEMATIC SHOWING THE INTERACTIONS BETWEEN IL1RACp AND OPG AND THE INTERLEUKIN RECEPTORS, ST2 AND IL1-R1.....	94
FIGURE 3.9- OPG WAS FOUND TO BIND 4 NOVEL BINDING PARTNERS, FAS, IL1RACp, GAP43 AND TMPRSS11D.....	97
FIGURE 4.1- PATHWAY FOLD ENRICHMENT IN OPG-STIMULATED HPA-SMCs.....	104
FIGURE 4.2- HEAT MAP OF KAM PROTEIN EXPRESSION AND PHOSPHORYLATION.....	106
FIGURE 4.3- IN CELL WESTERN ANALYSIS OF OPG-INDUCED PROTEIN PHOSPHORYLATION.....	108
FIGURE 4.4- WESTERN BLOT ANALYSIS OF OPG-INDUCED ERK1/2 AND HPS27 PROTEIN PHOSPHORYLATION IN HPA-SMCs.....	110
FIGURE 4.5- WESTERN BLOT ANALYSIS OF OPG-INDUCED CDK4 PHOSPHORYLATION AND CDK5 EXPRESSION IN HPA-SMCs.....	111
FIGURE 4.6- WESTERN BLOT ANALYSIS OF OPG-INDUCED DAXX EXPRESSION IN HPA-SMCs.....	113
FIGURE 4.7- WESTERN BLOT ANALYSIS OF OPG-INDUCED FADD EXPRESSION IN HPA-SMCs.....	114
FIGURE 4.8- WESTERN BLOT ANALYSIS OF OPG-INDUCED PHOSPHO-mTOR, ATG13 AND ATG7 EXPRESSION IN HPA-SMCs.....	117
FIGURE 4.9- PATHWAY FOLD ENRICHMENT OF GENES IN OPG-STIMULATED HPA-SMCs.....	121
FIGURE 4.10- HEAT MAP OF PAH-ASSOCIATED GENES REGULATED BY OPG.....	123
FIGURE 4.11- TAQMAN ANALYSIS OF RNA EXPRESSION IN HPA-SMCs.....	125
FIGURE 4.12- OPG INDUCES THE PHOSPHORYLATION OF CDK4 AND ERK1/2 IN PA-SMCs.....	129
FIGURE 4.13- OPG INDUCES THE EXPRESSION OF PDGFRA RNA.....	130
FIGURE 4.14- CAV-1 AND TNC INDUCE PA-SMC GROWTH AND PROLIFERATION (JONES & RABINOVITCH 1996; IVY ET AL. 2005).....	132
FIGURE 4.15- OPG INDUCES THE PHOSPHORYLATION OF HSP27.....	135
FIGURE 4.16- PROPOSED SCHEMATIC FOR OPG SIGNALLING IN PA-SMCs.....	138
FIGURE 5.1- THE EFFECT OF FAS BLOCKADE ON OPG-INDUCED GENE EXPRESSION IN PA-SMCs.....	143
FIGURE 5.2- FAS BLOCKADE REDUCES OPG-INDUCED PA-SMC PROLIFERATION.....	145
FIGURE 5.3- SIMULTANEOUS FAS AND TRAIL BLOCKADE FURTHER INHIBITS OPG-INDUCED PA-SMC PROLIFERATION.....	146
FIGURE 5.4- OPG, FAS AND TRAIL SIGNALLING IN NORMAL AND DISEASED PA-SMCs.....	149
FIGURE 5.5- TRAIL BLOCKADE, FAS BLOCKADE AND SIMULTANEOUS TRAIL AND FAS BLOCKADE IN PA-SMCs.....	151

LIST OF TABLES

TABLE 2.1 LICOR ODYSSEY SA SYSTEM SCANNING PARAMETERS	51
TABLE 2.2 FAS IP REACTIONS	55
TABLE 2.3 IL1RACP IP REACTIONS.....	55
TABLE 3.1- LIST OF PRIMARY HITS.....	79
TABLE 3.2- RESULTS OF THE CONFIRMATION SCREEN.....	81
TABLE 4.1- SUMMARY OF KINEX PROTEIN EXPRESSION AND PROTEIN PHOSPHORYLATION SIGNIFICANTLY ALTERED BY OPG IN PA-SMCs	102
TABLE 4.2- SUMMARY OF THE VALIDATED CHANGES IN PROTEIN EXPRESSION AND PHOSPHORYLATION IN PA-SMCs FOLLOWING OPG STIMULATION.	120
TABLE 7.1- ANTIBODIES (PAN-SPECIFIC AND PHOSPHO-SPECIFIC) SCREENED IN THE KINEX ANTIBODY MICROARRAY FOR OPG-STIMULATED LYSATES AT 10 MINUTES AND 60 MINUTES.....	180
TABLE 7.2- RNA INTEGRITY NUMBERS (RIN) FOLLOWING BIOANALYSER ANALYSIS OF RNA EXTRACTED FROM UNSTIMULATED AND OPG-STIMULATED HPA-SMC LYSATES.....	207

ABBREVIATIONS

%	Percent
®	Registered trademark
Ab	Antibody
ACVRL1	Activin A receptor type II-like 1
Alk-1	Activin receptor-like kinase 1
ANOVA	Analysis of variance
ApoE	Apolipoprotein E
Atg	Autophagy related
BMP	Bone morphogenetic protein
BMPR1A	Bone morphogenetic protein receptor 1A
BMPR2	Bone morphogenetic protein receptor 2
BSA	Bovine serum albumin
CAD	Coronary artery disease
CAV1	Caveolin-1
CDK	Cyclin-dependent kinase
cDNA	Complementary deoxyribonucleic acid
cGMP	Cyclic guanosine monophosphate
CKD	Chronic kidney disease
cm	Centimetre
Co-IP	Co-immunoprecipitation
CSA	Cross-sectional area
CTEPH	Chronic thromboembolic pulmonary hypertension
d	Day
DAVID	The Database for Annotation, Visualization and Integrated Discovery
DCR	Decoy receptor
DMEM	Dulbeccos minimum essential medium
DNA	Deoxyribonucleic acid
DR	Death receptor
EC	Endothelial cell
ECM	Extracellular matrix
EDTA	Ethylene diamine tetra acetic acid
ENG	Endoglin
eNOS	Endothelial nitric oxide synthase
ERK1/2	Extracellular signal-regulated kinase 1/2
ET-1	Endothelin-1
FADD	Fas-associated via death domain
FBS	Foetal bovine serum
FGF	Fibroblast growth factor
FPAH	Familial pulmonary arterial hypertension
g	Grams
GAP43	Growth associated protein 43
h	Hour

HHT	Hereditary haemorrhagic telangiectasia
HIV	Human immunodeficiency virus
HMVEC	Human microvascular endothelial cell
HPA-SMC	Human pulmonary arterial smooth muscle cell
HSP27	Heat shock protein 27
HuDMEC	Human dermal microvascular cell
HUVEC	Human umbilical vein endothelial cells
ICW	In-cell western
IgG	Immunoglobulin G
IL	Interleukin
IL-1R1	Interleukin-1 receptor 1
IL1RAcP	Interleukin-1 receptor accessory protein
IPAH	Idiopathic pulmonary arterial hypertension
KAM	Kinex™ antibody micorarray
KCNK3	Potassium channel, subfamily K, member 3
kDa	Kilodalton
LDLR	Low density lipoprotein receptor
LTB ₄	Leukotriene B ₄
MAPK	Mitogen activated kinase
MCP1	Monocyte chemotactic protein 1
MCT	Monocrotaline
Min	Minute
ml	Millilitre
mmHg	Millimetres of mercury
MMP	Matrix metalloprotease
MOPS	3-(N-morpholino)propanesulfonic acid
mPAP	Mean pulmonary arterial pressure
mRNA	Messenger ribonucleic acid
mTOR	Mammalian target of rapamycin
NaCl	Sodium Chloride
NF-κB	Nuclear factor-kappa B
nm	Nanometre
NO	Nitric oxide
OCIF	Osteoclastogenesis inhibitory factor
OPG	Osteoprotegerin
PA	Pulmonary artery
PA-EC	Pulmonary artery endothelial cell
PA-SMC	Pulmonary arterial smooth muscle cell
PAH	Pulmonary arterial hypertension
PAWP	Pulmonary arterial wedge pressure
PBS	Phosphate buffered saline
PCR	Polymerase chain reaction
PDGF	Platelet derived growth factor
PH	Pulmonary hypertension
PLCγ2	Phospholipase C-gamma2
PPH	Primary pulmonary hypertension
RANK	Receptor activator of nuclear factor-kappa B
RANKL	Receptor activator of nuclear factor-kappa B ligand
RHF	Right heart failure
RNA	Ribonucleic acid

rRNA	Ribosomal ribonucleic acid
RT-qPCR	Real-time quantitative polymerase chain reaction
RVH	Right ventricular hypertrophy
RVSP	Right ventricular systolic pressure
s	Seconds
SDC-1	Syndecan-1
SDS	Sodium dodecyl sulfate
SEM	Standard error of the mean
SERT	Serotonin transporter
siRNA	Short interfering ribonucleic acid
SMAD	Mothers against decapentaplegic homolog
SmBm	Smooth muscle basal medium
SMC	Smooth muscle cell
SuHx	Sugen-Hypoxia
TGF- β	Transforming growth factor beta
TGFBR1	Transforming growth factor, beta receptor I
TGFBR2	Transforming growth factor, beta receptor II
TMPRSS11D	Transmembrane protease, serine 11D
TNF	Tumour necrosis factor
Tph1	Tryptophan hydroxylase 1
TRAIL	Tumour necrosis factor related apoptosis-inducing ligand
TREM1	Triggering receptor expressed on myeloid cells 1
TRIS-HCl	Tris(hydroxymethyl)aminomethane hydrochloride
VEGF	Vascular endothelial growth factor
VIPR	Vasoactive intestinal peptide receptor
VSMC	Vascular smooth muscle cell
vWF	von willebrand factor
WHO	World Health Organisation
WPB	Weibel Palade bodies
xg	Gravity
μ g	Microgram
μ l	Microlitre
™	Trademark

SUMMARY

Pulmonary arterial hypertension (PAH) is a rare but fatal lung disease with a high mortality. Pathologically, PAH is characterised by progressive pulmonary vascular remodelling and it is well known that pulmonary arterial smooth muscle cell (PA-SMC) proliferation and migration is a key driver of this remodelling. Recently, the secreted glycoprotein, osteoprotegerin (OPG) has been implicated as an important pathogenic mediator in PAH. OPG is elevated within the serum and pulmonary vascular lesions from patients with PAH and OPG induces PA-SMC proliferation and migration *in vitro*. Furthermore, genetic deletion or antibody blockade of OPG can prevent and reverse established disease in pre-clinical animal models of PAH. However, it remains unclear how OPG signals to induce PA-SMC proliferation. Therefore, the work undertaken in this thesis aimed to characterise the OPG signalling cascade in PA-SMCs and identify the receptor through which this is mediated.

OPG was found to induce significant expression of CDK5, phospho-CDK4, phospho-ERK1/2, phospho-HSP27 and significantly altered expression of phospho-mTOR in PA-SMCs. OPG significantly altered the expression of 57 PAH-associated genes in PA-SMCs. Investigations into identifying an OPG binding partner revealed four novel interactions between OPG and Fas, IL1RAcP, GAP43 and TMPRSS11D. The interaction between OPG and Fas was confirmed in PA-SMCs. Fas expression was elevated in PA-SMCs, the pulmonary artery and right ventricle from idiopathic PAH patients. Fas blockade significantly inhibited OPG-induced gene expression in PA-SMCs and significantly inhibited OPG-induced PA-SMC proliferation by 34%, which was further reduced by simultaneous TRAIL blockade.

These data begin to reveal the receptor and novel intracellular signalling mechanisms through which OPG induces PA-SMC proliferation. As well as further highlighting OPG as a potential therapeutic target in PAH, these data also suggest a more diverse role for OPG in other biological systems.

1. INTRODUCTION

1.1 The Normal Pulmonary Circulation and Right Ventricle

The pulmonary circulation delivers deoxygenated blood from the body to the lungs, via the heart, where it is replenished with oxygen (Boron 2005). From the right atria, blood is pumped into the right ventricle, where it is then pumped out through the pulmonary artery (PA), which branches and divides to form smaller pulmonary arterioles and capillaries within the lungs. The pulmonary vascular bed branches throughout the lungs to enable gaseous exchange to occur between each of the millions of alveoli and the capillaries surrounding them (Boron 2005).

As such, the pulmonary vasculature is a high flow, low-pressure system with a low resistance to blood flow to allow gaseous exchange (Naeije 2013). Under normal physiological conditions, the pulmonary artery exhibits a mean pulmonary arterial pressure (mPAP) of ~7-19 mmHg (Naeije & Westerhof 2011). The right ventricle is a crescent-shaped, thin-walled structure that pumps this low-pressure system. The right ventricle is naturally adaptive to the demands of exercise by producing an elevation in mPAP of up to 40 mmHg (Pokreisz et al. 2007). However, because of its thin-walled structure, the right ventricle cannot acutely generate an mPAP of >40 mmHg.

1.2 Pulmonary Hypertension

The accumulation of vascular changes, sustained pulmonary vascular vasoconstriction and progressive pulmonary vascular remodelling leads to a persistent and prolonged elevation in mPAP. This once low pressure, low resistance network of vessels becomes a fatally diseased system where a devastating lung disease, known as pulmonary hypertension, manifests. Pulmonary hypertension (PH) is a progressive lung disease that is diagnosed at right heart catheterisation as an mPAP of >25 mmHg at rest. Pre-capillary PH, pulmonary arterial hypertension, is diagnosed by a pulmonary arterial wedge pressure (PAWP) of <15 mmHg and post-capillary PH is diagnosed by a PAWP of >15 mmHg (Hoepfer, Bogaard, et al. 2013). PH was first described over a century ago and since then, major developments in our understanding of the disease have led to a better characterisation and diagnosis of the disease.

1.2.1 Historical Classification of Pulmonary Hypertension

In 1865, the German physician, Klob, reported on the case of a 59-year-old man who suffered cyanosis, oedema and dyspnoea prior to his death and post-mortem revealed pulmonary arterial narrowing and arteriosclerosis (van Wolferen et al. 2007). Later in 1891, another German physician, Ernst Von Romberg, described a 24-year-old patient with abnormalities in the pulmonary artery and right ventricular hypertrophy. Pulmonary hypertension was later coined “Ayerza’s disease” following several reports made by Arrillaga, a physician who was first alerted to the condition by his professor, Ayerza (van Wolferen et al. 2007).

Heath and Whitaker later described the clinical and histologic features of PH after discussing six case studies of patients admitted to the cardiovascular unit in Sheffield (United Kingdom). All cases presented with cyanosis and classical symptoms of PH. Autopsy revealed enlargement of the heart, right ventricular hypertrophy and atrial dilation (Heath & Whitaker 1956). Histologic analysis also revealed muscularisation of previously non-muscular pulmonary arteries (<100 µm diameter) and larger pulmonary arteries (100-1000 µm diameter), with medial necrosis and luminal occlusion. Patients also presented with adventitial fibrosis and pulmonary arterial dilation (Heath & Whitaker 1956). This work described, for the first time, the specific pulmonary arterial remodelling that occurs in PH patients.

The first attempt at classifying pulmonary hypertension was made by Brenner (1957), where pulmonary hypertension patients were divided into 5 groups: 1) chronic bronchitis and emphysema, 2) left to right heart shunt, 3) primary pulmonary hypertension, 4) primary pulmonary arteriosclerosis and 5) pulmonary embolism (Brenner 1957). However, in 1973, the World Health Organisation (WHO) held the first conference on pulmonary hypertension to review the scientific information, discuss the pathogenesis and clinical presentation of primary pulmonary hypertension (Hatano et al. 1975). This meeting resulted in a classification based on aetiology consisting of two groups: secondary PH, which was described as PH of known cause, such as pulmonary hypertension due to pulmonary thromboembolism, pulmonary veno-occlusive disease, or left-to-right shunt (Group 2) and primary PH, which was

described as PH of unknown cause and cases were only assigned to this category once all possible known causes had been excluded (Group 1) (Hatano et al. 1975).

However, at the second WHO symposium held in Evian, a clinical classification was introduced. This resulted in five groups being established: 1) Pulmonary arterial hypertension (PAH) (including primary pulmonary hypertension), 2) pulmonary vascular hypertension, 3) PH associated with disorders of the respiratory system or hypoxia, 4) PH caused by thrombotic or embolic disease and 5) PH caused by disease affecting the pulmonary vasculature (Simonneau et al. 2004). The “Evian classification” abandoned the term “secondary pulmonary hypertension” because it was deemed confusing. The term “primary pulmonary hypertension” was later discontinued at the third WHO symposium in 2003 and instead, PAH was split into the subgroups IPAH, familial PAH (FPAH) and PAH related to risk factors or associated conditions (Simonneau et al. 2004).

In 2008, the decision was made at the fourth WHO symposium, held at Dana Point, to include genetic causes of PH, pulmonary veno-occlusive disease and/or pulmonary capillary hemangiomatosis (Group 1'), chronic thromboembolic pulmonary hypertension (Group 4) and PH with unclear multifactorial mechanisms (Group 5) (Simonneau et al. 2009). Finally, in 2013, the fifth most recent WHO symposium was held in Nice, France and the classification was further updated still. The most recent classification of PH established at the symposium in Nice symposium is shown in Figure 1.1, with modifications to the previous 2008 Dana Point classification shown in bold.

1. Pulmonary arterial hypertension
 - 1.1 Idiopathic PAH
 - 1.2 Heritable PAH
 - 1.2.1 BMPR2
 - 1.2.2 ALK-1, ENG, **SMAD9**, **CAV1**, **KCNK3**
 - 1.2.3 Unknown
 - 1.3 Drug and toxin induced
 - 1.4 Associated with:
 - 1.4.1 Connective tissue disease
 - 1.4.2 HIV infection
 - 1.4.3 Portal hypertension
 - 1.4.4 Congenital heart diseases
 - 1.4.5 Schistosomiasis
- 1' Pulmonary veno-occlusive disease and/or pulmonary capillary hemangiomatosis
- 1''. **Persistent pulmonary hypertension of the newborn (PPHN)**
2. Pulmonary hypertension due to left heart disease
 - 2.1 Left ventricular systolic dysfunction
 - 2.2 Left ventricular diastolic dysfunction
 - 2.3 Valvular disease
 - 2.4 **Congenital/acquired left heart inflow/outflow tract obstruction and congenital cardiomyopathies**
3. Pulmonary hypertension due to lung diseases and/or hypoxia
 - 3.1 Chronic obstructive pulmonary disease
 - 3.2 Interstitial lung disease
 - 3.3 Other pulmonary diseases with mixed restrictive and obstructive pattern
 - 3.4 Sleep-disordered breathing
 - 3.5 Alveolar hypoventilation disorders
 - 3.6 Chronic exposure to high altitude
 - 3.7 Developmental lung diseases
4. Chronic thromboembolic pulmonary hypertension (CTEPH)
5. Pulmonary hypertension with unclear multifactorial mechanisms
 - 5.1 Hematologic disorders: **chronic hemolytic anemia**, myeloproliferative disorders, splenectomy
 - 5.2 Systemic disorders: sarcoidosis, pulmonary histiocytosis, lymphangiomyomatosis
 - 5.3 Metabolic disorders: glycogen storage disease, Gaucher disease, thyroid disorders
 - 5.4 Others: tumoral obstruction, fibrosing mediastinitis, chronic renal failure, **segmental PH**

Figure 1.1- Updated Clinical Classification of Pulmonary Hypertension, Nice, France 2013 (Fifth WHO symposium).

*BMPR2 = bone morphogenetic protein receptor type II, Alk-1 = activin receptor-like kinase 1, ENG = endoglin, SMAD9 = mothers against decapentaplegic homolog 9, CAV1 = caveolin 1, KCNK3 = potassium channel, subfamily K, member 3. Modifications to Dana Point classification (2008) are shown in **bold** (Simonneau et al. 2013)¹.*

¹ Reprinted from Journal of the American College of Cardiology, Vol 62, Gerald Simonneau, Michael A. Gatzoulis, Ian Adatia, David Celermajer, Chris Denton, MD, Ardeschir Ghofrani, Miguel Angel Gomez Sanchez, R. Krishna Kumar, Michael Landzberg, Roberto F. Machado, Horst Olschewski, Ivan M. Robbins, Rogiero Souza, Updated Clinical Classification of Pulmonary Hypertension, D34-D41, Copyright 2013, with permission from Elsevier.

The updated classification of PH consists of five groups, 1) pulmonary arterial hypertension, 2) pulmonary hypertension due to left heart disease, 3) pulmonary hypertension due to lung disease and/or hypoxia, 4) chronic thromboembolic pulmonary hypertension (CTEPH) and 5) pulmonary hypertension with unclear multifactorial mechanisms (Figure 1.1). Pre-capillary PH includes Group 1, Group 3, Group 4 and Group 5 of the updated clinical classification of PH and post-capillary PH consists of only Group 2. However, the work described throughout this thesis focuses on PAH, in particular, idiopathic PAH.

1.3 Pulmonary Arterial Hypertension

PAH, or Group 1, is defined as pre-capillary PH and is diagnosed as an mPAP of >25 mmHg and a pulmonary capillary wedge pressure of <15 mmHg (Hoepfer, Bogaard, et al. 2013). PAH can be further divided into four subgroups (Figure 1.1, Group 1). The first subgroup, IPAH, refers to those patients who present with sporadic disease, with no known aetiology, no family history of the disease and no identified risk factor (Simonneau et al. 2013). The second group describes heritable PAH. In these families where there are multiple cases of PAH, 80% present with mutations in the transforming growth factor-beta (TGF- β) super family member, bone morphogenetic protein receptor 2 (*BMPR2*) mutations and 5% present with mutations in the other TGF- β superfamily members activin receptor-like kinase 1 (*ALK-1*, *ACVRL1*), endoglin (*ENG*) and Mothers Against Decapentaplegic Homolog 9 (*SMAD9*) (Figure 1.1, Group 1.2). Mutations in caveolin-1 (*CAVI*) and potassium channel, subfamily K, member 3 (*KCNK3*) have also been identified and all of these mutations are discussed in further detail in Chapter 1.4.7. However, in 20% of families presenting with PAH, the mutation is currently unknown (Simonneau et al. 2013). Group 1.3 describes PAH that is induced by drug and toxins, such as the anorexigen aminorex (Kay et al. 1971). Finally, Group 1.4 describes PAH associated with other disorders, including connective tissue disease (Group 1.4.1), HIV infection (Group 1.4.2), portal hypertension (Group 1.4.3), congenital heart disease (Group 1.4.4) and schistosomiasis (Group 1.4.5).

PAH currently affects 3482 patients in the UK and 44.9% of patients diagnosed with PH have PAH. Collectively, IPAH, HPAH and anorexigen-associated PAH have an incidence rate of 1.1 cases per million in the United Kingdom (McGoon et al. 2013). PAH is more common in women than men, with a ratio of 1.8:1. Those affected have a median age of 62 years in the UK (<http://www.hscic.gov.uk/catalogue/PUB13318>, Health and Social Care Information Centre, 2013). Of these cases, 34.6% have idiopathic PAH, 32.1% congenital heart disease, 25.7% connective tissue disease, 3.9% portal hypertension, 1.4% familial PAH, 0.8% HIV and 0.4% drug-induced PAH (<http://www.hscic.gov.uk/catalogue/PUB13318>, Health and Social Care Information Centre, 2013). Patients with PAH have a one-year survival rate of 88% and a three-year survival rate of 68% (<http://www.hscic.gov.uk/catalogue/PUB13318>, Health and Social Care Information Centre, 2013).

1.3.1 Clinical Presentation and Diagnosis

Symptoms of PAH typically present when the mPAP reaches 30-40 mmHg (Eddahibi et al., 2002). In a study of 187 patients with pulmonary arterial hypertension, the most common symptom reported was breathlessness (60%) with the second most common symptom being fatigue (19%). Patients also reported chest pain, fainting, oedema and palpitations (Rich et al. 1987). However, during this study, the time between the onset of the first symptom and diagnosis was reported to be 2.03 years \pm 4.9 years and although 90% patients were diagnosed within 3 years, some patients reported symptom onset 20 years before diagnosis (Rich et al. 1987).

Diagnosis can be made by non-invasive methods such as chest x-ray, electrocardiogram, vasodilator challenge and 6-minute walk test, however these methods often require confirmation by right heart catheterization (Elliot & Kiely 2006; Kiely et al. 2013). Both electrocardiogram and x-ray can appear normal in PAH patients, hence PAH may be overlooked or misdiagnosed. Unfortunately, due to the extent of vascular remodelling that has already developed during the asymptomatic stage of disease and the obstacles that sometimes arise during diagnosis, median survival without therapy is 2.8 years (Elliot and Kiely, 2006), with right heart failure being the major cause of mortality (Pokreisz et al., 2007). Because symptoms often present late, it is imperative

that diagnosis is made early to ensure patients can be treated as soon as possible to prolong patient life as much as possible.

1.3.2 PAH and the Right Heart

As discussed in Chapter 1.1, the pulmonary vascular system is low in pressure, and the right ventricle can naturally adapt to acute elevations in pressure (Pokreisz et al., 2007). During prolonged periods of elevated pressure, the right ventricle employs compensatory mechanisms to tolerate chronic hypertension. Cardiomyocytes undergo hypertrophy to reduce cardiac wall stress and maintain cardiac output. However, without improved pressure or afterload, there is a decline in blood flow to the right myocardium. Ischemia and apoptosis of right ventricle cardiomyocytes results in right ventricular dilation, stiffening and impaired stroke volume, poor ventricular filling, reduced cardiac function, inadequate organ perfusion and eventual right heart failure (RHF) in PAH patients (Davies & Morrell 2008; Pokreisz et al. 2007).

1.4 The Pathogenesis of Pulmonary Arterial Hypertension

The pathogenesis of PAH is an incredibly complex process that affects all layers, intima, media and adventitia, of the pulmonary arteries (Humbert et al. 2004). PAH typically affects the smaller, more distally located arterioles of the pulmonary circulation (Rabinovitch 2008). Endothelial cell (EC) apoptosis, EC and smooth muscle cell (SMC) proliferation, sustained pulmonary arterial vasoconstriction, inflammation and the immune system all play an important role in PAH and contribute to loss of lumen diameter and increased pulmonary pressure. Although the initial stimulus preceding the sustained pulmonary vasoconstriction and cell proliferation is currently unknown, there is a hypothesis that injury to the endothelium causes EC apoptosis, which is believed to be the early initial insult (Budhiraja et al. 2004; Voelkel et al. 2012). Proliferation of apoptosis-resistance ECs, and then PA-SMCs is then thought to follow EC injury and apoptosis (Voelkel et al. 2012). Dysfunctional endothelial cells are also thought to underlie the imbalance between vasodilators and vasoconstrictors that leads to pulmonary vasoconstriction in PAH (Rabinovitch 2008). Muscularisation of previously non-muscular pulmonary arterioles is thought to occur through the proliferation and migration of pulmonary arterial smooth muscle cells (PA-SMCs). Although it is currently unclear whether

inflammation is causal or a consequence of disease pathogenesis, it is probable that the inflammation that occurs in PAH may be a result of inflammation that has not been resolved following pulmonary vascular injury (Voelkel et al. 2012).

Although the initial cause of remodelling and abnormal cell growth remains unknown, the identification of mutations in the TGF- β superfamily member, *BMPR2*, identified the cause of some cases of heritable PAH (Thomson et al. 2000; Atkinson et al. 2002). However, the literature suggests that only 20% of *BMPR2* mutation carriers will actually develop disease (Newman et al. 2004).. This that there is a need for “multiple hits” in the development of PAH, such as genetic mutations in other genes, for example the serotonin receptor (*HTR2B*), in addition to *BMPR2* mutations (Yuan & Rubin 2005).

1.4.1 Endothelial Cell Apoptosis

As discussed above in Chapter 1.4, endothelial cell apoptosis is thought to be the initial early insult in PAH. Endothelial cell apoptosis is thought to occur as a result of endothelium injury caused by a number of factors including shear stress from increased pulmonary blood flow, infection, such as HIV, hypoxia, genetic susceptibility, such as *BMPR2* mutations and epigenetic factors such as microRNAs (Budhiraja et al. 2004; Voelkel et al. 2012).

In 1974, Meyrick et al reported on the case of a 41 year-old male with pulmonary hypertension who displayed a reduction in the number and size of vessels and slightly reduced filling at the apices of the lung (Meyrick et al. 1974). However, there has been controversy as to whether the apparent loss of vessels was actually caused by inadequate perfusion of distally located vessels due to the luminal narrowing and increased vasoconstriction, rather than an actual loss of vessels (Michelakis et al. 2008). However, there is now evidence that loss of distal vessels occurs in PAH and the underlying cause of this loss is likely to be endothelial cell apoptosis (Zhao et al. 2005). Recent evidence suggesting that loss of functional *BMPR2* signalling actually induces EC apoptosis further supports the idea that EC apoptosis may indeed contribute to the pathogenesis of PAH (Teichert-Kuliszewska 2006). In animal models, pulmonary EC apoptosis is observed prior to and accompanying disease

development, in addition to EC proliferation (Taraseviciene-Stewart et al. 2001). This further supports the idea that EC apoptosis is an early event in the pathogenesis of PAH and underpins the loss of distally located pulmonary arterioles.

1.4.2 Endothelial Cell Proliferation

Endothelial cell proliferation has been hypothesised to occur either as a result of endothelium injury or following endothelial cell apoptosis (Tuder & Graham 2010; Voelkel et al. 2012; Humbert et al. 2008). The mechanisms that lead to EC proliferation are currently unclear, however, endothelium injury may be a stimulus for EC proliferation (Humbert et al. 2008). EC proliferation may also occur after EC apoptosis causes a population of apoptosis-resistant ECs to emerge, which then proliferate, perhaps to compensate for the preceding EC death, and form plexiform lesions (Tuder & Graham 2010; Voelkel et al. 2012). It is thought that the proliferation of the endothelial cells and matrix deposition, which contributes to the formation of concentric and constrictive lesions within the intimal layer cause the greatest reduction in pulmonary artery lumen size (Stenmark & Frid 2011).

The proliferation of dysfunctional apoptosis-resistant ECs causes the formation of plexiform lesions, the hallmark of end-stage disease that occludes the lumen and narrows the pulmonary artery (Tuder & Graham 2010). Plexiform lesions are colonies of proliferating ECs lined by SMCs, myofibroblasts and connective tissue matrix that frequently form where the pulmonary artery branches (Pietra et al. 2004). The vigorous EC growth that contributes to lesion formation was first reported by Tuder et al (1994) after proliferating cells stained positive for the EC markers factor VIII and vimentin and exhibited low immunoreactivity for SMC specific markers. It was later identified that the ECs within plexiform lesions were monoclonal (Lee et al. 1998). Although plexiform lesions are described in PAH, the contribution of these plexiform lesions to the increase in pulmonary vascular resistance observed in PAH still remains unclear (Tuder & Graham 2010). In fact, there has been some reports of the plexiform lesion being a marker for endothelial cell abnormality, rather than being haemodynamically relevant (Humbert et al. 2008), however other literature contests the claim that plexiform lesions do not contribute to haemodynamic changes (Tuder & Graham 2010). However, it is clear from the literature that the exact cause of EC dysfunction and subsequent plexiform lesion formation is still ambiguous.

1.4.3 Pulmonary Vasoconstriction

The initial stimulus preceding pulmonary vasoconstriction is unknown, however endothelium injury is also thought to alter the effect ECs have on vascular homeostasis, as well as causing EC apoptosis and proliferation (Budhiraja et al. 2004; Humbert et al. 2008). Endothelium injury is thought to cause EC dysfunction and subsequently affect the release of vasoactive compounds (Humbert et al. 2008). An imbalance of vasoactive mediator release from dysfunctional ECs leads to sustained pulmonary vasoconstriction and subsequent reduction in lumen diameter that contributes to the increase in pulmonary vascular resistance in PAH (Schermuly et al. 2011). PAH patients show reduced levels of the vasodilators prostaglandin I₂, nitric oxide and cyclic guanosine monophosphate (cGMP) and increased levels of the vasoconstrictors thromboxane A₂, angiotensin II, endothelin-1 and serotonin, which cause excessive vasoconstriction (Schermuly et al. 2011). Furthermore, these vasoactive mediators also contribute to PA-SMC proliferation, a key pathogenic process in PAH, which is discussed in further detail below (Hassoun et al. 1992; Giaid et al. 1993; Lee et al. 1994; Hervé et al. 1995; Christman et al. 1992; Giaid & Saleh 1995; Farber & Loscalzo 2007).

1.4.3.1 Endothelin 1

Plasma levels of Endothelin-1 (ET-1), a vasoconstrictor produced in ECs are increased in patients with PAH (Farber and Loscalzo, 2004, McLaughlin and McGoon, 2006). Furthermore, ET-1 protein and mRNA was detected in the endothelial cells of pulmonary arteries displaying medial thickening (Giaid et al. 1993). ET-1 induces PA-SMC contraction by binding to ET_A and ET_B receptors present on PA-SMCs. ET_B receptors present on ECs potentiate vasoconstriction by inducing the release of thromboxane, another vasoconstrictive compound (McLaughlin and McGoon, 2006, Rabinovitch, 2008). ET-1 also acts as a mitogen for PA-SMCs and ET-1 induces PA-SMC proliferation via ET_A and ET_B receptors (Hassoun et al. 1992; Davie et al. 2002). Interestingly, Davie et al (2002) also showed ET-1 binding sites of a higher number in the distal PAs of primary pulmonary

hypertension (PPH) patients compared to control subjects. This could help to explain why smaller, distally located arterioles are affected more frequently in PAH.

1.4.3.2 Serotonin

Serotonin is a vasoconstrictor shown to induce PA-SMC hyperplasia and hypertrophy (Lee et al. 1994; Rabinovitch 2008). The involvement of serotonin in PAH pathogenesis was proposed in the 1960s after a correlation between increased risk of PAH and individuals taking the anorexigen, Aminorex, was observed (Eddahibi et al., 2002, MacLean, 2007a). Increased plasma levels of serotonin have been reported in PAH patients and PAH has been associated with the depletion in serotonin platelet content and subsequent increased plasma levels due to reduced uptake of serotonin from plasma (Hervé et al. 1995). PA-ECs synthesize serotonin from tryptophan through the catalytic actions of tryptophan hydroxylase 1 (tph1), which is subsequently secreted from PA-ECs to act on different serotonin receptors (MacLean, 2007a). *TPHI* expression is also increased within the lungs and PA-ECs of idiopathic PAH patients (Eddahibi et al. 2006).

1.4.4 Pulmonary Arterial Smooth Muscle Cell Proliferation

In the normal pulmonary vasculature, PA-SMCs are usually contractile and show low levels of proliferation, even though there are growth factors present in the vasculature that could potentially exert a mitogenic effect on PA-SMCs. Instead, medial vascular smooth muscle cells are embedded within the extracellular matrix consisting of proteins, produced by the vascular SMCs, that inhibit SMC proliferation, such as collagen I, collagen IV and heparin sulphate (Fritze et al. 1985; Koyama et al. 1996). However, in PAH, an increase in mitogenic factors and reduction in these anti-proliferative factors cause PA-SMCs to acquire a dysfunctional, hyper-proliferative phenotype.

The hallmark of all classes of pulmonary hypertension is the increase in pulmonary artery wall thickness and all three layers of the pulmonary artery, intima, media and adventitia show an increase in thickness (Chazova et al. 1995). Just like many of the pathogenic processes in PAH, the underlying cause of PA-SMC proliferation is

currently unknown and may be due to an inherent property of PA-SMCs, or may be caused by preceding EC dysfunction (Humbert et al. 2008). EC injury may cause the leakage of vascular elastase that degrades the vascular matrix to allow proliferative mediators to permeate the vascular wall and initiate the growth of smooth muscle cells within the medial layer (Budhiraja et al. 2004). The proliferation of smooth muscle cells and myofibroblasts cause an increase in medial thickness and the proliferation and accumulation of fibroblasts, myofibroblasts and increased matrix deposition underlies adventitial thickening (Stenmark & Frid 2011).

Abnormal proliferation and migration of α -smooth muscle actin positive cells, referred to as PA-SMCs from here on, underpin the characteristic pulmonary arterial remodelling observed in PAH (Davies and Morrell, 2008, Eddahibi et al., 2002). PA-SMC hyperplasia and hypertrophy result in the medial muscularisation of distal pulmonary arteries (Davies and Morrell, 2008, Eddahibi et al., 2002, Rabinovitch, 2008). The tunica media was originally believed to be a homogenous population of cells, however this view has changed dramatically due to evidence that cells of the media actually belong to a heterogeneous population. Different subpopulations of PA-SMCs are found throughout the pulmonary vasculature and at different sites along the vasculature. Frid et al (1994) have shown that the tunica media consists of different cell populations, with non-muscular cells located in the sub-endothelial layer of the inner media, SMCs within the middle media and both SMCs and non-muscular cells in the outer media (Frid et al. 1994). Furthermore, the different populations of cells within the media display distinct markers when stimulated with serum: the middle media SMCs expressed both the proliferation marker Ki-67 and smooth muscle-myosin, however serum stimulation of the outer media SMCs resulted in a reduction in smooth muscle-myosin (Frid et al. 1997). This may provide an important clue as to why only certain populations of cells, for example cells located in the smaller pulmonary arteries, undergo pathogenic changes in disease (Frid et al. 1997).

A number of different factors that are dysfunctional or dysregulated in PAH can induce the proliferation of PA-SMCs. Growth factors, such as PDGF, which has been shown to be increased in IPAH patients, induce that proliferation of PA-SMCs (Yu et al. 2003; Perros et al. 2008). Additionally, the BMP ligands BMP2, BMP4 and BMP7 that usually bind BMPR2 to inhibit SMC proliferation, no longer inhibit PA-SMC

proliferation when BMPR2 is mutated in FPAH and IPAH patients (Atkinson et al. 2002; Tajsic & Morrell 2011). Instead, this loss of signalling causes the proliferation of PA-SMCs. An imbalance between vasoactive compounds, which also act as mitogens and inhibitors of PA-SMC proliferation, also contribute to the excessive PA-SMC proliferation. Endothelin-1, serotonin (5-hydroxytryptamine, 5-HT), angiotensin-II and thromboxane A2 are all potent vasoconstrictors that are upregulated in PAH and induce the proliferation of PA-SMCs (Hassoun et al. 1992; Giaid et al. 1993; Lee et al. 1994; Hervé et al. 1995; Christman et al. 1992).

Coupled with the increase in mitogenic factors, there is also a reduction in the vasodilators nitric oxide (NO) and prostacyclin, which usually inhibit PA-SMC proliferation (Giaid & Saleh 1995; Farber & Loscalzo 2007). In addition to the growth factors and vasoactive compounds, and of direct relevance to this thesis and discussed in further detail later, OPG and TRAIL have recently been shown to play an important role in PAH pathogenesis and the proliferation and migration of PA-SMCs (Secchiero et al. 2003; Hameed et al. 2012; Lawrie et al. 2008; Condliffe et al. 2012). The role of these mitogens and dysfunctional signalling pathways in PAH pathogenesis will be discussed in more detail below, as their effects are not limited to a single action on a single cell type, but rather they exert complex and intertwining effects on a variety of cell types in disease.

1.4.5 Fibroblast Activation and Proliferation

The adventitial layer is thought to be an injury-sensing layer, which contains fibroblasts that respond to injury. These fibroblasts are activated by a variety of stresses, including inflammatory and environmental stresses, such as hypoxia. Upon activation, the fibroblasts acquire a proliferative phenotype, begin to express the contractile protein α -smooth muscle actin and extracellular matrix proteins. The fibroblasts also increase secretion of chemokines and cytokines, growth factors and angiogenic factors (Stenmark et al. 2012). Activated fibroblasts, which have acquired this hyper-proliferative phenotype, are observed in the pulmonary artery adventitia of PAH patients and animal models of PH (El Kasmi et al. 2014). Fibroblasts derived from the hypoxic calf model of PH exhibited a pro-inflammatory phenotype and were also found to induce the migration, adhesion and activation of monocytes, a process

found to be mediated by paracrine IL-6 signalling (M. Li et al. 2011; El Kasmi et al. 2014). Interestingly, fibroblasts derived from the hypoxic calf were found to have an active form of protein kinase C zeta (PKC-zeta), which instead of repressing replication and reducing DNA synthesis as in normal adventitial fibroblasts, actually caused an increase in fibroblast proliferation (Das et al. 2008). This suggests that the increase in fibroblast proliferation may be due to an activated form of PKC-zeta present in the remodelled vascular wall that induces proliferation instead of inhibiting DNA synthesis.

1.4.6 Inflammation

Inflammation is now widely acknowledged as playing an important role in the pathogenesis of PAH. Whether inflammation is causal or a consequence of disease is currently debated, however, it is probable that PH occurs when inflammation of pulmonary vascular injury is not resolved (Voelkel et al. 2012). Inflammation may also be caused by the release of chemokines from dysfunctional ECs that cause inflammatory cell recruitment. For example, IPAH PA-ECs markedly enhanced monocyte migration, a response that was abolished by CC chemokine ligand 2 inhibition (Sanchez et al. 2007; Humbert et al. 2008;) There have been a number of cytokines and chemokines implicated in PAH pathogenesis. Serum levels of the inflammatory cytokines, interleukin-1 (IL-1) and interleukin-6 (IL-6) are increased in patients with IPAH (Humbert et al. 1995). IL-6 induces the migration of PA-SMCs *in vitro* and IL-6 levels are increased in the chronic hypoxic and monocrotaline (MCT) rat model of PAH (Savale et al. 2009; Bhargava et al. 1999). Furthermore, IL-6 has also been shown to promote the development and progression of the pathogenic pulmonary vascular remodelling in mice overexpressing IL-6 (Steiner et al. 2009). Inhibition of IL-6 attenuated disease development in the MCT rat and IL-6 knockout also prevented disease development in the chronic hypoxic mouse model of PAH (Savale et al. 2009; Bhargava et al. 1999).

IL-1 serum levels are also elevated in IPAH patients and work published by Voelkel et al (1994) showed that the naturally occurring IL-1 receptor antagonist IL-1ra (anakinra) protected against disease development in the MCT rat model, but did not protect against disease development in the chronic hypoxic model. Authors proposed

that this was due to the fact that IL-1 α stimulates the vasodilator, nitric oxide (NO); therefore IL-1ra caused an inhibition in NO production in the chronic hypoxic mouse model. Hence, disease was maintained due to the reduction in NO production (Voelkel et al. 1994). In the Paigen-fed ApoE^{-/-} mouse model of PAH, animals exhibit increased IL-1 β and IL-6 levels, however, ApoE^{-/-}IL-1R1^{-/-} mice deficient in the IL1 receptor surprisingly develop a more severe phenotype and further increased IL-1 β and IL-6 levels (Lawrie et al. 2011). Consequently, an alternatively spliced, lung specific IL-1R1 transcript was identified that actively signals IL-1 in the lung, but is still inhibited by IL-1ra (Lawrie et al. 2011). Alongside the IL-1 and IL-6 inflammatory cytokines, monocyte chemotactic protein 1 (MCP1) and fractalkine have also been implicated as potential mediators in PAH pathogenesis (Sanchez et al. 2007; Perros, Dorfmueller, Souza, Durand-Gasselino, Godot, et al. 2007) and inflammatory cells, including T-cells, B-cells and macrophages have been identified in plexiform lesions of PAH patients (Tuder et al. 1994a).

Alongside pulmonary vascular remodelling, there is an infiltration of inflammatory cells and the formation of lymphoid tissue within the pulmonary artery. Perivascular infiltrates occur in pulmonary vascular lesions and comprise of T-lymphocytes, B-lymphocytes, macrophages, dendritic cells and mast cells (Rabinovitch et al. 2014). Studies have also shown that the inflammatory pathology is more advanced in the presence of *BMPR2* mutations (Rabinovitch et al. 2014). Regulatory T cells have been implicated in PAH, with abnormal numbers and function CD4 positive T cells being observed in conditions associated with PAH, for example HIV and systemic sclerosis (Speich et al. 1991; Radstake et al. 2009). Furthermore, in T cell deficient athymic nude rats, Sugen5416 treatment resulted in macrophage, mast cell and B cell infiltration in the lung due to vascular injury and endothelial cell apoptosis, which immune-restricted rats were protected from (Tamosiuniene et al. 2011).

Macrophages are also found to infiltrate the pulmonary arteries and macrophages have been identified as constituents of obliterative plexiform lesions in both PAH patients and animal models of PH (Tuder et al. 1994b; Savai et al. 2012; Frid et al. 2006; Vergadi et al. 2011). Alongside macrophage recruitment, macrophages were found to secrete leukotriene B₄ (LTB₄), which induced PA-EC injury and apoptosis, along with PA-SMC proliferation and hypertrophy in athymic nude rats. Interestingly, blockade

of macrophage-derived LTB₄ reversed experimental PH (Tian et al. 2013), implicating macrophages and the macrophage-derived leukotriene LTB₄ in the pathogenesis of PAH.

Natural killer cells, which usually have a beneficial effect on PH, can also acquire a pathogenic phenotype and in doing so, increase their matrix metalloprotease (MMP) production and reduce the amount of interferon- γ production (Rabinovitch et al. 2014). PAH patients also show an increase in the number of functionally deficient, CD56⁻/CD16⁺ natural killer cell subset (Ormiston et al. 2012). Dendritic cells have also been found to accumulate in the remodelled pulmonary arteries of both patients and animal models of PH (Perros, Dorfmueller, Souza, Durand-Gasselin, Mussot, et al. 2007) and aggregates of ectopic lymphoid tissue have been observed in the pulmonary vasculature of IPAH lungs, some of which were structurally similar to lymph nodes (Carragher et al. 2008). Studies now suggest, at least in animal models, that inflammation precedes vascular remodelling, indicating that inflammation may be causal, rather than consequential, in disease development (Rabinovitch et al. 2014; Tamosiuniene et al. 2011).

1.4.7 Genetics of Pulmonary Arterial Hypertension

In 2004, the decision was made at the fourth WHO symposium held at Dana Point, to include genetic causes of PH after the identification of genetic causes in a number of cases of PAH (Simonneau et al. 2009). Mutations in a number of genes, including a number of genes belonging to the TGF- β superfamily, have been identified in patients with both FPAH and IPAH.

1.4.7.1 Bone Morphogenetic Protein Receptor 2 Mutations

As mentioned previously, *BMPR2* mutations which lead to dysfunctional BMP signalling, can induce the proliferation of PA-SMCs and induce EC apoptosis (Tajsic & Morrell 2011; Teichert-Kuliszewska 2006). In non-diseased cells, *BMPR2* has been shown to protect ECs from apoptosis and conversely induce PA-SMC apoptosis (Majka et al. 2011; Teichert-Kuliszewska 2006; Zhang et al. 2003). Mutations in *BMPR2* have been identified in familial PAH (Lane et al. 2000; Deng et al. 2000) and

IPAH (Thomson et al. 2000) and these mutations were predicted to effect ligand binding, kinase activity and dimer formation (Lane et al. 2000). Mutations in *BMPR2* underpin heritable forms of PAH and reduced expression is associated with dysfunctional SMAD1/5/8 signalling and PA-SMC proliferation (Nishihara et al. 2002; Rudarakanchana et al. 2002). Additionally, in IPAH PA-SMCs, BMP ligands did not inhibit PA-SMC proliferation, and instead of inducing apoptosis, TGF β actually stimulated PA-SMC proliferation (Morrell et al. 2001). Mouse EC studies also revealed that a reduction in *BMPR2* cell surface expression may further increase p38 MAPK phosphorylation and thus activate proliferative pathways which may also contribute to PA-SMC proliferation (Eddahibi et al. 2002). This disruption in *BMPR2* signalling caused by the *BMPR2* mutations is now believed to underlie the dysfunctional EC apoptosis and exuberant PA-SMC proliferation observed in PAH.

Over 300 mutations in the *BMPR2* gene have now been identified and *BMPR2* mutations have been identified in 75% of FPAH and 25% of IPAH patients (Soubrier et al. 2013). However, as the literature suggests, only 20% of *BMPR2* mutation carriers will actually develop disease, and these statistics suggest that “multiple hits” may be required for the onset of PAH pathogenesis (Newman et al. 2004). These “hits” may include mutations and polymorphisms in modifier genes or exposure to environmental influences such as HIV infection that trigger disease development in these patients (Geraci et al. 2010).

1.4.7.2 Activin Receptor-Like Kinase 1 and Endoglin Mutations

Interestingly, mutations in the TGF- β receptor superfamily type 1 receptor, *ACVRL1* (also known as ALK-1, activin receptor-like kinase 1) and type III receptor, Endoglin (*ENG*), have been identified in hereditary haemorrhagic telangiectasia (HHT)-associated PAH (Harrison et al. 2003; McAllister et al. 1994). Mutations in *ACVRL1* and *ENG* were identified in patients with HHT, an autosomal dominant condition in which vascular dysplasia gives rise to symptoms including recurrent epistaxis (bleeding from the nose), gastro-intestinal haemorrhage and arteriovenous malformations in the pulmonary, cerebral and hepatic vessels (Johnson et al. 1996). *ACVRL1* mutations have been mapped to a second locus linked to HHT type 2 (Johnson et al. 1996). Harrison et al (2003) then identified mutations in *ACVRL1* in

patients with HHT that also presented with symptoms of PAH. There is now evidence that the mutations in *ACVRL1* are also present in FPAH and IPAH patients that do not show any symptoms of HHT (Fujiwara et al. 2008).

Mutations in *ENG*, which is expressed in ECs, were also found to underlie HHT (McAllister et al., 1994) and were identified in patients with HHT presenting with PAH symptoms (Harrison et al., 2003). More recent work has identified mutations in *ACVRL1* and *ENG* in Chinese patients with HHT-associated pulmonary hypertension (Eyries et al. 2012; Chen et al. 2013).

1.4.7.3 SMAD9

Mutations in the TGF- β signal transducer, SMAD9 have also been identified in PAH patients. The *SMAD9* gene encodes the protein SMAD8 which forms a complex with SMAD4 after being phosphorylated, along with SMAD1 and SMAD5, by the activated type 1 BMP receptor (Majka et al. 2011). Shintani et al (2009) identified a mutation in *SMAD9* in an IPAH patient that did not have mutations in *BMPR2* or *ACVRL1*. This mutation was also identified in the father of this patient (Shintani et al. 2009). Variants in SMAD1, SMAD4 and SMAD9 have also been identified in a cohort of 324 PAH cases (Nasim et al. 2011).

1.4.7.4 Caveolin-1

In addition to the mutations in the TGF- β superfamily, mutations in the *CAVI* gene have also been identified in a family of PAH patients (Austin et al. 2012). *CAVI* encodes the protein caveolin-1, an important component of plasma membrane invaginations called caveolae. Caveolae are abundant in cell surface receptors, which are critical for cellular signalling cascades, including the TGF- β signalling cascade (Soubrier et al. 2013). Austin et al (2012) used whole genome sequencing to identify a mutation in a family with multiple sufferers of PAH but who lacked mutations in other PAH-associated genes, such as *BMPR2*. The *CAVI* mutation was identified in both the family members who had PAH, and those who did not have PAH. Hence, the *CAVI* mutation also has variable penetrance like the other PAH-associated genes (Austin et al. 2012).

1.4.7.5 KCNK3

KCNK3 (TASK-1) is a mammalian potassium channel whose subunits consist of four transmembrane domains and two pore domains (Reyes et al. 1998). Mutations in *KCNK3* were recently identified by whole exome sequencing in members of the same family who were diagnosed with PAH (Ma et al. 2013). Whole-cell patch-clamp studies also revealed that the mutations were all loss-of-function mutations (Ma et al. 2013). Potassium channels open to allow potassium to enter the cell, causing membrane hyperpolarisation. This hyperpolarisation then causes voltage-gated calcium channels to close, reducing the intracellular calcium and hence cause vasodilation (Olschewski et al. 2006). Conversely, the inhibition of potassium channels leads to membrane depolarisation, calcium entry, cell contraction and vasodilation (Olschewski et al. 2006). Knocking down *KCNK3* caused PA-SMC depolarisation and hypoxia has also been reported to inhibit *KCNK3* function (Olschewski et al. 2006). It is therefore speculated that these loss-of-function mutations contribute to membrane depolarisation and cause subsequent smooth muscle cell contraction and pulmonary vasoconstriction.

1.4.7.6 Serotonin Transporter

The serotonin transporter allows the reuptake of serotonin into cells. *SERT* is encoded by a single gene located on chromosome 17q11.2 (MacLean 2007). The L-allelic variant of the *SERT* gene promoter present in 65% of IPAH patients potentiates *SERT* activity (MacLean 2007; McLaughlin & McGoan 2006). Activation of *SERT* is hypothesized to contribute to PAH pathogenesis by increasing serotonin reuptake in PA-SMCs, thus inducing PA-SMC proliferation through the induction of cyclin and c-Fos, production of calcium binding proteins, MAPK and ERK1/2 phosphorylation (Rabinovitch, 2008). Overexpression of *SERT* in mice has been reported to worsen hypoxia induced PAH (Rabinovitch, 2008). Mutations in *BMPR2* are suspected to increase *SERT* activity, exasperating the effects of both mutated *BMPR2* and *SERT* on PASMC proliferation. However, the involvement of *SERT* in pathogenesis remains ambiguous, with other research groups suggesting this variant is not a sufficient risk factor for disease development (Maclean 2007).

1.5 TRAIL in Pulmonary Arterial Hypertension

TRAIL (tumour necrosis factor-related apoptosis-inducing ligand) belongs to the tumour necrosis factor (TNF) receptor family and induces apoptosis of tumour cell lines, both *in vivo* and *in vitro*, through activation of death receptors at the cell surface (Spierings et al., 2004). TRAIL acts on 4 receptors: TRAIL R1 (Death receptor (DR) 4), TRAIL R2 (DR5), TRAIL R3 (decoy receptor (DCR) 1) and TRAIL R4 (DCR2), and also binds a fifth decoy receptor, osteoprotegerin (OPG) (Spierings et al., 2004; Vitovski et al., 2007). TRAIL R1 and TRAIL R2 each contain a death receptor in their cytoplasmic domain, thus induce tumour cell apoptosis, a process not observed in normal cells (Spierings et al., 2004; Vitovski et al., 2007). TRAIL R3 and R4 are termed “decoy receptors”. R3 lacks a complete death domain and R4 possesses only a partial death receptor in the cytoplasmic domain, hence both fail to induce apoptosis (Spierings 2004; Vitovski et al. 2007). However, TRAIL has also been found to induce the proliferation and migration of both rat and human vascular SMCs (VSMCs) through TRAIL R1 and R3 interaction and subsequent ERK1/2 phosphorylation rather than inducing cell apoptosis as expected (Secchiero et al., 2004) and plays an important role in PAH (Hameed et al. 2012; Dawson et al. 2014).

TRAIL RNA expression is elevated in IPAH PA-SMCs and TRAIL has been shown to induce the proliferation and migration of PA-SMCs *in vitro*, an effect mediated through the TRAIL R1 and TRAIL R3 receptors, which are also elevated in IPAH PA-SMCs, and ERK1/2 phosphorylation (Hameed et al. 2012). TRAIL expression was found to correlate with disease development in the MCT rat model of PAH, with an increase in TRAIL expression in the pulmonary arterioles, epithelial and endothelial cells observed in animals with disease (Hameed et al. 2012). Interestingly, TRAIL expression in the pulmonary vascular tissue is responsible for driving disease pathogenesis (Hameed et al. 2012).

Blockade of TRAIL by either antibody blockade or genetic deletion prevents and reverses disease in animal models of PAH. Administration of an anti-TRAIL antibody from the start of disease induction prevented MCT injected developing disease and

even reversed established disease in the Paigen diet-fed ApoE^{-/-} mouse model (Hameed et al. 2012). Disease reversal in the Paigen diet-fed ApoE^{-/-} mouse was accompanied by an increase in apoptosis and a reduction in proliferating cells, medial thickness and vessel muscularisation (Hameed et al. 2012). Genetic deletion of TRAIL was also found to prevent disease development in the chronic hypoxia and sugen-hypoxia model and the paigen-diet fed ApoE^{-/-} mouse model of PAH (Hameed et al. 2012; Dawson et al. 2014). This therefore makes TRAIL an attractive target for future PAH therapies.

1.6 Current Treatments for PAH

There is currently no curative treatment for PAH apart from lung transplantation (McLaughlin and McGoon, 2006). However, transplants are very limited and so this is not a feasible option for many patients. In the most recent National Audit of Pulmonary Hypertension, less than 1% of all PAH patients underwent transplantation. Left untreated, the median life expectancy for IPAH patients was 2.8 years, however in some patients, we now see a median life expectancy of up to and over 5 years (D'Alonzo et al. 1991; Hurdman et al. 2012).

Treatments for PAH include anti-coagulants and calcium channel blockers, as well as diuretics and long-term oxygen therapy, all treatments that are used for heart failure. Specific therapies approved for PAH target the underlying vasoconstriction and can offer successful relief from symptoms. Specific PAH treatments target the three main vasoactive pathways that are important in the pathogenesis of PAH and induce vasodilation. Endothelin receptor antagonists, such as Bosentan and Macitentan, dual endothelin (ET) receptor antagonists that block both the ET_A and ET_B receptors, and Ambrisentan, a selective ET_A receptor antagonist, all block the effects of endothelin and induce vasodilation (Galiè et al. 2013). Prostanoids, such as Baraprost, Epoprostanol, Iloprost and Trepostinil are active analogues of the vasodilator, prostacyclin, and hence induce vasodilation. Selexipeg is a selective prostacyclin IP-receptor agonist and induces vasodilation through binding the prostacyclin IP receptor (Galiè et al. 2013). Riociguat stimulates nitric oxide-soluble guanylate cyclase and enhances cGMP production to promote vasodilation. Sildenafil, Tadalafil and vardenafil are all phosphodiesterase-5 (PDE-5) inhibitors that prevent cGMP

degradation via PDE-5 and hence induce vasodilation of pulmonary arterioles (Galie et al. 2013).

It is clear from the literature that research is now aimed at increasing our understanding of the pathogenesis of PAH in order to identify novel therapeutic targets. As mentioned briefly in Chapter 1.4.4, and of direct relevance to this thesis, osteoprotegerin has recently been identified as an important mediator in PAH pathogenesis. Osteoprotegerin will now be discussed in detail.

1.7 Osteoprotegerin

OPG, meaning “to protect bone”, was first unknowingly described as the osteoclastogenesis inhibitory factor (OCIF), originally purified from human fibroblast conditioned media (Tsuda et al. 1997). OCIF was known to be a cytokine that inhibited bone reabsorption (Tsuda et al., 1997). Within the same year, Simonet et al (1997) identified OPG as an important regulator of bone density after transgenic mice overexpressing OPG developed osteopetrosis, an increase in bone density, and a decrease in the bone resorbing cells, osteoclasts. Analysis of a foetal rat intestinal library revealed a 401 amino acid-long, secreted cytokine with an N-terminus analogous to TNF receptor superfamily members (Simonet et al. 1997). We now know OPG to be a heparin-binding secreted glycoprotein belonging to the TNF receptor superfamily that exists as a 55-62 kDa monomer or a 110-120 kDa disulphide-linked homodimer (Simonet et al. 1997; Zauli et al. 2009).

OPG is a 401 amino acid-long protein that contains a 21 amino-acid long signal peptide that is cleaved to generate the mature, 380 amino-acid long form (Zauli et al. 2009). OPG consists of seven structural domains. Domains 1-4 are cysteine rich domains that share structural similarities with the TNF receptor extracellular domains (Yamaguchi et al. 1998). Domains 1-4 were found to be sufficient to abolish osteoclastogenesis, a process that OPG is involved in and this will be discussed below. Domains 5 and 6 contain death domains, which share similarities with the Fas and TRAIL death receptors and domain 7 consists of 50 amino acids and the cys-400 residue that is essential for disulphide bond formation and the dimerisation of OPG (Yamaguchi et al. 1998). Domain 7 may also play an important role in regulating the

release and activity of OPG (Zauli et al. 2009). The structure of full length OPG is shown in Figure 1.2. To enhance the activity of OPG, an OPG-Fc protein has also been synthesised, in which the cysteine-rich domains are fused to the Fc domain of human IgG1 and the signal peptide, death domains and heparin binding domains have been removed (Zauli et al. 2009). The structure of the OPG-Fc protein is also shown in Figure 1.2.

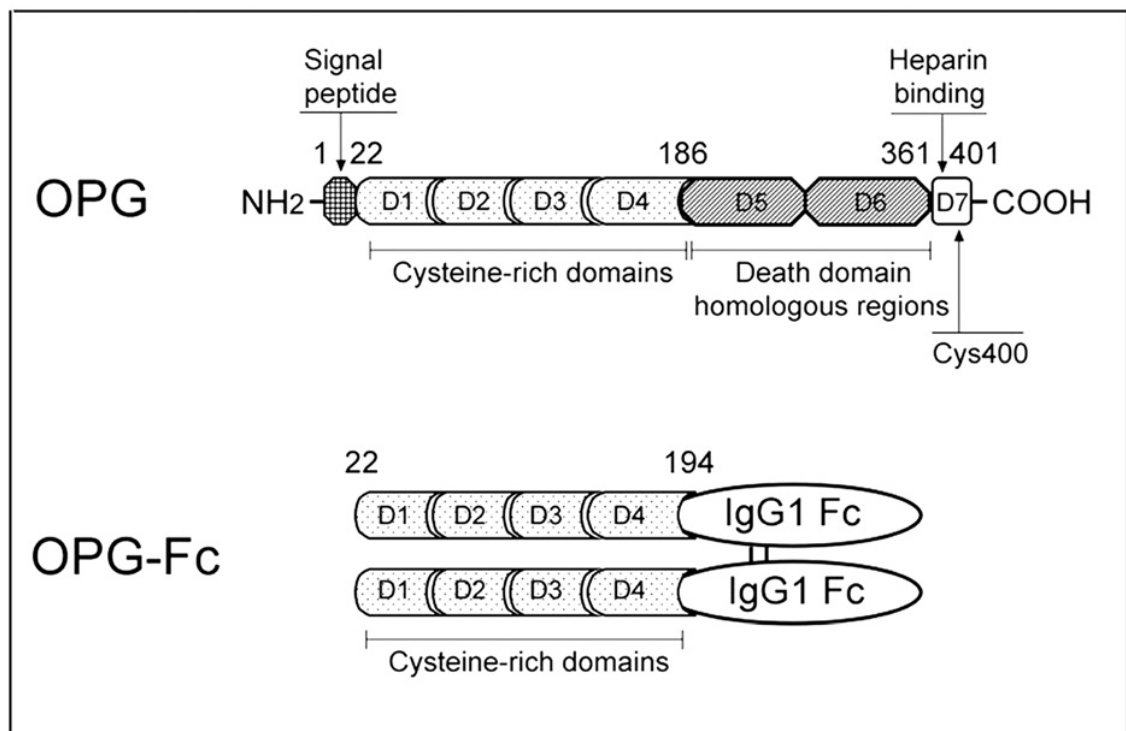


Figure 1.2- The structure of full length OPG and the synthesised OPG-Fc protein.

OPG consists of four cysteine-rich domains (domains 1-4), two death domain homologous regions (domains 5 and 6) and a heparin-binding domain (domain 7), containing at cysteine residue at amino acid position 400, which is required for dimerization. The synthesised OPG-Fc protein however consists only of the four cyctein-rich domains and is fused to the Fc domain of human IgG1².

² Springer and Cellular and Molecular Life Sciences, 66, 2009, 841-851, Role of full-length osteoprotegerin in tumor cell biology, Zauli. G, Melloni. E, Capitani. S and Secchiero. P, Figure 1, original copyright notice is given to Cellular and Molecular Life Sciences, with kind permission from Springer Science and Business Media.

OPG is expressed in a variety of tissues, including the human heart, kidney, placenta and lung (Simonet et al. 1997). A variety of cells express and secrete OPG, including bone marrow stromal cells and cells belonging to the osteoblastic cell lineage, B cells, megakaryocytes, platelets, vascular endothelial cells and smooth muscle cells, including PA-SMCs (Zauli et al. 2009; Li et al. 2007; Collin-Osdoby et al. 2001; Condliffe et al. 2012; Olesen et al. 2005). OPG was first identified, and is probably best known, for its role in bone biology as a soluble decoy receptor for RANKL (receptor activator of nuclear factor-kappa B ligand). OPG has also been shown to be a decoy receptor for TRAIL and since its discovery in 1997, OPG has been implicated in a variety of processes and diseases, including vascular calcification, angiogenesis, atherosclerosis and hypertension.

1.7.1 The OPG/RANKL/RANK Axis in Bone Biology

As discussed briefly above, OPG was first identified as an inhibitor of osteoclastogenesis and an important regulator of bone reabsorption. Yasuda et al (1998) identified RANKL as a ligand for OPG and reported that RANKL also played an important role in bone biology, with RANKL-induced osteoclast-like cell formation being inhibited by OPG (Yasuda et al. 1998). We now know that the interactions between OPG, RANKL and RANK (receptor activator of nuclear factor-kappa B), the receptor of RANKL, to be very important in the regulation of bone density.

The OPG/RANKL/RANK axis is important in bone remodelling with OPG playing a central role in regulating osteoclast production and function (Vitovski et al., 2007). Bone is continuously renewed through the removal of bone at trabeculae by osteoclasts; multinucleated bone reabsorbing cells, and is then laid down by bone forming cells, termed osteoblasts (Boyce & Xing 2007; Hofbauer & Schoppet 2004). Osteoclasts form from the cytoplasmic fusion of myeloid haematopoietic precursors (Boyce and Xing, 2007). Osteoclastogenesis requires binding of RANKL, a type 2 homotrimeric transmembrane protein expressed on mature osteoblasts, to its receptor, RANK, a type 1 homotrimeric transmembrane protein expressed on osteoclast precursor cells (Boyce & Xing 2007; Hofbauer & Schoppet 2004; Vitovski et al. 2007). Upon formation, this receptor ligand complex induces osteoclast formation,

activation and survival to prevent precursor differentiation into macrophages (Boyce and Xing, 2007; Hofbauer and Schoppet, 2004; Vitovski et al., 2007) by activating NF- κ B through recruitment of adaptor protein, TRAF6 (Boyce and Xing, 2007). NF- κ B then translocates to the nucleus to induce c-Fos expression, which subsequently results in osteoclastogenic gene transcription. OPG, secreted from osteoblasts, acts as a decoy receptor for RANKL, preventing the RANKL/RANK interaction, osteoclast activation and subsequent bone reabsorption (Hofbauer and Schoppet, 2004, Vitovski et al., 2007).

Post-natal OPG is critical for the maintenance of bone density and disrupted OPG expression *in vivo* results in the development of bone disorders (Bucay et al. 1998). OPG knockout mice exhibit osteoporosis, a reduction in bone density due to excessive bone reabsorption (Bucay et al., 1998). Conversely, elevated OPG levels or inactive RANKL result in osteopetrosis, elevated bone density due to reduced bone reabsorption (Simonet et al. 1997; Vitovski et al. 2007). In order to protect against excessive bone reabsorption, OPG mRNA is upregulated during bone formation (Tanaka et al. 2011). Mutations in OPG have also been associated with idiopathic hyperphosphatasia, an autosomal recessive bone disease that results in long bone deformation (Whyte et al. 2002). Although OPG was first identified and studied for its role in bone biology as a decoy receptor for RANKL, OPG interaction with TRAIL and the ability of OPG to block TRAIL-induced apoptosis of cancer cell lines has been known and studied for over a decade.

1.7.2 OPG in Tumour Cell Biology

Emery et al (1998) discovered that OPG acts as a decoy receptor for TRAIL. Immunoprecipitation revealed OPG to be a binding partner for membrane-bound or secreted TRAIL (Emery et al., 1998). OPG and TRAIL interaction was confirmed *in vitro* after OPG was reported to inhibit TRAIL-induced apoptosis of Jurkat cells and TRAIL repressed OPG inhibition of osteoclastogenesis (Emery et al., 1998). A role for OPG in tumour cell biology was identified by the ability of OPG to inhibit TRAIL-induced apoptosis of cancer cells (Cross et al., 2006). OPG has been reported to prevent TRAIL-induced apoptosis of ovarian cancer cell lines, in an $\alpha_v\beta_3$ integrin and $\alpha_v\beta_5$ integrin-dependant manner (Lane et al. 2012; Lane et al. 2013). OPG has

also been reported to prevent TRAIL-induced apoptosis of human microvascular endothelial cells (HMVECs), a process also requiring $\alpha_v\beta_3$ (Pritzker et al. 2004). Taken together, these findings support a role for OPG in the survival of cancer cells, a process that appears to be mediated through the $\alpha_v\beta_3$ and $\alpha_v\beta_5$ integrin.

Along with cancer cell survival, OPG has also been implicated in angiogenesis, the formation of new blood vessels, which is required for the development and progression of tumours (Cross et al. 2006). OPG expression was identified in the endothelium of malignant colorectal, breast and metastatic cancer tumours, but not in the endothelium of benign tumours or normal tissue. OPG induces human dermal microvascular cells (HuDMECs) to form cord-like capillary structures (Cross et al. 2006). Furthermore, OPG was also found to induce vessel-formation *in vivo* via heparin binding, which suggests a role for the heparin-binding domain in OPG signalling (McGonigle et al. 2008). More recently, work undertaken by Benslimane-Ahmim and colleagues has shown that OPG induces the migration and differentiation of endothelial colony-forming cells into cord-like structures, promotes fibroblast growth factor-2 (FGF2)-induced neoangiogenesis *in vivo* and increases endothelial colony-forming cell adhesion to fibronectin *in vitro* (Benslimane-Ahmim et al. 2011).

1.7.3 OPG and Calcification

The development of calcified arteries alongside osteoporosis in OPG^{-/-} mice first revealed a role for OPG in vascular biology and accumulating evidence supports a protective role for OPG against calcification (Bucay et al., 1998). Administration of recombinant OPG or restoring OPG expression reverses experimental calcification and VSMC calcification is reduced with OPG treatment *in vitro* (Schoppet et al., 2011). High concentrations of calcium, previously shown to induce VSMC calcification, were found to induce OPG mRNA expression in healthy VSMCs (Schoppet et al., 2011). Active NF- κ B induced OPG mRNA expression through $\alpha_v\beta_3$ integrin in ECs, with OPG protecting against apoptosis of cells hosting inactive NF- κ B (Malyankar et al. 2000). However, the transcriptional regulators controlling OPG expression remain unknown (Zhang et al. 2002).

Extracellular calcific stimuli induce the release of nanoparticles containing OPG protein from viable and apoptotic VSMCs (Schoppet et al., 2011). A study conducted recently reported that OPG reduced VSMC calcification in rat VSMCs. These data suggest an inhibitory role of OPG against calcification (Zhou et al. 2013). However, concentrations of OPG equivalent to those in coronary artery disease (CAD) and chronic kidney disease (CKD) patient serum appear to have no experimental effect against calcification (Schoppet et al., 2011). Olesen et al (2012) reported that OPG had no effect on VSMC calcification, however this may be due to the variation between the different donors used for this study (Olesen et al. 2012). Evidently, the role of OPG against calcification in disease still remains elusive.

1.7.4 OPG and Vascular Cell Proliferation

Interestingly, there is now accumulating evidence showing the ability of OPG to induce the proliferation of vascular endothelial cells. OPG increases HuDMEC and HUVEC proliferation and both cell types were found to secrete OPG (Cross et al., 2006). Authors state that both HuDMECs and HUVECs were insensitive to TRAIL, suggesting that the OPG-induced EC proliferation may be through TRAIL-independent signalling mechanisms (Cross et al., 2006). However, there have been reports in the literature that show TRAIL can alter HUVEC and HuDMEC phenotype (Pritzker et al. 2004; Secchiero et al. 2004). Evidently, due to the contradictions in the literature, it cannot be concluded whether OPG-induced EC proliferation is due to a TRAIL-independent signalling mechanism. OPG was also reported to induce human microvascular endothelial cell proliferation and migration through $\alpha_v\beta_3$ and $\alpha_v\beta_5$ integrins (Kobayashi-Sakamoto et al. 2008) and induce the survival of serum-deprived aortic SMCs (Bennett et al. 2006).

1.7.5 OPG in Cardiovascular Disease

OPG has been implicated as a potential mediator in cardiovascular disease and a patient study conducted by Stepien et al (2011) revealed elevated OPG in hypertensive patients compared to control patients. Elevated OPG levels have also been observed within pericardium of malignant and non-malignant pericardial effusion compared to pericardial fluid from coronary artery disease patients

(Karatolios et al. 2012). Ziegler et al (2005) reported a positive correlation between the severity of peripheral artery disease (PAD) and plasma values of OPG; however, this study does not determine whether OPG is causative of disease.

OPG and RANKL expression have been observed within the failing myocardium and OPG, RANKL and RANK are all upregulated in experimental and clinical heart failure. Elevated levels of OPG, RANKL and RANK mRNA within ischemic areas of the left ventricle and increased systemic OPG expression in patients with severe aortic stenosis also support the involvement of OPG, alongside RANKL and RANK, in heart failure (Ueland et al. 2012). Furthermore, OPG plasma levels are also a predictor of asymptomatic coronary artery disease in type-2 diabetic patients and OPG plasma levels are also significantly higher in patients with systemic hypertension, decreased kidney function and type-1 diabetic patients with nephropathy and signs of cardiovascular disease (Avignon et al. 2005; Rasmussen et al. 2006).

OPG has also been implicated as playing an important atheroprotective role. OPG is considered to be a negative regulator of atherosclerotic lesion development after studies revealed that the absence of OPG causes an increase in lesion area and calcification in the innominate artery of older (40 week and 60 week old) OPG^{-/-} ApoE^{-/-} mice (Bennett et al. 2006). Furthermore, bone marrow transplantation data published recently by the same group has implicated both vessel wall-derived and bone marrow-derived OPG as being sufficient to reduce lesion size and calcification in the innominate artery of mice (Callegari et al. 2013).

However, there are conflicting reports regarding the role of OPG in atherosclerosis. High-fat diet fed LDLR^{-/-} mice show a reduction in calcification after treatment with the recombinant OPG-Fc protein; however, this has no effect on atherosclerotic lesion size (Morony et al. 2008). This may be due to a calcification-induced inflammatory response already activated in the vessels, one that OPG can no longer modulate. OPG has been identified as a potential marker of atherosclerosis in patients with atherosclerosis, as plasma levels of OPG increase with increasing severity of atherosclerosis (Hosbond et al. 2012; Jinkwon Kim et al. 2013). LDLR^{-/-} mice have increased OPG levels upon disease onset, which did not increase with disease progression, suggesting that OPG may be a marker disease onset (Morony et al.

2008), however, this may not be the case in atherosclerosis patients. It is clear from the literature that the role of OPG in atherosclerosis still requires investigation.

1.7.6 Osteoprotegerin in Pulmonary Arterial Hypertension

Data published by Lawrie et al (2008) implicates OPG as a potential mediator in the pathogenesis of PAH. OPG is regulated by BMP signalling, serotonin and interleukins, predominantly IL-1, which have all been implicated in the pathogenesis of PAH (Lawrie et al., 2008). Lawrie et al (2008) hypothesised that the signalling pathways employed by BMPs, serotonin and the inflammatory cytokine IL-1 all converge to dysregulate OPG expression, thus causing the proliferation and migration of PA-SMCs. Immunohistochemical analysis of human lungs revealed an increase in OPG release from SMCs in patients with IPAH compared to healthy controls. Furthermore, immunohistochemical staining for OPG binding partners, TRAIL and RANKL, was elevated in ECs and SMCs present within IPAH patient lungs. Increased serum levels of OPG in IPAH patients further suggest a role for OPG in PAH (Lawrie et al., 2008).

Investigations into the effect of OPG on PA-SMC phenotype and dysfunctional signalling on OPG release generated also revealed that recombinant OPG increased proliferation and migration of PA-SMCs in a dose dependent manner. Human PA-SMCs transfected with siRNA (to mimic the heterozygous loss of function *BMPR2* mutation) demonstrated increased OPG release, as did PA-SMCs treated with 5HT and IL-1. For the first time, these data demonstrate that OPG is upregulated in patients of PAH and furthermore, OPG can influence the proliferation and migration of human PA-SMCs (Lawrie et al., 2008).

A recent patient study conducted by Condliffe et al (2012) revealed elevated OPG mRNA expression in human PA-SMCs isolated from IPAH patients. Serum levels of OPG were increased in IPAH patients and a significant correlation between OPG serum and pulmonary arteriole remodelling in rodent models was identified. These findings also support the role of OPG as an important biomarker in disease (Condliffe et al., 2012).

In addition to patient data and the effects of OPG in vitro, unpublished data from the Pulmonary Vascular Research Group at the University of Sheffield have shown that genetic deletion of OPG can prevent disease development in the Sugden-hypoxic (SuHx) mouse model of PH (Figure 1.3A) and blockade of OPG, though administration of an anti-OPG antibody, can reverse disease in the Paigen diet fed ApoE^{-/-} mouse model of PH (Figure 1.3B).

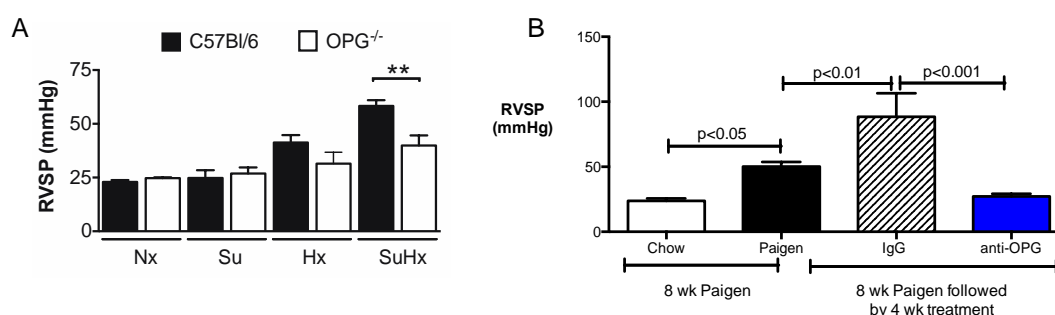


Figure 1.3- Genetic deletion of OPG prevents disease development in the SuHx mouse model and antibody blockade of OPG reverses disease in the Paigen fed ApoE^{-/-} mouse model of PH .

A) Disease was induced in C57Bl/6 and OPG^{-/-} using the Sugden5416/hypoxia method by administering weekly injections of Sugden5416 during 3 weeks exposure to normoxia or hypoxia, alongside normoxic control mice. Mice exposed to SuHx developed disease as shown by a significant increase in RVSP, compared to Sugden alone or hypoxia alone. However, OPG^{-/-} mice exposed to Sugden-hypoxia are protected against disease development. B) Male ApoE^{-/-} mice fed on a high fat Paigen diet (8 weeks) develop elevated RVSP compared to those animals fed on normal chow diet (8 weeks). However, 4-week administration of an anti-OPG antibody after 8 weeks Paigen diet reverses disease in ApoE^{-/-} mice, shown by a reduction in RVSP. Error bars represent mean \pm SEM, n=3-6. **p<0.01. Data generated by the Pulmonary Vascular Research Group, Department of Cardiovascular Science, University of Sheffield. Dawson et al manuscript in preparation.

These data show that blockade of OPG, through genetic deletion or antibody blockade prevents and reverses disease development animal models of PAH. These data provide evidence that OPG is an important pathogenic mediator in disease, and contributes directly to disease progression in PAH animal models. However, the mechanisms by which OPG exerts its effects in order to influence PA-SMC phenotype are still unknown.

1.8 Hypothesis and Aims

I hypothesised that OPG was binding to a previously undescribed cell surface receptor to active a previously undescribed signalling pathway in PA-SMCs. I also hypothesised that blocking the interaction between OPG and the identified receptor would prevent OPG-induced PA-SMC proliferation.

I therefore aimed to identify the receptor to which OPG was binding on PA-SMCs and the intracellular signalling mechanism through which OPG was inducing PA-SMC proliferation.

In order to identify a mechanism through which OPG signals in PA-SMCs, there were four aims to be addressed in this thesis:

- 1) To determine which receptor(s) OPG is binding on PA-SMCs in order to initiate a signalling cascade.
- 2) To determine which intermediate proteins OPG is signalling through in order to induce downstream mRNA transcription and PA-SMC proliferation.
- 3) To identify which genes are transcribed as a result of OPG signalling in PA-SMCs.
- 4) To determine whether blocking the interaction between OPG and the identified receptor(s) can modulate PA-SMC phenotype.

These aims are represented in the schematic below (Figure 1.4) and I will be aiming to answer each of these questions in the three results chapters that follow.

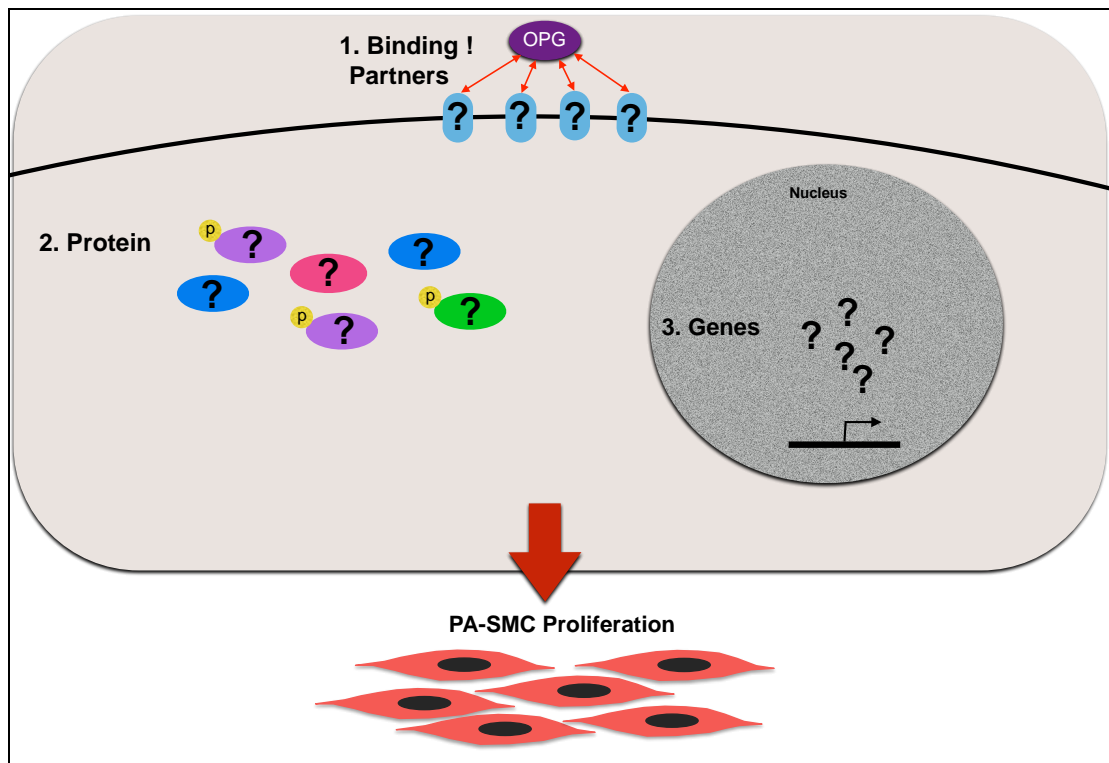


Figure 1.4- Aims to be addressed in this thesis.

In order to identify the mechanism through which OPG induces PA-SMC proliferation, 1) the receptor to which OPG is binding on PA-SMCs must be identified, 2) the changes in protein expression and activation and 3) the changes gene expression that OPG induces in PA-SMCs must be investigated. Finally, the effect on blocking the interaction between OPG and its binding partner on PA-SMC proliferation must also be assessed to determine the importance of the interaction in modulating PA-SMC phenotype.

2. GENERAL METHODS

2.1 Cell Culture

All cell culture was performed in a Class II laminar flow hood in a sterile environment, using aseptic techniques. Cells were cultured in sterile, disposable T75 cm² cell culture flasks, until ready for experimentation, in incubators at 37°C in 95% room air with 5% carbon dioxide (CO₂). All experiments were then carried out using disposable, sterile consumables, sterile reagents and media.

2.1.1 Human Pulmonary Arterial Smooth Muscle Cells (HPA-SMC)

2.1.1.1 HPA-SMC Culture and Passage

HPA-SMCs were purchased from Lonza (Basel, Switzerland) and grown in T75 cm² cell culture flasks, prior to experimentation, in sterile SmBM (Smooth Muscle Basal Medium), containing the SmGm-2 SingleQuots: 5% v/v foetal bovine serum (FBS) (CC-4102D, SmGM-2 SingleQuots, Lonza, Basel, Switzerland), 0.1% v/v insulin, 0.2% v/v hFGF-β, gentamicin (30 µg/ml) and amphotericin (15 ng/ml) (full growth media) (Lonza, Basel, Switzerland) at 37°C (5% CO₂).

Once HPA-SMCs reached ~80% confluence, the cells were then passaged and transferred into T75 cm² cell culture flasks to continue growth, or T25 cm² cell culture flasks or 96 well plates for experimentation. SmBM growth media was removed from the T75 cm² cell culture flasks and cells were washed three times in 1xPBS. All traces of PBS were removed and 5 ml 1x Trypsin/EDTA was added to each T75 cm² cell culture flask. Flasks were then incubated at 37°C for 5 minutes. Flasks were then removed from the incubator and cells displaced from the bottom of the flask by gentle tapping. To ensure cells were fully trypsinized, cells were observed using a microscope. Once fully trypsinized, 5 ml trypsin neutralisation solution was added to flask. Cells were then transferred to a 15 ml tube and cells were pelleted by centrifuging for 5 minutes at 1,200 xg. The cell pellet was then resuspended in 9 ml SmBm full growth media and the cells were split 1:3 (one T75 cm² cell culture flask

split into three T75 cm² cell culture flasks or nine T25 cm² cell culture flasks) or plated into flat bottom 96 well plates at a specific seeding density.

2.1.1.2 HPA-SMC Haemocytometer Counts

HPA-SMCs were removed from the T75 cm² cell culture flasks by trypsinisation as detailed in Chapter 2, Section 2.1.1.1. 1 ml trypsinized cells were then transferred into 10 ml SmBm-2 full growth media and mixed gently. 10 µl cell suspension was then pipetted onto each side of a haemocytometer. Cells were then counted under the microscope at a 10x magnification, by counting cells in the centre square and only counting cells overlapping the boundary of the centre square on the left and top boundaries. Cells in the centre square of each side of the haemocytometer were counted and an average of both sides were taken. An estimate of cell number was the calculated as follows:

$$\text{Cell number (cells/ml)} = ((\text{Cell N}^{\circ} \text{ centre square side 1} + \text{Cell N}^{\circ} \text{ centre square side 2}) / 2) \times 10^4$$

2.1.1.3 HPA-SMC Synchronization

Prior to stimulation of cells for all following experiments detailed in this Chapter, HPA-SMCs were synchronized for 48 hours with growth arrest media (DMEM, 0.2% v/v FBS, 0.5% v/v penicillin and streptomycin), unless stated otherwise. Synchronization of HPA-SMC cell cycles was performed to ensure all HPA-SMC cell cycles were halted between the G1 and S-Phase of the cell cycle prior to stimulation. This was to ensure that any changes in proliferation, protein or RNA expression were due to the stimulation of the cells and not due to the completion of cell cycles in a sub-population of cells. Cells were synchronized by removing all traces of SmBm-2 full growth media and washing the cells twice in 10 ml 1 x PBS. 10 ml growth arrest media was then pipetted into T75 cm² cell culture flasks, 4 ml into T25 cm² cell culture flasks or 100 µl per well of 96 well plates.

2.2 Pierce™ 660 nm Protein Assay

Protein concentration of cell lysates was measured using the Pierce 660 nm protein assay. The Pierce 660 nm protein assay is a dye-based assay that uses an acidic buffer reagent containing a proprietary dye-metal complex. Upon dye-metal complex binding to the protein in the acid environment of the buffer, the dyes maximum absorption is shifted. The reddish-brown colour of the buffer changes to green when protein binds to the dye-metal complex. The maximum absorption of the dye is then measured at 660 nm, with the colour change produced being proportional to the amount of protein. The colour change is due to the binding of positively charged basic proteins to the de-protonated dye at low pH. The Pierce 660 nm protein assay was used to measure protein concentration because, unlike other protein assays, it is compatible with most detergents that are used in the preparation of protein lysates.

2.2.1 Preparation of Bovine Serum Albumin (BSA) Standards

Bovine serum albumin (BSA) standards were prepared at 2000 µg/ml, 1500 µg/ml, 1000 µg/ml, 750 µg/ml, 500 µg/ml, 250 µg/ml, 125 µg/ml, 25 µg/ml and 0 µg/ml by diluting one 2000 µg/ml bovine serum albumin standard ampule (stock) (Pierce) as follows:

Vial	BSA Standard Concentration (µg/ml)	Volume and Source of BSA (µl)	Volume of distilled water
A	2000	300 of stock	0
B	1500	375 of stock	125
C	1000	325 of stock	325
D	750	175 of vial B dilution	175
E	500	325 of vial C dilution	325
F	250	325 of vial E dilution	325
G	125	325 of vial F dilution	325
H	25	100 of vial G dilution	400
I	0	0	400

2.2.2 Microplate Procedure for Protein Assay

Lysates were defrosted on ice and 1 g Ionic Detergent Compatibility Reagent added to 20 ml Pierce 660 nm Protein Assay Reagent and mixed well. Following the microplate procedure, 10 μ l of each BSA standard or lysate was then added in duplicate to a separate well of a 96 well plate. 150 μ l Protein Assay Reagent was then added to each well containing the BSA standards and samples. The 96 well plate was then covered, mixed for 1 minute on a plate shaker and incubated at room temperature for 5 minutes. The plate was then scanned at 700 nm using the LiCOR Odyssey Sa system.

2.3 Western Blotting

2.3.1 General Protocol

Western blotting is an analytical technique used to detect proteins within a protein lysate using gel electrophoresis and antibodies against specific proteins. Western blotting uses gel electrophoresis to separate proteins within the lysate based on the length of polypeptides (denatured gel) or based on the structure of proteins (native gel). Following electrophoresis, proteins are then transferred onto a membrane to allow easier manipulation during staining with specific antibodies. For all western blot protein analysis discussed throughout this thesis, the following protocol was performed prior to staining the membranes with specific antibodies. Gel electrophoresis was performed on denatured proteins using the XCell SureLock™ Mini-Cell Electrophoresis system (Life Technologies, Paisley, UK) and NuPAGE Novex 4-12% Bis-Tris 1.0 mm 10 well precast mini-gels (NP0321BOX, Life Technologies, Paisley, UK). Protein samples were prepared as discussed later in this chapter for each specific experiment.

2.3.1.1 Sample Preparation

Prior to electrophoresis, 30 μ l protein lysate aliquots were defrosted on ice and protein loading buffer (928-4004, Licor, Bad Homburg, Germany) added to the eppendorf containing the lysate (1 μ l per 3 μ l lysate). NuPAGE reducing agent (NP0009, Life Technologies, Paisley, UK) was then added to the eppendorf (1 μ l per 10 μ l lysate and protein loading buffer). Eppendorfs containing the protein lysate, loading buffer and

reducing agent were then mixed by vortexing for 15 seconds and heated at 70°C for 10 minutes to ensure the proteins were denatured.

2.3.1.2 Electrophoresis System Set-up and Sample Loading

Prior to sample loading, the gels were inserted into the XCell SureLock™ Mini-Cell Electrophoresis system by removing the gels from the pouch and peeling off the tape at the bottom of the gel. The Upper Chamber was then filled with 200 ml NuPAGE MOPS SDS 1x running buffer (Life Technologies, Paisley, UK) to check the tightness of the seal and ensure the Upper Chamber was not leaking. Once the seal was tight, additional NuPAGE MOPS SDS 1x running buffer was added to the Upper Chamber to ensure the buffer level exceeded the tops of the wells and 500 µl NuPAGE antioxidant (NP0005, Life Technologies, Paisley, UK) was added to the running buffer in the Upper Chamber. 30 µl of the denatured protein lysates was then added to the appropriate wells, along with 5 µl Novex Sharp™ pre-stained protein standard (LC5800, Life Technologies, Paisley, UK). The Lower Buffer Chamber was filled with 400 ml running buffer.

2.3.1.3 Gel Electrophoresis

The gels were exposed to electrophoresis for 45 minutes at 200 V. When running only one gel, a second, blank gel with the tape still intact was used to form the Upper Chamber.

2.3.1.4 Protein Wet Transfer

Once electrophoresis was complete, the gels were removed from the XCell SureLock™ Mini-Cell Electrophoresis system. The gel plates were then separated using a Gel Knife and the gel foot and wells removed using the Gel Knife. The proteins were then transferred onto Whatman nitrocellulose membrane (10401196, GE Healthcare Life Sciences, Amersham, UK) using wet transfer. Prior to transfer, 1x NuPAGE transfer buffer (NP0001, Life Technologies, Paisley, UK) containing 10% v/v methanol (when transferring one gel) or 20% v/v methanol (when transferring two gels) (VWR Chemicals) and 1 ml antioxidant was prepared and sponges, filter paper and nitrocellulose membrane were pre-soaked before transferring the gels using the

XCell II™ Blot Module, as shown in Figure 2.1. Gels were transferred facing the cathode core and any air bubbles were rolled out before inserting the blot module into the Lower Buffer Chamber. The Upper Chamber was then filled with 1x NuPage transfer buffer until the gel/membrane assembly was covered and the Lower Chamber was filled with 300 ml transfer buffer. The gels were then transferred for 60 minutes at 30 V.

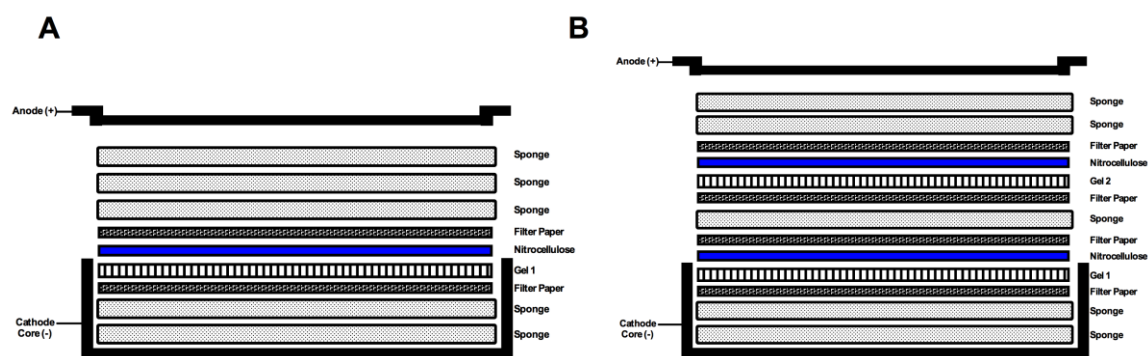


Figure 2.1- Wet transfer set-up.

After electrophoresis, proteins were transferred from the gel onto nitrocellulose membrane to allow easier manipulation during blocking and staining with specific antibodies. Proteins were transferred onto nitrocellulose membrane using wet transfer, where all components of the transfer system shown in **A** and **B** were pre-soaked in transfer buffer. When transferring one gel, the transfer set-up in **A** was used and when transferring two gels, the transfer set-up in **B** was used.

2.3.1.5 Membrane Blockade

Once the proteins were transferred, membranes were placed in blocking buffer (5% w/v low fat milk in 1x PBS or 30% v/v Odyssey blocking buffer (927-4000, Licor, Bad Homberg, Germany) in 1x PBS) for 1.5 hours at room temperature, with gentle rocking.

2.3.1.6 Primary Antibody Incubation

Membranes were incubated with desired primary antibodies, diluted as appropriate (as discussed throughout the chapter for each specific experiment) in 30% v/v Odyssey Sa blocking buffer or 5% w/v low fat milk, overnight at 4°C.

2.3.1.7 Secondary Antibody Incubation

After primary antibody incubation, membranes were washed for 3 x 10 minute washes in 0.1% v/v Tween-20 (in 1X PBS) before incubating with desired secondary antibodies. All IRDye 680LT and 800CW secondary antibodies were diluted 1:15000 in 30 % Odyssey blocking buffer containing 0.1% v/v SDS or 5% w/v low fat milk. Membranes were incubated with secondary antibodies for 1 hour at room temperature, protected from light, with gentle rocking. Membranes were then washed for 3 x 10 minute washes in 0.1% v/v Tween-20 in 1 x PBS.

2.3.1.8 Membrane Scanning

Following primary and secondary antibody incubation, membranes were scanned on the Licor Odyssey Sa system using the following parameters shown in Table 2.1.

Table 2.1 Licor Odyssey Sa System Scanning Parameters

	Channel	
	700 nm	800 nm
Resolution	200 µm	200 µm
Intensity	7.0	7.0
Focus Offset	3.0 mm	3.0 mm

Membranes were analysed using the Western Analysis tool. The amount of protein was proportional to the number of pixels detected (“total”). Amount of protein in each lane was then analysed by using the “Add Band” tool, subtracting lane background from each lane and expressing protein as a percentage of the control sample, normalised to the loading control. Protein expression was calculated as follows:

Protein expression = Pixels detected (total) Protein / Pixels detected (total) loading control

Protein expression (% control)= Protein expression / Control sample protein expression

2.3.1.9 Membrane Stripping

When required, antibodies were stripped from the membranes using 1X Re-blot Plus mild antibody stripping solution (2502, Millipore, Massachusetts, USA). Membranes were incubated in 20 ml 1X Re-blot Plus mild antibody stripping solution for 15 minutes at room temperature, with gentle rocking. Membranes were then washed two times 5 minutes in 30% v/v Odyssey blocking buffer. If required, membranes were re-probed with the appropriate secondary antibody using the methods described in Chapter 2, Section 2.3.1.7 and scanned using the methods described in Chapter 2, Section 2.3.1.8 to ensure all traces of primary antibody was removed. The membranes were then incubated with primary and secondary antibodies using the methods described in Chapter 2, Section 2.3.1.6 through to 2.3.1.7.

2.4 Retrogenix Cell Microarray

In order to identify OPG binding partners, a Retrogenix Cell microarray was carried out by Retrogenix (Sheffield, UK). In this Retrogenix cell microarray, binding between OPG and 2505 human plasma membrane proteins was determined by expressing each membrane protein in HEK293 cells. Retrogenix, Sheffield, UK, carried out all experimental methods outlined in Chapter 2.4.1 to Chapter 2.4.3 below.

2.4.1 Pre-Screen

Firstly, a pre-screen was conducted to determine optimal OPG and antibody concentrations to use in the primary screen. OPG was screened against HEK cells expressing syndecan-1 (positive control) and pIRES-hEGFR-IRES-ZsGreen1 or the membrane protein TREM1 (negative control) and pIRES-hEGFR-IRES-ZsGreen1 with varying concentrations of rhOPG (2 µg/ml and 0.5 µg/ml) and the anti-OPG antibody (2 µg/ml and 0.5 µg/ml). Secondary antibody, Alexafluor 647 rabbit anti-goat, was then added to the cells to determine levels of OPG binding to syndecan-1 and TREM1 membrane proteins and determine any background binding.

2.4.2 Primary Screen

Following the pre-screen, human embryonic kidney 293 (HEK293) cells were grown on top of duplicate expression vectors consisting of green fluorescent protein (GFP) and one full-length human plasma membrane protein. The expression vector pIRES-hEGFR-IRES-ZsGreen1 was spotted onto every slide to ensure minimum threshold of transfection was achieved. Cells were reverse transfected, fixed and the slides were treated with 0.5 µg/ml rhOPG (Peprotech, London, UK), 0.5 µg/ml anti-OPG (Peprotech, London, UK) followed by Alexafluor647 anti-goat antibody. Two replicate screens were performed and fluorescent images were analysed and quantified using ImageQuant software. A hit was then defined as a duplicate spot showing a raised signal compared to background levels. Hits were classified as weak, medium or strong depending on the spot intensity.

2.4.3 Confirmation Screen

Hits identified in one or both primary screens were then confirmed and analysed following the same methodology as for the primary screen. Vectors encoding hits were then sequenced to confirm protein identity. OPG plus anti-OPG plus secondary antibody, anti-OPG plus secondary antibody or OPG plus secondary antibody were used as controls in the conformation screen. (<http://www.retrogenix.com/default.asp>).

2.5 Co-Immunoprecipitation

Immunoprecipitation is a technique that uses an antibody against a specific protein to purify the protein antigen from a solution. Co-immunoprecipitation (Co-IP) uses this principle to isolate protein complexes from a solution, by using an antibody against a known protein within the complex to precipitate the protein complex and thus allow identification of unknown protein components within the complex. Co-IP was therefore used to pull down unknown OPG binding partners using an antibody against OPG and confirm OPG interaction with identified OPG binding partners.

2.5.1 Preparation of CHAPS Lysis Buffer

Prior to cell stimulation, a 1% v/v CHAPS cell lysis buffer was prepared in 30 mM TRIS-HCl (pH 7.5), 150 mM NaCl. Immediately before use, HALT™ protease inhibitor (10 µl/ml) (87786, Pierce Thermo Scientific) and EDTA (10 µl/ml) were added.

2.5.2 Preparation of HPA-SMC lysate

HPA-SMCs (P5) were grown T75 cell culture flasks in fully supplemented SmBm growth media until 80% confluent. Cells were then stimulated with rhOPG (500 ng/ml) in SmBm full growth media for 30 minutes at 37°C, without synchronization of cell cycles. After stimulation, cell culture flasks were placed on ice and washed twice with ice-cold PBS, ensuring all trace of PBS was removed. Cells were lysed in 1 ml CHAPS lysis buffer and incubated on ice for 15 minutes with occasional rocking. Following cell lysis, cells were scraped using a 25 mm cell scraper, transferred to a fresh 1.5 ml Eppendorf and disrupted by passing through a 21 gauge needle 5 times. The HPA-SMC lysate was clarified by centrifugation at 12,000 x g for 10 minutes at 4°C. The protein concentration of the HPA-SMC lysate was then measured by Pierce 660 nm protein assay and kept on ice until use after concentration quantification.

2.5.3 Preparation of Co-IP Reactions

Co-IP reactions were then prepared in 1.5 ml Eppendorfs by adding the reagents as described in Table 2.2 for the Fas IP and in Table 2.3 for the IL1RAcP IP.

Table 2.2 Fas IP reactions

Eppendorf	Antibody (Ab)	Lysate	rhOPG	rhFas	CHAPS buffer
1.1	Fas Ab (2 µg)	250 µl (50 µg) lysate	-	-	-
1.2	No Ab	250 µl (50 µg) lysate	-	-	-
1.3	Fas Ab (2 µg)	-	rhOPG 0.1 µg	rhFas 0.1 µg	250 µl CHAPS
1.4	No Ab	-	rhOPG 0.1 µg	rhFas 0.1 µg	250 µl CHAPS
1.5	Fas Ab (2 µg)	-	rhOPG 1 µg	rhFas 1 µg	250 µl CHAPS
1.6	No Ab	-	rhOPG 1 µg	rhFas 1 µg	250 µl CHAPS
1.7	Fas Ab (2 µg)	-	-	rhFas 1 µg	250 µl CHAPS
1.8	No Ab	-	-	rhFas 1 µg	250 µl CHAPS

Table 2.3 IL1RAcP IP Reactions

Eppendorf	Antibody	Lysate	rhOPG	rhIL1RAcP	CHAPS buffer
2.1	IL1RAcP Ab (2 µg)	250 µl (50 µg) lysate	-	-	-
2.2	No Ab	250 µl (50 µg) lysate	-	-	-
2.3	IL1RAcP Ab (2 µg)	-	rhOPG 0.1 µg	rhIL1RAcP 0.1 µg	250 µl CHAPS
2.4	No Ab	-	rhOPG 0.1 µg	rhIL1RAcP 0.1 µg	250 µl CHAPS
2.5	IL1RAcP Ab (2 µg)	-	rhOPG 1 µg	rhIL1RAcP 1 µg	250 µl CHAPS
2.6	No Ab	-	rhOPG 1 µg	rhIL1RAcP 1 µg	250 µl CHAPS
2.7	IL1RAcP Ab (2 µg)	-	-	rhIL1RAcP 1 µg	250 µl CHAPS
2.8	No Ab	-	-	rhIL1RAcP 1 µg	250 µl CHAPS

The 1.5 ml Eppendorfs containing the Co-IP reactions were then incubated at 4°C, overnight, with end-over-end mixing to allow immune complexes to form.

2.5.4 Precipitation of Immune Complexes

Following overnight incubation, 50 µl nProteinG sepharose 4 Fast Flow beads (50% slurry) were added to each Co-IP reaction and precipitated for 1 hour at 4°C with end-over-end mixing. Each Co-IP reaction was then centrifuged at 12,000 x g for 20 seconds and the pellet washed 3 times with 1 ml CHAPS lysis buffer and once with wash buffer (50 mM TRIS, pH 8.0).

2.5.5 Dissociation of Immune Complexes

The pellet was re-suspended in one times NuPAGE sample reducing agent and 5% v/v SDS. The pellet was then heated at 95°C for 5 minutes and centrifuged at 12,000 x g for 20 seconds. The supernatant was then transferred to a new Eppendorf and one times LiCOR lane marker added to each Eppendorf.

2.5.6 Analysis of Immune Complexes

The supernatants were then analysed by Western Blotting using the protocol described in Chapter 2, Section 2.3 to 2.3.1.9. Following membrane blockade in 30% v/v odyssey blocking buffer, membranes were incubated with goat polyclonal anti-OPG antibody (SC8468, Santa Cruz Biotechnology), for 3 hours at room temperature. OPG antibody was added at a 1:1000 dilution in 30% v/v odyssey blocking buffer. After incubation with the primary antibody, the membranes were washed 3 times 10 minutes in one times PBS plus 0.1% v/v tween-20. Membranes were then incubated with secondary antibody IRDye 680LT Donkey anti-goat (926-32214, LiCOR, Bad Homberg, Germany) at a 1:15,000 dilution in 30% v/v Odyssey blocking buffer for 1 hour at room temperature. The membranes were then washed 3 times 10 minutes in one times PBS plus 0.1% v/v Tween-20. The membranes were then scanned using the LiCOR Odyssey Sa system using the parameters detailed in Chapter 2, Section 2.3.1.8.

2.6 Immunohistochemistry

Histological slides of the pulmonary artery and right ventricle from donors with idiopathic PAH and control subjects undergoing lung resection for cancer or from donor lung were obtained from the Papworth Hospital NHS Trust tissue bank. All subjects gave informed written consent, and the study was approved by the Local Research Ethics Committee. Immunohistochemical analysis of the sections was then performed by Ms Nadine Arnold, Pulmonary Vascular Research Group, Department of Cardiovascular Science, University of Sheffield.

Briefly, tissue sections were de-waxed and rehydrated through graded alcohols to water. Endogenous peroxidases were blocked by incubation in 3% v/v hydrogen peroxide in water for 10 minutes. Slides were rinsed in tap water and antigen retrieval was performed by incubating the slides in citrate buffer (10 mMol/L, pH 6.0) for 20 minutes at 95°C. Slides were cooled for 20 minutes at room temperature before permeabilisation in 0.5% v/v Triton X-100 in PBS for 10 minutes and non-specific binding sites were blocked with 1% w/v low fat milk in 1 x PBS for 30 minutes at room temperature. Excess milk was then blotted away and primary antibodies, Fas monoclonal antibody (Mouse, Enzo Life Sciences, ADI-AMM-227-E) (1:100 dilution) or IL1RAcP polyclonal antibody (Rabbit, Abcam, Ab8110) (1:1000 dilution), were added and incubated overnight at 4°C. Primary antibodies were then washed off in 3 changes of PBS, incubating slides for 5 minutes between each wash. Slides were incubated with biotinylated anti-rabbit (1:200) biotinylated anti-mouse (1:200) secondary antibodies for 30 minutes at room temperature. All primary and secondary antibodies were diluted in 1 x PBS. Slides were washed in 3 changes of 1 x PBS, 5 minutes each. Slides were incubated with ABC complex for 30 minutes at room temperature and then washed in 3 changes of 1 x PBS, incubating slides for 5 minutes in each change of 1 x PBS. DAB substrate was then added for 10 minutes and slides were then rinsed in tap water. Slides were counterstained with Carazzi's haematoxylin for 1 minute, washed in tap water and dehydrated through graded alcohols to xylene. Slides were mounted using DPX mountant and left to dry overnight. Images were then captured using a Zeiss LSM 510 NLO inverted confocal microscope.

2.7 Kinex Antibody Microarray

In order to identify OPG-induced changes in protein phosphorylation and expression, Kinexus, Canada, performed a Kinex Antibody Microarray. Following cell synchronization and stimulation, Kinexus, Canada, performed all experimental methods outlined in Chapter 2, Section 2.7. HPA-SMCs were synchronized with 0.2% v/v FBS in growth arrest media for 48 hours and stimulated with 0.2% v/v FBS, rhOPG (50 ng/ml) and PDGF (20 ng/ml) for 10 and 60 minutes. Phosphorylation targets were identified from protein lysates by Kinex antibody microarray (Kinexus, Canada). Briefly, 50 µg lysate protein was covalently tagged with fluorescent dye and untagged protein removed by gel filtration. Non-specific binding sites were blocked and the samples were loaded side by side (control vs. stimulated) onto incubation chambers mounted on the microarray. The microarray consisted of 812 polyclonal and monoclonal antibodies (262 phospho-specific and 550 pan-specific), in duplicate. Samples were incubated and unbound protein washed away. Binding of proteins to their corresponding antibodies was detected in the form of 16-bit images captured by Perkin-Elmer ScanArray Reader laser array scanner (Waltham, MA). Signal quantification was performed by ImaGene 8.0 (Biodiscovery, El Segundo, CA) and Z-ratios calculated. A Z-ratio of ± 1.5 was deemed significant.

2.8 DAVID (The Database for Annotation, Visualization and Integrated Discovery) Analysis of Kinex Antibody Microarray Results

Uniprot accession codes of proteins deemed significantly regulated by OPG (z-ratio of ± 1.5) were then analysed using DAVID functional annotation to generate fold enrichment pathway analysis through the Kegg Pathway Database. An intersection of ≥ 2 fold change and $p \leq 0.05$ was used for the pathway fold enrichment analysis. Protein targets identified by the Kinex antibody microarray were then selected for validation based on involvement in different signalling pathways and time-dependent regulation by rhOPG.

2.9 Kinex Antibody Microarray Validation

2.9.1 In-Cell Western Assay

2.9.1.1 HPA-SMC Stimulation

HPA-SMCs (P4-P7) were grown as described in Chapter 2, Section 2.1.1.1 and transferred into 96 well plates (Corning Costar, Sigma, Dorset, UK) at a seeding density of 5×10^3 cells/well. Cells were synchronized as described in Chapter 2, Section 2.1.1.3 and then stimulated with rhOPG (50 ng/ml) for 10 and 60 minutes alongside quiesced cells (negative control).

2.9.1.2 HPA-SMC Fixing and Permeabilization

Cells were then fixed with fixing solution (PBS containing 3.7% v/v formaldehyde), by removing the cell culture media and adding 150 μ l fixing solution to each well by pipetting the fixing solution down the sides of the wells. Cells were fixed for 20 minutes at room temperature. Fixing solution was then removed removed by pipetting and 200 μ l 0.1% v/v Triton X-100 in 1 x PBS was added to each well, by pipetting the solution down the sides of the wells to prevent cell detachment. Three times 10-minute washes in Triton X-100 were performed at room temperature, with gentle shaking.

2.9.1.3 Cell Blockade

Cells were blocked in 150 μ l blocking solution (5% w/v low-fat milk in PBS) for 1.5 hours at room temperature, with gentle shaking.

2.9.1.4 Primary Antibody Incubation

Intracellular phospho-proteins were detected by incubating each column of wells of the 96 well plate with blocking solution containing one of the following antibodies: phospho-CDK2, phospho-CDK4, phospho-HSP27 (S15), phospho-p38, phospho-p44/p42 MAPK, phospho-PLC γ 2 or phospho-AKT. All primary antibodies were diluted 1:200, in blocking buffer. Cells were incubated with 50 μ l of each of the primary antibodies, overnight at 4°C, with gentle shaking. Following overnight

incubation, cells were washed in wash solution (PBS, 0.1% Tween), for 5 times 5 minutes with gentle shaking.

2.9.1.5 Secondary Antibody and Nuclear Staining

Following primary antibody incubation and washing, cells were incubated with anti-Rabbit IRDye 800 and anti-Mouse IRDye 800 (1:15,000 dilutions) in blocking solution containing 0.1% v/v Tween. Nuclear stains DRAC5 (1: 10,000 dilution) and Sapphire 700 (1:1000 dilution) were also added to secondary antibody solutions. Background wells were prepared by incubating cells with blocking buffer (containing 0.1% v/v Tween-20) containing only secondary antibody to determine non-specific antibody binding. Cells were incubated with secondary antibodies, nuclear stains and blocking buffer for 1 hour at room temperature, with gentle rocking. Cells were then washed with wash solution for 5 times 5 minutes.

2.9.1.6 Plate Analysis

Plates were analyzed using the Licor Odyssey Sa system, using the parameters described in Table 2.1. Cell number (nuclear stain) was detected in the 700 nm channel and phospho-proteins detected in the 800 nm channel. Signal quantification was calculated by subtracting background, normalizing the 800 channel (protein phosphorylation) to 700 channel (cell number) and calculating percentage response in the 800 channel relative to quiesced cells. A summary of this protocol is shown in Figure 2.2.

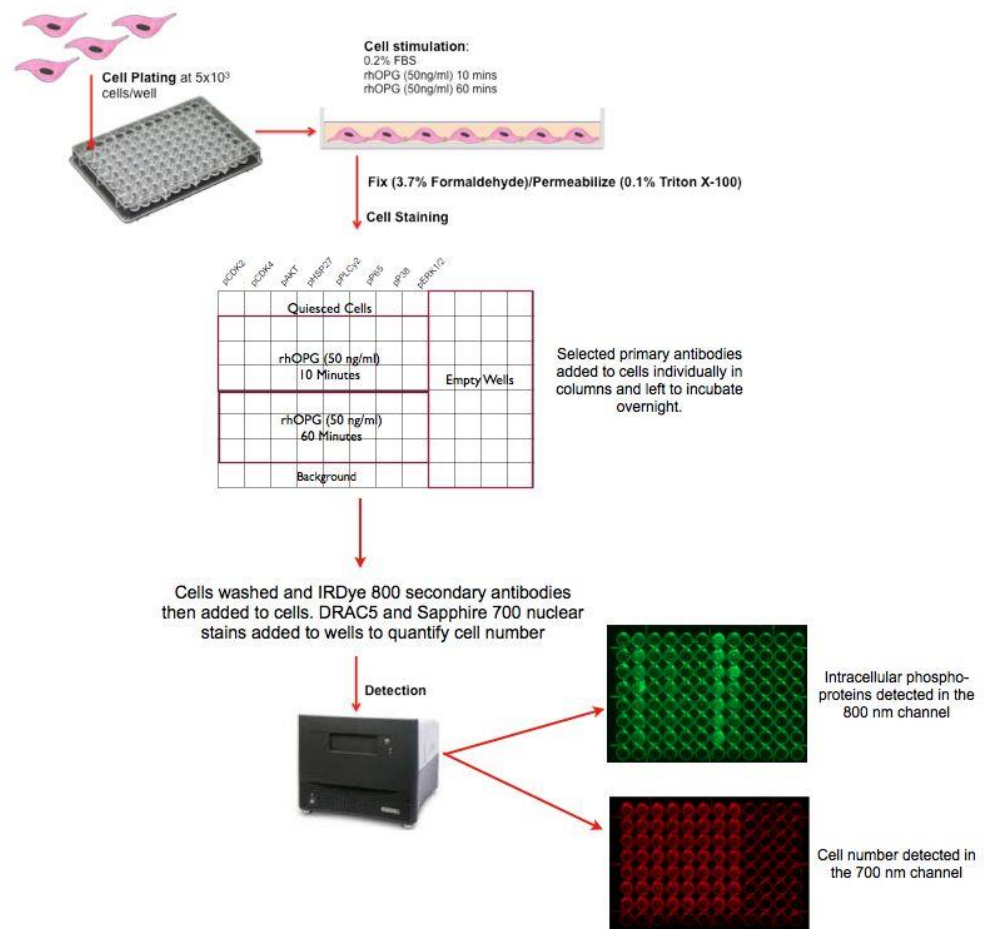


Figure 2.2- ICW Assay Protocol.

HPA-SMCs plated into 96 well plates were quiesced for 48 hours and stimulated with rhOPG (50 ng/ml) and 0.2% FBS for 10 and 60 minutes. Cells were then fixed and permeabilised, blocked and probed with primary antibodies against intracellular phospho-proteins, overnight. Cells were then washed and probed with secondary antibodies and nuclear stains to quantify cell number. Cells were then washed and scanned using the LiCOR Odyssey Sa System. Phospho-proteins were then detected in the 800 nm channel and cell number detected in the 700 nm channel.

2.9.2 Western Blotting

2.9.2.1 HPA-SMC Stimulation

HPA-SMCs (P4-P7) were grown as described in Chapter 2, Section 2.1.1.1 and passaged into 9x T25 cell culture flasks (1:3 split). Cells were then grown until cells reached ~80% confluence. Cells were then synchronised as described in Chapter 2

section 2.1.1.3. Growth arrest media was then removed after 48 h and cells were stimulated with 0.2% FBS (starve media) or rhOPG (50 ng/ml) diluted in starve media) for 10 minutes and 60 minutes.

2.9.2.2 HPA-SMC Lysis

2.9.2.2.1 Sodium Orthovanadate Lysis

Immediately before lysing, cell lysis buffer (78% v/v ddH₂O, 1% v/v 1M Tris HCl, 1% v/v 100 mM SDS, 100 mM sodium orthovanadate, 10% v/v protease inhibitor cocktail) was prepared and boiled for 5 minutes. After stimulation, cell culture media was removed and cells were washed three times in cold PBS. All trace of PBS was removed with a pipette and 300 µl of lysis buffer heated to 95°C was added to each flask and incubated for 5 minutes. Cells were then scraped using a cell scraper and the lysate was transferred to a fresh 1.5 ml Eppendorf. Lysates were boiled for 5 minutes at 100°C and then centrifuged at 4°C, 14,000 rpm for 10 minutes to clarify the cell lysate. Following centrifugation, the supernatant was then transferred into fresh 0.5 ml Eppendorfs in 30 µl aliquots and immediately frozen at -80°C until required. Sodium orthovanadate lysis buffer was used to lyse cells prior to performing western blotting to detect phospho-proteins.

2.9.2.2.2 Triton X-100 Lysis

Immediately before lysing, cell lysis buffer (150 mM NaCl, 20 mM Tris, 1% v/v Triton X-100, 0.1% v/v SDS in 1 x PBS) was prepared. Immediately before use, HALT Protease Inhibitor cocktail (100X) was added to the cell lysis buffer. After cell stimulation, cell culture media was removed from the T25 cm² cell culture flask and the cells were washed three times in cold PBS. All trace of PBS was removed using a pipette and 300 µl cell lysis buffer was added per T25 cm² cell culture flask. Flasks were then immediately frozen at -80°C, ensuring an even layer of lysis buffer was spread over the bottom of the cell culture flask. Immediately before western blotting, T25 cm² cell flasks were defrosted on ice, and aliquotted into 30 µl aliquots before freezing at -80°C.

2.9.2.3 Primary Antibody Incubation

Western blotting was performed on cell lysates according to the protocol described in Chapter 2 section 2.3. After gel electrophoresis and blocking as described in Chapter 2, Section 2.3, the blot was incubated with blocking buffer (5% w/v low fat milk (Marvel) in 1xPBS) containing phospho-CDK4, phospho-ERK1/2 phospho-p44/p42 MAPK or phospho-HSP27 primary antibodies (1:1000 dilutions), or mTOR, phospho-mTOR, CDK5, FADD, Atg7, Atg13 or Daxx primary antibodies in 30% v/v Odyssey blocking buffer, overnight at 4°C. β -actin and p44/p42 primary antibodies (1:1000 dilutions) were also added and used for loading controls. Following primary antibody incubation, membranes were washed in 0.1% v/v Tween-20, for 3 times 10 minutes washes.

2.9.2.4 Secondary Antibody Incubation

Secondary antibodies Donkey anti-Rabbit IRDye 800 and Goat anti-Mouse IRDye 800 were diluted 1:15000 in blocking buffer and incubated for 1 hour at room temperature, protected from light. Following secondary antibody incubation, membranes were washed in 0.1% v/v Tween-20, for 3 times 10 minutes washes.

2.9.2.5 Membrane Scanning

Each blot membrane was then scanned and signal detected using the Licor Odyssey Sa system. Band density was quantified by subtracting background and counting the number of pixels in each band (number of pixels proportional to density). Band density of phospho-proteins was then normalised to the band density of loading controls.

2.10 Agilent RNA Microarray

A microarray consists of thousands of genes spotted onto a slide that are used to look at gene expression in samples, for example healthy cells versus cancer cells, in order to gain insight into the causes and development of disease. An Agilent RNA microarray was performed in order to investigate changes in gene expression in HPA-SMCs stimulated with rhOPG compared to unstimulated cells.

When a gene is activated in cells, mRNA is transcribed. RNA is then isolated from the cells and reverse transcribed into cDNA. Fluorescently labelled cRNA is then synthesised from the cDNA using fluorescent nucleotides. In a two-colour microarray, a different fluorescent nucleotide is used for the stimulated, for example Cy3, and unstimulated control, for example Cy5. The fluorescently labelled cRNA from both samples is then combined and added to the microarray slide consisting of thousands of oligonucleotides. In a one-colour microarray, each sample is labelled with the same fluorescent nucleotide, for example Cy3, and each sample is run on a different sub-array on the microarray slide. If the mRNA is expressed in the samples, the cRNA then hybridizes to the complementary oligonucleotide on the slide. The more mRNA is expressed in the sample, the more cRNA hybridises to the oligonucleotides. The colour of fluorescence detected provides information on whether the mRNA is expressed in the stimulated or unstimulated samples.

2.10.1 HPA-SMC Stimulation

HPA-SMCs (P7) were grown as previously described in Chapter 2, Section 2.1.1.1, and synchronized in T25 cm² cell culture flasks as previously described in Chapter 2, Section 2.1.1.3. After 48 hours, growth arrest media was removed and HPA-SMCs were stimulated with rhOPG (50ng/ml) or growth arrest media (0.2% FBS, negative control). Nine T25 cm² cell culture flasks per condition were stimulated. Cells were stimulated for 6 hours, before cell culture media was removed and 500 µl TRIzol reagent was added to each T25 cm² cell culture flask. Flasks were then frozen at -80°C, ensuring an even layer of TRIzol was spread over the bottom of the cell culture flask.

2.10.2 HPA-SMC RNA Isolation

T25 cm² cell culture flasks previously stimulated and frozen at -80°C (described in Chapter 2.10.1) were defrosted on ice and RNA was extracted by J. Iremonger (Pulmonary Vascular Research Group, Department of Cardiovascular Science, University of Sheffield) using the DirectZol RNA extraction kit.

2.10.3 Bioanalyzer Analysis of RNA Quality

The quality of extracted RNA was then assessed using Agilent 2100 Bioanalyzer. RNA quality analysis was carried out by J. Iremonger (Pulmonary Vascular Research Group, Department of Cardiovascular Science, University of Sheffield), according to the Agilent RNA 6000 Nano Kit Guide.

2.10.4 Agilent RNA Microarray

Agilent 8-plex, single colour human gene expression microarrays were then performed to analyse gene expression in HPA-SMCs stimulated with rhOPG (50 ng/ml) or 0.2% FBS (growth arrest media). RNA was pooled from 3 individual samples per sub-array, with three sub-arrays being run for each condition (rhOPG or 0.2% FBS). Microarray analysis was performed, as described in the Agilent One-Colour Microarray-Based Gene Expression Analysis Protocol Low input Quick Amp Labeling protocol (version 6.6, September 2012 Agilent technologies, G4140-90040). Successful hybridization of the RNA to sixty thousand complimentary probes was detected by scanning the microarrays using the Agilent G2565BA microarray scanner by J. Iremonger (Pulmonary Vascular Research Group, Department of Cardiovascular Science, University of Sheffield).

2.10.5 Agilent RNA Microarray Analysis

Dr Alex Rothman (Pulmonary Vascular Research, Department of Cardiovascular Science, University of Sheffield) performed the microarray data handling. The data were background corrected and Log₂ transformed using Bioconductor and Lima programs in the programming language R. Log₂ fold change was calculated by subtracting the raw data of unstimulated control samples from the raw data of OPG-stimulated PA-SMCs. Output files were then organised by removing duplicate probes and using the intersection of Log₂ fold change >0.3 and p<0.05 for further analysis and heat map generation.

2.10.6 Heat Map Generation

A heat map was generated using R, with the help of Dr Alex Rothman, Department of Cardiovascular Science, University of Sheffield. PAH associated genes were identified using the search term “pulmonary hypertension” in Medline (Pubmed). A heat map was then generated to show mean \pm SD (standard deviation) of OPG-regulated genes that are associated with PAH. Mean \pm SD was calculated for each data value by: 1) calculating the mean of all 6 arrays (3x OPG and 3x unstimulated). 2) Standard deviation of all 6 arrays was calculated and finally 3) the mean of all 6 arrays was subtracted from each data value before dividing by the SD of all 6 arrays ((Data value-mean of all 6 arrays)/SD of all 6 arrays).

2.10.7 DAVID (The Database for Annotation, Visualization and Integrated Discovery) Analysis of Agilent RNA Microarray

Agilent Oligo IDs of genes regulated by OPG (Log₂ Fold change >0.3 and p<0.05) were then analysed using DAVID functional annotation to generate fold enrichment pathway analysis through the Kegg Pathway Database. Intersections of ≥ 2 fold change and p ≤ 0.05 were used for the pathway fold enrichment analysis.

2.11 TaqMan® Real-time Quantitative Polymerase Chain Reaction

In order to validate the RNA microarray and measure the RNA expression levels of identified targets in HPA-SMC lysates, real-time quantitative polymerase chain reaction (RT-qPCR) was performed. PCR is a technique that allows sequences within DNA, generated from a cDNA template, to be amplified thousands of times. The PCR product (amplicon) is then detected and quantified, often by post-PCR electrophoresis, after the last PCR cycle has been completed. RT-PCR however, allows the PCR product to be detected and quantified after the completion of each individual PCR cycle has been completed, in real time. RT-PCR therefore allows the starting amount of DNA to be theoretically calculated. Theoretically, there is a doubling of DNA with each PCR cycle and the DNA is amplified exponentially. However, the reaction eventually plateaus. In RT-PCR, fluorescent markers are incorporated into the DNA during each cycle; hence the fluorescence is proportional to the amount of amplicon

produced. Fluorescence is then plotted against cycle number to generate an amplification plot representing accumulation of amplicons over PCR duration. If a DNA sequence expression is abundant, amplification is detected in earlier cycles. However, if expression is low, amplification is detected in later cycles.

Taqman RT-qPCR uses fluorescent probes as the fluorescent detection system. The Taqman probe contains a 5' reporter dye, usually a FAM™ or VIC™ dye, covalently linked to a quencher dye, usually TAMRA™ or a non-fluorescent dye at the 3' end. The proximity of the quencher dye to the report dye suppresses the fluorescence of the reporter dye. If the specific DNA target sequence is present, the probe anneals to the DNA between the forward and reverse primer sites. The AmpliTaq Gold® DNA polymerase, which exhibits 5' to 3' activity, then cleaves the probe between the report and quencher dye. The probe then displaces from the DNA target sequence, the cleaved reporter dye fluoresces and polymerization of the DNA sequence continues. The 3' end of the probe is blocked and thus is not extended during the reaction. The fluorescence then accumulates exponentially as each PCR cycle is completed repeating the process above.

2.11.1 HPA-SMC stimulation

HPA-SMCs (P4-P7) were passaged into T25 cell culture flasks and grown until cells reached ~80% confluence. Cells were then synchronised as described in Chapter 2 section 1.1.1.3. Growth arrest media was removed after 48 h and cells were stimulated with 0.2% v/v FBS (starve media) or rhOPG (50 ng/ml diluted in starve media) for 6 hours at 37°C. Following stimulation, the media was removed and 500 µl TRIzol reagent was added directly to the T25 cell culture flasks. Flasks were then frozen at -80°C until RNA was extracted.

2.11.2 DirectZol RNA Extraction

2.11.2.1 Preparation of DNase I Cocktail

Before RNA extraction, all areas and equipment were cleaned with RNaseZap®. Immediately before RNA extraction, a DNase I cocktail was prepared by

reconstituting 250 units lyophilized DNase I in 250 µl DNase/RNase-free water. 5 µl (5 units) DNase I were then added to 8 µl 10X DNase I reaction buffer, 3 µl DNase/RNase-free Water and 64 µl RNA wash buffer in an RNase-free tube and mixed gently.

2.11.2.2 RNA Extraction

Immediately before RNA extraction, T25 cm² cell culture flasks were defrosted on ice. 500 µl ethanol (96-100%) was then added directly to the cell homogenate and mixed well by pipetting. The mixture was then loaded into a Zymo-Spin™ IIC Column placed in a collection tube and centrifuged for 1 minute at 10,000 xg. The flow through was discarded and the Zymo-Spin™ IIC Column was transferred into a new collection tube. 400 µl RNA wash buffer was then added to the Zymo-Spin™ IIC Column, placed in a collection tube, and centrifuged for 1 minute at 10,000 xg. The flow through was discarded. 80 µl of the DNase I cocktail was then added directly to the matrix of the Zymo-Spin™ IIC Column in a collection tube. The column was then incubated at 37°C for 15 minutes, then centrifuged at 10,000 xg for 30 seconds.

400 µl Direct-Zol™ RNA pre-wash was then added to the column and centrifuged for 1 minute at 10,000 xg and the flow through was discarded. 700 µl RNA wash buffer was then added to the column and centrifuged for 1 minute and the flow through discarded. The column was then centrifuged for a further 2 minutes in an empty collection tube to ensure complete removal of the wash buffer. The column was then transferred carefully into an RNase-free tube. 50 µl of DNase/RNase water was then added directly to the column matrix and centrifuged at 14,000 xg for 1 minute. The concentration of the eluted RNA was then measured using the Nanodrop 1000 and then frozen immediately at -80°C until required.

2.11.2.3 Nanodrop 1000 Spectrophotometer

The concentration of RNA isolated from samples as described for each experiment was measured using the Nanodrop 1000 Spectrophotometer (ThermoScientific, United Kingdom). Prior to RNA measurement, all areas and equipment were cleaned with RNaseZap® and RNA samples were defrosted on ice. The pedestals of the Nanodrop

1000 were cleaned with a clean, lint-free tissue. The “Nucleic Acids” program on the Nanodrop software was launched and a 1 µl RNase-free water sample was loaded on the pedestal. Once the machine was calibrated, the machine was then blanked to RNase-free water that the RNA samples were suspended in. Once blanked, the pedestals were cleaned with a clean, lint-free tissue. 1 µl sample was then pipetted onto the pedestal and the RNA concentration was measured. The pedestals were then cleaned with a clean, lint-free tissue. This process was repeated for each sample, with the machine being re-blanked after every 15 samples.

2.11.3 Reverse Transcription of Isolated RNA

Before reverse transcription, all areas and equipment were cleaned with RNaseZap®. Complementary DNA (cDNA) was synthesized from RNA by reverse transcription using the Applied Biosystems High Capacity RNA-to-cDNA™ kit (4387406, Invitrogen, Life Technologies, Paisley, UK). In order to yield 2000 ng cDNA output, 1000 ng RNA was added to each reaction. A total of 9 µl RNA was added to 10 µl 2X RT buffer and 1 µl 20X enzyme to ensure a total of 20 µl for each reaction. A control reaction containing no RNA and no enzyme was also prepared. The volume of RNA and RNase free-water required was calculated as follows:

Volume RNA sample required (µl) = RNA sample concentration (µg/µl) / RNA input required (ng)

Volume of RNase-free water required (µl) = 20 – (volume RNA sample required (µl) + volume 2X RT buffer (µl) + volume 20X enzyme (µl)).

cDNA was then synthesized using the Applied Biosystems Verti 96 well thermocycler at 37°C for 60 minutes and 95°C for 5 minutes followed by incubation at 4°C. The cDNA was then stored at -20°C until required.

2.11.4 TaqMan RT-qPCR Reaction Set-up

Before Taqman RT-qPCR reactions were set up, all areas and equipment were cleaned with RNaseZap®. Taqman RT-qPCR reactions were set up in triplicate wells of a

384-well clear bottom plate. 50 ng cDNA was added to each appropriate well by diluting 20 µl cDNA previously synthesised in 180 µl RNase-free water and pipetting 5 µl diluted cDNA into each well. 0.5 µl of 20x probe, 18S, ACVRL1, BMPR1A, CAV1, FAS, GAP43, IL1RAcP, PDGFRA, TGFBR1, TGFBR2, TMPRSS11D, TNC, TRAIL, VEGFA and VIPR1 (Appendix 7.1.11), was then added to each appropriate well. 4.5 µl Taqman Universal Mastermix was then added to each well.

2.11.5 TaqMan 7900HT Fast Real Time PCR System Set-up

The Taqman RT-qPCR was performed using the 7900HT Fast Real Time PCR System (Life Technologies), using the 9600 Emulation setting and 45 cycles. The thermal profile was used as follows for each cycle: 2 minutes at 50°C, 10 minutes at 95°C, 15 seconds at 95°C and 1 minute at 60°C.

Taqman validation was performed using cDNA generated from the nine individual unstimulated (0.2% v/v FBS) and OPG-stimulated samples used for the microarray and a further four unstimulated (0.2% v/v FBS) and OPG-stimulated HPA-SMC samples generated separately from the microarray samples.

2.11.6 TaqMan data analysis

Taqman data was normalised using $\Delta\Delta CT$ with 18S rRNA as the endogenous control.

2.12 Fas and TRAIL neutralisation to assess OPG-induced proliferation of HPA-SMC

2.12.1 HPA-SMC Pre-Incubation with Antibodies

HPA-SMCs were grown in fully supplemented media as described in Chapter 2 Section 2.1.1.1, until ~80% confluent. Cells were then trypsinized and seeded into 96 well plates at 5×10^4 cells/ml (200 µl/well). Three wells were left empty without any cells added to the wells, however media was added to the wells. Cells were left to adhere for 24 hours at 37°C (5% CO₂) before cell cycles were synchronized for 48 h in growth arrest media as described in Chapter 2 Section 2.1.1.3. Cells were then

washed 3 times in PBS and incubated with Fas neutralising antibody (Mouse Monoclonal Fas Antibody (human, neutralising), clone ZB4, Millipore, Darmstadt, Germany) (1500 ng/ml), TRAIL neutralising antibody (1500 ng/ml) or both Fas and TRAIL antibody (1500 ng/ml) diluted in growth arrest media, for 30 minutes (37°C, 5% CO₂).

2.12.2 HPA-SMC Stimulation

Following pre-incubation with antibodies, cells were stimulated with OPG (30 ng/ml), PDGF (20 ng/ml) or 0.2% v/v FBS in the presence or absence of Fas, TRAIL or both Fas and TRAIL antibodies for 72 h (37°C, 5% CO₂). All stimulants and antibodies were added in triplicate wells and to a final volume of 200 µl in each well, diluted in growth arrest media.

2.12.3 CellTiter-Glo® Measurement of HPA-SMC Proliferation

The CellTiter Glo® assay is a luminescent cell viability assay that was used to perform a high-throughput cell proliferation assay. The assay principally uses the Luciferase enzyme to catalyse the oxidation of its chemical substrate, luciferin, using ATP as a co-substrate. After cell lysis, ATP is released from the cells, which the luciferase enzyme uses to catalyse luciferin oxidation to generate light. Therefore, the luminescence generated by luciferase is proportional to the amount of ATP, which is proportional to the number of cells.

2.12.3.1 CellTiter-Glo® Assay

Prior to performing the CellTiter-Glo® assay, the CellTiter-Glo® Buffer and CellTiter-Glo® substrate were equilibrated to room temperature before use. 10 ml CellTiter-Glo® buffer was added to CellTiter-Glo® substrate and mixed to form the CellTiter-Glo® Reagent. 100 µl of the CellTiter-Glo® reagent was then added directly to the 96 wells containing the stimulations, including the wells containing media only (background wells). The plate was then mixed for 2 minutes on a plate shaker to lyse the cells. The plate was then incubated for 10 minutes to allow the luminescence signal to stabilize, before reading the luminescent signal on a VarioSkan Flash (Thermo Scientific) plate reader.

2.13 Fas neutralisation to assess RNA expression in HPA-SMCs

HPA-SMCs were grown and synchronised in T25 cm² cell culture flasks as previously described in Chapter 2, section 2.1.1. Cells were then incubated for 30 minutes with Fas neutralising antibody (Mouse Monoclonal Fas Antibody (human, neutralising), clone ZB4, Millipore, Darmstadt, Germany) (1500 ng/ml) in growth arrest media. Following pre-incubation with the Fas antibody, cells were stimulated with rhOPG (50 ng/ml) for 6 hours in the presence or absence of Fas neutralising antibody. The media was then removed and 500 µl Trizol solution was immediately added to each T25 cm² cell culture flask. Flasks were then frozen at -80°C before extracting the RNA using the DirectZol RNA extraction kit (Chapter 2.11.2). Expression of TRAIL, PDGFRA, TNC, VIPR, VEGF and Cav-1 was then analysed by TaqMan qPCR (Chapter 2.11).

3. IDENTIFICATION OF NOVEL OPG BINDING PARTNERS

3.1 Introduction

As discussed in the introduction to this thesis (Chapter 1.7), OPG is a secreted glycoprotein that can exist as a 55-62 kDa monomer or a 110-120 kDa homodimer (Simonet et al. 1997; Zauli et al. 2009). Trimers of OPG have also been detected in nanoparticles at a molecular weight of 180 kDa (Schoppet et al. 2011). Interactions between OPG and several proteins have already been reported in the literature. OPG is perhaps best known for its role as a decoy receptor for RANKL and as a decoy receptor for TRAIL. By binding to TRAIL, OPG can prevent TRAIL-induced apoptosis of tumour cell lines (Cross et al., 2006) and by binding to RANKL, can block osteoclastogenesis (Yasuda et al. 1998; Hsu et al. 1999). However, in both cases, OPG has simply been shown to bind and prevent the interaction of RANKL and TRAIL with their receptors, to block signalling, rather than signalling itself.

The ability of OPG to form homodimers has been found to influence the ability of OPG to bind to RANKL. OPG homodimers have been identified as having a higher affinity for binding RANKL than OPG monomers (Schneeweis et al. 2005) and although TRAIL trimers have been identified to bind to TRAIL receptor trimers, TRAIL trimers have been found to bind to only one OPG receptor molecule (Bosman et al. 2014). Therefore, the ratio to which OPG binds TRAIL and RANKL is different and the formation of OPG dimers and trimers may also influence the affinity to which OPG binds to different ligands.

Although OPG is known to bind RANKL and TRAIL, it is possible that OPG may be binding to a different binding partner to induce the pathogenic phenotype in PASMCS. Although both RANKL and TRAIL are expressed in patient lesions (Lawrie et al., 2008), current literature would suggest that OPG is binding to TRAIL and RANKL to block their respective signalling, rather than signalling through the OPG ligands, TRAIL and RANKL.

OPG also binds to syndecan-1 (SDC-1) (Standal et al. 2002; Mosheimer et al. 2005) and the OPG-SDC-1 interaction has been found to be important in monocyte migration (Mosheimer et al. 2005). However, SDC-1 was not detected within PAH patient lesions (Lawrie et al., 2008) suggesting that SDC-1 is not likely to be the receptor through which OPG induces the PA-SMC phenotype to contribute to disease pathology and induce disease in patients.

OPG binding to von Willebrand Factor (vWF) and thrombospondin-1 (vWF reductase) has also been reported (Zannettino et al., 2005). vWF is a protein localised to Weibel Palade bodies (WPB) found exclusively in ECs (Zannettino et al. 2005), therefore, it seemed unlikely that the interaction with vWF would mediate an OPG response in PA-SMCs. Finally, Kobayashi-Sakamoto et al (2008) suggested an interaction between OPG and $\alpha_v\beta_3$ and $\alpha_v\beta_5$, after blockade of $\alpha_v\beta_3$ and $\alpha_v\beta_5$ was reported to reduce OPG-induced human microvascular EC (HMVEC) migration. However, the interaction between OPG and $\alpha_v\beta_3$ and $\alpha_v\beta_5$ was not confirmed and therefore remains to be determined.

Interestingly, work by Yamaguchi et al (1998) has shown that domains 5 and 6 of OPG can induce cell apoptosis when included in a chimeric OPG-Fas protein consisting of the Fas transmembrane domain. OPG does not have a transmembrane domain and although domains 5 and 6 are structurally similar to the death domains belonging to Fas, overexpression of OPG did not induce cell apoptosis (Yamaguchi et al. 1998). These findings suggest that domains 5 and 6 of OPG have the potential to signal and induce apoptosis but may not in normal cell biology due to the absence of a transmembrane domain. However, these findings show the ability of OPG to induce phenotypic changes in cells when expressed as a chimeric protein with Fas. Fas, like TRAIL, belongs to the TNF superfamily and it would therefore be interesting to determine whether there may be an interaction between OPG and Fas that allows OPG to signal in PA-SMCs.

After examining the reported OPG interactions, it seems that OPG may induce changes in PA-SMC phenotype by binding to different proteins than those mentioned

above. Therefore, I used an unbiased screening approach to identify potential OPG binding partners.

3.2 Aims

In order to gain more insight into how OPG induces changes in PA-SMC phenotype, I sought to identify human plasma membrane proteins expressed on PA-SMCs to which OPG binds to cause the proliferation of PA-SMCs. The three main aims of this chapter were to:

1. Identify human plasma membrane proteins to which OPG binds by Retrogenix cell microarray.
2. Confirm selected interactions between OPG and human membrane proteins in PA-SMC lysates using co-immunoprecipitation.
3. Determine the expression of receptors in IPAH patient tissue (right ventricle and pulmonary artery) using immunohistochemical staining.

3.3 Methods

3.3.1 Retrogenix Cell Microarray

The identification of OPG human protein binding partners was performed for OPG using the Retrogenix Cell Microarray (Sheffield, UK). Optimal binding conditions were first established using syndecan-1 (positive control) and TREM-1 (negative control). HEK293 cells were reverse transfected with expression vectors consisting of one of 2505 (~60% of all known) human plasma membrane proteins and OPG binding was assessed (<http://www.retrogenix.com/default.asp>) (Chapter 2.4).

3.3.2 TaqMan RT-qPCR

RNA was extracted from 0.2% FBS-stimulated or OPG-stimulated (50 ng/ml) PA-SMCs after 6-hour stimulation. Expression of Fas, IL1RAcP, GAP43 and TMPRSS11D mRNA in PA-SMCs was quantified by TaqMan RT-qPCR (Chapter 2.11). Fas expression in IPAH patient PA-SMCs was analysed by TaqMan RT-qPCR

on RNA previously extracted, prior to me joining the Pulmonary Vascular Research group, as described by Hameed et al (2012).

3.3.3 Co-Immunoprecipitation

Co-immunoprecipitation was used to pull down OPG binding partners and confirm the interaction between OPG and the binding partners identified by the Retrogenix cell microarray. Co-immunoprecipitation was performed as described in Chapter 2.5.

3.3.4 Immunohistochemistry

Immunohistochemical analysis of pulmonary artery and right ventricle sections from donors with IPAH was performed by Ms Nadine Arnold, Pulmonary Vascular Research Group, Department of Cardiovascular Science, University of Sheffield, as described in Chapter 2.6. The sections were stained for OPG, Fas and IL1RAcP.

3.3.5 Statistical Analysis

All data are represented as mean \pm SEM. Treatments were compared using Two-way ANOVA followed by Tukey's post hoc test for multiple comparisons. When comparing only two groups, an unpaired T-test was used. $P < 0.05$ was deemed statistically significant. The n numbers refer to the number of separate experiments performed. For all experiments, each condition was performed in duplicate or triplicate.

3.4 Results

3.4.1 Identification of OPG Binding Partners

As I discussed in the introduction to this chapter, although OPG has been reported to bind to several proteins, I believed that OPG might be binding to different proteins than those discussed in the introduction to induce PA-SMC proliferation. Therefore, I first aimed to identify human membrane proteins to which OPG binds. To do this, an unbiased Retogenix cell microarray was performed in order to identify interactions between OPG and ~60% of all known human plasma membrane proteins.

Pre-screening of rhOPG and antibody concentrations was performed to determine optimum binding conditions of rhOPG and the anti-OPG antibody. Based on the pre-screen, optimum conditions were determined to be 0.5 µg/ml rhOPG and 0.5 µg/ml anti-OPG antibody (Figure 3.1, condition 5). This condition showed successful binding of OPG to syndecan-1, with the lowest levels of background detected (2.1 fold over the glass slide alone), in the absence of non-specific binding to TREM1. The other conditions tested generated high background and non-specific binding to TREM1 (Figure 3.1, conditions 1 and 4) or specific binding to syndecan-1 but with high background (Figure 3.1, condition 2). For the primary and confirmation screens, 0.5 µg/ml OPG and 0.5 µg/ml anti-OPG antibody was then used during experimentation.

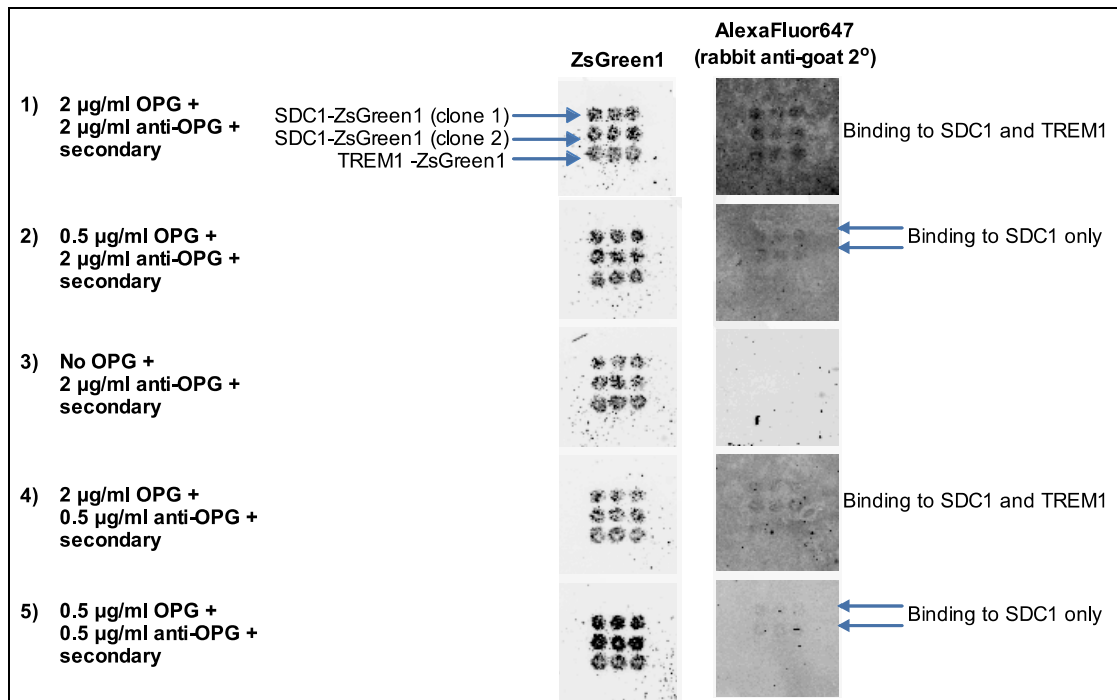


Figure 3.1- Pre-screen to determine background levels and binding.

Pre-screen of rhOPG and anti-OPG antibody concentrations was conducted to determine optimum binding conditions of OPG and the anti-OPG antibody. 1) 2 $\mu\text{g/ml}$ OPG and anti-OPG antibody generated binding to both syndecan-1 (positive) and TREM1 (non-specific binding to negative control). 2) Binding of OPG to syndecan-1 was detected in the presence of 0.5 $\mu\text{g/ml}$ OPG and 2 $\mu\text{g/ml}$ anti-OPG antibody, however background levels detected were high. 3) Background generated in the presence of anti-OPG antibody only. 4) Binding of OPG to syndecan-1 in the presence of 2 $\mu\text{g/ml}$ OPG and 0.5 $\mu\text{g/ml}$ anti-OPG antibody was detected, however non-specific binding to the negative TREM1 control was detected. 5) 0.5 $\mu\text{g/ml}$ OPG and 0.5 $\mu\text{g/ml}$ anti-OPG antibody generated binding to syndecan-1 only with lower background levels that condition 2 (2.1 fold over glass slide alone). Based on the pre-screen, optimum conditions were determined to be 0.5 $\mu\text{g/ml}$ OPG and 0.5 $\mu\text{g/ml}$ anti-OPG antibody. Successful transfection of both SDC1 and TREM1 membrane proteins (ZsGreen1 panels) was shown by detection of ZsGreen1 fluorescence (black spots).

Results of the primary screen revealed an interaction between OPG and 16 human membrane proteins, in one or both of the screens. The 16 “hits” are shown in Table 3.1.

Table 3.1- List of Primary Hits

In the primary screen, 2505 expression vectors, each encoding one full-length human membrane protein, were arrayed across 7 slides. Each slide was arrayed in duplicate and the slides were screened with 0.5 µg/ml OPG, followed by addition of 0.5 µg/ml anti-OPG primary antibody and secondary AlexaFluor647 rabbit anti-goat secondary antibody. A total of 16 hits, duplicate spots identified as a “hit” in one or both of the replicate slides, were identified and the intensity of the duplicate spots were quantified using the ImageQuant software (GE).

Hit Number	Gene Id	Intensity of Duplicate Spots
1	FCGR1A	Weak/medium
2	SLC13A3	Inverse
3	TLR7/CDC42	Weak
4	FGFR1	Weak
5	GAP43	Very weak
6	FCGR2B	Medium
7	CXCR7	Inverse
8	TNFSF11	Strong
9	TAAR9	Medium
10	FAS	Strong
11	IL1RAcP	Strong
12	PTPRN/LYD6B	Medium
13	SDC1	Medium
14	TMPRSS11D	Medium
15	FGF6	Diffuse
16	FCGR2A	Medium

Inverse hits, CXCR7 and SLC13A3, were visible as white spots caused by the fluorescence level detected being less than background levels. Binding of OPG to the FC-gamma receptors FCGR1A, FCGR2A and FCGR2A was also observed. FGF6 was also identified as a diffuse hit.

The identity of each vector for the 16 primary hits (Table 3.1) was confirmed by sequencing before proceeding to the confirmation screen. As identified in the primary screen, binding of OPG to the FC-gamma receptors was found to be present in all conditions, even in the negative controls where rhOPG or anti-OPG antibody had not been added to the cells (Table 3.2). These “hits” were therefore regarded as non-specific and thus discounted. The inverse SLC13A3 hit and diffuse FGF6 binding was again observed in the confirmation screen (Table 3.2) and these “hits” were also discounted. After discounting the non-specific, inverse and diffuse hits, 6 confirmed interactions between OPG and syndecan-1 (SDC1), RANKL (TNFSF11), Growth Associated Protein 43 (GAP43), Fas, IL1-receptor accessory protein (IL1RAcP) and transmembrane protease, serine 11D (TMPRSS11D) (Table 3.2) were identified. Images of the spot intensities and binding controls for the 6 confirmed interactions described are represented visually in Figure 3.2. Successful transfection of all vectors was achieved for the confirmation screen and controls, shown by ZsGreen1 fluorescence (Figure 3.3).

Table 3.2- Results of the Confirmation Screen.

Each of the 16 hits identified in the primary screen were re-spotted and probed with 0.5 µg/ml OPG and 0.5 µg/ml anti-OPG antibody and AlexaFluor647 rabbit anti-goat secondary antibody. No rhOPG (anti-OPG primary antibody and AlexaFluor647 rabbit anti-goat secondary antibody) and no anti-OPG primary antibody (rhOPG and AlexaFluor647 rabbit anti-goat secondary antibody) negative controls were also included to determine non-specific binding of OPG and the anti-OPG primary antibody to the human membrane proteins. Binding to FC gamma receptors was present in all conditions, even in the negative controls where no OPG or anti-OPG primary antibody was added. SLC13A3 was identified as an inverse hit (white spots detected where fluorescence levels are less than background levels) and FGF6 was identified as a diffuse hit. 6 OPG specific hits were identified as GAP43, TNFSF11, Fas, IL1RAP, SDC1 and TMPRSS11D. Background levels detected in the presence of OPG, anti-OPG and secondary antibodies were classified as medium/high and low in the negative controls.

Hit No:	1 2 3 4 5 6 7 8 9 10 11 12 13 14 15 16 17 18																		Background	
	Gene Id:	FCGR1A	SLC13A3	TLR7	CDC42	FGFR1	GAP43	FCGR2B	CXCR7	TNFSF11	TAAR9	FAS	IL1RAcP	PTPRN	LYPD6B	SDC1	TMPRSS11D	FGF6		FCGR2A
Condition	Rep. No																			
OPG + anti-OPG + secondary	1	Strong	Inverse				Medium	Strong				V.strong	Weak	Medium		Weak	Weak	Diffuse	Strong	Med/high
OPG + anti-OPG + secondary	2	Strong	Inverse				Medium	Strong				V.strong	Weak	Medium		Weak	Weak	Diffuse	Strong	Med/high
Anti-OPG + secondary (no OPG)	1	Strong						Strong											Strong	Low
Anti-OPG + secondary (no OPG)	2	Strong						Strong											Strong	Low
OPG + secondary (no anti-OPG)	1	Strong						Strong											Strong	Low
OPG + secondary (no anti-OPG)	2	Strong						Strong											Strong	Low

 Binding of antibodies to FC-gamma receptors
 OPG specific hits

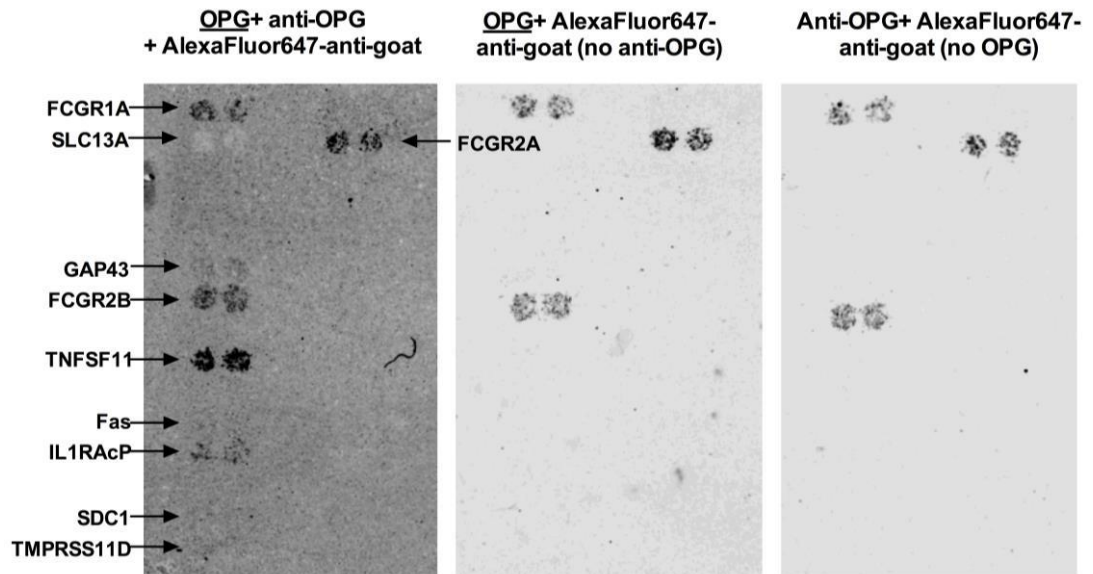


Figure 3.2- Confirmation Screen Results.

Left Panel: Binding to FCGR1A, SLC13A3, GAP43, FCGR2B, TNFSF11, Fas, IL1RAcP, SDC1, TMPRSS11D and FCGR2A was confirmed and fluorescence detected from the AlexaFluor647 secondary antibody is visible as black spots. The inverse hit, SLC13A3 is visible as white spots. **Centre and right Panels:** Binding to the FC-gamma receptors, FCGR1A, FCGR2B and FCGR2A, was detected in the negative controls: OPG + AlexaFLuor647 secondary (centre panel) and anti-OPG primary + AlexaFluor647 secondary (right panel).

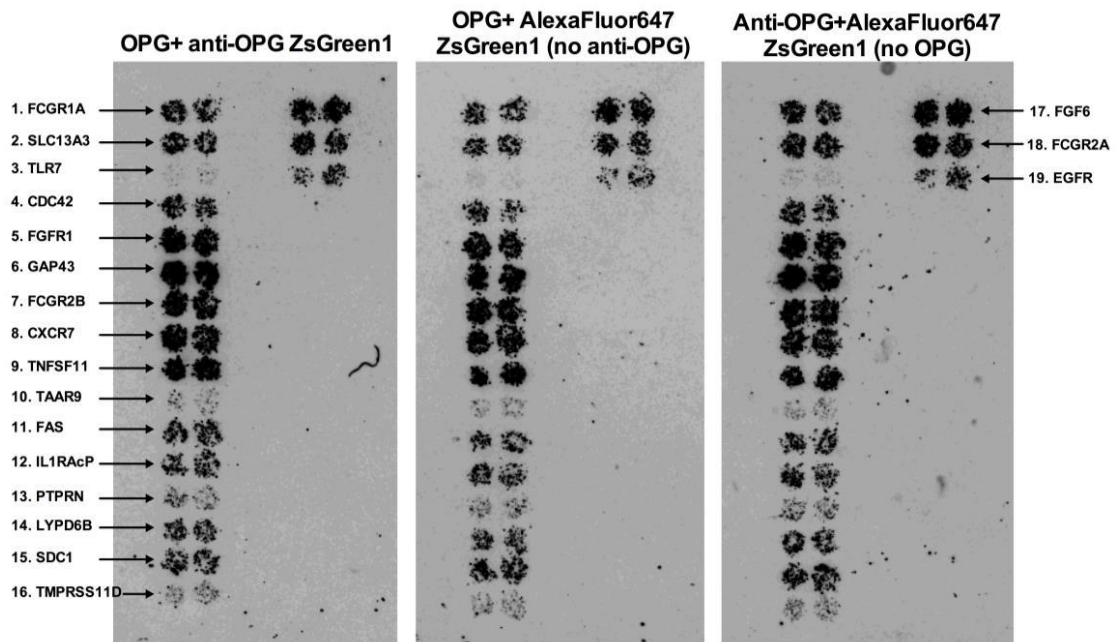


Figure 3.3- Retrogenix transfection confirmation (ZsGreen1 fluorescence).

All vectors of hits identified in the primary screen were successfully transfected into HEK293 cells for the confirmation screen (Left panel) and two negative controls: OPG + AlexaFluor647 (no anti-OPG, Centre Panel) and Anti-OPG + AlexaFluor647 (no OPG, Right Panel).

The interactions between OPG and syndecan-1 and RANKL were already known prior to the cell microarray. The Retrogenix cell microarray therefore identified 4 potential novel interactions between OPG and GAP43, Fas, IL1RAP and TMPRSS11D.

3.4.2 Fas, IL1RAcP and Gap43 RNA Expression in PA-SMCs

Because the putative OPG binding partners were identified by expressing human plasma membrane proteins on HEK293 cells, the next step was to determine whether they are expressed in PA-SMCs, the cells that proliferate in vitro following OPG stimulation.

TMPRSS11D RNA was not expressed in quiesced or OPG-stimulated PA-SMCs (data not shown). Expression of Fas, IL1RAcP and GAP43 RNA was confirmed in quiesced and OPG-stimulated PA-SMCs (Figure 3.4). Fas RNA was most abundantly expressed in quiesced PA-SMCs ($p < 0.01$) and OPG-stimulated PA-SMCs ($p < 0.001$), compared to IL1RAcP and GAP43 RNA expression in quiesced and OPG-stimulated PA-SMCs, respectively. Fas expression was also significantly increased in response to OPG-stimulation ($p < 0.05$), compared to unstimulated cells (Figure 3.4).

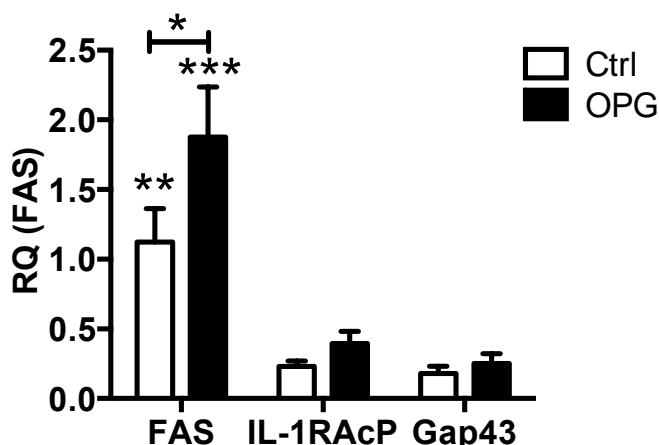


Figure 3.4- FAS, IL1RAcP and GAP43 RNA expression levels in quiesced and OPG-stimulated PA-SMCs.

*Fas, IL1RAcP and GAP43 RNA is expressed in PA-SMCs. However Fas RNA expression was significantly higher than IL1RAcP and GAP43 PA-SMCs and Fas expression was significantly increased in OPG-stimulated PA-SMCs, compared to unstimulated PA-SMCs. All data normalised using $\Delta\Delta CT$ with 18S rRNA as the endogenous control gene and normalising ΔCT to Fas expression. Bar graphs represent mean \pm SEM. Ctrl= control, quiesced PA-SMCs. OPG= OPG-stimulated (50 ng/ml) PA-SMCs. * $p < 0.05$, ** $p < 0.01$, *** $p < 0.001$, $n = 4$.*

Based on these findings, the interaction between OPG and TMPRSS11D was not chosen at this stage for further investigation, because the absence of RNA suggests that TMPRSS11D is not expressed in PA-SMCs. Fas RNA expression was not only most abundant, but was OPG-responsive in PA-SMCs. Therefore, OPG binding to Fas was selected for validation. Although IL1RAcP expression levels were significantly lower than Fas, IL1RAcP was also selected for further validation because the IL-1 signalling is already known to play a role in the pathogenesis of PAH and can increase the secretion of OPG (Humbert et al. 1995; Lawrie et al. 2008; Lawrie et al. 2011).

3.4.3 Validating the Interaction of OPG with Endogenous Fas and IL1RAcP in PA-SMC Lysates

Data from the Retrogenix cell microarray suggest that OPG interacts with Fas and IL1RAcP when these human membrane proteins are expressed on the surface of HEK293 cells. However, I could not conclude from these data that OPG interacts with these proteins in PA-SMCs, even though Fas and IL1RAcP RNA was detected in PA-SMCs. I therefore wanted to determine whether OPG could interact with endogenously expressed Fas and IL1RAcP on PA-SMCs.

Using co-immunoprecipitation, I was able to demonstrate that using an anti-Fas antibody to immunoprecipitate endogenous Fas also pulled down OPG from HPA-SMC lysates. This can be seen by a band in lane 2 at 50 kDa (Figure 3.5). OPG was also co-immunoprecipitated from an in vitro mixture of recombinant human Fas and recombinant human OPG, shown by a band in lane 3 at 50 kDa (Figure 3.5). Furthermore, no bands were detected at 50 kDa in the no antibody negative controls (Lanes 3 and 5, Figure 3.5). An anti-IL1RAcP antibody used to immunoprecipitate endogenous IL1RAcP from HPA-SMC lysates was also found to pull down OPG from HPA-SMC lysates, shown by a band at 50 kDa in lane 6 (Figure 3.5). OPG was also co-immunoprecipitated from an in vitro mixture of recombinant human IL1RAcP and recombinant human OPG, shown by a band in lane 8 at 50 kDa (Figure 3.5). Furthermore, no bands were detected at 50 kDa in the no antibody negative controls (Lanes 7 and 9, Figure 3.5).

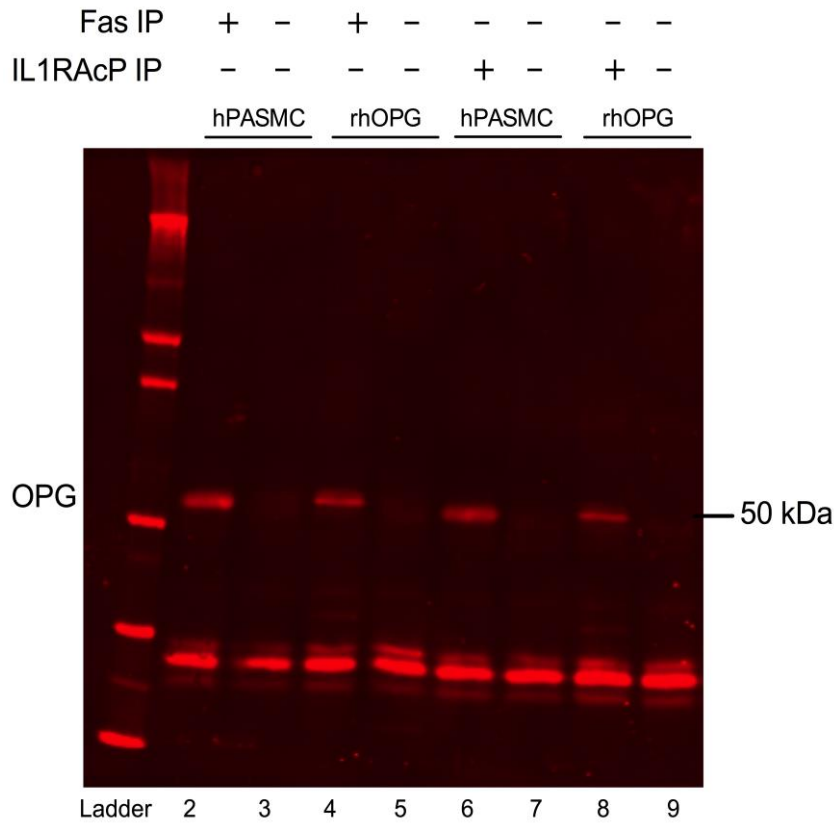


Figure 3.5- Co-immunoprecipitation of OPG from PA-SMC lysates and recombinant human proteins.

Lanes 2-8: OPG was co-immunoprecipitated from HPA-SMC lysates and recombinant human proteins using Fas antibody or IL1RAcP antibody. Lane 1: Novex pre-stained protein standards. Lane 2: Fas antibody + HPA-SMC lysate- Fas antibody was found to pull down OPG from PA-SMC lysates, shown by a band at 50 kDa. Lane 3: No Fas antibody+ HPA-SMC lysate- No bands detected at 50 kDa in the negative control. Lane 4: Fas antibody + rhFas + rhOPG- Fas antibody was found to pull down OPG from an in vitro mixture of rhFas and rhOPG, shown by a band at 50 kDa. Lane 5: No Fas antibody+ rhFas + rhOPG- No bands detected at 50 kDa in the negative control. Lane 6: IL1RAcP antibody + HPA-SMC lysate- IL1RAcP antibody was found to pull down OPG from PA-SMC lysates, shown by a band at 50 kDa. Lane 7: No IL1RAcP antibody + HPA-SMC lysate- No bands detected at 50 kDa in the negative control. Lane 8: IL1RAcP antibody + rhIL1RAcP + rhOPG- IL1RAcP antibody was found to pull down OPG from an in vitro mixture of rhIL1RAcP and rhOPG, shown by a band at 50 kDa. Lane 9: No IL1RAcP antibody+ rhIL1RAcP + rhOPG- No bands detected at 50 kDa in the negative control.

3.4.4 OPG, Fas and IL1RAcP Expression in Human IPAH Tissues

After validating the interaction between OPG and Fas and IL1RAcP in PA-SMCs, the next aim was to determine whether the binding partners were expressed in human tissues and whether this expression was altered in PAH patient tissue.

Immunohistochemical analysis revealed that OPG was barely detectable in the control pulmonary artery, however diffuse medial and cellular OPG staining was observed in the IPAH pulmonary artery (Figure 3.6 A). Weak immunoreactivity was detected for Fas in the control pulmonary artery, however diffuse Fas staining was detected throughout the IPAH pulmonary artery (Figure 3.6 A). IL1RAcP immunoreactivity was barely detectable in the control pulmonary artery and although an increase in immunoreactivity was detected in the IPAH pulmonary artery, levels of IL1RAcP staining detected in the pulmonary artery was not as diffuse as OPG or Fas staining (Figure 3.6 A).

Interesting, OPG and Fas immunoreactivity was detected in the right ventricle of both the control and IPAH sections (Figure 3.6 B). Although IL1RAcP immunoreactivity was also increased in right ventricle from patients with IPAH, IL1RAcP staining appeared to be less prominent than Fas protein expression in the IPAH sections (Figure 3.6 B). This staining shows that the potential OPG binding partners, Fas and IL1RAcP are expressed, along with OPG, in the pulmonary artery and right ventricle of IPAH patients. However, IL1RAcP immunoreactivity was weaker than both Fas and OPG staining in the control and IPAH pulmonary artery and right ventricle (Figure 3.6 A and B).

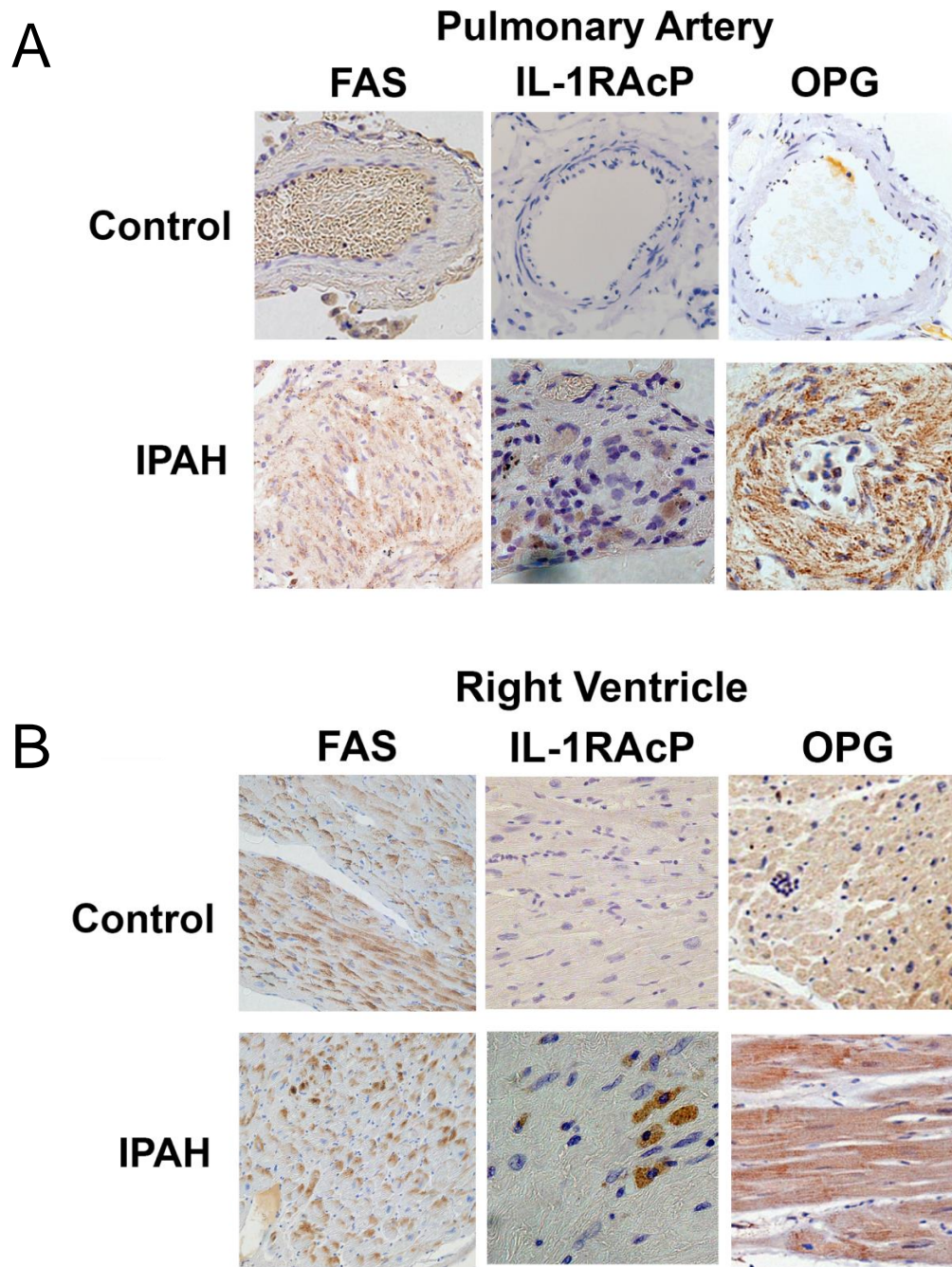


Figure 3.6- Immunohistochemical staining of Fas, ILIRAcP and OPG in the pulmonary artery and right ventricle.

Brown Fas, ILIRAcP and OPG staining visible in the pulmonary artery and right ventricle from IPAH patients, compared to the control sections.

Because Fas RNA expression in PA-SMCs was the highest out of the four identified binding partners, and diffuse Fas immunostaining was observed, along with OPG, in the pulmonary artery and right ventricle of IPAH patients, Fas RNA expression was also measured in the PA-SMCs from IPAH patients. Fas RNA expression was found to be significantly higher in PA-SMCs from IPAH patients, compared to healthy, control PA-SMCs (Figure 3.7). Furthermore, previously published data by Condcliffe et al (2012) has shown a significant increase in OPG mRNA expression in IPAH PA-SMCs. Taken together, the increase in OPG mRNA and Fas mRNA supports the immunohistochemistry data and further shows that OPG and the potential OPG binding partner, Fas, are both elevated in diseased PA-SMCs.

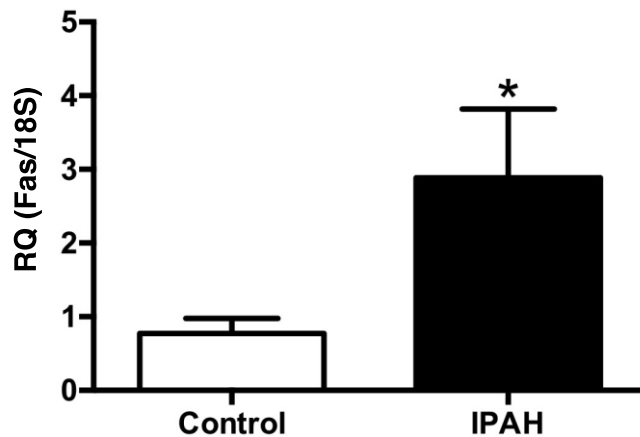


Figure 3.7- Fas RNA expression in IPAH patient lungs.

*Fas RNA expression is 3-fold higher in PA-SMCs isolated from IPAH patient lungs compared to Fas RNA levels in PA-SMCs isolated from healthy, control patient lungs. Bars represent mean \pm SEM. Control= healthy PA-SMCs, IPAH= IPAH PA-SMCs. N=3, * p <0.05.*

3.5 Discussion

The aim of this chapter was to identify the human plasma membrane proteins to which OPG binds. Although OPG has previously been shown to bind to several proteins, including TRAIL, RANKL, SDC-1 and vWF, I felt that OPG was binding to an undescribed cell surface receptor, for reasons discussed in the introduction to this chapter. An unbiased cell microarray was therefore conducted to screen OPG binding to ~60% of all known human plasma membrane proteins. Four novel interactions between OPG and Fas, IL1RAcP, GAP43 and TMPRSS11D were identified by the cell microarray. Expression of TMPRSS11D RNA was not detected in PA-SMCs, however Fas RNA expression was found to be significantly higher than IL1RAcP and GAP43 RNA expression and was significantly increased by OPG stimulation. Therefore, the interaction between OPG and Fas was then confirmed in PA-SMCs. Although levels of IL1RAcP RNA were lower than Fas levels, the interaction between OPG and IL1RAcP was also confirmed in PA-SMCs because IL-1 signalling is known to play a role in PAH (Humbert et al. 1995; Lawrie et al. 2008; Lawrie et al. 2011). Fas protein was identified, along with OPG, in the pulmonary artery and right ventricle of IPAH patients, however, only low levels of IL1RAcP was detected. Fas RNA levels were also significantly increased in PA-SMCs from IPAH patients.

After reviewing the literature, it seems that Fas and IL1RAcP are the two proteins most likely to be acting as receptors for OPG, rather than GAP43 or TMPRSS11D. Firstly, GAP43 (neuromodulin, B-50, P-57, F1, pp46) is reported by the literature to be a neuron-specific protein, predominantly associated with nerve growth (Denny 2006; Strittmatter et al. 1991). GAP-43 is synthesized on free ribosomes and is transported in vesicles to the plasma membrane (Denny 2006). GAP-43 is highly concentrated at the growth cone plasma membrane and is involved in filopodia formation, neurotransmitter release, endocytosis and synaptic vesicle recycling at the pre-synaptic membrane. Neuronal growth cones deficient in GAP-43 show reduced adhesion, spreading and branching (Denny 2006). Although GAP-43 levels decline in neurons after mature synapses have formed, GAP-43 persists at the synapses of the limbic system and neocortex and is also present in the adult retina and cornea. GAP-43 appears to be nervous system specific and currently, there are no reports in the

literature of a role for GAP-43 outside of the nervous system. Although findings in this chapter show for the first time that GAP43 RNA is expressed in PA-SMCs, based on the literature, it seems unlikely that GAP43 is the OPG receptor responsible for the pathogenic phenotype in PA-SMCs.

Secondly, TMPRSS11D (human airway trypsin-like protease, HAT) is a type-II transmembrane trypsin-like serine protease that was identified from the sputum of chronic airway disease patients (Yasuoka et al. 1997; C. Liu et al. 2013). Expression of TMPRSS11D has been found in cells of the submucosal serous glands located in the trachea and bronchi (Yasuoka et al. 1997) and bronchial ciliated endothelial cells (Takahashi et al. 2001). Literature suggests TMPRSS11D may function in normal airway epithelium (Takahashi et al. 2001) and may play a role in mucous secretion (Chokki et al. 2004). Interestingly, OPG levels are increased in the sputum of chronic obstructive pulmonary disease patients (To et al. 2011), however interaction between OPG and TMPRSS11D in the sputum of healthy individuals or COPD patients has not been investigated. Although other serine proteases, such as elastase, have been implicated in cardiovascular disease and are involved in pathogenic processes, such as atheromatous plaque formation, vascular damage, endothelial cell apoptosis and vascular SMC proliferation (Sharony et al. 2010), TMPRSS11D has not been implicated in such cardiovascular biological function or pathogenic processes.

Although binding of OPG to GAP43 and TMPRSS11D was not further pursued at this stage, the interactions between OPG and these proteins will require further investigation in the future to fully understand the implications of these interactions on cell function. Although TMPRSS11D RNA expression was not detected in PA-SMCs, expression has not been analysed in endothelial cells or fibroblasts, two more cell types that play an important role in PAH pathogenesis. The interaction between OPG and TMPRSS11D may be important in other lung diseases such as COPD. However, the importance of the OPG-TMPRSS11D interaction and expression of TMPRSS11D RNA in PA-SMCs this has not been investigated because this is outside the scope of this thesis.

The interaction between OPG and Fas and IL1RAcP was successfully confirmed in PA-SMCs. IL1RAcP belongs to the interleukin-1 (IL-1) receptor family, a subgroup

of the Toll-IL-1-receptors (TIR) (Boraschi & Tagliabue 2013). IL1RAcP is one of the ten members of the IL-1 receptor family and is a homologue of IL1R1. IL1RAcP acts a co-receptor for other IL-1 receptor family members and does not bind directly to ligands (Boraschi & Tagliabue 2013). IL1RAcP binds to IL-1R1 is required for IL-1 signalling through IL-1R1 (Wesche et al. 1997).

The ligand for the IL-1R1/IL1RAcP complex, IL-1 is a key player in inflammation, cytokine production, the immune response and inflammatory disorders (Boraschi & Tagliabue 2013; Vicenová et al. 2009). Many cell types constitutively express IL-1 α and synthesis is stimulated by inflammation (Vicenová et al. 2009). IL-1 β however, is not produced unless inflammatory signals are received and cleavage to the mature form by caspase-1 is carefully regulated. Macrophages are the main IL-1 producing cells, however neutrophils, lymphocytes, dendritic cells, keratinocytes, ECs, hepatocytes, fibroblasts and muscle cells have also been shown to produce IL-1 (Vicenová et al. 2009).

IL-1 plays an important role in PAH pathogenesis. Interactions between vascular cells and inflammation are important in vascular dysfunction and PAH pathogenesis. Inflammatory cytokines, including IL-1 and IL-6, are upregulated in PAH (Dorfmueller et al. 2002; Humbert et al. 1995; Sanchez et al. 2007; Perros, Dorfmueller, Souza, Durand-Gasselin, Godot, et al. 2007). Voelkel et al (1994) reported that the monocrotaline rat model of PAH is protected against disease development when treated with IL-1Ra, shown by a reduction in pulmonary artery blood pressure and right ventricular hypertrophy (Voelkel et al. 1994). ApoE^{-/-} mice fed on a high fat Paigen diet develop PAH, however IL-1^{-/-} mice were protected from PAH. Interestingly however, ApoE^{-/-}/IL-1R1^{-/-} mice developed a more severe PAH phenotype (Lawrie et al. 2011). It was reported that the ApoE^{-/-}/IL-1R1^{-/-} mice expressed a lung-specific alternative IL-1R1 receptor form that may contribute to a more severe disease phenotype (Lawrie et al. 2011).

IL1RAcP can also form complexes with ST-2 (suppressor of tumorigenicity) (Palmer et al. 2008), to facilitate the binding of the ST-2 ligand, IL-33. ST-2 can exist as a membrane bound or soluble form (sST-2) and ST-2 is expressed by endothelial cells, myocytes and fibroblasts of the cardiovascular system (Shao et al. 2014). Both

ST-2 and its ligand, IL-33, have also been implicated in PAH. Patients with IPAH show elevated serum levels of soluble ST2 (sST-2) and elevated sST-2 levels also correlate with disease worsening (Zheng et al. 2014; Carlomagno et al. 2013). Conversely however, ST2^{-/-} mouse pulmonary fibroblasts were shown to hyperproliferate to normoxia and hypoxia (Mahmood et al. 2010).

Although increased ST-2 has been observed in PAH, no difference in IL-33 levels were found between patient or control sera (Carlomagno et al. 2013). However, IPAH ECs show a reduction in nuclear IL-33 expression and a 50% reduction in IL-33 mRNA levels have been observed in IPAH lungs (Shao et al. 2014). IL-33 is considered to have a beneficial effect and displays anti-hypertrophy, anti-fibrosis actions and can reduce cardiac hypertrophy and fibrosis in mice (Carlomagno et al. 2013; Shao et al. 2014). Furthermore, PAH patients with elevated sST-2 levels show an increase in myocardial fibrosis (Carlomagno et al. 2013). Therefore, it has been suggested that sST-2 acts as a decoy receptor for IL-33 and blocks the beneficial actions of IL-33.

Because of the involvement of IL-1 in PAH, it would seem possible that OPG might bind to IL1RAcP protein on PA-SMCs and may be inducing pathogenic changes in the cells through this interaction. OPG may also be binding to IL1RAcP to facilitate the binding of ST-2 to IL-33, which may also have pathogenic effects on myocardial hypertrophy and fibrosis. The possible binding interactions between OPG, IL1RAcP and the interleukin receptors and ligand are shown in Figure 3.8. However, due to the fact that IL1RAcP is a co-receptor for other IL-1 receptors, I suspect that another receptor may be required to induce signalling events in PA-SMCs upon OPG binding to IL1RAcP. The possibility of another receptor and the interaction between OPG and IL1RAcP will however require further characterisation. Although the interaction between OPG and IL1RAcP was confirmed in PA-SMCs, PA-SMC IL1RAcP RNA levels and immunoreactivity in the pulmonary artery and right ventricle were lower than Fas RNA and immunoreactivity. This was surprising to find, however the low levels of IL1RAcP expression in the patient tissue may be due to an issue with the time at which the tissues were collected. The tissues that were stained were from patients with end-stage disease, by which time IL1RAcP expression may be reduced. IL1RAcP expression therefore needs to be assessed in tissues collected at an early

stage of disease.

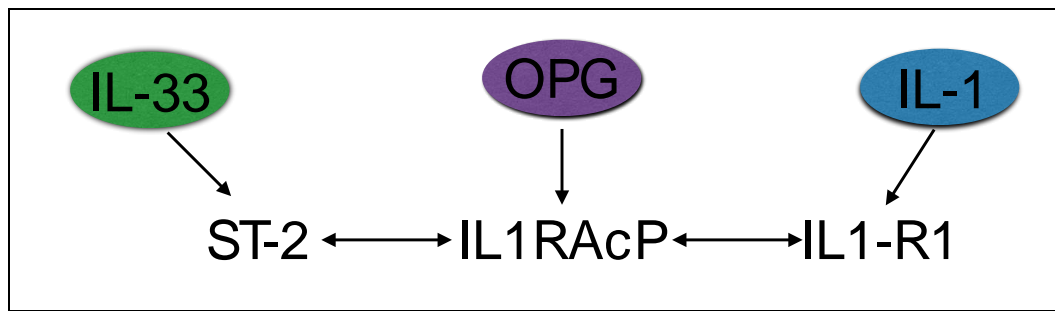


Figure 3.8-Schematic showing the interactions between IL1RAcP and OPG and the interleukin receptors, ST2 and IL1-R1.

IL-1 binds to the IL1-R1 receptor and IL-33 binds to the ST-2 receptor.

The fact that both OPG and Fas are so abundantly expressed in the right ventricle and pulmonary artery of IPAH patients suggests that Fas may indeed be a receptor for OPG that plays a role in disease. Fas (cluster of differentiation 95, CD95, APO-1, TNFRSF6) is a 45 kDa, type 1 membrane protein belonging to TNF receptor family and plays an important role in cell apoptosis (Serrao et al. 2001; Aggarwal et al. 1995; Hamann et al. 2000; Sata et al. 2000; Trauth et al. 1989; Yonehara et al. 1989). Fas consists of an N-terminal, containing 3 cysteine-rich domains (CRDs), a transmembrane domain and an intracellular region containing a death domain (Brint et al. 2013). The death domain (DD) is approximately 80 amino acids long and is responsible for transducing the apoptotic signal (Brint et al. 2013). Fas is constitutively expressed throughout various tissues of the body, including endothelial cells of the biliary tract, intestine, reproductive system, activated fibroblasts and osteoclasts (Leithäuser et al. 1993). The natural ligand for the Fas receptor is Fas ligand (FasL), a transmembrane protein (Brint et al. 2013), however expression of FasL is not ubiquitous and expression is restricted to haematopoietic cells and the immune privileged sites of the eye and testes (Brint et al. 2013).

Fas induces apoptosis through either the extrinsic pathway, where pro-caspase-8 and the DISC complex act to amplify the signal, or through the intrinsic pathway, where mitochondria amplify the apoptotic signal (Scaffidi et al. 1998). Fas induces apoptosis of activated mature T cells, virally infected or cancer cells and immune cells which

enter immune privileged sites (Ashkenazi & Dixit 1998; Brint et al. 2013).

Fas protein expression has been shown in human alveolar lung basal epithelial (A549) cells (Serrao et al. 2001), rabbit alveolar epithelium, macrophages and airway epithelium (Matute-Bello et al. 2001). HUVECs have also been shown to express Fas mRNA (Sata et al. 2000). The downstream apoptotic mediator of Fas, FADD (Fas-associated protein with death domain), caspase-1 and caspase-3 are elevated in the lungs from patients with idiopathic pulmonary fibrosis (Maeyama et al. 2001). FasL is also expressed on HUVECs (Sata et al. 2000) and FasL induces apoptosis of a variety of different cell types, including rabbit type II (Matute-Bello et al. 2001) and mouse macrophage RAW cells (Lu et al. 2002).

However, more specific to findings in this chapter, Fas mRNA and protein is expressed in vascular smooth muscle cells (Sata et al. 2000; Geng et al. 1997). Interestingly, Fas expression has been identified in the lipid core and fibrous caps of atherosclerotic plaques (Geng et al. 1997). Furthermore, apoptotic SMCs express Fas in atherosclerotic plaques (Geng et al. 1997). Although the role of Fas in apoptosis has been extensively reported, Fas has also been shown to induce the proliferation of normal human foreskin diploid fibroblasts (Aggarwal et al. 1995) and ligation has been shown to induce CD3 activated T-cell and naïve T-cell proliferation (Alderson et al. 1993). Fas also interacts with LC3B-II and caveolin-1 to mediate a dynamic switch between apoptosis and autophagy in lung epithelial cells (Tanaka et al. 2012). This is interesting because autophagy has recently been implicated as an important process in PAH pathogenesis (Long et al. 2013; Lee et al. 2011).

Although Fas has not been implicated in PAH, TRAIL, another member of the TNF superfamily, is also an important mediator PAH (Hameed et al. 2012). Having previously been reported to induce cancer cell apoptosis (Emery et al. 1998), TRAIL is now known to induce VSMC and PA-SMC proliferation and migration and TRAIL R1 and TRAIL R3 receptors are both significantly upregulated in IPAH PA-SMCs (Secchiero et al. 2004; Hameed et al. 2012). Taking into account the fact that Fas is expressed in PA-SMCs, both from healthy and IPAH donors, Fas is expressed along with OPG in IPAH patient sections and that TRAIL and the TRAIL receptors R1 and R3 are important in the pathogenesis of PAH, this all supports the possibility that

OPG binding to Fas may be mediating pathogenic changes in PA-SMCs.

To summarise, the aim of this chapter was to identify potential binding partners for OPG on PA-SMCs. These data reveal for the first time, four novel interactions between OPG and GAP-43, TMPRSS11D, IL1RAcP and Fas receptor (Figure 3.9). However, it seems most likely that Fas may be acting as the binding partner for OPG in diseased PA-SMCs. The importance of the OPG-Fas interaction in mediating PA-SMC phenotype will be investigated further in the following chapters. After identifying potential OPG binding partners, the proteins through which OPG is signalling and the genes that are transcribed as a result of OPG signalling in PA-SMCs will be investigated in the next chapter. Several known downstream signalling proteins of TMPRSS11D, GAP43, IL1RAcP and Fas are also shown in Figure 3.9. In the next chapter, I will investigate whether OPG can induce changes in these, and many other intracellular proteins, and induce changes in gene expression, by using an unbiased screening approach. This will allow me to identify OPG-induced changes in protein expression and activation and gene expression that may be causing PA-SMC proliferation.

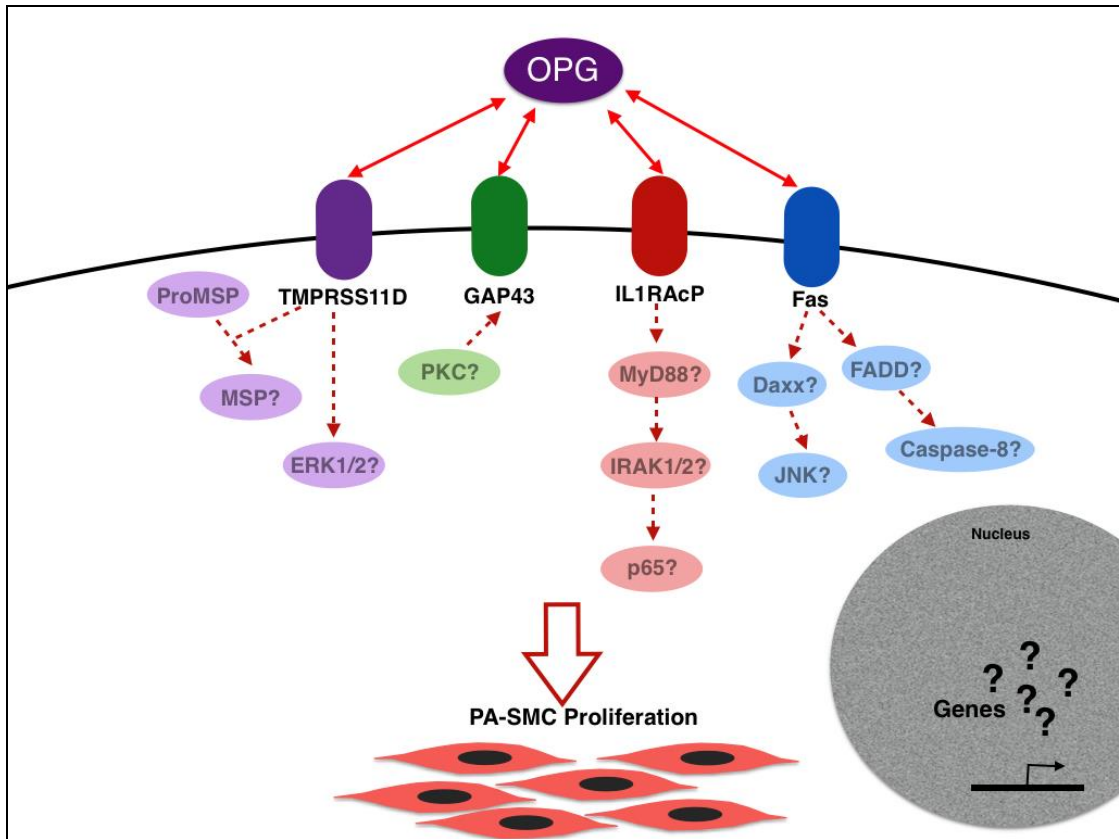


Figure 3.9- OPG was found to bind 4 novel binding partners, Fas, IL1RAcP, Gap43 and TMPRSS11D.

Several proteins that signal downstream of TMPRSS11D (Orikawa et al. 2012; Matsushima et al. 2006), GAP43 (Strittmatter et al. 1991; Denny 2006), IL1RAcP (Boraschi & Tagliabue 2013) and Fas (Brint et al. 2013) are also shown, however whether these proteins are involved in mediating the receptor signalling has yet to be investigated.

4. IDENTIFICATION OF OPG REGULATED PROTEIN AND RNA EXPRESSION IN PULMONARY ARTERIAL SMOOTH MUSCLE CELLS

4.1 Introduction

The results in the previous chapter identified four potential novel binding partners for OPG, with Fas being the most likely candidate for the receptor to which OPG is binding to induce pathogenic changes in PA-SMCs. The aim of the work presented in this chapter was to examine the intracellular mechanisms that are activated as a result of OPG binding to the receptor on the cell surface. Firstly, the intermediate protein signalling that leads to gene transcription was investigated by assessing changes in the expression and activation of proteins in PA-SMCs. Secondly, the changes in gene expression induced by OPG in PA-SMCs was assessed. Exploring the changes in gene and protein expression and protein activation in OPG-stimulated cells will help build our understanding of how OPG is inducing pathogenic changes in PA-SMCs and potentially identify any targets that may offer therapeutic potential in the future. Furthermore, this will provide evidence as to whether OPG can alter the expression of proteins that signal downstream of the binding partners that were identified in Chapter 3 (Figure 3.9), particularly the IL-1 and Fas-signalling pathways. This will provide more evidence as to whether the interactions between OPG and Fas and IL1RAcP are driving the phenotypic changes in PA-SMCs.

OPG has been found to induce the phosphorylation of ERK1/2 in HMVEC (Kobayashi-Sakamoto et al. 2008) and ERK1/2, Akt and mTOR in endothelial-colony forming cells (Benslimane-Ahmim et al. 2011) but there have been no reports about changes in protein or gene expression induced by OPG in PA-SMCs. Therefore, an unbiased array approach was used, much like the cell microarray used in Chapter 3, to identify OPG-induced changes in protein activation and gene expression in PA-SMCs.

4.2 Aims

The first aim of this chapter was to determine OPG-induced changes in protein expression and activation in PA-SMCs and validate selected targets by in-cell western and traditional western blotting. The second aim was to identify OPG-induced changes in gene expression and subsequently validate selected genes by TaqMan quantitative RT-PCR.

4.3 Methods

4.3.1 Kinex Antibody Microarray

In order to identify OPG-induced changes in protein phosphorylation and expression, a Kinex antibody microarray (Kinex, Canada) was performed on unstimulated and OPG-stimulated HPA-SMC lysates, at 10 minute and 60 minute time points, as previously described in chapter 2.7. Uniprot accession codes of proteins deemed significantly regulated by OPG (z-ratio of ± 1.5) were then analysed using DAVID functional annotation to generate fold enrichment pathway analysis through the Kegg Pathway Database. Intersections of ≥ 2 fold change and $p \leq 0.05$ were used for the pathway fold enrichment analysis (Chapter 2.7 and 2.8).

4.3.2 In-Cell Western Assay (primary validation of the KAM)

Results from the Kinex Antibody Microarray were validated using an In-Cell western assay, as previously described in chapter 2.9.1. HPA-SMCs (P4-P7) were stimulated with rhOPG (50 ng/ml) or 0.2% v/v FBS for 10 and 60 minutes. Cells were fixed and permeabilised before incubating with phospho-CDK2, phospho-CDK4, phospho-HSP27 (S15), phospho-ERK1/2, phospho-PLC γ 2 or phospho-AKT primary antibodies. Cells were then incubated with secondary antibodies and the nuclear stains, DRAC5 and sapphire 700 for signal normalisation to cell number (Chapter 2.9).

4.3.3 Western Blotting (secondary validation of the KAM)

Western blotting was performed on cell lysates stimulated with OPG (50 ng/ml) or 0.2% v/v FBS (unstimulated) for 10 minutes and 60 minutes, as described in Chapter 2.9.2. Membranes were incubated with phospho-CDK4, phospho-ERK1/2, phospho-HSP27, CDK5, Daxx, phospho-mTOR, Atg13, Atg5, GβL and FADD. Following secondary antibody incubation, membranes were washed and scanned using the LiCor Odyssey Sa system (Chapter 2.9.2).

4.3.4 Agilent 8-plex single colour RNA microarray

RNA was extracted from HPA-SMCs after 6 hour stimulation with OPG or 0.2% v/v FBS (negative). Agilent 8-plex, single colour human gene expression microarrays were then performed to analyse gene expression in HPA-SMCs. The data was background corrected and Log₂ transformed using Bioconductor and Lima programs in the programming language R. Output files were then organised by removing duplicate probes and using the intersection of Log₂ fold change >0.3 and p<0.05. A heat map was generated to show OPG-regulated genes that are associated with PAH (Appendix 7.5). Agilent Oligo IDs of genes regulated by OPG were then analysed using DAVID functional annotation to generate fold enrichment pathway analysis through the Kegg Pathway Database (Chapter 2.10).

4.3.5 Real-time TaqMan qPCR Validation

Taqman validation was performed on the RNA from the nine unstimulated RNA samples and nine OPG stimulated RNA samples used for the microarray, and a further four unstimulated (0.2% v/v FBS) and four OPG-stimulated HPA-SMC samples generated separately from the microarray samples. Taqman data was normalised using $\Delta\Delta\text{CT}$, with 18S rRNA as the endogenous control (Chapter 2.11).

4.3.6 Statistical analysis

All data are represented as mean \pm SEM. Treatments were compared using One-way ANOVA followed by Tukey's post hoc test for multiple comparisons. When comparing only two groups, an unpaired T-test was used. P<0.05 was deemed

statistically significant. The n numbers refer to the number of separate experiments performed and for each experiment performed, each condition was performed in duplicate or triplicate.

4.4 Results

4.4.1 Kinex Antibody Microarray

Out of the 812 antibodies (262 phospho-specific and 550 pan-specific antibodies) screened in the Kinex antibody microarray (KAM), OPG was found to significantly up-regulate or down-regulate the expression or phosphorylation of 89 proteins (Table 4.1). Of these 89 proteins, phosphorylation of 12 proteins and expression of 77 proteins were significantly altered by OPG (Table 4.1). Alterations in protein expression and phosphorylation were observed at 10 minutes and 60 minutes, however for a number of proteins, these changes were found to persist between 10 minutes and 60 minutes (Table 4.1). However, 89 proteins was a large number of proteins to validate and subsequently investigate in more detail. Therefore, further analysis of the protein list was paramount to interpolate the biological meaning of the proteins altered by OPG. To do this, the protein list was analysed using DAVID to look at the pathway fold enrichment.

OPG was found to alter the expression and phosphorylation of proteins that function in a wide variety of signalling pathways, including p53, VEGF, apoptosis, Toll-like receptor, MAPK, chemokine signalling and focal adhesion (Figure 4.1), all of which are known to be involved in PAH pathogenesis. Interestingly, OPG altered the expression and activation of proteins belonging to a variety of cancer pathways, including non-small cell lung cancer, chronic myeloid leukaemia, bladder cancer, glioma, small cell lung cancer, pancreatic cancer, prostate cancer, endometrial cancer, acute myeloid leukaemia, colorectal cancer and melanoma. The fact that OPG altered proteins involved in cancer pathways is very interesting because PAH shares similarities to cancer pathogenesis (Rai et al. 2008) (Figure 4.1).

Table 4.1- Summary of Kinex protein expression and protein phosphorylation significantly altered by OPG in PA-SMCs

Serial No.	Antibody Codes	Target Protein Name	Phospho Site (Human)	Full Target Protein Name	Z-ratio (50ng/mL OPG 10', 0.2% FCS 10')	Z-ratio (50ng/mL OPG 60', 0.2% FCS 60')	Refseq	Uniprot Link
5	NK001	Abl	Pan-specific	Abelson proto-oncogene-encoded protein-tyrosine kinase	-0.21	9.79	NP_005148	P00519
9	NK002	ACK1	Pan-specific	Activated p21cdc42Hs protein-serine kinase	1.73	-1.12	NP_005772	Q07912
21	NK007	ASK1 (MAP3K5)	Pan-specific	Apoptosis signal regulating protein-serine kinase	-1.60	1.67	NP_005914	Q99683
17	NN004	APG1	Pan-specific	Hsp 70-related heat shock protein 1 (osmotic stress protein 94 (OSP94))	-1.40	2.24	NP_055093	Q95757
18	NN122	APG2	Pan-specific	Hsp 70-related heat shock protein 4 (HSP70RY)	0.16	2.03	BAA75062	P34932
21	NK007	ASK1 (MAP3K5)	Pan-specific	Apoptosis signal regulating protein-serine kinase	-1.60	1.67	NP_005914	Q99683
27	NK008-1	Aurora A (AIK)	Pan-specific	Aurora Kinase A (serine/threonine protein kinase 6)	0.31	1.64	NP_940835	Q14965
43	NN009	Bid	Pan-specific	BH3 interacting domain death agonist	0.47	1.52	NP_001187	P55957
133	NN025	c-IAP1	Pan-specific	Cellular inhibitor of apoptosis protein 1 (baculoviral IAP repeat-containing protein 3, apoptosis inhibitor 2 (API2))	3.35	-2.62	NP_001156	Q13490
53	PN015	Caldesmon	S789	Caldesmon	1.53	-0.19	NP_004333	Q05682
69	NK021-2	CaMK4	Pan-specific	Calcium/calmodulin-dependent protein-serine kinase 4	-3.13	-0.51	NP_001735	Q16566
75	NN011-NN125	CASP1ab	Pan-specific	Pro-caspase 1 (Interleukin-1 beta convertase) alpha/beta isoform	-1.78	0.85	NP_001214	P29466
80	NN016	CASP6	Pan-specific	Pro-caspase 6 (apoptotic protease Mch2)	-3.27	-0.16	NP_001217	P55212
139	PN130	c-Myc	T58/S62	Myc proto-oncogene protein	-0.05	3.29	NP_002458.2	P01106
88	NP003	Cdc25C	Pan-specific	Cell division cycle 25C phosphatase	0.71	-1.84	NP_001781	P30307
96	NK025-4	CDK1 (CDC2)	Pan-specific	Cyclin-dependent protein-serine kinase 1	1.62	2.49	NP_001777	P06493
102	PK007-3	CDK1/2	Y15	Cyclin-dependent protein-serine kinase 1/2	-2.91	-1.74	NP_001777	P06493
110	NK026-6	CDK2	Pan-specific	Cyclin-dependent protein-serine kinase 2	3.06	3.60	NP_001789	P24941
112	NK027-2	CDK4	Pan-specific	Cyclin-dependent protein-serine kinase 4	1.67	0.14	NP_000066	P11802
116	NK028-4	CDK5	Pan-specific	Cyclin-dependent protein-serine kinase 5	6.58	2.84	NP_004926	Q00535
118	NK029-2	CDK6	Pan-specific	Cyclin-dependent protein-serine kinase 6	2.38	3.98	NP_001250	Q00534
121	NK030-2	CDK7	Pan-specific	Cyclin-dependent protein-serine kinase 7	5.53	0.32	NP_001790	P50613
125	NK031-5	CDK8	Pan-specific	Cyclin-dependent protein-serine kinase 8	2.22	2.84	NP_001252	P49336
127	NK032	CDK9	Pan-specific	Cyclin-dependent protein-serine kinase 9	1.79	-0.89	NP_001252	P50750
104	NK033	CDK10	Pan-specific	Cyclin-dependent protein-serine kinase 10 [PISLRE]	0.66	1.87	NP_003665	Q15131
131	NK035	Chk2	Pan-specific	Checkpoint protein-serine kinase 2	1.90	-0.01	NP_009125	Q96017
134	NK036	CK1d	Pan-specific	Casein protein-serine kinase 1 delta	0.38	2.45	NP_001884	P48730
136	NK198	CK1g	Pan-specific	Casein kinase I gamma 1 isoform	2.84	-0.09	NP_071331	Q8IXA3
137	NK040	CK1g2	Pan-specific	Casein protein-serine kinase 1 gamma 2	2.37	-0.09	NP_001310	P78368
144	NK042	COT	Pan-specific	Osaka thyroid oncogene protein-serine kinase (Tpl2)	-0.31	3.07	NP_005195	P41279
158	NK044-2	Csk	Pan-specific	C-terminus of Src tyrosine kinase	1.16	-9.53	NP_004374	P41240
164	NN032	Cyclin G1	Pan-specific	Cyclin G1	-1.61	-2.84	NP_004051	P51959
165	NN033	CytoC	Pan-specific	Cytochrome C	0.78	-1.76	NP_061820	P99999
168	NK046	DAPK2	Pan-specific	Death-associated protein kinase 2	-1.70	-0.53	NP_055141	Q9UIK4
169	NN034	DAXX	Pan-specific	Death-associated protein 6 (BINC2)	-1.15	-1.56	NP_001341	Q8UER7
173	NK048-2	DNAPK	Pan-specific	DNA-dependent protein kinase catalytic subunit	-1.65	-2.16	NP_008835.5	P78527
179	PK009	EGFR	Y1092	Epidermal growth factor receptor-tyrosine kinase	-1.75	-0.61	NP_005219	P00533
209	NK206-1	Erk5	Pan-specific	Extracellular regulated protein-serine kinase 5 (Big MAP kinase 1 (BMK1))	-3.78	2.13	NP_620602	Q13164
224	NN042	FAS	Pan-specific	Tumor necrosis factor superfamily member 6 (Apo1, CD95)	-2.98	1.43	NP_003789	P25445
232	NN044	Fos	Pan-specific	Fos-c FBJ murine osteosarcoma oncoprotein-related transcription factor	-0.69	2.18	NP_005243	P01100
234	NK065	Fyn	Pan-specific	Fyn proto-oncogene-encoded protein-tyrosine kinase	-1.93	1.40	NP_002028	P06241
258	PN035	Histone H1	hospho CDK1 site	Histone H1 phosphorylated	1.64	0.17	NP_005316	Q02539
265	PN101-2	Histone H3	T3	Histone H3.3	-1.56	1.67	NP_003521	P84243
267	NN052-2	HO1	Pan-specific	Heme oxygenase 1	-0.24	2.51	NP_002124	P09601
270	NN054	Hsc70	Pan-specific	Heat shock 70 kDa protein 8	-2.11	3.06	NP_006588	P11142
277	PN040-1	Hsp27	S15	Heat shock 27 kDa protein beta 1 (HspB1)	3.48	0.14	NP_001531	P04792
303	NN061-11	Hsp90a	Pan-specific	Heat shock 90 kDa protein alpha	1.85	1.53	NP_005339	P07900
310	NN061-17	Hsp90b	Pan-specific	Heat shock 90 kDa protein beta	-1.90	0.53	NP_031381	P08238
318	NN064-2	IkBa	Pan-specific	Inhibitor of NF-kappa-B alpha (MAD3)	-0.07	-1.84	NP_065390	P25963
324	NK075-2	IKKa	Pan-specific	Inhibitor of NF-kappa-B protein-serine kinase alpha (CHUK)	1.76	-1.32	NP_001269	Q15111
328	PK030-PK031	IKKa/b	S180/S181	Inhibitor of NF-kappa-B protein-serine kinase alpha/beta	1.84	-0.19	NP_001269	Q15111

329	NK076-1	IKKb	Pan-specific	Inhibitor of NF-kappa-B protein-serine kinase beta	4.13	-4.33	NP_001547	O14920
334	NK078-3	ILK1	Pan-specific	Integrin-linked protein-serine kinase 1	3.54	-0.24	NP_034692	O13418
336	PN044	Integrin b1	S785	Integrin beta 1 (fibronectin receptor beta subunit, CD29 antigen)	2.43	0.61	NP_002202	P05556
340	PK033	IR/IGF1R (INSR)	Y1189/Y1190	Insulin receptor / Insulin-like growth factor 1 receptor	1.62	1.60	NP_000866	P06213
344	NK081-2	IRAK2	Pan-specific	Interleukin 1 receptor-associated kinase 2	1.91	0.01	NP_001561	O43187
350	PN046-2	IRS1	Y1179	Insulin receptor substrate 1	2.23	1.95	NP_005535	P35568
363	NK088-2	JNK1/2/3	Pan-specific	Jun N-terminus protein-serine kinases (stress-activated protein kinase (SAPK)) 1/2/3	3.61	-0.02	NP_002741	P45983
366	NK196	JNK2/3	Pan-specific	Jun N-terminus protein-serine kinase (stress-activated protein kinase (SAPK/b)) 2/3	-1.86	0.16	NP_002743.3	P45984
401	NN155	MEF-2	Pan-specific	Myelin expression factor 2 (MYEF2)	-6.42	-2.35	NP_057216.2	Q9P2K5
422	NK101	MEK3 (MAP2K3)	Pan-specific	MAPK/ERK protein-serine kinase 3 (MKK3)	-0.21	1.75	NP_659732	P46734
430	NK103	MEK4 (MAP2K4)	Pan-specific	MAPK/ERK protein-serine kinase 4 (MKK4)	-1.39	5.74	NP_003001	P45985
480	NK207	NIK	Pan-specific	NF-kappa beta-inducing kinase	-0.74	-2.46	NP_003945.2	Q99558
490	NN080	p27 Kip1	Pan-specific	p27 cyclin-dependent kinase inhibitor 1B	0.73	-2.47	NP_004055	P46527
492	NN081-NN120	p35, p25	Pan-specific	CDK5 regulatory subunit 1, p35, p25	-0.85	-2.31	NP_003876	Q15078
494	PK060-2	p38a MAPK	T180+Y182	Mitogen-activated protein-serine kinase p38 alpha	1.56	-1.67	NP_001306	Q16539
514	NP008	PAC1	Pan-specific	Dual specificity MAP kinase protein phosphatase	-0.68	6.84	NP_004409	Q05923
531	PN060-1	Paxillin 1	Y118	Paxillin 1	-1.65	-1.90	NP_002850	P49023
533	NN087	PCNA	Pan-specific	Proliferating cell nuclear antigen	3.87	1.70	NP_002583	P12004
540	NK126-2	PDK1	Pan-specific	3-phosphoinositide-dependent protein-serine kinase 1	-2.01	-0.38	NP_002604	O15530
543	NN088	PERP	Pan-specific	p53-induced protein PIGPC1	1.69	-1.45	NP_071404	Q9H230
550	NK213	PITSLRE	Pan-specific	PITSLRE serine/threonine-protein kinase CDC2L1	2.73	-4.08	NP_277028.1	P21127
576	PK074	PKCa/b2	T638/T641	Protein-serine kinase C alpha, beta 2	-1.76	-0.44	NP_002728	P17252
577	NK133	PKCb1	Pan-specific	Protein-serine kinase C beta 1	-2.03	0.66	NP_002729	P05771
589	NK136-2	PKCe	Pan-specific	Protein-serine kinase C epsilon	-1.76	1.80	NP_005391	Q02156
591	NK137	PKCg	Pan-specific	Protein-serine kinase C gamma	0.35	-2.28	NP_002730	P05129
599	NK142	PKCm (PKD)	Pan-specific	Protein-serine kinase C mu (Protein kinase D)	-2.52	0.38	NP_002733	Q15139
616	NN156	PLC R(PLCg2)	Pan-specific	1-phosphatidylinositol-4,5-bisphosphate phosphodiesterase gamma-2	-0.36	2.71	NP_002652.2	P16885
638	NP020	PP4C	Pan-specific	Protein-serine phosphatase X - catalytic subunit (PPX/C)	-2.44	0.14	NP_002711	P60510
645	NK148	PRK1 (PKN1)	Pan-specific	Protein kinase C-related protein-serine kinase 1	-2.00	1.97	NP_002732	Q16512
674	NK155-4	Raf1	Pan-specific	Raf1 proto-oncogene-encoded protein-serine kinase	2.09	2.31	NP_002871	P04049
677	NK205-2	RafA (Araf)	Pan-specific	A-Raf proto-oncogene serine/threonine-protein kinase	1.83	-0.23	NP_001645.1	P10398
719	NK170	SGK3	Pan-specific	Serum/glucocorticoid regulated kinase 3	0.69	2.69	NP_037389.4	Q96BR1
729	NN145	Socs2	Pan-specific	Suppressor of cytokine signaling 2	1.50	1.99	NP_003868.1.	O14508
740	NK172-4	Src	Pan-specific	Src proto-oncogene-encoded protein-tyrosine kinase	1.50	0.18	NP_005408	P12931
757	NN106	STAT5B	Pan-specific	Signal transducer and activator of transcription 5B	0.91	-1.78	NP_036580	P51692
780	NK220-2	TBK1	Pan-specific	Serine/threonine-protein kinase TBK1	-0.23	2.23	NP_037386	Q9UHD2
790	NK181-2	Tyk2	Pan-specific	Protein-tyrosine kinase 2 (Jak-related)	-9.07	1.69	NP_003322	P29597
803	NK186	Yes	Pan-specific	Yamaguchi sarcoma proto-oncogene-encoded tyrosine kinase	-2.01	0.10	NP_005424	P07947

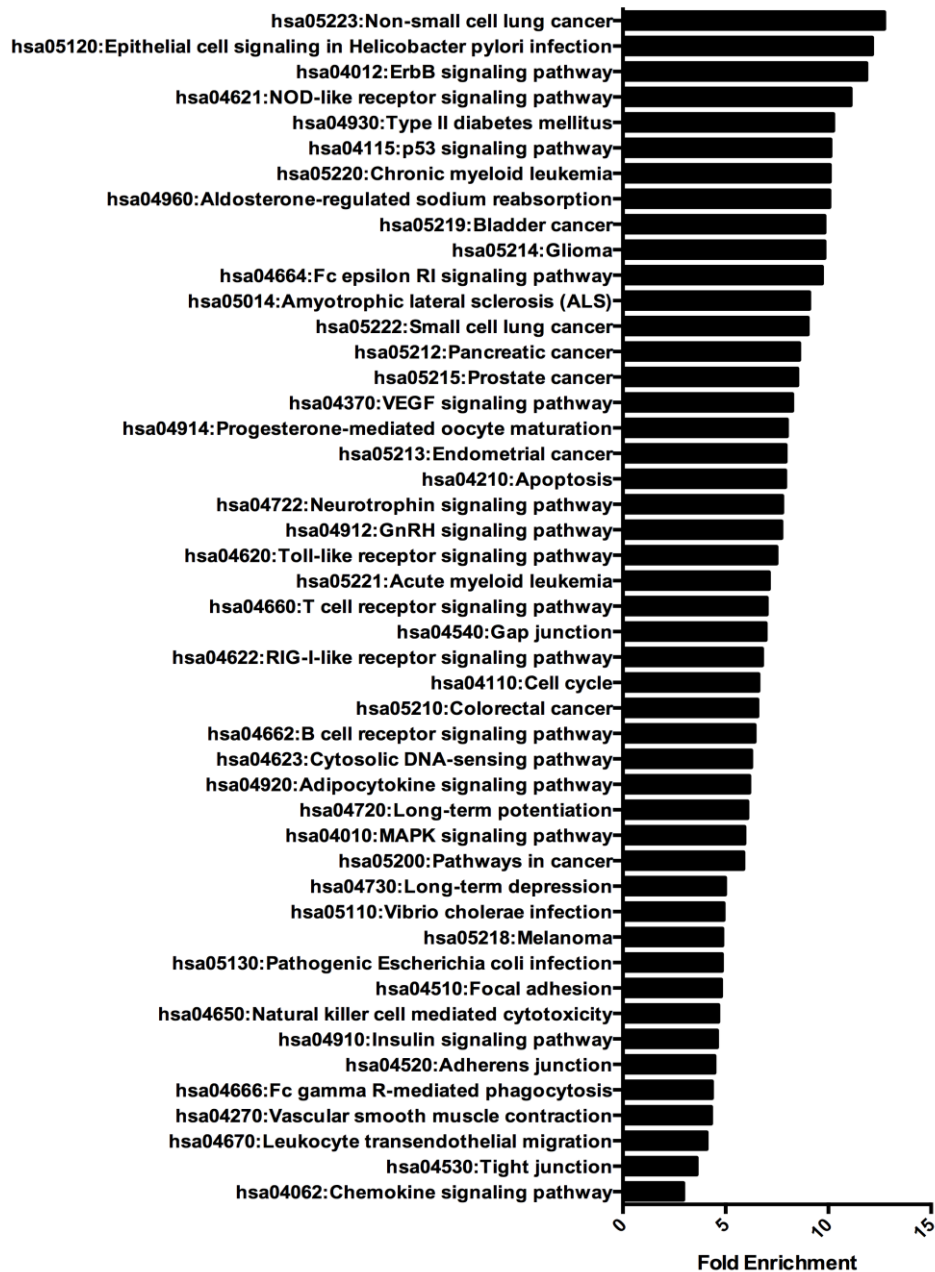


Figure 4.1- Pathway fold enrichment in OPG-stimulated HPA-SMCs.

Fold enrichment of different pathways was calculated using DAVID. The fold enrichment of a certain pathway demonstrates how many fold were proteins of the pathway altered than would be expected by chance. Uniprot accession codes of proteins deemed significantly regulated by OPG (z-ratio of ± 1.5) were then analysed using DAVID functional annotation to generate fold enrichment pathway analysis through the Kegg Pathway Database. Intersections of ≥ 2 fold change and $p \leq 0.05$ were used for the pathway fold enrichment analysis.

However, even after looking at the different pathways in which the proteins altered by OPG signalled in, I wanted to further focus my attention on several proteins that I would go on to validate. Therefore, OPG-regulated protein expression at the two different time points, proteins that were significantly regulated by OPG at both 10 minutes and 60 minutes (as shown in Table 4.1) were then presented as a heat map (Figure 4.2). This was done to allow for better visual interpretation of the results to select the proteins whose expression and phosphorylation was altered by OPG at different time points.

Interestingly, OPG was found to increase the expression of cell cycle proteins Abl, c-myc, chk2 and the cyclin dependent kinases CDK1, CDK2, CDK4, CDK5, CDK6, CDK7, CDK8 and CDK9 and alter the expression and phosphorylation of heat shock proteins HSP27, HSP70 and HSP90 (Table 4.1 and Figure 4.2). The ability of OPG to alter Abl was interesting because Imatinib, a small tyrosine kinase inhibitor used to treat the chronic myeloid leukaemia by targeting the BCR-ABL fusion protein (Ciarcia et al. 2012), has also been considered as a PH treatment.

Furthermore, OPG was found to increase expression of the IL-1 signalling pathway kinase IRAK2 (Interleukin-1 receptor-associated kinase-like 2) and decreased expression Fas at 10 minutes and Daxx, a cytoplasmic protein that can interact with Fas and mediate Fas signalling, at 10 and 60 minutes. However, Fas expression was increased at 60 minutes (Table 4.1 and Figure 4.2). The finding that OPG was able to alter the expression of Fas and Daxx was of particular interest after finding that OPG was able to interact with Fas (previously discussed in Chapter 3). Interestingly, although the Z-score was not deemed significant, OPG was found to reduce the expression of mTOR, an inhibitor of autophagy (Z-score ratio -1.05, Appendix 7.3).

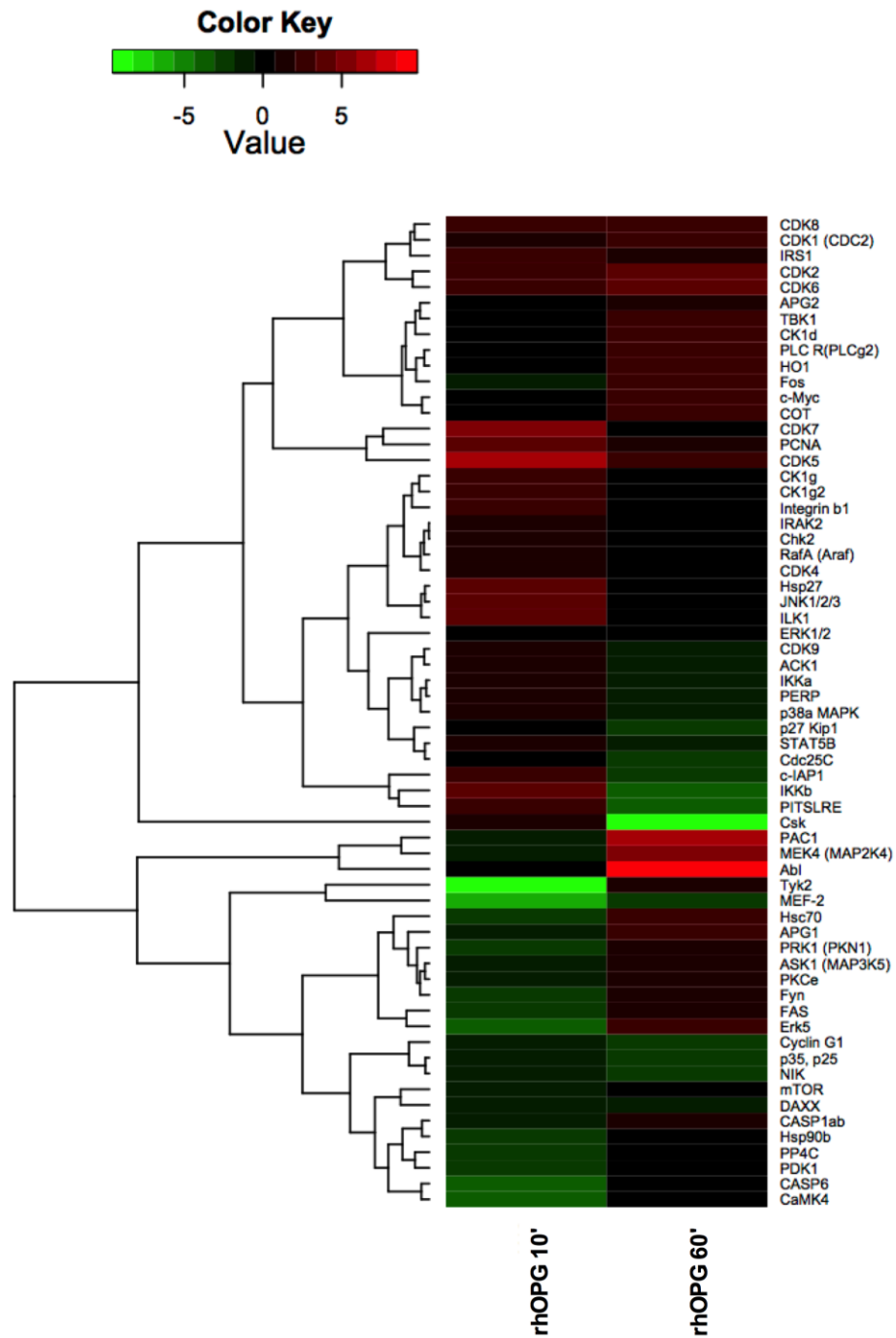


Figure 4.2- Heat map of KAM protein expression and phosphorylation.

Kinex antibody microarray revealed OPG both positively and negatively regulates protein phosphorylation and total protein expression. Heat map shows Z-ratio of protein phosphorylation and total protein expression.

4.4.2 In-Cell Western Validation of OPG-induced Protein Expression and Phosphorylation

To validate the KAM results, several protein targets were selected for validation by in-cell western assay. The proteins selected for validation based on KAM results and pathway analyses were phospho-CDK2, phospho-HSP27, phospho-PLC γ 2, phospho-Akt and ERK1/2. Targets were selected for validation based on Z-ratio, differential time-dependent regulation or involvement in pathways relevant to PAH disease pathogenesis and HPA-SMC phenotype. Although results of the KAM revealed a change in total CDK4 in response to OPG stimulation, phospho-CDK4, the activate form of CDK4, was also selected for analysis by the in-cell western.

Signal quantification of the in-cell western assay revealed rhOPG significantly induced the phosphorylation of CDK4, HSP27 and ERK1/2 (Figure 4.3 B, D and F respectively). Compared to quiesced HPA-SMCs, rhOPG induced a 67% increase in CDK4 phosphorylation at 10 minutes (Figure 4.3 B) and a 90% increase in CDK4 phosphorylation at 60 minutes (Figure 4.3 B). Signal quantification also revealed significant ERK1/2 phosphorylation in OPG-stimulated HPA-SMCs compared to quiesced HPA-SMCs. Compared to unstimulated, quiesced cells, OPG induced a 182% increase in ERK1/2 phosphorylation at 10 minutes (Figure 4.3 F) and a 133% increase in ERK1/2 phosphorylation at 60 minutes (Figure 4.3 F). Additionally, rhOPG induced a 242% in HSP27 phosphorylation in HPA-SMCs at 10 minutes and a 311% increase in HSP27 phosphorylation at 60 minutes compared to unstimulated, quiesced HPA-SMCs (Figure 4.3 D). OPG had no effect on phosphorylation of CDK2, Akt or PLC γ 2 (Figure 4.3 A, C and E respectively).

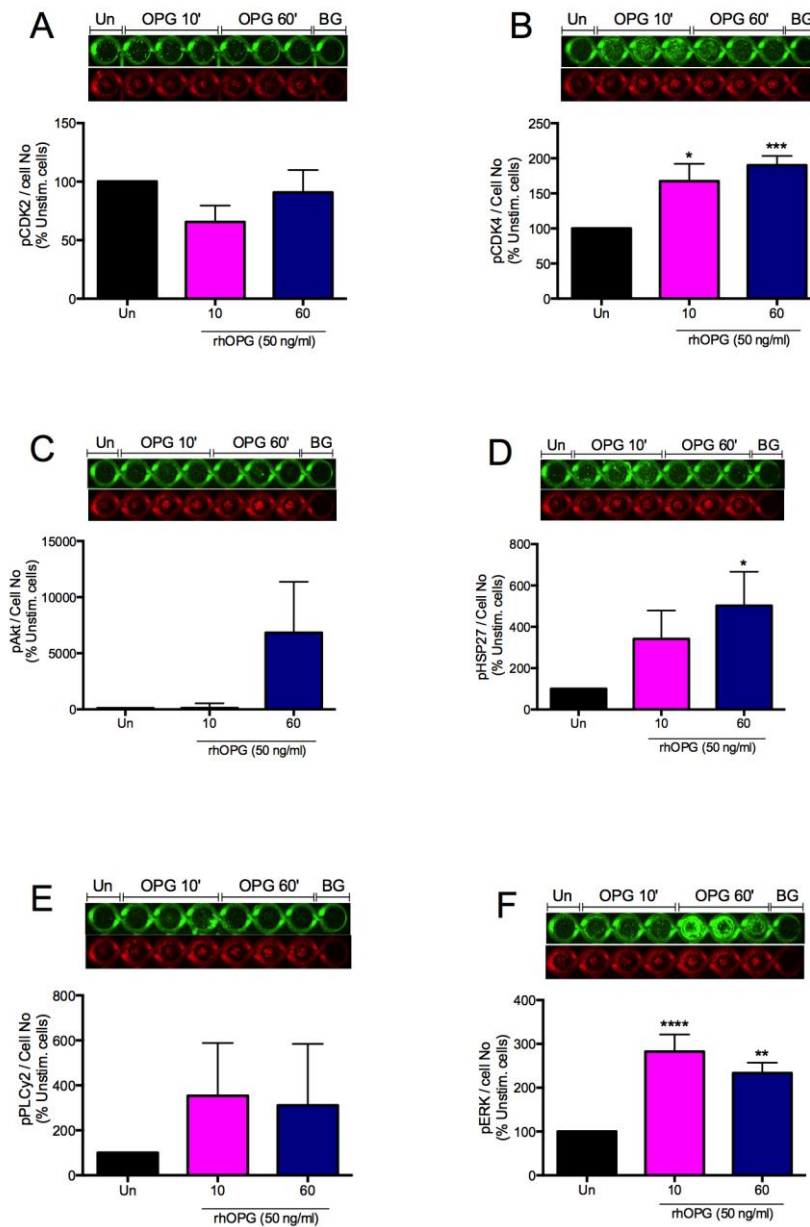


Figure 4.3- In cell western analysis of OPG-induced protein phosphorylation.

Graphs A-G show the effect of OPG stimulation at 10 minute and 60 minute time points on A) CDK2, B) CDK4, C) Akt, D) HSP27, E) PLC γ 2 and F) ERK1/2 in HPA-SMCs, compared to unstimulated, quiesced control HPA-SMCs. OPG was found to significantly increase phosphorylation of B) CDK4, D) HSP27 and F) ERK1/2 at 10 and 60 minutes compared to unstimulated, control cells. Representative images are shown above the bar graphs. Un= unstimulated (quiesced) HPA-SMCs, B=Background wells, 10= 10 minutes, 60= 60 minutes. Error bars represent mean \pm SEM. N=6 individual experiments. * p <0.05, ** p <0.01, *** p <0.001, **** p <0.0001.

4.4.3 Western blot validation of OPG-induced protein expression and phosphorylation

4.4.3.1 Effect of OPG on ERK1/2 and HSP27 Phosphorylation

The in-cell western assay is also a relatively high-throughput technique compared to traditional western blotting techniques. Therefore, the phosphorylation of proteins found to be significantly altered by OPG in the in-cell western assay were examined in OPG-stimulated HPA-SMCs using gold standard western blotting. OPG was found to induce a significant, almost 3-fold, increase in pERK1/2 at 10 minutes ($p < 0.0001$) and a significant 2-fold increase at 60 minutes ($p < 0.001$) in HPA-SMCs, compared to unstimulated cells (Figure 4.4 A). OPG however had no statistically significant effect on the levels of phospho-HSP27 expression after 10-minute or 60-minute stimulation (Figure 4.4 B). However, results show a trend towards increased HSP27 in HPA-SMCs, which may require further repeats to achieve statistical significance.

These data therefore support data from the in-cell western assay (Figure 4.3) showing that OPG significantly induced the phosphorylation of ERK1/2 at 10 and 60 minutes (Figure 4.4 A).

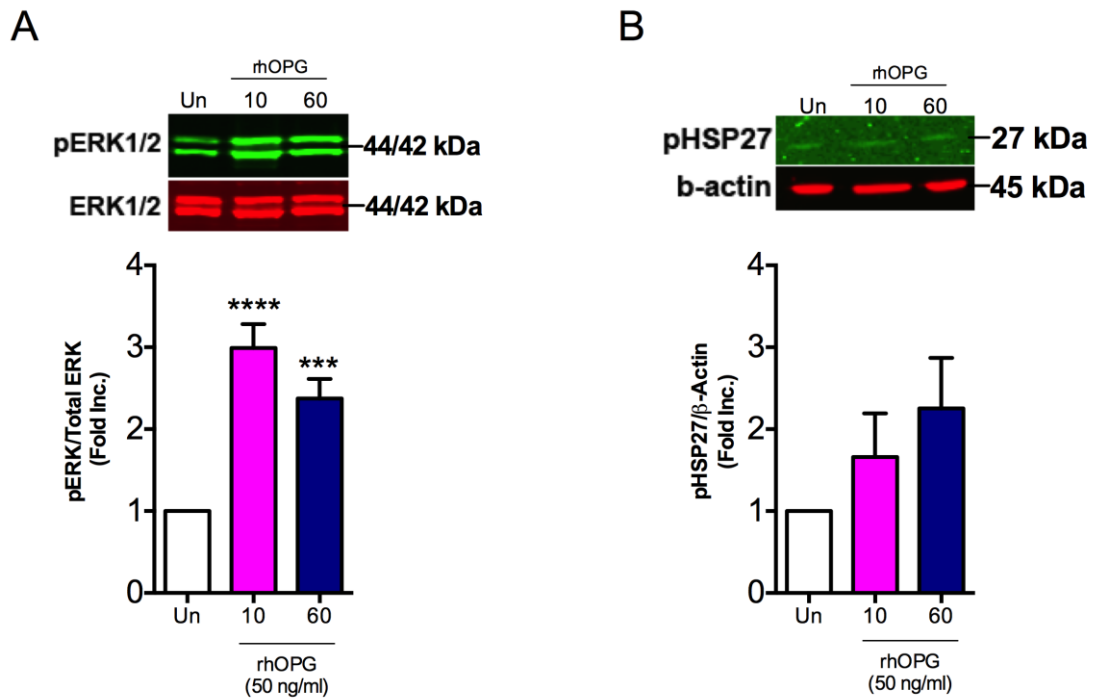


Figure 4.4- Western blot analysis of OPG-induced ERK1/2 and HSP27 protein phosphorylation in HPA-SMCs.

Graphs A and B show the effect of OPG stimulation at 10 minute and 60 minute time points on A) ERK1/2 and B) HSP27 phosphorylation in HPA-SMCs compared to unstimulated, quiesced control cells. A) OPG significantly increased the phosphorylation of ERK1/2 at 10 minutes and 60 minutes compared to unstimulated cells. Phospho-ERK1/2 levels were normalised to total ERK1/2 loading controls. B) OPG did not have any significant effect on the phosphorylation of HSP27 in HPA-SMCs. Phospho-HSP27 levels were normalised to β -actin loading controls. Relative band densities of pERK1/2 and pHSP27 are shown by the bar charts and representative western blot images shown above the graph. Un=Unstimulated cells, 10= 10 minutes, 60= 60 minutes. Bars represent mean \pm SEM, $n=5-10$. *** $p<0.001$, **** $p<0.0001$.

4.4.3.2 Effect of OPG on CDK4 Phosphorylation and CDK5 Expression

Levels of CDK4 phosphorylation were also measured by western blotting, however, CDK4 phosphorylation was not found to be significantly altered by OPG at 10 minutes or 60 minutes (Figure 4.5 A). However, results of the KAM revealed that the expression of another cyclin dependent kinase, CDK5, was found to be significantly increased by OPG (Table 4.1, Figure 4.2). CDK5 expression was found to be significantly increased by OPG after 60 minutes, compared to 10 minutes stimulation. However, when compared to unstimulated HPA-SMCs, there was no significant change in CDK5 protein levels detected in HPA-SMCs following 10-minute and 60-minute OPG stimulation ($p < 0.05$, Figure 4.5).

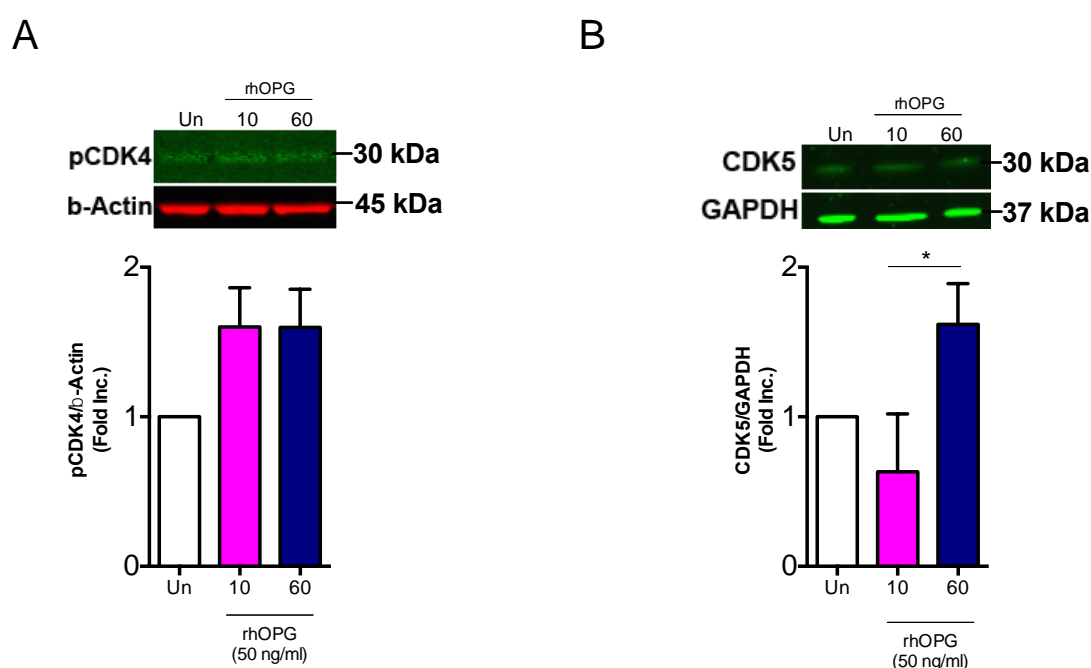


Figure 4.5- Western blot analysis of OPG-induced CDK4 phosphorylation and CDK5 expression in HPA-SMCs.

Graphs show the effect of OPG stimulation at 10 minute and 60 minute time points on A) CDK4 phosphorylation and B) CDK5 expression in HPA-SMCs compared to unstimulated cells. A) OPG was found to have no significant effect on CDK4 phosphorylation at 10 minutes or 60 minutes. Phospho-CDK4 levels were normalised to β -actin loading controls. B) OPG significantly increased CDK5 expression at 60 minutes, compared to 10-minute stimulation ($p < 0.05$). CDK5 levels were normalised to β -actin loading controls. Relative band densities of pCDK4 and CDK5 are shown by the bar charts and representative western blot images shown above the graph.

*Un=Unstimulated cells, 10= 10 minutes, 60= 60 minutes. Bars represent mean ± SEM, n=4-6. *p<0.05.*

So far, this chapter has focused on investigating the effects of OPG stimulation on the phosphorylation and expression of different proteins that are involved in anti-apoptotic (phospho-HSP27, CDK5), pro-proliferative (phospho-ERK1/2) and pro-survival (phospho-CDK4) pathways. However, my data shows that OPG can bind to the Fas receptor on PA-SMCs (Chapter 3). I therefore wanted to investigate whether OPG had any effect on the expression or activation of proteins belonging to the Fas signalling pathway.

4.4.3.3 Effect of OPG on Daxx and FADD Expression

Upon FasL binding, the Fas receptor multimerizes on the cell membrane and complexes with another death domain-containing protein, FADD (Fas-associated death domain), to signal through the caspases to induce apoptosis (Mollinedo & Gajate 2006; Brint et al. 2013; Ouyang et al. 2012). However, Fas-induced apoptosis is not exclusively mediated through FADD and the caspases. Another protein, Daxx, also associates with Fas to facilitate Fas-induced apoptosis.

Interestingly, results of the KAM revealed a significant reduction in Daxx expression, a protein known to associate with Fas to mediate apoptotic signalling in cells, after 60-minute stimulation with OPG, which was accompanied by an increase in Fas expression at 60 minutes. Western blotting revealed that OPG had no significant effect on Daxx expression at 10 minutes or 60 minutes (Figure 4.6). PA-SMCs were also stimulated with OPG for 24 hours in an attempt to determine whether OPG could induce changes in Daxx protein expression at a later time point. However, even after 24-hour stimulation, OPG had no significant effect on Daxx expression (Figure 4.6).

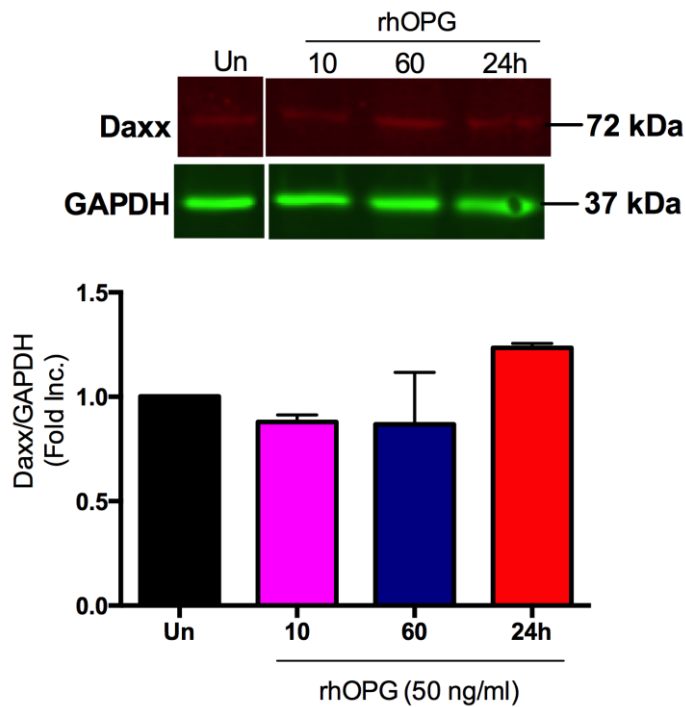


Figure 4.6- Western blot analysis of OPG-induced Daxx expression in HPA-SMCs. Graph shows the effect of OPG stimulation at 10 minute, 60 minute and 24-hour time points on Daxx expression in HPA-SMCs compared to unstimulated, quiesced control cells. OPG had no significant effect on Daxx expression in HPA-SMCs. Daxx levels were normalised to the GAPDH loading control. Relative band densities of Daxx are shown by the bar charts and representative western blot images shown above the graph. Un=Unstimulated cells, 10= 10 minutes, 60= 60 minutes, 24h= 24 hours. Error bars represent mean \pm SEM, n=3.

However, in addition to the interaction with Daxx, Fas forms a complex with another death domain-containing protein, FADD (Fas-associated death domain), to induce apoptosis through the intrinsic and extrinsic apoptotic pathways (Mollinedo & Gajate 2006). I therefore next sought to determine whether OPG could induce changes in FADD expression. However, western blotting revealed that OPG has no significant effect on FADD expression in PA-SMCs following 10-minute, 60-minute or 24-hour stimulation (Figure 4.7). I also analysed the expression of phospho-FADD in OPG-stimulated cells, however no bands were detected for phospho-FADD (data not shown).

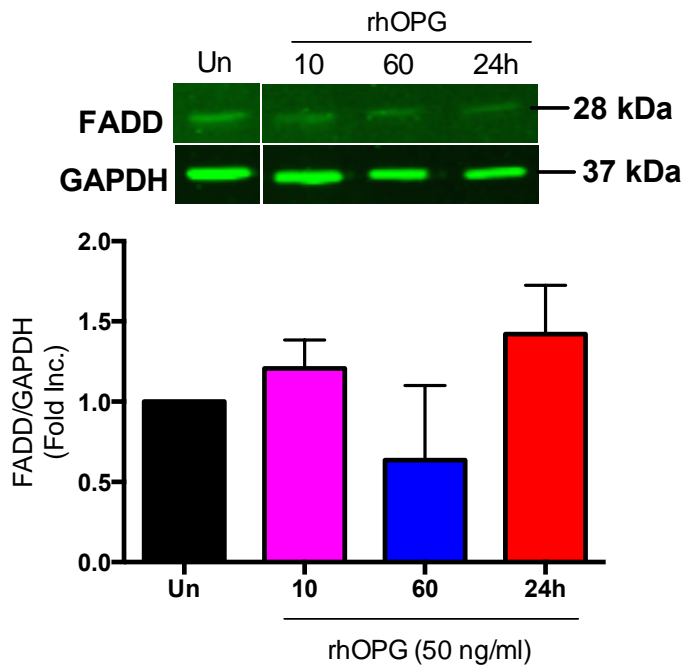


Figure 4.7- Western blot analysis of OPG-induced FADD expression in HPA-SMCs.

Graph shows the effect of OPG stimulation at 10 minute, 60 minute and 24-hour time points on FADD expression in HPA-SMCs compared to unstimulated, quiesced control cells. OPG had no significant effect on FADD expression in HPA-SMCs. FADD levels were normalised to the GAPDH loading control. Relative band densities of FADD are shown by the bar charts and representative western blot images shown above the graph. Un=Unstimulated cells, 10= 10 minutes, 60= 60 minutes, 24= 24 hours. Error bars represent mean \pm SEM, $n=3$.

My data show that OPG has no significant effect on the expression of Daxx and FADD. Furthermore, phospho-FADD was not detected in PA-SMCs. These data suggest that the OPG-Fas interaction may not be signalling directly through components the Fas signalling pathway in PA-SMCs. However, cross-talk between Fas and the autophagy pathway has recently been reported (Chen et al. 2010; Zhang et al. 2011; Tanaka et al. 2012). I therefore decided to investigate whether OPG was altering the expression of proteins belonging to the autophagy pathway.

4.4.3.4 Investigating the Effect of OPG on mTOR Phosphorylation, Atg13, Atg7 and GβL Expression in PA-SMCs

The autophagy pathway is a pro-survival pathway, which may be activated by OPG in PA-SMCs via Fas. The autophagy proteins that I selected to investigate the expression of are highlighted in Figure 4.8 A (yellow and red stars). I chose to investigate whether OPG could significantly change the expression of phospho-mTOR because the KAM revealed a reduction in mTOR expression in PA-SMCs following OPG stimulation (Figure 4.8 A, red star), although this reduction was not statistically significant. However, based on this result, I began to speculate that OPG might be inducing changes in the autophagy signalling pathway. Along with phospho-mTOR, the autophagy inhibitor, I also chose to examine expression changes of proteins that function in different branches of the autophagy pathway that were not analysed by the KAM to determine whether OPG stimulation was inducing changes in autophagy proteins that form complexes with, or signal downstream, of mTOR (Figure 4.8 A, yellow stars).

OPG was found to cause a significant difference in phospho-mTOR between 10 minutes and 60 minutes stimulation ($p < 0.05$, Figure 4.8 B). However, when compared to unstimulated HPA-SMCs, no significant change in phospho-mTOR was detected following OPG-stimulation at 10 minutes and 60 minutes (Figure 4.8 B). This suggests that OPG stimulation may cause a rapid reduction in mTOR activation to prevent autophagy inhibition and allow activation of downstream autophagy signalling, a response that recovers by 60 minutes.

After finding that OPG could induce changes in phospho-mTOR, I then went on to determine whether OPG could induce changes in the protein GβL, which binds to mTOR to activate the kinase activity of mTOR, facilitate complex formation with other proteins and mediate the downstream signalling of mTOR (Kim et al. 2003). However, OPG was not found to induce any significant changes on GβL expression in PA-SMCs following 10-minute, 60-minute or 24-hour stimulation with OPG (Figure 4.8 E).

In order to determine whether the change observed in mTOR phosphorylation was indeed having downstream effects on the autophagy signalling pathway, the

expression of two important autophagy proteins, Atg7 and Atg13, was examined in OPG-stimulated HPA-SMCs. However, OPG did not induce any significant changes in Atg13 or Atg7 expression at 10 minutes, 60 minutes or 24 hours, compared to unstimulated cells (Figure 4.8 C and D, respectively).

A) Autophagy schematic showing the proteins selected for investigation using western blotting (yellow stars). Expression of mTOR (red star) was also shown by the KAM to be reduced by OPG stimulation and although this result was not statistically significant, mTOR was also selected for validation by western blotting. Illustration reproduced courtesy of Cell Signaling Technology, Inc. (www.cellsignal.com). Bar graphs show the effect of OPG stimulation at 10 minute, 60 minute and 24-hour time points on B) phospho-mTOR, C) Atg13, D) Atg7 and E) GβL expression in HPA-SMCs compared to unstimulated, quiesced control cells. Relative band densities of phospho-mTOR, Atg13, Atg7 and GβL are shown by the bar charts and representative western blot images shown above the graph. Un=Unstimulated cells. Error bars represent mean ± SEM, n=3-6.

Having failed to see a significant change in the expression of Atg7, I next wanted to determine whether OPG could induce changes in the expression of LC3B-II. This was because LC3B-II plays an important role in the formation of the autophagosome, a double membrane vesicle into which cell organelles are packed into for recycling during autophagy (Tanaka et al. 2012). LC3B-II is formed from the LC3 precursor, which is first processed by Atg4 to form LC3-I and then LC3-I is activated, to form LC3B-II by Atg7 and Atg3, through the addition of a phosphatidylethanolamine (PE) group (He & Klionsky 2009; Codogno et al. 2012). Therefore, despite not observing any changes in Atg7, I sought to establish whether OPG could alter the expression of LC3B-II, perhaps through a mechanism that was independent of Atg7. Unfortunately, no bands were detected for LC3B-II after analysing OPG-stimulated PA-SMC lysates by western blotting (data not shown).

Data presented so far in this chapter suggest that OPG can alter the phosphorylation of CDK4, HSP27, ERK1/2 and mTOR and OPG can induce the expression of CDK5 in PA-SMCs. However, OPG was found to have no significant effect on the expression of Daxx and FADD, proteins belonging to the Fas signalling pathway, or the autophagy proteins Atg7, Atg13 and G β L. A summary of the validated changes in protein expression and phosphorylation that have been investigated in this chapter thus far is shown in Table 4.2.

Table 4.2- Summary of the validated changes in protein expression and phosphorylation in PA-SMCs following OPG stimulation.

Protein	Pan-Specific / Phospho-specific	OPG-induced changes in expression
HSP27	Phospho-specific	Significantly increased at 60 minutes (results of ICW).
CDK4	Phospho-specific	Significantly increased at 10 minutes and 60 minutes (results of ICW).
CDK5	Pan-specific	Significantly increased at 60 minutes (results of western blotting)
Daxx	Pan-specific	No significant change
FADD	Pan-specific	No significant change
mTOR	Phospho-specific	Significantly increased at 60 minutes (results of western blotting)
Atg13	Pan-specific	No significant change
Atg7	Pan-specific	No significant change
GβL	Pan-specific	No significant change
ERK1/2	Phospho-specific	Significantly increased at 10 minutes and 60 minutes (results of ICW and western blotting).

After investigating the changes in protein expression and phosphorylation, the next aim of this chapter was to examine the changes in gene expression caused by OPG stimulation. To do this, an mRNA expression microarray was performed on unstimulated and OPG-stimulated cells to compare differences in gene expression between the two conditions.

4.4.4 Microarray Analysis of OPG-induced Changes in Gene Expression in HPA-SMCs

After conducting a microarray to investigate OPG-regulated changes in gene expression in HPA-SMCs, OPG was found to alter the expression of 1732 genes out of the 60,000 probes analysed. Such a large gene list is hard to analyse manually, therefore, the list was analysed using DAVID in order to identify pathways that the genes altered by OPG belonged too. OPG was found to regulate the expression of genes involved in several signalling pathways, including p53, ECM receptor interaction, TGF-β, focal adhesion, PPAR, the cell cycle and pathways in cancer (Figure 4.9). Interestingly, OPG was previously found to alter the expression and

phosphorylation of proteins belonging to the p53 pathway, focal adhesion pathway, cell cycle and pathways involved in cancer (discussed above), as well as altering the expression of genes also belonging to these pathways (Figure 4.9).

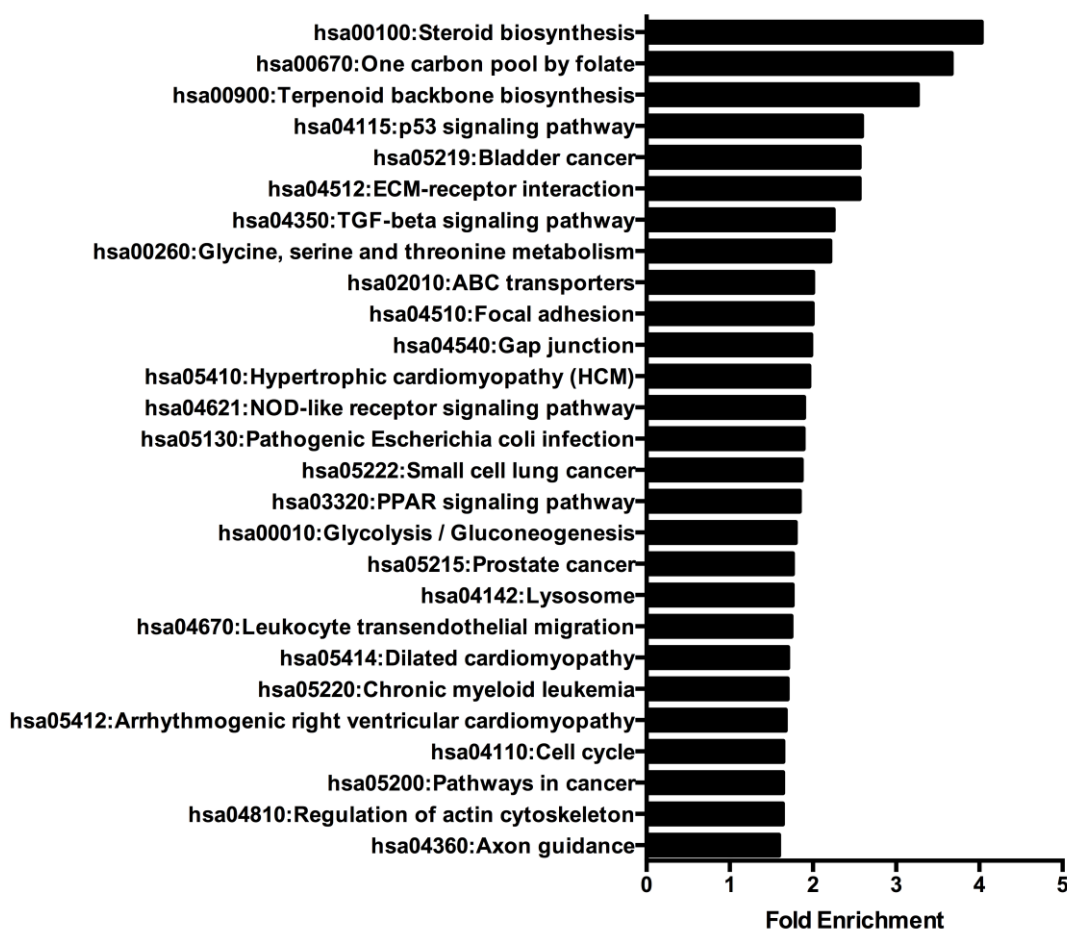


Figure 4.9- Pathway fold enrichment of genes in OPG-stimulated HPA-SMCs.

Fold enrichment of different pathways was calculated using DAVID. The fold enrichment of a certain pathway demonstrates how many fold were proteins of the pathway altered than would be expected by chance. Agilent IDs of genes deemed significantly regulated by OPG (Log₂ fold change of >0.4 and P<0.05) were analysed using DAVID functional annotation to generate fold enrichment pathway analysis through the Kegg Pathway Database. Intersections of ≥2 fold change and p≤0.05 were used for the pathway fold enrichment analysis. OPG was found to alter the expression of genes in a number of different pathways, including the p53 signalling pathway, ECM-receptor interaction, focal adhesion, PPAR signalling pathway, cell cycle and pathways in cancer.

Although the pathway analysis allowed us to see which pathways the genes altered by OPG belonged to, such a large number of genes and pathways make it hard to pinpoint exactly which changes to gene expression are causing PA-SMCs to acquire a pathogenic phenotype. I next wanted to determine whether the gene list contained any genes that were already associated with PAH pathogenesis. Consequently, the list of 1732 genes was compared to a list of genes already known to be involved in the pathogenesis of PAH (Appendix 7.5). OPG was found to positively and negatively regulate the expression of 57 (40%) genes already associated with the pathogenesis of PAH (Figure 4.10).

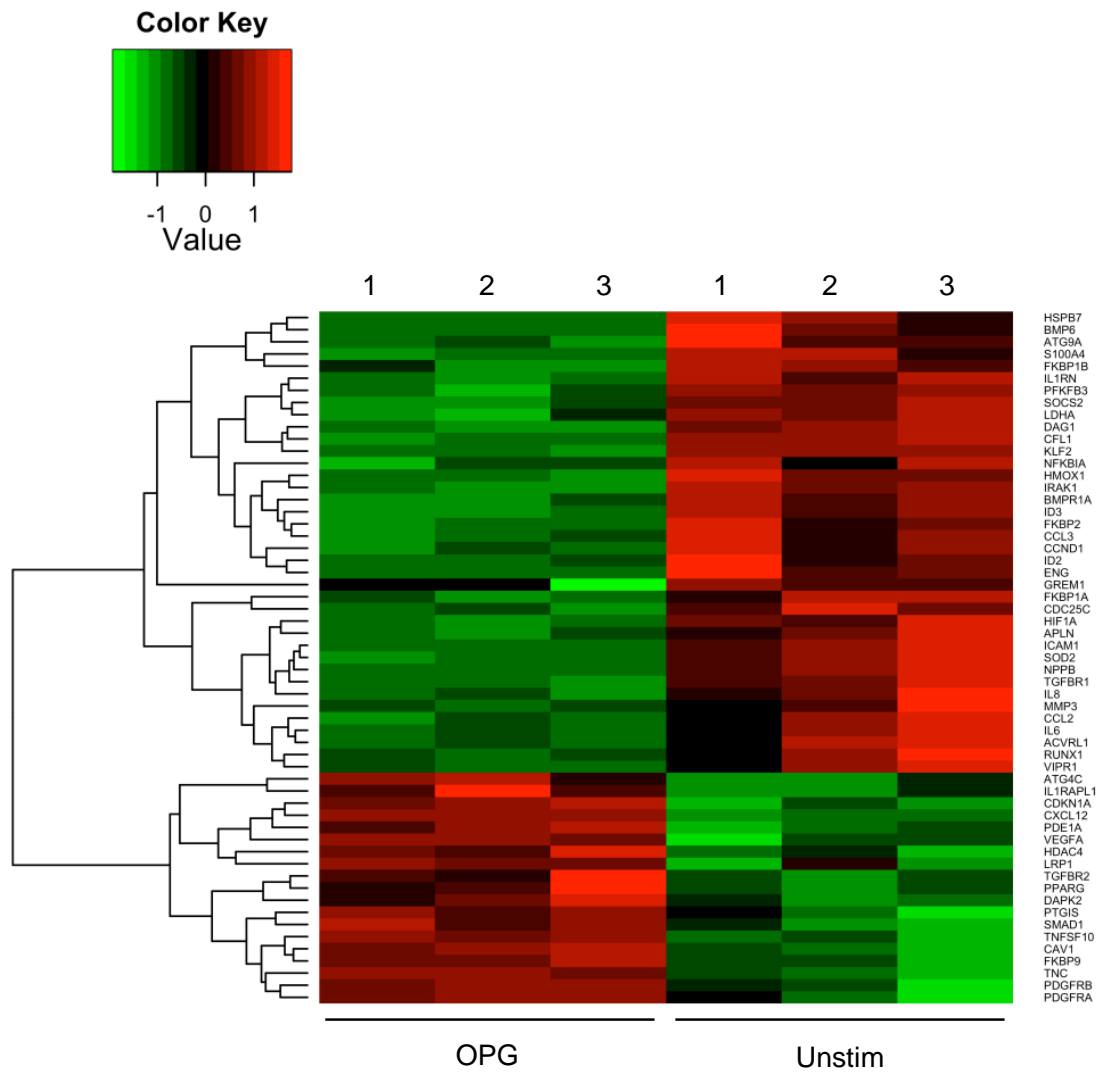


Figure 4.10- Heat map of PAH-associated genes regulated by OPG.

When compared to unstimulated PA-SMCs, OPG was found to both positively and negatively regulate the expression of genes that have already been associated with PAH in PA-SMCs. Each column represents each of the three individual sub-arrays used to analyse 3 pooled RNA samples from each condition. Heat map shows Z-score ratio.

After these findings that a number of PAH-associated genes were altered by OPG in PA-SMCs, several genes were subsequently selected for validation to ensure results of the microarray were reproducible.

4.4.5 TaqMan Validation of the mRNA Microarray

Ten genes of the 57 were selected for validation based on their known involvement in PAH pathogenesis (Appendix 7.5). The TGF β signalling pathway is now widely acknowledged to play an important role in the pathogenesis of PAH. Mutations in the TGF β superfamily have been identified as important genetic defects underpinning PAH. Mutations in ACVRL1 (ALK-1) have been identified in hereditary haemorrhagic telangiectasia (HTT)-associated PAH (Harrison et al. 2003) and TGFBR2 mutations have been identified in IPAH vascular lesions (Yeager et al. 2001). Furthermore, the expression of BMPR1A (Du et al. 2003), TGFBR1 and TGFBR2 (Gore et al. 2014; Richter et al. 2004) are altered in IPAH patients. Therefore the TGF β superfamily members ACVRL1, BMPR1A, TGFBR1 and TGFBR2 were selected for validation. TRAIL (Hameed et al. 2012), PDGFRA (Perros et al. 2008) and TNC (Jones et al. 1997; Ihida-Stansbury et al. 2006) are all known to play an important role in PAH and mRNA and protein expression of these pathogenic mediators are also increased within IPAH patients. Furthermore, VEGF levels are increased in the serum and SMCs from PAH patients (Selimovic et al. 2009; Hirose et al. 2000). Therefore, TRAIL, PDGFRA, TNC and VEGFA expression was selected for validation. Cav-1 and VIPR were also selected for validation because there is increasing evidence suggesting that an increase in Cav-1 is important for the pathogenesis of PAH (Mathew et al. 2004; Mathew 2011) and finally VIP serum concentrations are reduced in IPAH patients (Petkov et al. 2003).

OPG was found to significantly increase the expression of TRAIL, PDGFRA, CAV-1, TNC and VEGFA in HPA-SMCs compared to unstimulated control cells (*Figure 4.11*). These results validate the changes in gene expression observed in the microarray. OPG also significantly decreased the expression of VIPR, compared to unstimulated HPA-SMCs, and these data also validate the changes in VIPR observed by the microarray analysis.

However, OPG had no significant effect on BMPR1A, TGFBR1, TGFBR2 or ACVRL1 expression (*Figure 4.11*). These data do not support the results of the microarray, which instead shows a reduction in BMPR1, ACVRL1 and TGFBR1 and an increase in TGFBR2 (*Figure 4.11*).

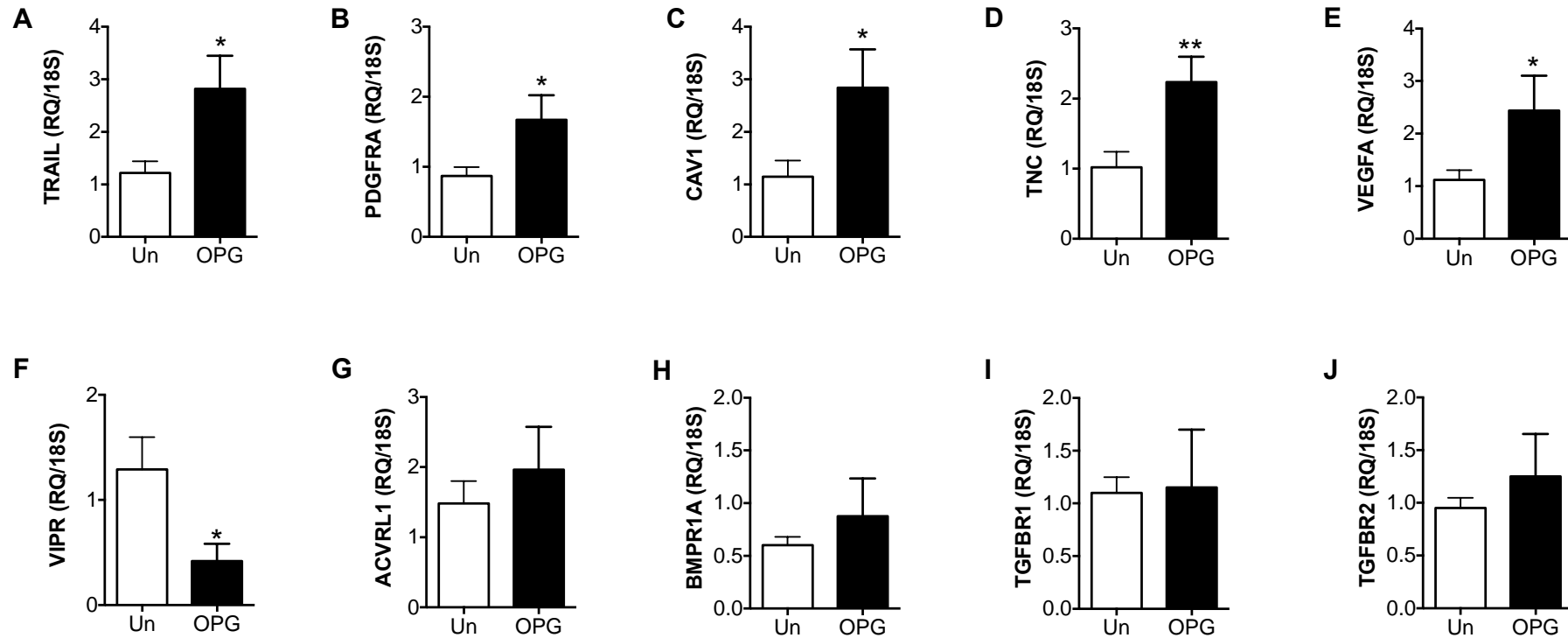


Figure 4.11- TaqMan analysis of RNA expression in HPA-SMCs.

Bar graphs show Taqman RT-qPCR validation of (A) TRAIL, (B) PDGFRA, (C) Cav-1, (D) TNC, (E) VEGFA, (F) VIPR, (G) ACVRL1, (H) BMPR1A, (I) TGFBR1 and (J) TGFBR2 RNA expression in OPG- stimulated PA-SMCs. All data are normalised using $\Delta\Delta CT$ with 18S rRNA as the endogenous control gene. Un= unstimulated PA-SMCs, OPG= OPG-stimulated (50 ng/ml) PA-SMCs. Error bars represent mean \pm SEM, * $p < 0.05$, ** $p < 0.01$, $n = 11$.

4.5 Discussion

Following the identification of potential binding partners for OPG in Chapter 3, this fourth chapter aimed to explore the intracellular signalling mechanisms through which OPG signals to induce pathogenic changes in PA-SMCs. In this chapter, I aimed to answer two questions, 1) which intermediate proteins is OPG signalling through to induce downstream mRNA transcription? and 2) which genes are transcribed as a result of OPG signalling in PA-SMCs? To do this, changes in protein phosphorylation and gene and protein expression were examined in OPG-stimulated PA-SMCs.

Results of the Kinex antibody microarray, undertaken to analyse protein phosphorylation, revealed that OPG both positively and negatively regulated the expression and activation of 89 proteins in PA-SMCs (Table 4.1). Pathway analysis revealed fold enrichment of a number of signalling pathways including p53, VEGF, apoptosis, Toll-like receptor, MAPK, chemokine signalling and focal adhesion (Figure 4.1). Interestingly, OPG was found to alter the expression and activation of proteins involved in cancer (Figure 4.1), which shares some similarities with PAH pathogenesis, such as abnormal and uncontrolled cell growth, migration and apoptosis evasion (Rai et al. 2008). OPG was found to induce the phosphorylation of the cyclin dependent kinases CDK4 and CDK5, along with the ERK1/2 and HPS27 and also to alter phosphorylation of the autophagy inhibitor mTOR. Microarray analysis revealed that OPG altered the expression of 1732 genes in PA-SMCs and pathway analysis showed the genes altered belonged 27 different signalling pathways. OPG was found to regulate the expression of 57 PAH-associated genes (Figure 4.10), including TRAIL, PDGFRA, CAV-1, TNC, VEGF and VIPR (Figure 4.11). These data highlight the diverse effects OPG has on gene expression in PA-SMCs and reveal that OPG can modulate the expression of genes belonging to many different signalling pathways.

My data show OPG interacts with Fas (Chapter 3), so I next looked at whether OPG could alter the expression of FADD and Daxx, which are proteins belonging to the Fas signalling pathway. Although expression of Daxx was reduced in the KAM, expression remained unchanged in the western blot analysis of OPG-stimulated PA-SMCs. Furthermore, OPG did not induce any significant change in FADD expression

in PA-SMCs. This suggests that the signalling mechanisms employed by OPG may not be occurring through the Fas signalling pathway. Instead, the data in this chapter suggest that OPG activates an atypical network of pro-proliferative, pro-survival and anti-apoptotic proteins in PA-SMCs.

4.5.1 The Effects of OPG on PA-SMC Proliferation

Data in this chapter revealed an increase in the expression of proteins and genes that are involved in pro-proliferative pathways. OPG was found to increase CDK4 phosphorylation in PA-SMCs. CDK4 is a cell cycle protein that, when complexed with at least one of the three D-type cyclins, D1, D2 and D3 and phosphorylated in the activation loop, can phosphorylate pRb and subsequently allow S-phase gene transcription and cell cycle progression (Meloche & Pouyssegur 2007; Hirai et al. 1995; Lukas et al. 1996). CDK4 activity and expression is increased in proliferating PA-SMCs (Ibe et al. 2008). Furthermore, CDK4 expression is reduced in HPA-SMCs where PDGF-induced proliferation is inhibited (G. Liu et al. 2013). Furthermore, ERK1/2 is required for the expression of the CDK4 activator, cyclin-D1 (Lavoie et al. 1996).

It is well known that ERK1/2 is important in SMC proliferation and migration. In proliferating SMCs, including PA-SMCs, ERK1/2 expression and phosphorylation is increased (G.-W. Li et al. 2011; Jia et al. 2012; Wilden et al. 1998; Yoshizumi et al. 1998; Kingsley et al. 2002) and ERK1/2 blockade reduces viability of PA-SMCs (Song et al. 2013). Furthermore, ERK1/2 expression is required for PDGF-BB-induced migration of VSMCs and has been implicated in ET-1 induced PA-SMC migration (Kingsley et al. 2002; Meoli & White 2010). Phospho-ERK1/2 also mediates TRAIL-induced PA-SMC proliferation and migration (Hameed et al. 2012). In my data, not only was OPG found to induce ERK1/2 phosphorylation in PA-SMCs, but OPG also increased TRAIL RNA expression in PA-SMCs and TRAIL has also been shown to induce PA-SMC proliferation through ERK1/2 phosphorylation (Hameed et al., 2012).

TRAIL protein expression, along with OPG expression, has been previously observed in concentric and plexiform lesions of IPAH patients and TRAIL RNA expression is

elevated in IPAH PA-SMCs (Hameed et al. 2012; Lawrie et al. 2008). TRAIL can also induce the proliferation and migration of VSMCs and PA-SMCs *in vitro*, a process that is mediated by ERK1/2 phosphorylation (Secchiero et al. 2004; Hameed et al. 2012). The OPG-induced increase in TRAIL gene expression in PA-SMCs suggests that, since TRAIL protein expression correlates with the changes seen in mRNA expression (Hameed et al. 2012), TRAIL may also be contributing to PA-SMC proliferation. I propose that TRAIL-induced PA-SMC proliferation may be occurring through an ERK1/2-dependent mechanism. In support of this, the TRAIL receptors, TRAIL R1 and R3 are also significantly upregulated in IPAH PA-SMCs (Hameed et al. 2012), therefore TRAIL may be causing this increase in phospho-ERK1/2 by binding to TRAIL R1 and R3. Thus, OPG may be directly activating pERK1/2 to induce PA-SMC proliferation, whilst also causing indirect proliferation through an increase in TRAIL expression and TRAIL-induced ERK1/2 phosphorylation.

I therefore propose that OPG is inducing PA-SMC proliferation through the activation of CDK4 and ERK1/2 and that the increase in TRAIL RNA expression caused by OPG might also be potentiating the pro-proliferative effect TRAIL has on PA-SMCs. This proposition is summarised in Figure 4.12.

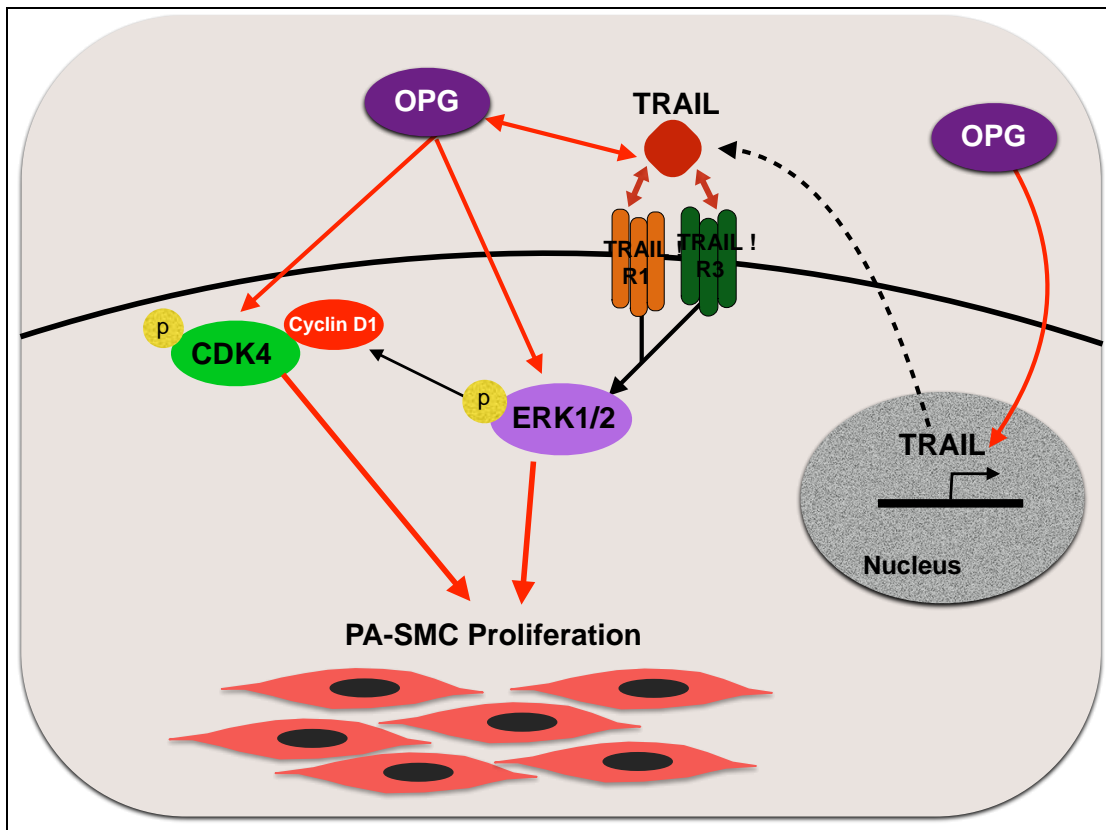


Figure 4.12- OPG induces the phosphorylation of CDK4 and ERK1/2 in PA-SMCs.

Activation of CDK4 and ERK1/2 may subsequently lead to the proliferation of PA-SMCs as both CDK4 and ERK1/2 activity has been identified in proliferating PA-SMCs (Ibe et al. 2008; G.-W. Li et al. 2011; Jia et al. 2012; Wilden et al. 1998; Yoshizumi et al. 1998; Kingsley et al. 2002). Phospho-ERK1/2 may also activate cyclin D (Lavoie et al. 1996), to result in further activation of CDK4 in PA-SMCs. OPG induces RNA expression of it's ligand, TRAIL and TRAIL has also been shown to induce PA-SMC proliferation through ERK1/2 (Hameed et al., 2012).

My data also suggest a role for the PDGF signalling pathway in OPG-induced PA-SMC proliferation as OPG increased PDGFRA mRNA expression. PDGFRA is a receptor tyrosine kinase that acts as a receptor, along with PDGFRB, for PDGF. PDGF can induce the proliferation and migration of PA-SMCs (Yu et al. 2003) and plays an important role in the pathogenesis of PAH, as evidenced by the mechanistic action of Imatinib, a drug previously approved for PAH treatment. Imatinib is a tyrosine kinase inhibitor that inhibits PDGF-induced PA-SMC proliferation and PDGFRA and PDGFRB receptor phosphorylation (Pankey et al. 2013).

PDGFRA mRNA expression is elevated in the small PAs from patients with severe PAH and protein expression is increased in proliferating SMCs of pulmonary vascular lesions (Perros et al. 2008). Interestingly, PDGF has also been shown to induce OPG mRNA expression and OPG protein secretion from human aortic SMCs (Zhang et al. 2002). It would be interesting to investigate whether PDGF induces an increase in OPG expression and release from PA-SMCs because if this is the case, there may be a feedback loop occurring between OPG and PDGF in PA-SMCs. The role I propose the PDGF signalling pathway plays in OPG-induced PA-SMC proliferation is shown below in Figure 4.13.

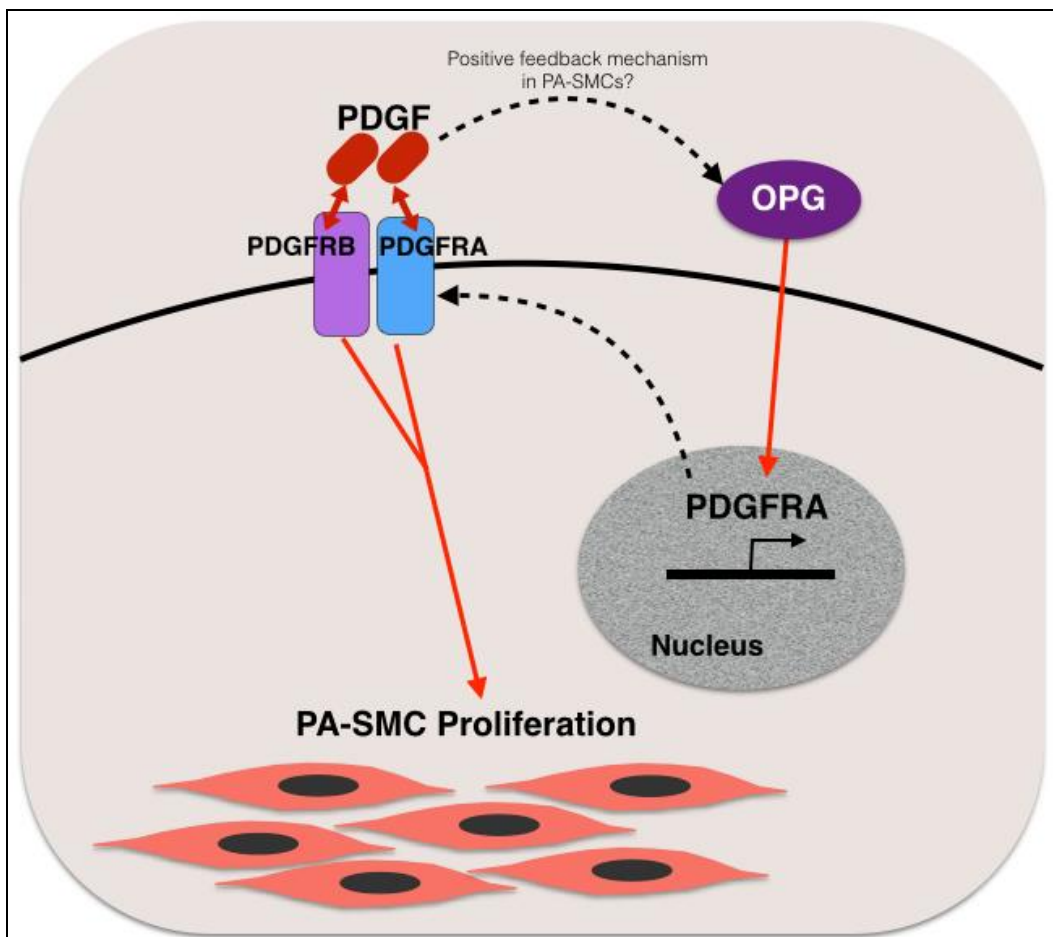


Figure 4.13- OPG induces the expression of PDGFRA RNA.

PDGF has been shown to induce the proliferation of PA-SMCs (Yu et al. 2003) and can induce OPG mRNA expression and secretion (Zhang et al. 2002). Therefore, there may be the possibility of a positive feedback loop existing between OPG and PDGF in PA-SMCs.

OPG was found to increase mRNA expression of TNC and Cav-1, both of which have been associated with PA-SMC proliferation. TNC is an extracellular matrix glycoprotein that can interact with a variety of receptors to induce a variety of different signalling pathways. Increased TNC expression is observed in animal models of PAH (Jones et al. 2002; Jones & Rabinovitch 1996; Ivy et al. 2005), in the adventitia and media of PAs and neointima of children with congenital heart disease and PAH (Jones et al. 1997) and in the occlusive vascular lesions and wall of remodelled PAs of FPAH patients, including those harbouring BMP2 mutations (Ihida-Stansbury et al. 2006). TNC also promotes VSMC growth (Jones & Rabinovitch 1996) and co-localises with proliferating SMCs (Jones & Rabinovitch 1996; Ivy et al. 2005).

Caveolin-1 is an important component of caveolae, membrane invaginations that are abundant in cell surface receptors, critical for cellular signalling cascades (Soubrier et al. 2013). Although mutations in the CAV1 gene have been identified in PAH patients (Austin et al. 2012), discussed in Chapter 2, there are still conflicting reports in the literature surrounding the role of Cav-1 in PAH. Cav-1 expression is reduced in the hypoxic, MCT and SuHx models of PAH (Zhao et al. 2002; Bauer et al. 2012; Achcar et al. 2006) and reduced Cav-1 has been reported in vascular lesions of PAH patients (Achcar et al. 2006). However, there are some conflicting reports that show Cav-1 expression is elevated in the SMC layer of pulmonary vessels from human IPAH lung sections (Patel et al. 2007). Additionally, Cav-1 mRNA is increased in PA-SMCs from IPAH patients and proliferation of PA-SMCs overexpressing Cav-1 is elevated, whereas Cav-1 inhibition in IPAH-PA-SMCs reduced proliferation of these cells (Patel et al. 2007). Literature now suggests that compartmentalisation of Cav-1 is important in PAH and it is the reduction in PA-EC Cav-1 and increase in PA-SMC Cav-1 expression that is important in PAH pathogenesis (Mathew, 2011; Mathew et al., 2004; Y. Zhao et al., 2009; Huang et al., 2012), with increased SMC Cav-1 been described in animal models and patients with PAH (Mathew, 2011; Huang et al., 2012). I therefore hypothesise that the increase in Cav-1 and TNC expression that is induced by OPG might also have pro-proliferative effects on PA-SMC phenotype (Figure 4.14).

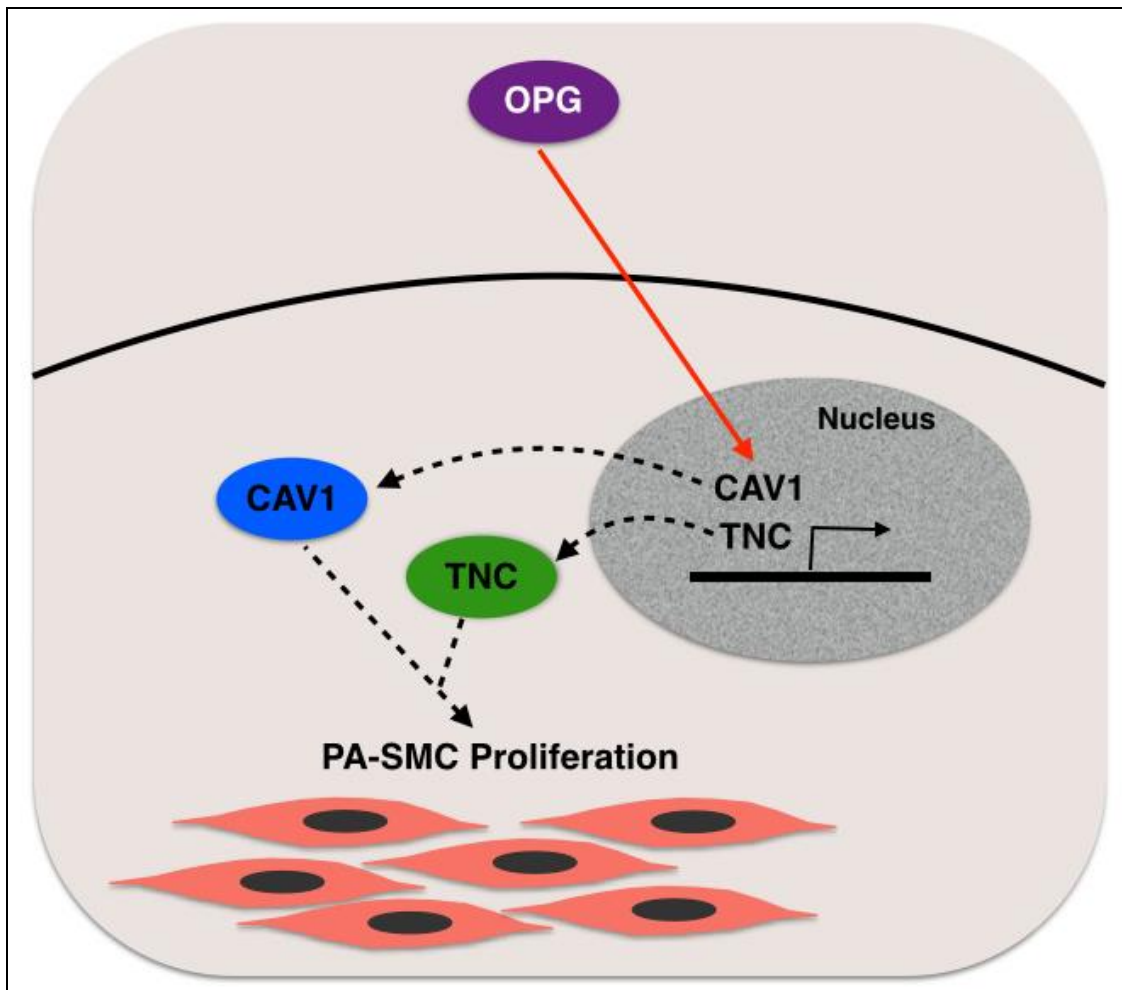


Figure 4.14- Cav-1 and TNC induce PA-SMC growth and proliferation (Jones & Rabinovitch 1996; Ivy et al. 2005).

OPG increased both CAV1 and TNC gene expression in PA-SMCs, therefore, Cav-1 and TNC protein may also be increased and inducing the proliferation and growth of PA-SMCs.

In addition to the pro-proliferative pathways discussed above, phosphorylation of HSP27 suggests that OPG is also activating anti-apoptotic pathways in HPA-SMCs. Historically, the induction of evolutionarily conserved heat shock proteins in response to stress has been shown to protect cells and this correlates with increased tolerance to stressful conditions (Samali & Cotter 1996). HSP27 has a number of protective roles in cells in response to heat, oxidative and mechanical stress and when phosphorylated, acts as an inhibitor of apoptosis by retaining cytochrome C9 to block the intrinsic apoptotic pathway (Ghayour-Mobarhan et al. 2012). Interestingly, dimers of

phosphorylated HSP27 have been shown to interact with Daxx to block Fas-induced apoptosis (Charette & Landry 2000; Charette et al. 2000). Upon Fas activation, Daxx translocates from the nucleus to the cytoplasm where Daxx then activates Ask1 to induce apoptosis. However, HSP27 is thought to block this translocation, maintaining Daxx localisation to the nucleus and blocking apoptosis (Charette & Landry 2000; Charette et al. 2000). This suggests that OPG may be blocking Fas-induced apoptosis through the Daxx-dependent pathway by inducing the phosphorylation of HSP27. This may also explain why no change in Daxx expression was detected if the mechanism by which HSP27 blocks Daxx-mediated apoptosis is through inhibiting Daxx translocation to the cytoplasm, rather than altering expression of Daxx.

In support of HSP27 being an important mediator, HSP27 expression has been observed in the ECs and SMCs of pulmonary arteries of congenital heart disease patients with pulmonary hypertension, and HSP27 expression was most prominent in the ECs and SMCs of pulmonary arteries that showed medial hypertrophy and proliferation (Geiger et al. 2009). Furthermore, HSP27 was detectable in the concentric and plexiform lesions of pulmonary arteries (Geiger et al. 2009). Interestingly, treating human retinal endothelial cells with a mixture of cytokines, interferon- γ , TNF α and IL-1 inhibit HSP27 expression, which correlated with an increase in cell apoptosis. Interferon- γ , TNF α and IL-1 β are all increased in patients with pulmonary hypertension (Humbert et al. 1995; Feinberg et al. 1999; George et al. 2014). This raises the question as to whether the increase in inflammatory cytokines observed in PAH may act to reduce HSP27 expression and contribute to the initial endothelial cell apoptosis commonly observed in PAH pathogenesis. Conversely, the increase in HSP27 observed in plexiform lesions, a hallmark of late stage disease, may contribute to the proliferation of endothelial cells in later stages of the disease (Geiger et al. 2009). Therefore, the OPG-induced increase in HSP27 observed in SMCs may act to promote SMC survival by protecting cells against apoptosis.

OPG was also found to induce the expression of another cyclin-dependent kinase, CDK5. Although a member of the cyclin-dependent kinase family, CDK5 plays no evident role in the cell cycle (Arif 2012). Expression of CDK5 and its activators were originally thought to be restricted to neurons (Xie & Tsai 2004). However, the functions of CDK5 are now known to extend beyond the nervous system and there is

increasing evidence to support an anti-apoptotic role for CDK5. CDK5 has been reported to bind to cyclin-I in mouse podocytes and neurons (Brinkkoetter et al. 2009). CDK5 inhibition increases the susceptibility of podocytes to apoptosis *in vitro* and inhibition of CDK5 and cyclin-I knockout both cause a reduction in the anti-apoptotic proteins Bcl-2 and Bcl-XL, as well as a reduction in pERK1/2 (Brinkkoetter et al. 2009). CDK5 has also been shown to directly phosphorylate Bcl-2 (Cheung et al. 2008). These data therefore suggest a pro-survival, anti-apoptotic role for CDK5, and its activator cyclin-I.

In support of this, CDK5 has also been implicated in cell proliferation, with CDK5 expression identified in proliferating bovine aortic endothelial cells and low levels of CDK5 have been detected in quiesced cells (Sharma et al. 2004). Interestingly, basic fibroblast growth factor (bFGF), shown to be increased in PAH patients and the MCT-rat model of PAH (Arcot et al. 1995; Benisty et al. 2004), induces CDK5 expression and inhibition of CDK5 causes the inhibition of bFGF-induced cell proliferation (Sharma et al. 2004). Inhibition of cell proliferation by angiotensin also causes a reduction in CDK5 expression (Sharma et al. 2004). I propose that the combination of increased HSP27 activation and CDK5 expression might be preventing PA-SMC apoptosis, hence promoting PA-SMC survival, as well as inducing PA-SMC proliferation and this is summarised below in Figure 4.15.

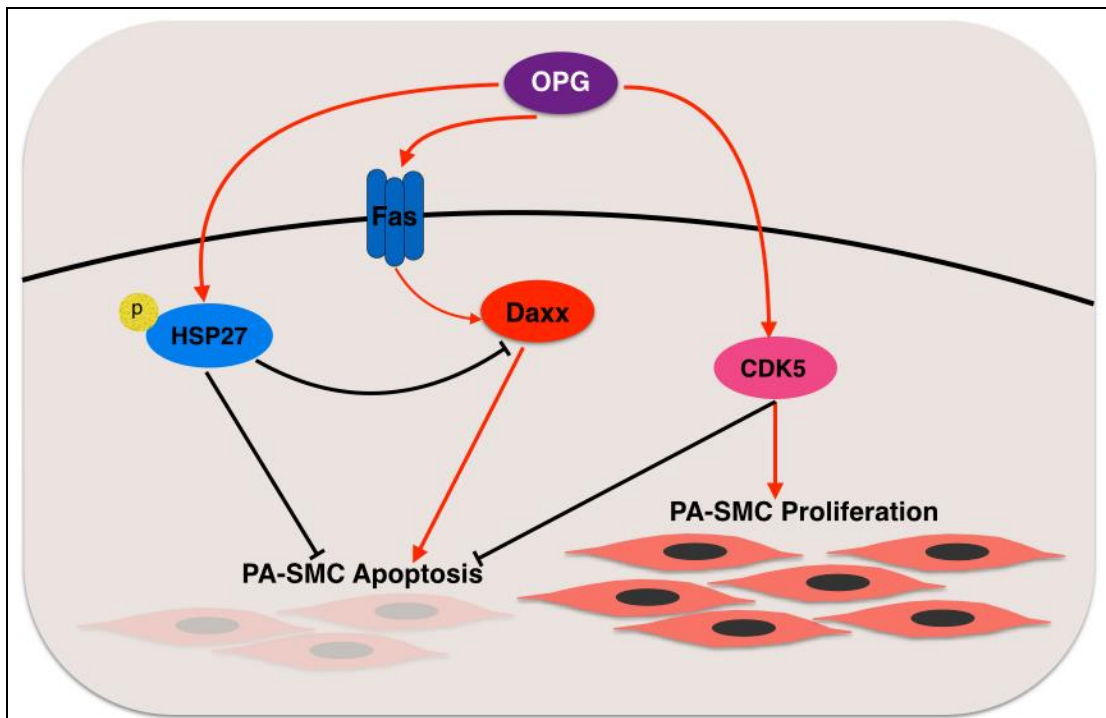


Figure 4.15- OPG induces the phosphorylation of HSP27.

Phospho-HSP27 is an inhibitor of apoptosis (Ghayour-Mobarhan et al., 2012) and might therefore inhibiting PA-SMC apoptosis. Furthermore, phospho-HSP27 has been shown to block the translocation of Daxx to prevent Fas-induced apoptosis (Charette & Landry 2000; Charette et al. 2000) and so might also be preventing Fas-induced apoptosis of PA-SMCs.

OPG was found to induce changes in phosphorylation of the autophagy inhibitor, mTOR. Autophagy has also been investigated as a potential mediator in PAH pathogenesis, however the exact role autophagy plays in PAH development still remains ambiguous. Increased levels of the autophagy marker, LC3B, have been reported in the lungs of PH patients and LC3B expression is increased in PA-ECs and PA-SMCs exposed to hypoxia, *in vitro*, suggesting autophagy contributes to PAH (Lee et al. 2011). However, LC3B knockout caused an increase in SMC proliferation and exaggerated disease in hypoxic mice, which on the contrary, suggests a protective role for autophagy in PAH (Lee et al. 2011). Furthermore, similar contradictory findings for the role of the autophagy protein, ATG5, have also been reported. ATG5 expression is increased within the heart of mice after haemodynamic stress, however ATG5 knockout actually causes more rapid heart failure in response to haemodynamic

stress (Nakai et al. 2007). However, a recent report by Long et al (2013) suggests a more definitive and pathogenic role for autophagy in PAH. Increased levels of LC3BII and ATG5 are observed in the MCT rat model of PAH and Chloroquine, an inhibitor of disease development, was shown to reduce autophagy (Long et al. 2013).

In my data, although OPG was found to cause a significant increase in phospho-mTOR levels at 60 minutes, compared to 10 minutes of stimulation, there were no changes detected in the autophagy proteins β LC3, ATG7 or ATG13. Levels of LC3B were also assessed in OPG-stimulated PA-SMC lysates after 10 minutes, 60 minutes and 24-hour of stimulation with OPG. No bands were detected by western blotting, even after attempting to optimise the western blotting process by using different antibody concentrations and amounts of protein loaded onto the gels. This may be due cells requiring longer stimulation with OPG, for example 48-hour or 72-hour stimulation, before changes in LC3B-II expression are observed. The LC3B-II antibody has been used successfully in several research papers (Chertov et al. 2011; Gao et al. 2011; Ouyang et al. 2012) and LC3B expression has been described in PA-SMCs (Lee et al. 2011). Therefore, I propose that the reason LC3B-II was not detected might have been due to the duration of OPG stimulation, rather than the antibody not successfully detecting LC3B-II or LC3B-II not being expressed in PA-SMCs. The duration of OPG stimulation may require further optimisation for changes in LC3B-II to be detected in PA-SMCs. Therefore, further investigation into changes in autophagy protein expression must be conducted in PA-SMCs in order to determine whether OPG is signalling through the autophagy pathway.

In addition to the genes mentioned above, OPG was also found to increase the expression of VEGFA RNA and to reduce VIPR RNA expression. Opposing findings for the role of VEGF in PAH have been reported in the literature. On the one hand, the literature has reported increased VEGF mRNA and protein expression, along with increased VEGF receptor mRNA expression, in the hypoxic rat model of PAH (Tuder et al. 1995). On the other hand, literature has reported a reduction in VEGF expression in the MCT-treated rat (Arcot et al. 1993) and the VEGFR2 antagonist, Sugen5416, is now used to induce PAH in animal models of PAH, either alone or combined with hypoxia (Taraseviciene-Stewart et al. 2001). Curiously, arterial and venous serum levels of VEGF are elevated in PAH patients and VEGF mRNA is expressed in

proliferative SMCs found in, and surrounding, plexiform lesions (Selimovic et al. 2009; Hirose et al. 2000). OPG was found to increase the expression of VEGF mRNA in PA-SMCs, which mirrors the increase observed in PAH patients. However, the effect of increased VEGF mRNA expression on PA-SMC phenotype requires further investigation to confirm whether increased VEGF mRNA expression correlates with increased VEGF protein expression and determine whether the increase in VEGF expression causes PA-SMC proliferation.

VIPR expression was also reduced in PA-SMCs stimulated with OPG. VIP binds to the receptors, VIPR (VIPR1, VPAC-1) and VIPR2 (VPAC-2) and acts as a systemic vasodilator and causes the relaxation of human pulmonary arteries (Greenberg et al. 1987). VIP also inhibits the proliferation of human airway and pulmonary arterial smooth muscle cells (Maruno et al. 1995; Petkov et al. 2003). VIP serum concentrations are reduced in IPAH patients (Petkov et al. 2003), however, VIPR levels are elevated in IPAH patient PA-SMCs and animal models of PAH (Vuckovic et al. 2009). VIP (aviptadil) inhalation has been trialled as a potential therapy for PH and although results showed significant selective pulmonary vasodilation and an improvement in stroke volume, results were modest and short-lived (Leuchte et al. 2008). Although the literature shows an increase in VIPR expression in PAH, PA-SMCs stimulated with OPG show a reduction in VIPR mRNA expression. Evidently, the phenotypic effects of this will require further investigation.

These data reveal for the first time that OPG can modulate the expression and activation of proteins that, although signal in different pathways, all may ultimately lead to the survival and proliferation of PA-SMCs via a multidirectional, cooperative network. This is shown in the proposed schematic (Figure 4.16), detailing the process that I reason occurs in PA-SMCs as a result of OPG stimulation *in vitro*. Although Fas was identified as the most likely OPG binding partner in the previous chapter, it still remains to be determined whether these intracellular protein changes are occurring as a result of OPG binding to Fas.

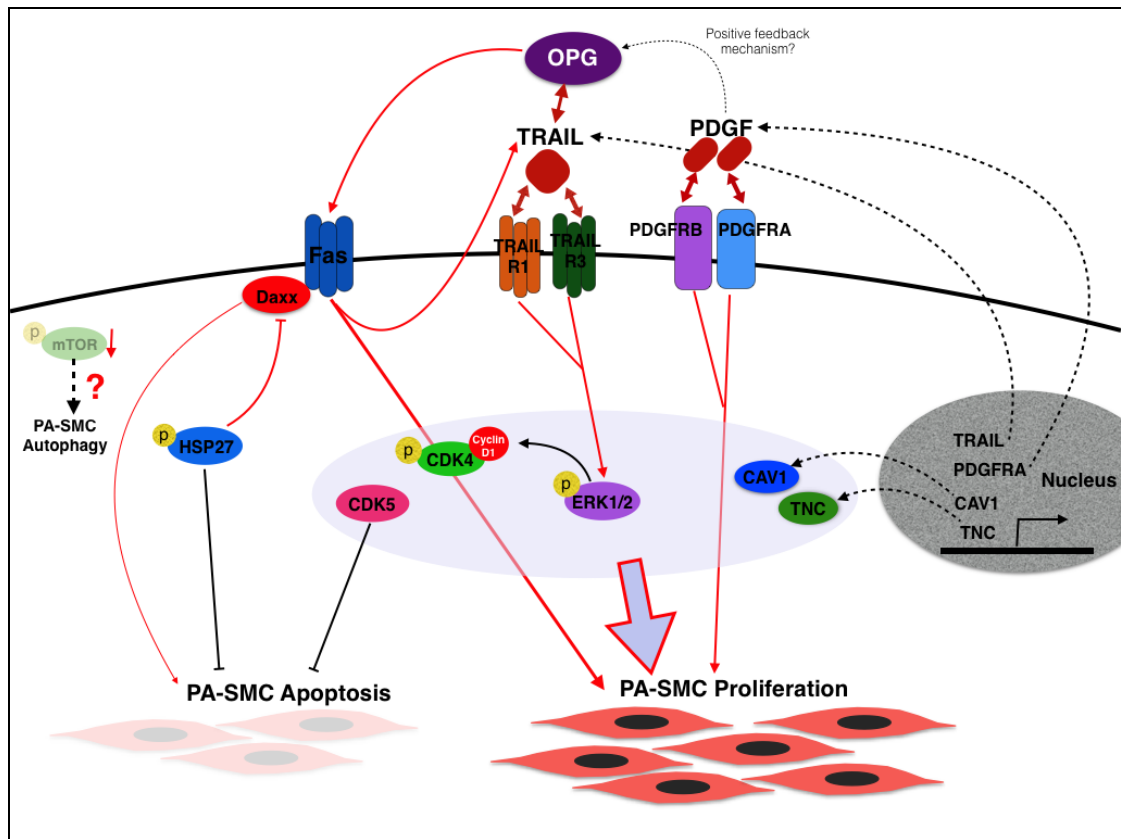


Figure 4.16- Proposed schematic for OPG signalling in PA-SMCs.

This schematic incorporates all the data discussed and the individual schematics (Figures 4.12-4.15) discussed throughout this chapter to illustrate the proposed signalling mechanisms activated by OPG to induce PA-SMC proliferation in vitro. OPG induces the phosphorylation of CDK4 and ERK1/2 and increases the protein expression of CDK5 to induce PA-SMC proliferation, as well as inducing HSP27 phosphorylation and CDK5 expression to block PA-SMC apoptosis. OPG induces the expression of the pro-proliferative genes Cav-1, TNC, PDGFRA and TRAIL, which may also induce PA-SMC proliferation if the changes in protein levels reflect the changes that are occurring at the mRNA level.

Although results of the microarray revealed a significant change in BMPR1A, ACVRL1, TGFBR1 and TGFBR2 expression in response to OPG, these results were not validated and OPG was found to have no effect on the expression of these genes when analysed by TaqMan. This may be due to the fact that the microarray data can vary due to the large amount of probes used on the array. Differences in probe

hybridization efficiency for each probe may mean that cDNA from some genes hybridize much more readily than cDNA for other probes (Geeleher et al. 2011). Although data are expressed as a ratio between OPG stimulated and unstimulated PA-SMCs to overcome this, it is important to note that the ratio does not give an absolute measure of the amount of mRNA in each PA-SMC sample. Furthermore, probes with a sequence that is closely related to other members of the same gene may fail to accurately differentiate between closely related members of the same family. This may lead to cross hybridization, causing some probes to bind the wrong cDNA from closely related gene family members (Geeleher et al. 2011). Therefore, the discrepancies in gene expression observed may be a limitation of the microarray.

As further analysis for my findings, it would be important to assess the levels of protein for all of the genes altered by OPG in this chapter to determine whether changes in mRNA levels reflect the changes at the protein levels. Therefore, all my conclusions about the effect changes in mRNA expression have on PA-SMC phenotype would need to be confirmed at the protein level. It would also be particularly interesting to see if there is any change in gene expression when the OPG-Fas interaction is blocked, and if this change in gene expression is accompanied by a change in OPG-induced PA-SMC proliferation. The effect of OPG-Fas blockade on gene expression and PA-SMC proliferation was therefore investigated in Chapter 5.

5. INVESTIGATING THE EFFECT OF BLOCKING THE OPG-FAS INTERACTION ON HUMAN PA-SMC PHENOTYPE

5.1 Introduction

The results presented in this thesis have thus far identified potential OPG binding partners on PA-SMCs and have begun to reveal the proteins and genes through which OPG may be mediating PA-SMC proliferation. These findings are summarized in Figure 4.16. However, it still remains to be determined whether the changes in protein activation and expression, along with changes in gene expression, are being mediated through interactions between OPG and the identified OPG binding partners. As discussed previously, Fas was identified as the most probable binding partner for OPG on PA-SMCs (Chapter 3), therefore I next determined whether OPG-induced changes in gene expression and PA-SMC proliferation were being mediated through an OPG-Fas interaction.

5.2 Aim

The aim of this chapter was to determine the effect of blocking the OPG-Fas interaction on OPG-induced changes in gene expression and PA-SMC proliferation.

5.3 Methods

5.3.1 Real-time TaqMan qPCR

Following 30-minute incubation in the presence or absence of Fas neutralising antibody, HPA-SMCs were stimulated with 0.2% v/v FBS or rhOPG (50 ng/ml) for 6 hours. RNA was then extracted using TRIzol reagent and the Zymo Direct-Zol RNA extraction kit. Complementary DNA (cDNA) was synthesized by reverse transcription and mRNA levels of TRAIL, PDGFRA, CAV1, VEGFA and TNC were quantified by TaqMan RT-qPCR (Chapter 2.13).

5.3.2 HPA-SMC Proliferation

HPA-SMCs were pre-incubated in the presence or absence of Fas neutralising antibody (1500 ng/ml), TRAIL neutralising antibody or both Fas and TRAIL antibody (1500 ng/ml) for 30 minutes prior to 72-hour stimulation with OPG (30 ng/ml), PDGF (20 ng/ml) or 0.2% v/v FBS. Proliferation was then measured using the CellTiter-Glo® luminescent assay. In order to analyse PA-SMC proliferation, results were expressed as a percentage response of unstimulated cells (0%) and PDGF (100%) (Chapter 2.12).

5.3.2.1 Statistics

All data are represented as mean \pm SEM. Treatments were compared using Two-way ANOVA followed by Tukey's post hoc test for multiple comparisons. $P < 0.05$ was deemed statistically significant. The n numbers refer to the number of separate experiments performed and for each experiment performed, each condition was performed in duplicate or triplicate.

5.4 Results

5.4.1 The Effect of Blocking the OPG-Fas Interaction on OPG-induced PAH-associated Gene Expression

To determine whether Fas truly was the key receptor driving the OPG-induced phenotype, I aimed to determine the effect of Fas blockade on OPG-induced gene expression.

In support of my data discussed in the previous results (Chapter 4, Figure 4.11), OPG stimulation of PA-SMCs induced a significant increase in TRAIL, PDGFRA, TNC, VEGFA and CAV1 expression (Figure 5.1). Interestingly, Fas blockade prior to OPG stimulation of PA-SMCs significantly inhibited the OPG-induced expression of PDGFRA, Cav-1, TNC and VEGFA expression (Figure 5.1). Although OPG did not induce a significant change in BMPR1A expression in PA-SMCs, these data support my TaqMan data in Chapter 4. Furthermore, Fas blockade did not have any significant effect on BMPR1A expression (Figure 5.1). Surprisingly however, Fas blockade induced a further significant increase in TRAIL expression in PA-SMCs following OPG stimulation, rather than inhibiting OPG-induced TRAIL expression (Figure 5.1).

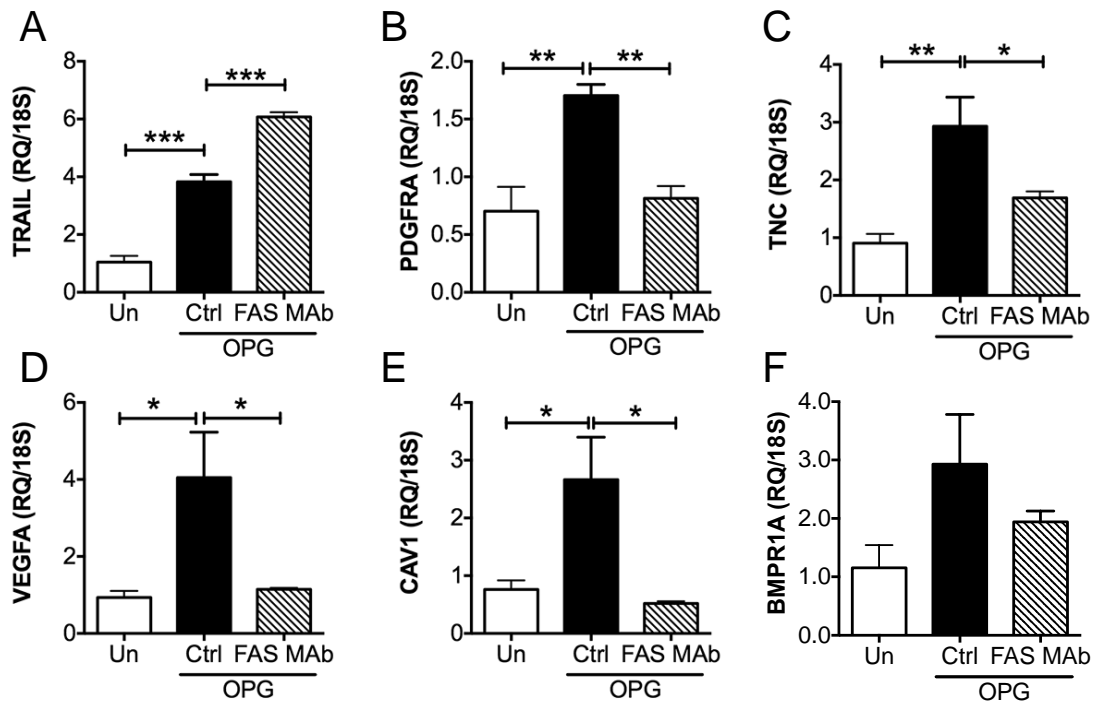


Figure 5.1- The effect of Fas blockade on OPG-induced gene expression in PA-SMCs.

Quiesced HPA-SMCs were incubated in the presence or absence of Fas neutralising antibody for 30 minutes prior to 6 h stimulation of cells with OPG (50 ng/ml) or 0.2% FBS (negative). The effect of Fas blockade on the expression of A) TRAIL, B) PDGFRA, C) TNC, D) VEGFA, E) CAV1 and F) BMPRIA RNA was assessed by TaqMan RT-qPCR. All data are normalised using $\Delta\Delta CT$ with 18S rRNA as the endogenous control gene. Fas mAb= Fas monoclonal antibody, Un = unstimulated PA-SMCs incubated with Fas mAb. Ctrl = control OPG-stimulated (50 ng/ml) cells. Fas mAb = cells pre-treated with Fas antibody for 30 minutes before stimulation with OPG (50 ng/ml). Error bars represent mean \pm SEM. N=4 experiments, each experiment with duplicate wells.

5.4.2 Investigating the Effect of Blocking the OPG-Fas Interaction on OPG-induced PA-SMC Proliferation

After finding that Fas blockade significantly inhibited OPG-induced gene expression of PDGFRA, TNC, VEGF and CAV1 in PA-SMCs, I next wanted to examine the effect of Fas blockade on OPG-induced PA-SMC proliferation as this is one of the

key drivers of PAH pathogenesis and blocking this process may help to stabilise disease and prevent disease progression. Investigating the effect of blocking Fas would also convince me of whether the OPG-Fas interaction would be important in PA-SMC proliferation.

As expected, OPG caused a significant increase ($p < 0.0001$) in cell proliferation, compared to unstimulated cells (Figure 5.2). Pre-treatment of cells with the Fas neutralising antibody had no significant effect on unstimulated cells or PDGF-induced proliferation of PA-SMCs (Figure 5.2). Conversely, pre-treating the cells with the Fas antibody prior to OPG stimulation caused a significant reduction of 34% in OPG-induced proliferation of PA-SMCs ($p < 0.01$), compared to OPG stimulated cells. This observation was intriguing as it suggests Fas is a significant contributor to the proliferative phenotype. However, these data also suggest that there may be another factor that is causing the proliferation of PA-SMCs, even in the presence of Fas blockade.

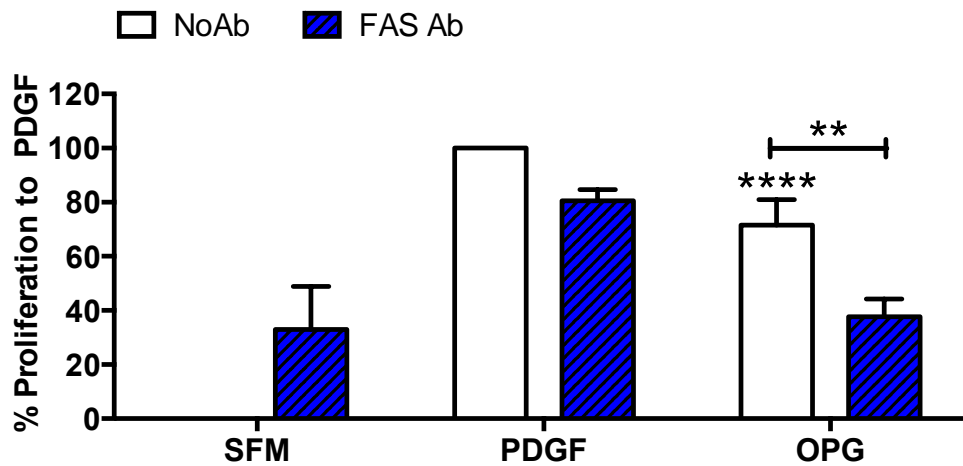


Figure 5.2- Fas blockade reduces OPG-induced PA-SMC proliferation.

*OPG significantly increased PA-SMC proliferation after 72 hours stimulation, compared to unstimulated PA-SMCs. However, pre-incubation with Fas neutralising antibody 30 minutes before OPG stimulation caused a significant reduction of 34% in OPG-induced PA-SMC proliferation. Fas blockade had no effect on PDGF-induced or unstimulated PA-SMC proliferation. Proliferation was normalised to unstimulated (0%) and PDGF stimulated (100%) cells. Error bars represent mean \pm SEM, n=4. ** p <0.01, **** p <0.0001. White bars= no antibody. Blue striped bars= Fas antibody pre-treatment 30 minutes before stimulation.*

After looking back at the changes in gene expression in the presence of Fas blockade, the change in TRAIL expression remained puzzling (Figure 5.1 A). Although changes in TRAIL RNA expression was not deemed significant, Fas blockade led to a further increase in TRAIL expression, rather than a reduction. TRAIL has already been shown to induce the proliferation of PA-SMCs in vitro (Hameed et al. 2012) and therefore TRAIL could possibly be the mitogen responsible for the remaining PA-SMC proliferation. This led me to speculate that TRAIL may be the additional factor responsible for the PA-SMC proliferation.

I therefore investigated the effect of blocking TRAIL on PA-SMC proliferation. TRAIL blockade alone however had no effect on unstimulated cells, PDGF-induced or OPG-induced proliferation (Figure 5.3). After observing that TRAIL blockade alone did not cause a reduction in OPG, I then looked at the effect of blocking both Fas and TRAIL simultaneously to see whether this could inhibit OPG-induced

proliferation more so than Fas blockade alone. As shown in Figure 5.3, treatment of PA-SMCs with both Fas and TRAIL antibody had no effect on PDGF-induced proliferation. However, Fas and TRAIL blockade significantly inhibited OPG-induced proliferation by 58%, a further 24% reduction than Fas blockade alone.

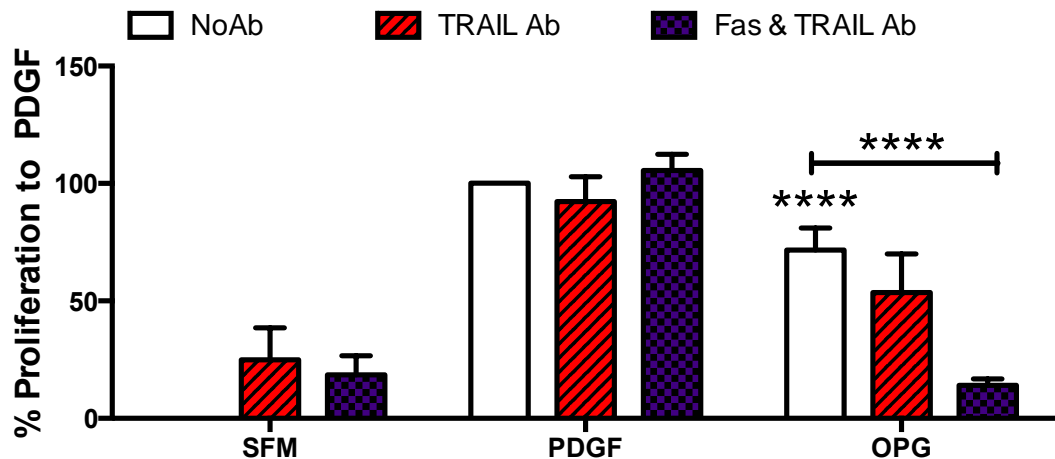


Figure 5.3- Simultaneous Fas and TRAIL blockade further inhibits OPG-induced PA-SMC proliferation.

*Pre-incubation with both the Fas neutralising antibody and TRAIL antibody had no effect on PDGF-induced or unstimulated PA-SMC proliferation. However, OPG-induced proliferation was significantly reduced by 58% when both Fas and TRAIL were blocked by antibody pre-treatment. Pre-incubation with TRAIL antibody 30 minutes before stimulation (red striped bars) had no effect on OPG-induced, PDGF-induced or unstimulated cell proliferation. Proliferation was normalised to unstimulated (0%) and PDGF stimulated (100%) cells. Error bars represent mean \pm SEM, n=4. ****p<0.0001. White bars= no antibody. Purple spotted bars= Fas and TRAIL antibody pre-treatment 30 minutes before stimulation.*

5.5 Discussion

In this chapter, I aimed to answer the last of the four questions set out in the Chapter 2 of this thesis to identify a mechanism by which OPG induces PA-SMC proliferation. The data show that Fas blockade significantly inhibited OPG-induced gene expression of PDGFRA, TNC, VEGFA, and CAV1. Furthermore, Fas blockade alone caused a significant reduction in OPG-induced PA-SMC proliferation.

Although Fas blockade was found to significantly inhibit OPG-induced gene expression, it would be interesting to assess the effect Fas antibody only treatment has on gene expression in unstimulated cells. This would ensure that the inhibition of OPG-induced gene expression in HPA-SMCs caused by Fas blockade is not due to the antibody treatment of cells. After observing that OPG-induced PA-SMC proliferation was only partially reduced by Fas blockade, I began to speculate whether there might be another factor that was inducing PA-SMC proliferation, in addition to OPG. Fas blockade significantly reduced PDGFRA, TNC, VEGFA and Cav-1 expression, Fas blockade induced a significant increase in TRAIL expression in OPG-stimulated cells pre-treated with a Fas neutralising antibody. The fact that TRAIL is a potent PA-SMC mitogen (Hameed et al. 2012) led me to suspect that TRAIL might also be inducing PA-SMC proliferation. TRAIL blockade alone had no effect on OPG-induced PA-SMC proliferation, confirming that OPG was not inducing pathogenic changes in PA-SMCs by binding to TRAIL. However, blockade of both Fas and TRAIL together caused a greater reduction in OPG-induced proliferation. I therefore propose that there may be a redundancy mechanism between Fas and TRAIL in PA-SMCs.

There are no reports in the literature of a redundancy mechanism between Fas and TRAIL. However, in support of my theory, a recent study has reported a redundancy mechanism for TRAIL-resistance. Resistance against TRAIL-induced apoptosis in normal, non-transformed human primary fibroblasts and SMCs was caused by cellular FLICE-like inhibitory protein (cFLIP), B-cell lymphoma 2 (Bcl-2) and XIAP (van Dijk et al. 2013). However, knockdown or inhibition of cFLIP, Bcl-2 or XIAP independently was not sufficient to induce sensitivity to TRAIL-induced apoptosis, which suggests a redundancy mechanism between these proteins (van Dijk et al. 2013). These data therefore support my theory that a redundancy mechanism may

exist in PA-SMCs. OPG-induced PA-SMC proliferation may be mediated by a redundancy mechanism that exists between Fas and TRAIL, and blocking Fas or TRAIL alone does not fully inhibit OPG-induced proliferation.

I therefore postulate that in normal PA-SMCs, where there are low levels of OPG, Fas, TRAIL and the TRAIL receptors, TRAIL R1 and TRAIL R3, there is a basal level of PA-SMC proliferation. Because OPG levels are low, there is only a small amount of OPG binding to Fas, hence a low amount of PA-SMC proliferation. This allows FasL to bind to Fas and induce PA-SMC apoptosis. In normal PA-SMCs, OPG might also be binding to TRAIL to prevent TRAIL binding to TRAIL R1 and TRAIL R3 and hence OPG prevents TRAIL-induced PA-SMC proliferation. Therefore, in normal, healthy PA-SMCs, there is a balance between PA-SMC proliferation and apoptosis maintained by the interaction of OPG with Fas and TRAIL. However, during PAH pathogenesis, there is an unknown insult or injury that triggers an increase in OPG, TRAIL and TRAIL receptor expression, which has already been shown by the literature (Lawrie et al. 2008; Condliffe et al. 2012; Hameed et al. 2012), and an increase in Fas expression caused by OPG stimulation of PA-SMCs, as shown by data in this thesis. I therefore propose that OPG-induced PA-SMC proliferation is increased by OPG binding to Fas, which then leaves TRAIL free to bind to the TRAIL R1 and TRAIL R3 receptors and subsequently induce PA-SMC proliferation. This is summarised in Figure 5.4.

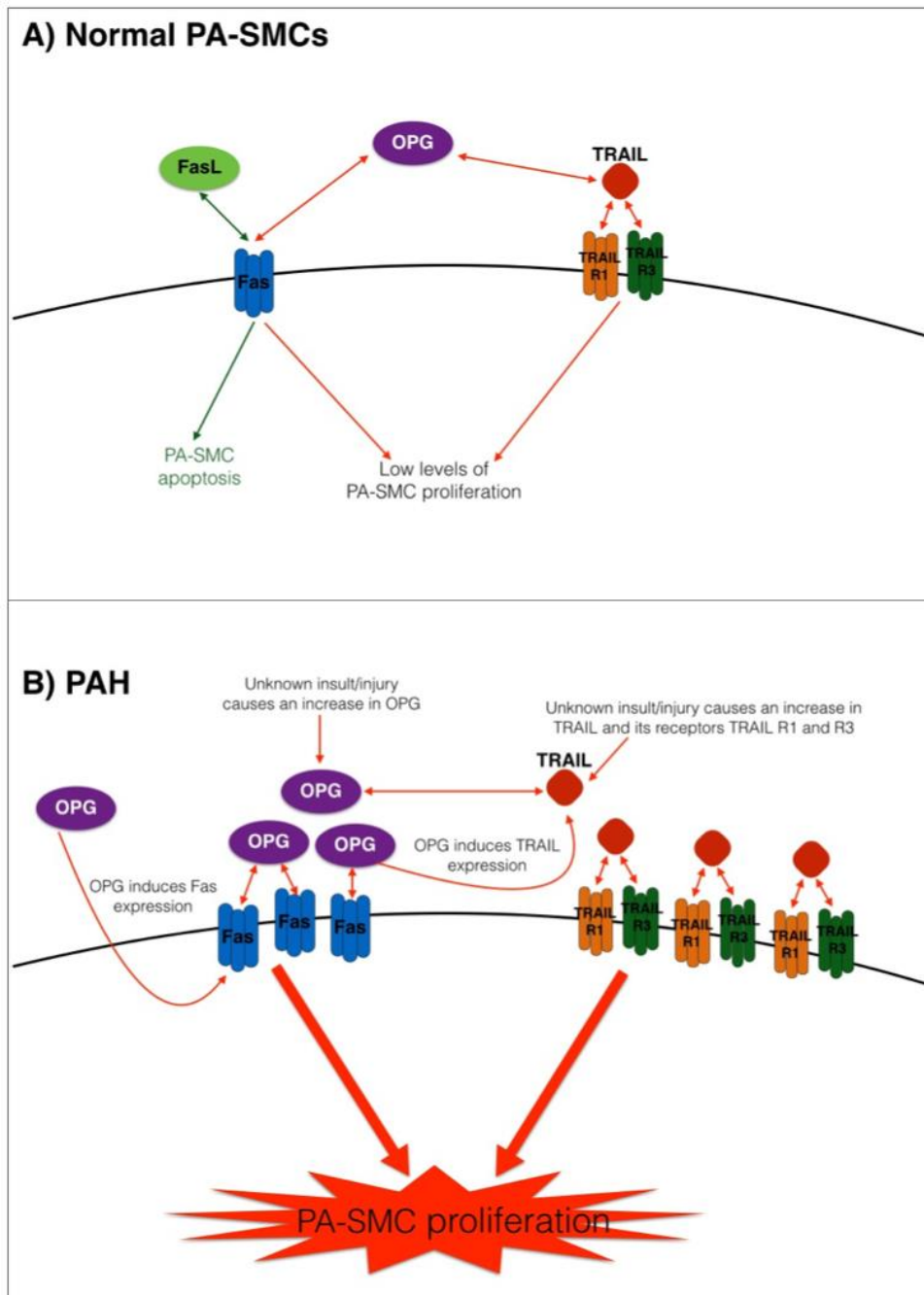


Figure 5.4- OPG, FAS and TRAIL signalling in normal and diseased PA-SMCs.

A) In normal PA-SMCs, there is a low level of Fas, OPG and TRAIL expression, hence a low level of PA-SMC proliferation. Due to low levels of OPG binding to Fas, FasL can still bind to Fas and induce apoptosis of PA-SMCs. Therefore, in normal PA-SMCs there is a balance between PA-SMC proliferation and apoptosis. B) However, in PAH, an unknown insult or injury causes an increase in OPG expression, which subsequently increases Fas expression and OPG binds to Fas to induce PA-SMC proliferation. An unknown insult/injury also increases TRAIL, TRAIL R1 and TRAIL R3 expression and TRAIL induces PA-SMC proliferation.

Blockade of TRAIL alone however had no effect on OPG-induced proliferation, suggesting that OPG-induced proliferation is not mediated through the OPG-TRAIL interaction. Fas blockade significantly reduced OPG-induced proliferation, however upon blockade of Fas, there was an increase in TRAIL expression. This TRAIL surplus may therefore continue to induce cell proliferation, even though the interaction between OPG and Fas is blocked and OPG is free to bind TRAIL. Therefore, both Fas and TRAIL blockade is required to inhibit PA-SMC proliferation and this is summarised in Figure 5.5.

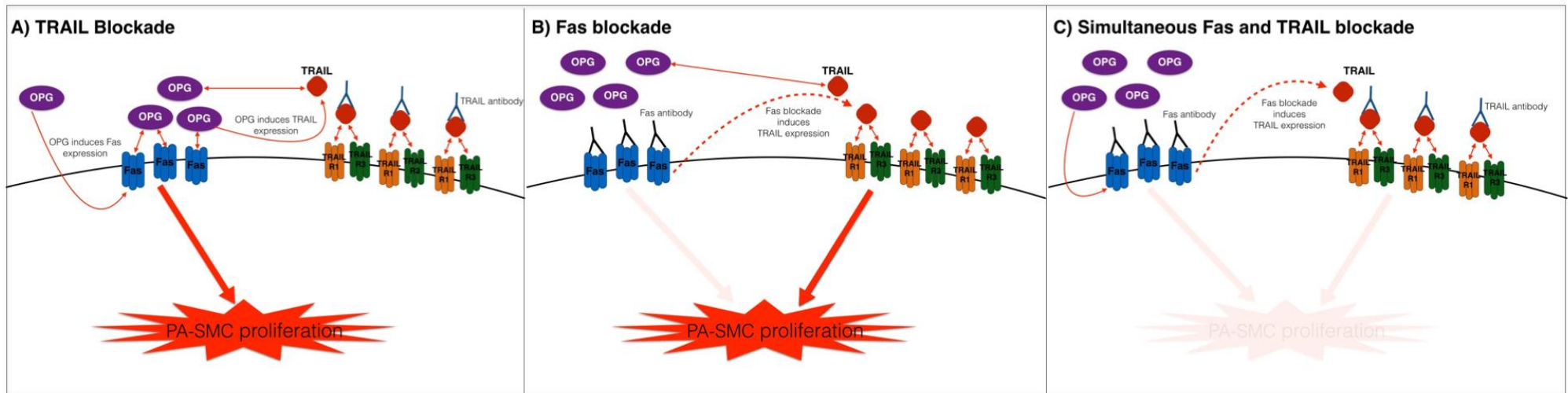


Figure 5.5- TRAIL blockade, Fas blockade and simultaneous TRAIL and Fas blockade in PA-SMCs.

A) TRAIL blockade alone has no effect on OPG-induced proliferation of PA-SMCs in vitro, however B) Fas blockade prevents OPG binding and thus inhibits OPG-induced PA-SMC proliferation. Fas blockade also induces TRAIL expression, which may also potentiate the TRAIL-induced proliferation that occurs in PA-SMCs, even when the OPG-Fas interaction is blocked. C) Simultaneous blockade of both Fas and TRAIL is therefore required to inhibit PA-SMC proliferation.

These data would therefore be important to consider if the OPG-Fas interaction was to be pursued as a therapeutic target. In this case, an antibody against OPG to block interaction with Fas may be more suitable than an antibody against Fas, due to the effect of blocking Fas on TRAIL expression. However, it would also be beneficial to develop an antibody that binds to OPG to block the interaction with Fas, but also still allow OPG to bind to TRAIL. This would allow OPG to “mop up” excess TRAIL to prevent TRAIL binding to its receptors, TRAIL R1 and TRAIL R3, thus preventing TRAIL-induced proliferation.

Although these data have provided evidence that the OPG-Fas interaction is responsible for the pathogenic changes in PA-SMCs, further work to investigate the effects of Fas blockade on PA-SMC phenotype should be conducted. Firstly, it would be interesting to assess the effect of Fas blockade on OPG-induced CDK4, HSP27, ERK1/2 and mTOR phosphorylation and CDK5 expression in PA-SMCs at different time points, for example, at 10 minutes, 60 minutes and 24 hours. This would provide further information about whether the changes in protein expression and activation are being mediated through the OPG-Fas interaction. It would also be interesting to determine the effect of Fas blockade on OPG-induced migration of PA-SMCs because Lawrie et al (2008) have reported that OPG induced the migration, as well as proliferation, of PA-SMCs *in vitro*.

In conclusion, the data presented in this chapter provide evidence that the interaction between the TNF receptor superfamily members, OPG and Fas, is responsible for the proliferation and changes in pathogenic gene expression in PA-SMCs induced by OPG. Furthermore, these data reveal a possible redundancy between Fas and another TNF superfamily member, TRAIL, in the proliferation of PA-SMCs. These data suggest that if the Fas blockade was to be considered as a therapeutic target, the need to also block TRAIL as well would have to be considered. Finally, these data reveal for the first time that blocking the Fas receptor can prevent OPG-induced pathogenic changes in PA-SMCs and may be of therapeutic potential in the future. As discussed in this chapter, I propose that OPG induces the survival and proliferation of PA-SMCs *in vitro* through the novel interaction with Fas. Furthermore, my data in Chapter 4, show that OPG induces changes in protein phosphorylation and expression and gene

expression, which may consequently be inducing the survival and proliferation of PA-SMCs *in vitro*.

6. GENERAL DISCUSSION

PAH is a devastating lung disease with a high mortality and a poor quality of life. PAH is defined as an mPAP of >25 mmHg at rest, however, symptoms often present late and are often misdiagnosed. Unfortunately, there is currently no cure for PAH and right heart failure is the major cause of mortality (Elliot & Kiely 2006; Kiely et al. 2013; Pokreisz et al. 2007). The pathogenesis of PAH is an incredibly complex process that affects all layers of the pulmonary arteries (Humbert et al. 2004). PAH is characterised by progressive pulmonary vascular remodelling, a key component of which is the proliferation and migration of pulmonary arterial smooth muscle cells (PA-SMCs) (Rabinovitch 2008). OPG has recently been implicated as an important pathogenic mediator in PAH and OPG also induces the proliferation and migration of PA-SMCs *in vitro* (Lawrie et al. 2008; Condliffe et al. 2012). Furthermore, recent unpublished data from the Pulmonary Vascular Research Group (Department of Cardiovascular Science, University of Sheffield) shows that OPG blockade, either by genetic deletion or anti-OPG antibody treatment prevents and reverses disease in animal models of PAH. OPG is therefore an attractive therapeutic target, but the mechanism through which OPG induces PA-SMC proliferation is currently unknown. Therefore, the work undertaken in this thesis aimed at identifying the binding partner and intracellular signalling mechanism through which OPG induces the proliferation of PA-SMCs.

6.1 Summary of Key Findings

The data presented in this thesis show for the first time that OPG can bind to four previously undescribed human membrane proteins: Fas, IL1RAcP, TMPRSS11D and GAP43. Although the interaction between Fas and IL1RAcP was confirmed in endogenous PA-SMC lysates, Fas mRNA expression levels in PA-SMCs were the greatest of the four binding partners identified by the Retrogenix cell microarray, Fas mRNA expression was increased upon PA-SMC stimulation with OPG and was significantly higher in IPAH PA-SMCs compared to control PA-SMCs. Fas protein was also expressed in the pulmonary artery and right ventricle of IPAH patients, along with OPG (Chapter 3).

After identifying a potential OPG binding partner, I then investigated OPG-induced changes in protein and gene expression in PA-SMCs. OPG was found to alter the expression and activation of proteins and expression of genes involved in pro-proliferative pathways (phospho-ERK1/2, TRAIL, PDGFRA, TNC, Cav-1), the cell cycle (phospho-CDK4), anti-apoptotic pathways (phospho-HSP27 and CDK5) and pro-survival pathways (phospho-mTOR) (Chapter 4).

Finally, in order to determine the importance of the OPG-Fas interaction, I then looked at the effect of blocking this interaction on OPG-induced gene expression and PA-SMC proliferation. Fas blockade significantly inhibited OPG-induced gene expression and PA-SMC proliferation, however simultaneous Fas receptor and TRAIL blockade resulted in an even greater inhibition of OPG-induced PA-SMC proliferation (Chapter 5).

Although only six proteins from the KAM list of 89 OPG-regulated proteins were chosen for validation, the KAM data indicated that a high proportion of proteins induced by OPG are involved in the cell cycle. These data suggest that OPG is exerting its mitogenic actions by pushing the cell cycle forward in cells by inducing the expression of cell cycle proteins, which subsequently promote PA-SMC division and hyperplasia. Importantly, the KAM also showed activation of a number of protein kinases, such as PKC, P38 MAPK, JNK, MEK, Raf and Abl (Chapter 4), which are known for their pro-proliferative actions, and anti-apoptotic proteins, such as the heat shock proteins. Activation of both these classes of proteins by OPG would all contribute to a pro-survival, pro-proliferative phenotype in PA-SMCs. Furthermore, constitutively active protein kinases and the inhibition of apoptosis are characteristically observed in neoplastic cells. Interestingly, PAH has been likened to cancer, with cells involved in PAH acquiring a hyperproliferative phenotype, which is also observed in neoplastic cells (Rai et al. 2008).

6.2 OPG, PAH and the Cancer Hypothesis

The idea that PAH shared characteristics with cancer first came from the finding that monoclonal endothelial cell proliferation was occurring in the plexiform lesions of remodelled pulmonary arteries (Tuder & Graham 2010). VEGF and VEGFR2 expression is detected in the endothelial cells with plexiform lesions and VEGF and its receptors are also expressed on a variety of tumour cells, including lung cancer cells (Tuder & Graham 2010; Goel & Mercurio 2013). The major similarities between PAH and cancer include altered cell crosstalk, proliferation and apoptosis-resistance (Rai et al. 2008; Guignabert et al. 2013). In support of this, *ex vivo* human IPAH PA-SMCs and PA-ECs have been shown to maintain their hyperproliferative, anti-apoptotic phenotype for longer than normal PA-SMCs and PA-ECs (Guignabert et al. 2013). Recent evidence also suggests pulmonary vascular cells acquire a “Warburg” phenotype, that is, they show a shift in energy production from mitochondrial oxidative phosphorylation to glycolysis, which is also observed in cancer cells (Guignabert et al. 2013). Furthermore, several markers detected in the IPAH lung have also been described in cancers, including Cav-1 and the PDGF receptors (Tuder & Graham 2010). Data presented in this thesis demonstrate the ability of OPG to alter expression of VEGFA, Cav-1 and PDGFRA, suggesting that the mechanism through which OPG induces PA-SMC proliferation may be similar to the dysregulated mechanisms seen in cancer cell growth and proliferation.

Although PAH shares the above similarities with cancer, there are also differences between PAH and cancer and it is clear that PAH is not actually a cancer (Rai et al. 2008; Guignabert et al. 2013). One important difference between PAH and cancer is the phenotype cells acquire during the pathogenesis of each disease (Guignabert et al. 2013). Cancer cells develop an aggressive, hyperproliferative phenotype and the cells continue to proliferate despite restricted space and nutrients. Cancer cells also invade and destroy adjacent tissue, as well as metastasising to other locations in the body (Guignabert et al. 2013). Although PA-SMCs and PA-ECs acquire a hyperproliferative, anti-apoptotic phenotype in PAH, these cells do not have invade other tissues or metastasise like cancer cells do (Guignabert et al. 2013).

A further difference is that, unlike cancer cells, which generate malignant cells through clonal expansion, PAH affects all layers of the vessel wall and affects multiple cell types, including SMCs, ECs and fibroblasts, rather than a single homogenous cell population (Guignabert et al. 2013). Interestingly, cancer cells show alterations in cell proliferation machinery, especially cyclins and cyclin dependent kinases that enable cancer cells to proliferate on their own (Guignabert et al. 2013). However, although there is currently no evidence in the literature of pulmonary vascular cells acquiring the ability to proliferate on their own, my data indicate that OPG induces the activation and expression cell cycle proteins, including phosphorylation of CDK4. My data therefore suggest that, although PA-SMCs may not develop alterations in cell cycle machinery like cancer cells do, OPG may be causing cell proliferation and hyperplasia by inducing cell cycle protein activation and expression, similar to cancer cells. These data therefore support the theory that PA-SMCs involved in PAH pathogenesis may acquire a phenotype similar to cancer cells. Despite the similarities between PAH and cancer, it is clear that the mechanisms that lead to the tumorigenic phenotype in cancer can not fully explain how PAH develops due to the differences discussed above. However, the similarities between PAH and cancer has identified a group of anti-proliferative, oncological drugs that may also prove therapeutically beneficial in PAH (Guignabert et al. 2013).

In addition to the activation of the pro-proliferative pathways, OPG was also found to activate anti-apoptotic heat shock proteins. HSP27 expression has been identified in the PA-ECs and PA-SMCs of congenital heart disease patients with pulmonary hypertension, remodelled pulmonary arteries and plexiform lesions (Geiger et al. 2009). Dimers of phosphorylated HSP27 have been shown to interact with Daxx to prevent its translocation from the nucleus to the cytoplasm, prevent subsequent Ask1 activation and block Fas-induced apoptosis (Charette & Landry 2000; Charette et al. 2000). Therefore, OPG may not only be binding to Fas to induce PA-SMC proliferation, but may be inhibiting the apoptotic effects of Fas by increasing levels of phosphorylated HSP27, which then blocks Fas-induced apoptosis. High levels of HSP27 expression are observed in treatment resistant cancers, such as prostate cancer and HSP27 is thought to contribute to apoptosis resistance in cancer cells (Zoubeidi & Gleave 2012). The HSP27 specific inhibitor, Apatorsen (OGX-427) is now undergoing phase II clinical trials to treat prostate and bladder cancer (Lamoureux et

al. 2014). It would therefore be interesting to assess the effect of inhibiting HSP27 on disease development and reversal in animal models of PAH to determine the therapeutic potential in of HSP27 in PAH.

OPG most significantly altered the expression of Abl in the KAM and this was very interesting because this supports the cancer hypothesis. As briefly mentioned in Chapter 4, Imatinib, is used to treat the myeloproliferative disorder, chronic myeloid leukaemia by competitively binding to and blocking the ATP binding site of the BCR-ABL fusion protein (Ciarcia et al. 2012). Imatinib has previously been shown to inhibit the PDGF receptor and c-Kit in addition to Abl and so was suspected of having therapeutic potential for the treatment of PAH (Galiè et al. 2013). Imatinib was previously shown to prevent MCT-induced PH and reverse PH in both the MCT rat model and hypoxic mouse model of PH (Schermyly et al. 2005; Pankey et al. 2013). Imatinib was also shown to inhibit proliferation and induce apoptosis of PDGF-stimulated IPAH PA-SMCs (Nakamura et al. 2012). However, despite these promising data, in a randomized, double blind placebo controlled trial of Imatinib as an add-on therapy for the treatment of PAH, a high number of serious adverse effects, such as subdermal hematoma, were reported (Hoepfer, Barst, et al. 2013). Consideration for Imatinib as a treatment for PH has currently been halted (Galiè et al. 2013). My data suggest that small molecule inhibitors against specific targets, such as HSP27 and Abl, might be useful as future PAH therapies.

A number of small molecule inhibitors that therapeutically target ERK1/2 activation have been approved to treat cancers. Vemurafenib and Selumetinib inhibit Raf and MEK1/2, respectively to block ERK1/2 activation (Sale & Cook 2013). ERK1/2 has also, like the proteins discussed above, been shown to be important in the pathogenesis of PAH, as well as in cancer. TRAIL-induced PA-SMC proliferation and migration is ERK1/2 dependent and recent work looking into the mechanism of the PH therapeutic, Sildenafil, revealed that Sildenafil reduced in ERK1/2 activation (Kiss et al. 2014). ERK1/2 may therefore be a therapeutic target in itself, and blocking ERK1/2 may prevent the proliferation of PA-SMCs.

6.3 The OPG-Fas Interaction as a Potential Therapeutic Target

As discussed previously in Chapter 5, Fas blockade inhibited OPG-induced PA-SMC proliferation. The OPG-Fas interaction may therefore be a potential therapeutic target in the treatment of PAH. However, if the OPG-Fas interaction were to be targeted, the effect of Fas blockade on TRAIL RNA expression and TRAIL-induced PA-SMC proliferation would need to be considered. It appears at this stage that targeting Fas would not be beneficial because Fas ligation resulted in an increase in TRAIL RNA expression and still did not completely inhibit OPG-induced proliferation, simultaneous Fas and TRAIL blockade was required. TRAIL has already been implicated as an important pathogenic mediator in PAH (Hameed et al. 2012) and considering the possible redundancy mechanism between Fas and TRAIL, Fas blockade may result in an undesirable increase in TRAIL expression if therapeutically blocked. Therefore, one possible way to target the OPG-Fas interaction would be to develop a monoclonal antibody that binds OPG to prevent interaction with Fas and inhibit PA-SMC proliferation.

Monoclonal antibodies (mAbs) are highly specific antibodies that recognize only a single epitope on any one antigen. This could be highly advantageous if targeting OPG because it may allow a mAb to be developed that binds specifically to the epitope to which Fas binds OPG, blocking the OPG-Fas interaction, but still leaving OPG free to interact with TRAIL. This would allow the role of OPG as a decoy receptor for TRAIL to be exploited, allowing OPG to bind excess TRAIL and prevent TRAIL-induced PA-SMC proliferation. This would however rely on the OPG binding sites for Fas and TRAIL being different and this has yet to be determined, for example by identifying the crystal structure of OPG by X-ray crystallography and investigating binding of Fas and TRAIL to OPG by surface plasmon resonance.

Although there are currently no mAb therapies that are approved for PAH therapies, there are now reports in the literature of mAbs being used to treat PAH that is associated with other conditions. The IL-6 mAb Tocilizumab has been successfully used to treat a patient with Castleman's disease-associated PAH who was resistant to conventional PH therapies, and a patient with adult onset Still's disease-associated

PAH (Arita et al. 2010; Kadavath et al. 2014). The successful treatment of Castleman's disease-associated PAH in a non-responder to conventional therapies provides a possibility that mAbs may offer an alternative therapy to these patients.

6.4 Limitations

Although the data presented in this thesis begin to reveal a novel receptor and the signalling mechanisms through which OPG may be inducing PA-SMC proliferation, there are several limitations to the work undertaken. The KAM was chosen to identify potential protein targets because it is a high-throughput, time-effective technique allowing hundreds of different proteins to be screened for changes in protein expression and phosphorylation in PA-SMCs following OPG stimulation. Because it is a high thorough-put technique, results had to be validated to ensure accurate interpretation of the results. However, the KAM showed expression and phosphorylation of 89 proteins were significantly altered in PA-SMCs following OPG stimulation. Only nine proteins were then selected for validation by In-cell western blotting or gold standard western blotting. This means that the remaining 80 proteins that were not selected for validation may also play an important role in mediating OPG-induced PA-SMC proliferation. Therefore, the role of the remaining 80 proteins would require further investigation, as discussed below in Chapter 6.5. The KAM also used non-denatured protein samples. Native proteins may not be accessible to certain antibodies due to the masking of specific epitopes when proteins are in their native form. This could be problematic if proteins activated by OPG form complexes, masking antibody-specific epitopes. However, despite the limitations, this technique allowed identification of potential phosphorylation targets of OPG that were previously unidentified and provided a much more time-effective and cost-effective way of screening hundreds of targets to identify proteins for validation.

Just as the KAM was used to investigate changes in protein expression and activation, the RNA microarray was used as a high-throughput screen to identify changes in RNA expression in OPG-stimulated PA-SMCs. Results of the microarray revealed that OPG significantly altered the expression of 1732 genes. However, I chose to focus on the 57 genes already associated with PAH pathogenesis and of these, ten genes were selected for validation. By only investigating the effects of OPG on PAH-associated

gene expression, this may have excluded genes not associated with PAH, but may still play an important role in OPG-induced PA-SMC proliferation. Results of the microarray will therefore require further investigation, as discussed in Chapter 6.5.

Finally, although the Retrogenix cell microarray identified four novel binding partners for OPG, only the interaction between OPG and Fas and IL1RAcP was validated. Furthermore, I only investigated the effect of blocking the OPG-Fas interaction on PA-SMC proliferation. I did not follow up the interactions between OPG and GAP43, IL1RAcP or TMPRSS11D on PA-SMC phenotype, or the role of these interactions in mediating the phenotype of other cell types, such as PA-ECs or fibroblasts. This would be important to do in the future work, discussed below, because these novel OPG interactions may reveal important roles for OPG in the biology of other cells and diseases, such as neurones and neurodegenerative disorders, which are beyond the scope of this thesis.

6.5 Future Directions

The data in this thesis implicate the novel OPG-Fas interaction as central in PA-SMC proliferation and show that OPG has the ability to induce changes in both protein expression and activation and PAH-associated gene expression in PA-SMCs. However, the identification of novel OPG interactions and downstream changes in gene and protein expression have created even more research questions that must be investigated to determine the importance of these in normal cell biology and in disease.

Future research leading on from this thesis could firstly investigate the expression and function of Fas in other cell types and animal models of PAH. It would be interesting to determine whether Fas protein expression is observed in other cell types important in PAH pathogenesis, such as ECs and fibroblasts, and whether this interaction might be important in inducing pathogenic changes in these cell types. It would also be important to determine whether Fas is expressed, or even correlates, with disease development of animal models of PH and if so, whether blocking Fas *in vivo* could prevent or even reverse experimental PH. Results discussed in this thesis provide evidence that the OPG-Fas interaction is a potential therapeutic target. Therefore,

research following on from this work is now developing human monoclonal antibodies against OPG. Future work will look at the effect of blocking OPG in animal models of PH to assess the efficacy and pharmacokinetics of the antibodies.

However, after identifying that OPG can bind to four novel human membrane proteins, it has become evident that knowing how OPG interacts with the binding partners, RANKL and TRAIL would be very beneficial to help with the design of therapeutics against OPG. Therefore, it would be very beneficial to determine the crystal structure of OPG, for example by X-ray crystallography, to model how OPG interacts with its binding partners. If OPG is capable with binding each of the binding partners at different binding sites, this would be an important consideration when screening anti-OPG antibodies for example, and might allow an anti-OPG antibody to be designed that blocks the binding site for Fas, but still allows OPG to bind to TRAIL and prevent the mitogenic actions of TRAIL in PA-SMCs.

The increase in HSP27 and CDK4 activation offers another line of therapeutics. Small molecule inhibitors against HSP27, such as Apatorsen, should be evaluated to see if HSP27 blockade could prevent or reverse disease in animal models of PH, because HSP27 may also be an important therapeutic target for the treatment of PAH. Additional work should also be undertaken to look at the effect of blocking cyclin dependant kinases on OPG-induced PA-SMC proliferation. This could be investigated in the future by inhibiting CDK activity *in vitro*, prior to OPG stimulation of PA-SMCs, using the pan-specific CDK inhibitor, BAY 1000394, which has been shown to inhibit proliferation of cancer cell lines (Siemeister et al. 2012)

Further work would also be required to investigate the changes in protein and gene expression in more detail. One limitation of this work is that only a selection of proteins were selected from the KAM and only PAH-associated genes were chosen from the microarray for validation and further investigation. Therefore, future work would be needed to thoroughly investigate the changes in protein and gene expression in greater detail, especially looking into the consequences of OPG-induced changes in genes that have not been implicated in PAH pathogenesis. There may be proteins and genes that have not been investigated in this thesis that may play an important role in PAH pathogenesis. It would also be interesting to determine whether Abl expression

correlates with disease progression or is reduced in animals that have received the anti-OPG intervention and prevention, or whether Abl expression is altered in PAH patients that are currently, or have previously received Imatinib treatment.

Data presented in this thesis identified that OPG induced an increase in ERK1/2 expression in PA-SMCs. ERK1/2 action is also required for TRAIL-induced PA-SMC proliferation and migration of PA-SMCs (Hameed et al. 2012). These data suggest that ERK1/2 is a common mediator in both OPG and TRAIL signalling. A microarray has recently been performed by the Pulmonary Vascular Research Group (University of Sheffield, UK), comparing TRAIL-stimulated to unstimulated PA-SMCs. Analysis of this microarray will provide more information about the distinct and overlapping signalling pathways that OPG and TRAIL employ in PA-SMCs to induce proliferation. This may then identify novel therapeutic targets, or biomarkers that help clinicians to diagnose PAH earlier.

Finally, the novel OPG interactions with TMPRSS11D, Gap43 and IL1RAcP will also require validation and their role in disease will need to be further studied. Firstly, the interaction between OPG and GAP43 and TMPRSS11D would need to be confirmed by co-immunoprecipitation. GAP43 RNA was detected in PA-SMCs, therefore the interaction between OPG and GAP43 would need to be investigated in PA-SMCs. TMPRSS11D expression would need to be investigated in other cell types involved in PAH pathogenesis to determine whether the interaction with TMPRSS11D may be important in the phenotype of ECs or fibroblasts for example. To investigate TMPRSS11D expression in different cell types, TaqMan RT-qPCR would determine RNA expression, and protein expression would be confirmed by western blotting. Expression of all four binding partners would need further examined in both healthy and diseased human tissue and animal tissue. The interaction with IL1RAcP would also need to be investigated to determine whether OPG can modulate inflammatory pathways through interactions with IL1RAcP, ST-2 and IL1-R1.

I believe that the data presented in this thesis begin to reveal a novel signalling pathway and cell surface receptor through which OPG induces PA-SMC proliferation. These data contribute to furthering our current understanding of the mechanisms that lead to the PA-SMC dysfunction and proliferation that is observed PAH. These data

provide further evidence that OPG is a critical mediator of PA-SMC phenotype and as such represents a potential therapeutic target for PAH. Furthermore, these data also suggest that OPG is not simply a decoy receptor for RANKL and TRAIL and through binding to previously undescribed cell membrane proteins, OPG might instead play a more diverse role in other biological systems.

7. APPENDIX

7.1 Product Suppliers

7.1.1 General Reagents

Reagent	Cat. No	Supplier	Location
CHAPS	C-5070	Sigma-Aldrich	Dorset, UK
Complete Protease Inhibitor Cocktail mini	11836153001	Roche	West Sussex, UK
Corning® Costar® 96-Well Cell Culture Plates	3595	Sigma-Aldrich	Dorset, UK
Di-Sodium hydrogen orthophosphate	301584L	AnalaR Normapur®, VWR International Ltd	Lutterworth, Leicestershire, UK
DTT	D0632	Sigma-Aldrich	Dorset, UK
Formaldehyde	101136C	AnalaR Normapur®, VWR International Ltd	Lutterworth, Leicestershire, UK
Methanol	451027S	VWR International Ltd	Lutterworth, Leicestershire, UK
NaCl	10040460	Fisher Scientific	Loughborough, Leicestershire, UK
PBS	BR0014	Oxoid	Basingstoke, UK
SDS	L3771	Sigma-Aldrich	Dorset, UK
Sodium Hydroxide	102525P	AnalaR Normapur®, VWR International Ltd	Lutterworth, Leicestershire, UK
Sodium Orthovanadate	S6508-50G	Sigma-Aldrich	Dorset, UK
Sodium Phosphate	342483	Sigma-Aldrich	Dorset, UK
TRIS	T/P630/60	Fisher Scientific	Loughborough, Leicestershire, UK
Triton X-100	T8787	Sigma-Aldrich	Dorset, UK
Tween-20	P1379	Sigma-Aldrich	Dorset, UK
β-Mercaptoethanol (β-ME)	M6250	Sigma-Aldrich	Dorset, UK

7.1.2 Cell Culture Reagents

Reagent	Cat. No	Supplier	Location
DMEM	BE12-604F	Lonza	Basel, Switzerland
Penicillin/streptomycin	15240062	Gibco, Life Technologies	Paisley, UK
SmBM growth media	CC-3181	Lonza	Basel, Switzerland
SmGm-2 SingleQuots	CC-4149	Lonza	Basel, Switzerland
Insulin	CC4021D		
hFGF-B	CC4068D		
GA-1000	CC4081D		
FBS	CC-4102D		
hEGF	CC-4230D		
T25 cm² cell culture flask	156367	Nunc, Thermo Fisher scientific	Rockford, Illinois, USA
T75 cm² cell culture flask	156499	Nunc, Thermo Fisher scientific	Rockford, Illinois, USA
Trypsin	R-001-100	Gibco, Life Technologies	Paisley, UK
Trypsin Neutralising Solution	R-002-100	Gibco, Life Technologies	Paisley, UK
Human Pulmonary Arterial Smooth Muscle Cells	CC-2581	Lonza	Basel, Switzerland

7.1.3 Co-Immunoprecipitation Reagents

Reagent	Cat. No	Supplier	Location
nProteinG sepharose 4 Fast Flow beads (Immunoprecipitation Starter Kit)	17-6002-35	GE Healthcare Life Sciences	Buckinghamshire, UK

7.1.4 In-Cell Western Assay Reagents

Reagent	Cat. No	Supplier	Location
DRAC5	DR50050	Biostatus	Leicestershire, UK
Sapphire 700	928-40022	LiCOR	Bad Homburg, Germany

7.1.5 Pierce 660 nm Protein Assay

Reagent	Cat. No	Supplier	Location
Bovine Serum Albumin Standard	23209	Pierce, Thermo Fisher Scientific	Rockford, Illinois, USA
Ionic Detergent Compatibility Reagent	22663	Pierce, Thermo Fisher Scientific	Rockford, Illinois, USA
Pierce 660nm Protein Assay Reagent	22660	Pierce, Thermo Fisher Scientific	Rockford, Illinois, USA

7.1.6 Primary Antibody Suppliers

Antibody	Cat. No	Supplier	Location
Human Atg13 rabbit monoclonal antibody	13273	Cell Signaling Technology	Danvers, MA, USA
Human Atg7 (D12B11) rabbit monoclonal antibody	8558	Cell Signaling Technology	Danvers, MA, USA
Human CDK5 (EP715Y) rabbit monoclonal antibody	AB40773	Abcam	Cambridge, UK
Human Daxx (7A11) mouse monoclonal antibody	NBP1-47453	Novus Biologicals	Cambridge, UK
Human ERK1/2 rabbit monoclonal antibody	4695	Cell Signaling Technology	Danvers, MA, USA
Human FADD rabbit polyclonal antibody	2782	Cell Signaling Technology	Danvers, MA, USA
Human Fas mouse monoclonal neutralising antibody (Clone ZB4)	05-338	Millipore Corporation	Massachusetts, USA
Human Fas rabbit polyclonal antibody	NBP1-49957	Novus Biologicals	Cambridge, UK
Human GβL rabbit monoclonal antibody	3274	Cell Signaling Technology	Danvers, MA, USA

antibody			
Human IL1RAcP mouse monoclonal antibody (Co-IP)	H00003556-PW1	Novus Biologicals	Cambridge, UK
Human monoclonal LC3B antibody	3868S	Cell Signaling Technology	Danvers, MA, USA
Human mTOR (7C10) rabbit monoclonal	2983	Cell Signaling Technology	Danvers, MA, USA
Human OPG goat polyclonal antibody	SC8468	Santa Cruz Biotechnology	
Human Phospho-CDK2 (Thr160) rabbit polyclonal antibody	2561	Cell Signaling Technology	Danvers, MA, USA
Human Phospho-CDK4 (Thr172) rabbit polyclonal antibody	58845	Cell Signaling Technology	Danvers, MA, USA
Human Phospho-ERK1/2 (Thr202/Tyr204) rabbit monoclonal antibody	4370	Cell Signaling Technology	Danvers, MA, USA
Human Phospho-HSP27 (Ser15) rabbit polyclonal antibody	2404	Cell Signaling Technology	Danvers, MA, USA
Human Phospho-mTOR rabbit polyclonal antibody (Ser2481)	2974	Cell Signaling Technology	Danvers, MA, USA
Human Phospho-PLCy2 (Tyr759) rabbit polyclonal antibody	3874	Cell Signaling Technology	Danvers, MA, USA
Human TRAIL goat polyclonal neutralising antibody	AF375	R&D Systems	Abingdon, UK

7.1.7 Proliferation Assay Reagents

Reagent	Cat. No	Supplier	Location
---------	---------	----------	----------

CellTiter-Glo® Luminescent Cell Viability Assay	G7571	Promega	Southampton, UK
---	-------	---------	-----------------

7.1.8 Recombinant Proteins

Recombinant Protein	Cat. No	Supplier	Location
rhFas-FC Chimera	326-FS-050/CF	R&D systems	Abingdon, UK
rhIL1RAcP-FC Chimera	676-CP-100	R&D systems	Abingdon, UK
rhOPG	185-OS-025	R&D systems	Abingdon, UK
rhPDGF-BB	PHG0045	Gibco, Life Technologies	Paisley, UK

7.1.9 RNA Extraction and RT-qPCR

Reagent	Cat. No	Supplier	Location
DirectZol RNA Extraction Kit	R250	Zymo, Cambridge Bioscience	Cambridge, UK
Maxwell LEV simply RNA tissue kit	AS1280	Promega	Southampton, UK
Qiagen AllPrep RNA/DNA/Protein tissue kit	80004	Qiagen	Manchester, UK
RNA-to-cDNA kit	4387406	Invitrogen, Life Technologies	Paisley, UK
RNA Later	R0901	Sigma-Aldrich	Dorset, UK
TaqMan Universal Mastermix	4440040	Applied Biosystems, Life Technologies	Paisley, UK
TRIzol Reagent	15596-029	Invitrogen, Life Technologies	Paisley, UK

7.1.10 Secondary Antibody Suppliers

Antibody	Cat. No	Supplier	Location
IRDye 680LT Donkey anti-goat	926-32214	LiCOR	Bad Homburg, Germany
IRDye 680LT Goat anti-mouse	926-68020	LiCOR	Bad Homburg, Germany
IRDye 800 CW Donkey anti-goat	926-32214	LiCOR	Bad Homburg, Germany
IRDye 800 CW Donkey anti-mouse	926-32212	LiCOR	Bad Homburg, Germany

IRDye 800 CW Donkey anti- rabbit	926-32213	LiCOR	Bad Homburg, Germany
---	-----------	-------	-------------------------

7.1.11 TaqMan Probes

Probe	Cat. No	Supplier	Location
18s	Hs03003631_g1	Invitrogen, Life Technologies	Paisley, UK
ACVRL1	Hs00953798_m1	Invitrogen, Life Technologies	Paisley, UK
BMPR1A	Hs01034913_g1	Invitrogen, Life Technologies	Paisley, UK
Cav-1	Hs00971716_m1	Invitrogen, Life Technologies	Paisley, UK
Fas	Hs00236330_m1	Invitrogen, Life Technologies	Paisley, UK
GAP43	Hs00967138_m1	Invitrogen, Life Technologies	Paisley, UK
IL1RAP	Hs00895050_m1	Invitrogen, Life Technologies	Paisley, UK
PDGFRA	Hs00998018_m1	Invitrogen, Life Technologies	Paisley, UK
TGFBR1	Hs00610320_m1	Invitrogen, Life Technologies	Paisley, UK
TGFBR2	Hs00234253_m1	Invitrogen, Life Technologies	Paisley, UK
TMPRSS11D	Hs00975370_m1	Invitrogen, Life Technologies	Paisley, UK
TNC	Hs01115665_m1	Invitrogen, Life Technologies	Paisley, UK
TNFSF10 (TRAIL)	Hs00921974_m1	Invitrogen, Life Technologies	Paisley, UK
VEGFA	Hs00900055_m1	Invitrogen, Life Technologies	Paisley, UK
VIPR1	Hs00270351_m1	Invitrogen, Life Technologies	Paisley, UK

7.1.12 Western Blotting Reagents

Reagent	Cat. No	Supplier	Location
Chromatography Paper	3030917	Fisher Scientific	Loughborough, Leicestershire, UK
Halt™ Protease Inhibitor	87786	Pierce, Thermo	Rockford, Illinois,

Cocktail (100x)		Fisher Scientific	USA
LiCOR Odyssey Blocking Buffer	927-40000	LiCOR	Bad Homburg, Germany
Marvel Skimmed Low Fat Milk	N/A	Premier International Foods Ltd	St Albans, UK
Nitrocellulose	10401196	GE Healthcare Life Sciences	Buckinghamshire, UK
Novex Sharp Pre-Stained Protein Standards	LC5800	Life Technologies	Paisley, UK
NuPAGE antioxidant	NP0005	Life Technologies	Paisley, UK
NuPAGE MOPS SDS running buffer (20x)	NP0001	Life Technologies	Paisley, UK
NuPAGE Novex Bis-Tris gels (1.0 mm, 10 wells)	NP0321BOX	Life Technologies	Paisley, UK
NuPAGE sample reducing agent (10x)	NP0009	Life Technologies	Paisley, UK
NuPAGE Transfer Buffer (20x)	NP00061	Life Technologies	Paisley, UK
Protein loading buffer (4x)	928-40004	LiCOR	Bad Homburg, Germany
Reblot Mild Antibody Stripping Solution	2502	Millipore	Watford, UK
XCell Surelock Mini Cell Electrophoresis System	EI0002	Life Technologies	Paisley, UK

7.2 Preparation of Solutions

7.2.1 General Solutions

Solution	Preparation
Phosphate Buffered Saline	A one times solution of PBS was prepared by dissolving one PBS tablet (Oxoid, BR0014G) in 100 ml distilled water. A 20x PBS solution was prepared by dissolving 20 PBS tablets in 100 ml distilled water. A one times PBS solution was prepared by diluting 25 ml 20x PBS in 475 ml distilled water.
10% w/v SDS	A 10% w/v SDS was prepared by adding 1 g SDS to 10 ml distilled H ₂ O.
5% v/v SDS	Protein samples were dissolved in a 1:2 dilution of 10% w/v SDS to give a final volume of 5% v/v SDS. For example, 30 µl sample was dissolved in 30 µl 10%

	w/v SDS to give a final concentration of 5% SDS.
0.1% v/v Tween-20 wash buffer	0.1% v/v Tween-20 wash buffer was prepared by adding 500 µl Tween-20 to 500 ml one times PBS.

7.2.2 Cell Culture Solutions

Solution	Preparation
Smooth Muscle Basal Medium (SmBM) for HPA-SMC	The SmGm-2 SingleQuots, containing 25 ml foetal calf serum (FBS), 500 µl insulin, 1000 µl hFGF-β, 500 µl gentamycin/amphotericin were defrosted overnight at 4°C prior to use. All SingleQuots and FBS were added to 500 ml SmBm-2 cell culture media to produce a media containing 5% v/v FBS, 0.1% v/v insulin, 0.2% v/v hFGF-β and 0.1% v/v gentamycin/amphotericin. 1% v/v penicillin/streptomycin was also added.
Growth Arrest Media for HPA-SMC	Growth arrest media was prepared to synchronize HPA-SMC cell cycles by adding 1 ml FBS and 5 ml 100 X penicillin/streptomycin (10,000 units/mL of penicillin, 10,000 µg/mL of streptomycin) to 500 ml DMEM. DMEM containing 0.2% v/v FBS. Therefore, a 0.2% v/v FBS, 1% v/v penicillin/streptomycin growth arrest media was produced.
Sodium Orthovanadate Lysis Buffer	1 M Tris-HCl (pH 7.4) was prepared by adding 157.6 mg Tris-HCl (molecular weight 157.56) to 1 ml distilled water. 100 mM sodium orthovanadate was prepared by adding 18.39 mg/ml sodium orthovanadate (molecular weight 183.908) to 1 ml distilled water and heating at 95°C, until clear to dissolve. 10% w/v SDS was prepared by adding 1 g SDS to 10 ml distilled water. Lysis buffer (10 mM Tris-HCl, 10 mM Sodium orthovanadate, 1% v/v SDS) was then prepared by adding 10 µl 1 M Tris-HCl, 10 µl 100 mM sodium orthovanadate and 100 µl 10% SDS to 780 µl distilled H ₂ O. Immediately before use, 10 µl HALT™ protease inhibitor was added to 1 ml lysis buffer.
Triton X-100 Lysis Buffer	A 1% Triton X-100 lysis buffer (150 mM

	NaCl, 20 mM Tris, 1% Triton X-100, 0.1% SDS) was prepared by adding 438.8 mg NaCl (molecular weight 58.44), 121.14 mg Tris (molecular weight 121.12), 500 µl Triton X-100 and 50 mg SDS in 50 ml PBS.
5% Milk Blocking Buffer	Low fat Marvel milk powder was purchased from the local supermarket. A 5% w/v milk blocking buffer was prepared by adding 5 g low fat milk to 100 ml one times PBS and mixing gently.

7.2.3 Pierce 660 nm Protein Assay Bovine Serum Albumin Standards Preparation

Albumin standards were prepared at 2000 µg/ml, 1500 µg/ml, 1000 µg/ml, 750 µg/ml, 500 µg/ml, 250 µg/ml, 125 µg/ml, 25 µg/ml and 0 µg/ml by diluting one 2000 µg/ml bovine serum albumin standard stock ampule as follows:

Vial	BSA Standard Concentration (µg/ml)	Volume and Source of BSA (µl)	Volume of distilled water
A	2000	300 of stock	0
B	1500	375 of stock	125
C	1000	325 of stock	325
D	750	175 of vial B dilution	175
E	500	325 of vial C dilution	325
F	250	325 of vial E dilution	325
G	125	325 of vial F dilution	325
H	25	100 of vial G dilution	400
I	0	0	400

7.2.4 Western Blotting Solutions

Solution	Preparation
Protein Loading Buffer	One times protein loading buffer (Licor) was prepared by diluting 1 µl protein loading buffer (4x) in 3 µl protein lysate

	(1:4 dilution).
NuPAGE Sample Reducing Agent	One times sample reducing agent (Life Technologies) was prepared by diluting 1 μ l sample reducing agent (10x) in 9 μ l protein lysate (1:10 dilution).
NuPAGE MOPS SDS Running Buffer	A one times solution of NuPAGE MOPS SDS running buffer (Life Technologies) was prepared by diluting 25 ml running buffer (20x) in 475 ml distilled water.
NuPAGE Transfer Buffer	A one times solution of NuPAGE transfer buffer (Life Technologies) containing 10% methanol was prepared by diluting 25 ml transfer buffer (20x) in 424 ml distilled water containing 50 ml methanol and 1 ml antioxidant (Life Technologies). A one times solution of NuPAGE transfer buffer containing 20% methanol was prepared by diluting 25 ml transfer buffer (20x) in 374 ml distilled water containing 100 ml methanol and 1 ml antioxidant.
30 % LiCOR Odyssey Blocking Buffer	A 30% solution of LiCOR Odyssey blocking buffer was prepared by diluting 15 ml blocking buffer in 35 ml PBS.
30 % LiCOR Odyssey Blocking Buffer + 0.1% v/v SDS	A 30% solution of LiCOR Odyssey blocking buffer was prepared by diluting 15 ml blocking buffer in 35 ml PBS. 500 μ l 10% w/v SDS was then added to 50 ml 30% v/v Odyssey blocking buffer.
Re-blot Plus Mild Antibody Stripping Solution	A one times antibody stripping solution was prepared by adding 2 ml 10 times Re-blot plus mild antibody stripping solution (Millipore) to 18 ml PBS.

7.2.5 Co-Immunoprecipitation Solutions

Solution	Preparation
CHAPS Lysis Buffer	5 M NaCl was prepared by adding 2922 mg NaCl (molecular weight 58.44) to 10 ml distilled H ₂ O. 5 M TRIS-HCl pH 7.4 was prepared by adding 7880 mg TRIS-HCl (molecular weight 157.6) to 10 ml distilled H ₂ O. 10% w/v CHAPS was prepared by adding 1 g CHAPS in 10 ml distilled H ₂ O. CHAPS lysis buffer (30 mM TRIS-HCl, 150 mM NaCl, 1% v/v CHAPS) was then prepared by adding 0.75 ml 5 M NaCl, 0.75 ml 5 M TRIS-HCl and 2.5 ml 10% CHAPS to 21 ml ddH ₂ O.

nProteinG Sepharose 4 Fast Flow beads (50% slurry)	A 50% slurry of nProteinG sepharose 4 Fast Flow beads was prepared by washing the beads 3 times in CHAPS lysis buffer, centrifuging at 12,000 x g for 20 seconds after each wash and discarding the supernatant. 250 µl beads were then re-suspended in 250 µl CHAPS lysis buffer.
Co-Immunoprecipitation Wash Buffer	Co-Immunoprecipitation wash buffer was prepared by adding 302.85 mg Tris (molecular weight 121.14) to 50 ml PBS and mixing gently.

7.2.6 Cell Assay Solutions

Solution	Preparation
3.7% Formaldehyde Cell Fixing Solution	A 3.7% formaldehyde cell fixing solution was prepared by adding 5 ml 37% formaldehyde to 45 ml one times PBS
0.1% Triton X-100 Permeabilization Solution	A 0.1% Triton X-100 permeabilization solution was prepared by adding 500 µl Triton X-100 to 500 ml one times PBS and mixing gently.
0.3% Triton X-100 Permeabilization Solution	A 0.1% Triton X-100 permeabilization solution was prepared by adding 1500 µl Triton X-100 to 500 ml one times PBS and mixing gently.
DRAC5/Sapphire 700 Nuclear Stain	DRAC5 (Biostatus) and Sapphire 700 (LiCOR) nuclear stain was prepared by diluting DRAC5 1:10,000 and sapphire 700 1:1000 in 30% v/v LiCOR Odyssey blocking buffer. 5 ml DRAC5/Sapphire 700 nuclear stain solution was prepared for each 96 well plate by adding 0.5 µl DRAC5 and 10 µl Sapphire 700 to 5 ml 30% v/v LiCOR Odyssey blocking buffer, mixing gently, protected from light.

7.2.7 RNA Isolation, Reverse Transcription and TaqMan RT-qPCR

Solution	Preparation
DirectZol DNase I Cocktail	A DNase I cocktail was prepared by reconstituting 250 units lyophilized DNase I in 250 µl DNase/RNase-free water. 5 µl (5 units) DNase I were then

	added to 8 μ l 10X DNase I reaction buffer, 3 μ l DNase/RNase-free Water and 64 μ l RNA wash buffer in an RNase-free tube and mixed gently.
RT Buffer (2x) Dilution	Applied Biosystems High Capacity RNA-to-cDNA™ RT buffer (2x) was diluted 1:2 by adding 10 μ l to 9 μ l RNA sample and 1 μ l Applied Biosystems High Capacity RNA-to-cDNA™ enzyme (20x).
Enzyme (20x) Dilution	Applied Biosystems High Capacity RNA-to-cDNA™ enzyme (20x) was diluted 1:20 by adding 1 μ l to 9 μ l RNA sample and 10 μ l Applied Biosystems High Capacity RNA-to-cDNA™ RT buffer (2x).

7.2.8 Preparation of Recombinant Proteins

Solution	Preparation
rhOPG	<p>0.1 μg rhOPG was added to the appropriate Co-IP reactions by pipetting 1 μl of the OPG stock (100 μg/ml) into 250 μl CHAPS solution in the appropriate Eppendorfs. 1 μg rhOPG was added to the appropriate Co-IP reactions by pipetting 10 μl of the OPG stock (100 μg/ml) into 250 μl CHAPS solution in the appropriate Eppendorfs.</p> <p>50 ng/ml rhOPG solution was prepared for cell stimulation by diluting 1μl 100 μg/ml stock solution in 2000 μl cell culture media.</p>
rhIL1RAcP	0.1 μ g rhIL1RAcP was added to the appropriate Co-IP reactions by pipetting 0.5 μ l of the IL1RAcP stock (200 μ g/ml) into 250 μ l CHAPS solution in the appropriate Eppendorfs. 1 μ g rhIL1RAcP was added to the appropriate Co-IP reactions by pipetting 5 μ l of the IL1RAcP stock (200 μ g/ml) into 250 μ l CHAPS solution in the appropriate Eppendorfs.
rhFAS Receptor	0.1 μ g rhFas was added to the appropriate Co-IP reactions by pipetting 1 μ l of the

	Fas stock (100 µg/ml) into 250 µl CHAPS solution in the appropriate Eppendorfs. 1 µg rhFas was added to the appropriate Co-IP reactions by pipetting 10 µl of the Fas stock (100 µg/ml) into 250 µl CHAPS solution in the appropriate Eppendorfs.
rhPDGF-BB	20 ng/ml solution for stimulation was prepared by diluting 1 µl 10 µg/ml stock solution in 500 µl growth arrest media.

7.2.9 Preparation of Primary Antibodies

Solution	Preparation
Human Atg13 rabbit monoclonal antibody	ATG13 antibody was diluted 1:500, by adding 2 µl of antibody to 1000 µl blocking buffer (30% v/v Odyssey blocking buffer in 1x PBS) for use in Western blotting.
Human Atg7 (D12B11) rabbit monoclonal antibody	ATG7 antibody was diluted 1:500, by adding 2 µl of antibody to 1000 µl blocking buffer (30% v/v Odyssey blocking buffer in 1x PBS) for use in Western blotting.
Human CDK5 (EP715Y) rabbit monoclonal antibody	CDK5 antibody was diluted 1:500, by adding 1 µl of antibody to 500 µl blocking buffer (30% v/v Odyssey blocking buffer in 1x PBS) for use in Western blotting.
Human Daxx (7A11) mouse monoclonal antibody	Daxx antibody was diluted 1:1000, by adding 1 µl, 1:500, by adding 2 µl and 1:250 µl of antibody to 1000 µl blocking buffer (30% v/v Odyssey blocking buffer in 1x PBS) for use in Western blotting.
Human ERK1/2 rabbit monoclonal antibody	ERK1/2 antibody was diluted 1:1000, by adding 1 µl of antibody to 1000 µl blocking buffer (30% v/v Odyssey blocking buffer in 1x PBS) for use in Western blotting.
Human FADD rabbit polyclonal antibody	FADD antibody was diluted 1:500, by adding 1 µl of antibody to 500 µl blocking buffer (30% v/v Odyssey blocking buffer in 1x PBS) for use in Western blotting.
Human Fas neutralising mouse monoclonal antibody	A working solution of Fas neutralising antibody (1500 ng/ml) was prepared by diluting the Fas antibody stock solution (1 mg/ml) 1:666.67 by adding 1.5 µl Fas neutralising antibody to 1000 µl growth arrest media.
Human Fas rabbit polyclonal antibody (Co-IP)	2 µg anti-Fas antibody was added to the appropriate Co-IP reactions by pipetting 20 µl of

		the anti-Fas antibody stock solution (100 µg/ml) into the appropriate Eppendorfs.
Human GβL rabbit monoclonal antibody		GβL antibody was diluted 1:500, by adding 1 µl of antibody to 500 µl blocking buffer (30% v/v Odyssey blocking buffer in 1x PBS) for use in Western blotting.
Human IL1RAcP mouse monoclonal antibody (Co-IP)		2 µg anti-IL1RAcP antibody was added to the appropriate Co-IP reactions by pipetting 10 µl of the anti-IL1RAcP antibody stock solution (200 µg/ml) into the appropriate Eppendorfs.
Human mTOR (7C10) rabbit monoclonal		MTOR antibody was diluted 1:500, by adding 2 µl of antibody to 1000 µl blocking buffer (30% v/v Odyssey blocking buffer in 1x PBS) for use in Western blotting.
Human OPG goat polyclonal antibody		OPG antibody 1:1000, by adding 1 µl of antibody to 1000 µl blocking buffer (30% v/v Odyssey blocking buffer in 1x PBS) for use in Western blotting.
Human Phospho-CDK2 (Thr160) rabbit polyclonal antibody		Phospho-CDK2 antibody was diluted 1:200, by adding 1 µl of antibody to 200 µl blocking buffer (5% w/v low-fat milk in 1xPBS) for use in the in-cell western assay.
Human Phospho-CDK4 (Thr172) rabbit polyclonal antibody		Phospho-CDK4 antibody was diluted 1:200, by adding 1 µl of antibody to 200 µl blocking buffer (5% w/v low-fat milk in 1xPBS) for use in the in-cell western assay. Phospho-CDK4 was diluted 1:1000, by adding 1 µl of antibody to 1000 µl blocking buffer (5% w/v low-fat milk in 1xPBS) for use in Western blotting.
Human Phospho-ERK1/2 (Thr202/Tyr204) rabbit monoclonal antibody		Phospho-ERK1/2 antibody was diluted 1:200, by adding 1 µl of antibody to 200 µl blocking buffer (5% w/v low-fat milk in 1xPBS) for use in the in-cell western assay. Phospho-ERK1/2 antibody was diluted 1:1000, by adding 1 µl of antibody to 1000 µl blocking buffer (5% w/v low-fat milk in 1xPBS) for use in Western blotting.
Human Phospho-HSP27 (Ser15) rabbit polyclonal antibody		Phospho-HSP27 antibody was diluted 1:200, by adding 1 µl of antibody to 200 µl blocking buffer (5% w/v low-fat milk in 1xPBS) for use in the in-cell western assay. Phospho-HSP27 was diluted 1:1000, by adding 1 µl of antibody to 1000 µl blocking buffer (5% w/v low-fat milk in 1xPBS) for use in Western blotting.
Human Phospho-mTOR		Phospho-mTOR antibody was diluted 1:500, by

rabbit polyclonal antibody (Ser2481)	adding 2 μ l of antibody to 1000 μ l blocking buffer (30% v/v Odyssey blocking buffer in 1x PBS) for use in Western blotting.
Human (Tyr759) Phospho-PLCγ2 rabbit polyclonal antibody	Phospho-PLC γ 2 antibody was diluted 1:200, by adding 1 μ l of antibody to 200 μ l blocking buffer (5% w/v low-fat milk in 1xPBS) for use in the in-cell western assay.
Human polyclonal antibody TRAIL neutralising goat	A working solution of TRAIL neutralising antibody (1500 ng/ml) was prepared by diluting the TRAIL antibody stock solution (200 μ g/ml) 1:133.3 by adding 7.5 μ l TRAIL neutralising antibody to 1000 μ l growth arrest media.

7.2.10 Preparation of Secondary Antibodies

Antibody	Preparation
IRDye 680LT Donkey anti-goat	IRDye 800 CW Donkey anti-goat was diluted 1:15,000, by adding 1 μ l of antibody to 15,000 μ l blocking buffer ((30% v/v Odyssey blocking buffer in 1x PBS, with 0.1% v/v SDS).
IRDye 680LT Goat anti-mouse	IRDye 800 CW Goat anti-mouse was diluted 1:15,000, by adding 1 μ l of antibody to 15,000 μ l blocking buffer ((30% v/v Odyssey blocking buffer in 1x PBS, with 0.1% v/v SDS).
IRDye 800 CW Donkey anti-goat	IRDye 800 CW Donkey anti-goat was diluted 1:15,000, by adding 1 μ l of antibody to 15,000 μ l blocking buffer ((30% v/v Odyssey blocking buffer in 1x PBS, with 0.1% v/v SDS).
IRDye 800 CW Donkey anti-mouse	IRDye 800 CW Donkey anti-mouse was diluted 1:15,000, by adding 1 μ l of antibody to 15,000 μ l blocking buffer ((30% v/v Odyssey blocking buffer in 1x PBS, with 0.1% v/v SDS).
IRDye 800 CW Donkey anti-rabbit	IRDye 800 CW Donkey anti-rabbit was diluted 1:15,000, by adding 1 μ l of antibody to 15,000 μ l blocking buffer ((30% v/v Odyssey blocking buffer in 1x PBS, with 0.1% v/v SDS).

7.3 Antibodies screened in the Kinex antibody microarray

Table 7.1- Antibodies (pan-specific and phospho-specific) screened in the Kinex antibody microarray for OPG-stimulated lysates at 10 minutes and 60 minutes.

Target Protein Name	Phospho Site (Human)	Full Target Protein Name	Z-ratio (50ng/mL OPG 10', 0.2% FBS 10')	Z-ratio (50ng/mL OPG 60', 0.2% FBS 60')
14-3-3 z	Pan-specific	14-3-3 protein zeta (cross-reacts with other isoforms)	-0.38	0.05
4E-BP1	S64	Eukaryotic translation initiation factor 4E binding protein 1 (PHAS1)	0.28	0.30
4E-BP1	T45	Eukaryotic translation initiation factor 4E binding protein 1 (PHAS1)	0.59	-0.10
4E-BP1	T69	Eukaryotic translation initiation factor 4E binding protein 1 (PHAS1)	-0.17	-0.41
Abl	Pan-specific	Abelson proto-oncogene-encoded protein-tyrosine kinase	-0.21	9.79
AcCoA carboxylase	S80	Acetyl coenzyme A carboxylase	0.44	1.01
Acetylated Lysine	Pan-specific	Acetylated Lysine	-0.73	-0.46
Acetylated Lysine	Pan-specific	Acetylated Lysine	1.93	0.08
ACK1	Pan-specific	Activated p21cdc42Hs protein-serine kinase	1.73	-1.12
Adducin a, g	S726, S693	Adducin alpha (ADD1)/gamma (ADD3)	0.12	-0.53
AIF	Pan-specific	Apoptosis inducing factor (programed cell death protein 8 (PDCD8))	-1.12	-0.18
AK2	Pan-specific	Adenylate kinase 2	0.04	1.07
ALK	Pan-specific	Anaplastic lymphoma kinase	0.14	-0.60
ALS2CR7 (PFTAIRE2)	Pan-specific	Amyotrophic lateral sclerosis 2 chromosomal region candidate gene protein-serine kinase 7	-1.33	0.01
AMPKa1/2	T183	5'-AMP-activated protein kinase subunit alpha 1/2	-0.17	-0.15
ANKRD3	Pan-specific	Ankyrin repeat domain protein-serine kinase 3 (RIPK4, DIK)	0.62	0.81
APG1	Pan-specific	Hsp 70-related heat shock protein 1 (osmotic stress protein 94 (OSP94))	-1.40	2.24
APG2	Pan-specific	Hsp 70-related heat shock protein 4 (HSP70RY)	0.16	2.03

Arrestin b1	Pan-specific	Arrestin beta 1	-0.21	-0.57
Arrestin b1	S412	Arrestin beta 1	-0.01	0.38
ASK1 (MAP3K5)	Pan-specific	Apoptosis signal regulating protein-serine kinase	-1.60	1.67
ASK1 (MAP3K5)	Pan-specific	Apoptosis signal regulating protein-serine kinase	-0.42	1.36
ASK1 (MAP3K5)	S1046	Apoptosis signal regulating protein-serine kinase	-0.55	0.02
ATF2	Pan-specific	Activating transcription factor 2 (CRE-BP1)	0.01	-0.16
ATF2	T69/T71	Activating transcription factor 2 (CRE-BP1)	-0.55	0.78
ATF2	T69/T71	Activating transcription factor 2 (CRE-BP1)	-0.40	-0.45
Aurora A (AIK)	Pan-specific	Aurora Kinase A (serine/threonine protein kinase 6)	0.31	1.64
Aurora A (AIK)	Pan-specific	Aurora Kinase A (serine/threonine protein kinase 6)	0.20	-0.30
Aurora B (AIM-1)	Pan-specific	Aurora Kinase B (serine/threonine protein kinase 12)	0.16	1.11
Aurora C (AIK3)	Pan-specific	Aurora Kinase C (serine/threonine-protein kinase 13)	-0.02	0.45
Axl	Pan-specific	Axl proto-oncogene-encoded protein-tyrosine kinase	0.33	0.58
MEK1/2+B23 (NPM)	S217+S221, S4	MAPK/ERK protein-serine kinase 1/2 (MKK1/2) + B23 (nucleophosmin, numatrin, nucleolar protein NO38)	-0.30	-0.59
B23 (NPM)	T199	B23 (nucleophosmin, numatrin, nucleolar protein NO38)	-0.35	-0.20
B23 (NPM)	T199	B23 (nucleophosmin, numatrin, nucleolar protein NO38)	-0.08	-0.50
B23 (NPM)	T234/T237	B23 (nucleophosmin, numatrin, nucleolar protein NO38)	-0.38	0.86
Bad	S75	Bcl2-antagonist of cell death protein	0.00	0.40
Bad	S99	Bcl2-antagonist of cell death protein	0.09	0.20
Bak	Pan-specific	Bcl2 homologous antagonist/killer (BCK2L7)	0.28	0.90
Bax	Pan-specific	Apoptosis regulator Bcl2-associated X protein	-0.57	0.56
Bcl2	Pan-specific	B-cell lymphoma protein 2 alpha	0.00	0.00
Bcl-xL	Pan-specific	Bcl2-like protein 1	-0.28	-0.05
Bcl-xS/L	Pan-specific	Bcl-xS/L	-0.01	-0.32
Bid	Pan-specific	BH3 interacting domain death agonist	0.47	1.52
BLK	Pan-specific	B lymphoid tyrosine kinase	-0.15	0.07
BLNK	Y84	B-cell linker protein	0.12	-0.04
BMX (Etk)	Pan-specific	Bone marrow X protein-tyrosine kinase	-0.28	0.70
BMX (Etk)	Y40	Bone marrow X protein-tyrosine kinase	0.37	-0.11
BRCA1	S1497	Breast cancer type 1 susceptibility protein	-0.53	-0.17
BRD2	Pan-specific	Bromodomain-containing protein-serine kinase 2	-0.07	0.24

Btk	Pan-specific	Bruton's agammaglobulinemia tyrosine kinase	0.42	1.40
Btk	Y223	Bruton's agammaglobulinemia tyrosine kinase	-0.24	0.25
BUB1A	Pan-specific	BUB1 mitotic checkpoint protein-serine kinase	0.00	-0.28
Caldesmon	S789	Caldesmon	1.53	-0.19
Calnexin	Pan-specific	Calnexin	0.24	0.89
Calnexin	Pan-specific	Calnexin	0.34	-0.43
Calnexin	Pan-specific	Calnexin	-0.16	0.51
Calreticulin	Pan-specific	Calreticulin	-0.33	0.52
CAMK1a	Pan-specific	Calcium/calmodulin-dependent protein-serine kinase 1 alpha	0.84	-0.35
CaMK1d	Pan-specific	Calcium/calmodulin-dependent protein-serine kinase 1 delta	-0.72	-0.39
CaMK1d	Pan-specific	Calcium/calmodulin-dependent protein-serine kinase 1 delta	-0.85	0.71
CaMK2a	T286	Calcium/calmodulin-dependent protein-serine kinase 2 alpha	-0.09	-1.00
CaMK2a	T286	Calcium/calmodulin-dependent protein-serine kinase 2 alpha	0.04	-0.10
CAMK2b	Pan-specific	Calcium/calmodulin-dependent protein-serine kinase 2 beta	-0.25	-0.79
CAMK2b	Pan-specific	Calcium/calmodulin-dependent protein-serine kinase 2 beta	-0.10	-0.60
CAMK2d	Pan-specific	Calcium/calmodulin-dependent protein-serine kinase 2 delta	-0.08	0.68
CAMK2d	Pan-specific	Calcium/calmodulin-dependent protein-serine kinase 2 delta	-0.32	0.82
CAMK2g	Pan-specific	Calcium/calmodulin-dependent protein-serine kinase 2 gamma	0.64	0.63
CaMK4	Pan-specific	Calcium/calmodulin-dependent protein-serine kinase 4	0.24	-0.51
CaMK4	Pan-specific	Calcium/calmodulin-dependent protein-serine kinase 4	-3.13	-0.51
CaMK4	Pan-specific	Calcium/calmodulin-dependent protein-serine kinase 4	-1.65	-0.28
CaMKK (CaMKK2)	Pan-specific	Calcium/calmodulin-dependent protein-serine kinase kinase	-0.74	-0.77
CAS	Pan-specific	Cellular apoptosis susceptibility protein (CSE1L)	-0.30	0.26
CASK/Lin2	Pan-specific	Calcium/calmodulin-dependent protein-serine kinase (Lin2 homolog)	0.01	-0.23
CASP12	Pan-specific	Pro-caspase 12 (mouse)	-1.48	-0.74
CASP1ab	Pan-specific	Pro-caspase 1 (Interleukin-1 beta convertase) alpha/beta isoform	-1.78	0.85
CASP2	Pan-specific	Pro-caspase 2 (ICH1 protease)	-0.46	-0.22
CASP3	Pan-specific	Pro-caspase 3 (apopain, cysteine protease CPP32)	-0.52	0.27
CASP4	Pan-specific	Pro-caspase 4 (ICH2 protease, ICE(rel)-II)	0.88	-0.41
CASP5	Pan-specific	Caspase 5 (ICH3 protease, ICE(rel)-III)	-1.62	-1.21
CASP6	Pan-specific	Pro-caspase 6 (apoptotic protease Mch2)	-3.27	-0.16
CASP7	Pan-specific	Pro-caspase 7 (ICE-like apoptotic protease 3 (ICE-LAP3), Mch3)	-0.10	-0.70

CASP9	Pan-specific	Pro-caspase 9 (ICE-like apoptotic protease 6 (ICE-LAP6), Mch6, APAF3)	-0.07	0.73
Catenin b1	Pan-specific	Catenin (cadherin-associated protein) beta 1	-0.26	-0.29
Caveolin 2	Pan-specific	Caveolin 2	-0.22	-0.66
Caveolin 2	S36	Caveolin 2	-0.09	-0.23
CD45	Pan-specific	Leukocyte common antigen CD45 receptor-tyrosine phosphatase (LCA, T200)	-0.39	-0.59
Cdc25B	Pan-specific	Cell division cycle 25B phosphatase	-0.31	0.45
Cdc25C	Pan-specific	Cell division cycle 25C phosphatase	0.71	-1.84
Cdc25C	S216	Cell division cycle 25C phosphatase	0.79	-0.49
CDC2L5 (CHED)	Pan-specific	Cell division cycle 2-like protein-serine kinase 5	0.10	0.26
Cdc34	Pan-specific	Cell division cycle 34 (ubiquitin-conjugating ligase)	-0.26	-0.37
Cdc42	Pan-specific	Cell division control protein 42 homolog	-0.12	-0.07
CDK1 (CDC2)	Pan-specific	Cyclin-dependent protein-serine kinase 1	0.08	0.24
CDK1 (CDC2)	Pan-specific	Cyclin-dependent protein-serine kinase 1	0.31	-0.36
CDK1 (CDC2)	Pan-specific	Cyclin-dependent protein-serine kinase 1	-0.15	-0.50
CDK1 (CDC2)	Pan-specific	Cyclin-dependent protein-serine kinase 1	1.62	2.49
CDK1 (CDC2)	Pan-specific	Cyclin-dependent protein-serine kinase 1	-1.45	2.41
CDK1 (CDC2)	Pan-specific	Cyclin-dependent protein-serine kinase 1	1.07	-0.94
CDK1/2	T14+Y15	Cyclin-dependent protein-serine kinase 1/2	0.05	-0.29
CDK1/2	Y15	Cyclin-dependent protein-serine kinase 1/2	-0.77	-0.81
CDK1/2	Y15	Cyclin-dependent protein-serine kinase 1/2	-0.57	2.19
CDK1/2	Y15	Cyclin-dependent protein-serine kinase 1/2	-2.91	-1.74
CDK1/2	T161	Cyclin-dependent protein-serine kinase 1/2	0.35	2.66
CDK10	Pan-specific	Cyclin-dependent protein-serine kinase 10 [PISSLRE]	0.66	1.87
CDK2	Pan-specific	Cyclin-dependent protein-serine kinase 2	1.74	1.09
CDK2	Pan-specific	Cyclin-dependent protein-serine kinase 2	-0.16	0.47
CDK2	Pan-specific	Cyclin-dependent protein-serine kinase 2	-0.27	1.03
CDK2	Pan-specific	Cyclin-dependent protein-serine kinase 2	1.35	0.62
CDK2	Pan-specific	Cyclin-dependent protein-serine kinase 2	0.20	0.52
CDK2	Pan-specific	Cyclin-dependent protein-serine kinase 2	3.06	3.60
CDK4	Pan-specific	Cyclin-dependent protein-serine kinase 4	-0.04	-0.25
CDK4	Pan-specific	Cyclin-dependent protein-serine kinase 4	1.67	0.14
CDK5	Pan-specific	Cyclin-dependent protein-serine kinase 5	1.96	-0.47

CDK5	Pan-specific	Cyclin-dependent protein-serine kinase 5	-0.56	0.26
CDK5	Pan-specific	Cyclin-dependent protein-serine kinase 5	1.47	2.84
CDK5	Pan-specific	Cyclin-dependent protein-serine kinase 5	6.58	-0.33
CDK6	Pan-specific	Cyclin-dependent protein-serine kinase 6	0.63	0.14
CDK6	Pan-specific	Cyclin-dependent protein-serine kinase 6	2.38	-0.11
CDK6	Pan-specific	Cyclin-dependent protein-serine kinase 6	0.59	3.98
CDK7	Pan-specific	Cyclin-dependent protein-serine kinase 7	1.90	0.00
CDK7	Pan-specific	Cyclin-dependent protein-serine kinase 7	5.53	0.32
CDK7	Pan-specific	Cyclin-dependent protein-serine kinase 7	1.59	0.18
CDK8	Pan-specific	Cyclin-dependent protein-serine kinase 8	1.47	-0.05
CDK8	Pan-specific	Cyclin-dependent protein-serine kinase 8	0.01	-1.01
CDK8	Pan-specific	Cyclin-dependent protein-serine kinase 8	2.22	2.84
CDK8	Pan-specific	Cyclin-dependent protein-serine kinase 8	-1.27	-0.10
CDK9	Pan-specific	Cyclin-dependent protein-serine kinase 9	1.79	-0.89
CDKL1	Pan-specific	Cyclin-dependent kinase-like 1	0.84	-0.20
Chk1	Pan-specific	Checkpoint protein-serine kinase 1	-0.04	0.18
Chk1	Pan-specific	Checkpoint protein-serine kinase 1	1.32	0.67
Chk2	Pan-specific	Checkpoint protein-serine kinase 2	1.90	-0.01
Chk2	T68	Checkpoint protein-serine kinase 2	0.22	-0.18
c-IAP1	Pan-specific	Cellular inhibitor of apoptosis protein 1 (baculoviral IAP repeat-containing protein 3, apoptosis inhibitor 2 (API2))	3.35	-2.62
CK1d	Pan-specific	Casein protein-serine kinase 1 delta	0.38	2.45
CK1e	Pan-specific	Casein protein-serine kinase 1 epsilon	-0.11	-0.37
CK1g	Pan-specific	Casein kinase I gamma 1 isoform	2.84	-0.09
CK1g2	Pan-specific	Casein protein-serine kinase 1 gamma 2	2.37	-0.09
CK2a	Pan-specific	Casein protein-serine kinase 2 alpha/ alpha prime	0.51	0.13
c-Myc	T58/S62	Myc proto-oncogene protein	-0.05	3.29
Cofilin 1	Pan-specific	Cofilin 1	-0.01	-0.78
Cofilin 1	S3	Cofilin 1	1.02	-0.28
Cofilin 2	S3	Cofilin 2	1.18	0.14
Cortactin	Y466	Cortactin (amplaxin) (mouse)	0.40	-0.76
COT	Pan-specific	Osaka thyroid oncogene protein-serine kinase (Tpl2)	-0.31	3.07
COT	Pan-specific	Osaka thyroid oncogene protein-serine kinase (Tpl2)	0.77	0.23
COX2	Pan-specific	Cyclo-oxygenase 2 (prostaglandin G/H synthase 2 precursor)	-0.04	-1.13

CPG16/Ca MKinase VI	Pan- specific	Serine/threonine-protein kinase DCAMKL1	0.46	-1.05
CREB1	S129+S133 3	cAMP response element binding protein 1	0.58	-0.36
CREB1	S133	cAMP response element binding protein 1	0.36	1.15
CREB1	S133	cAMP response element binding protein 1	-0.19	0.77
Crystallin aB	Pan- specific	Crystallin alpha B (heat-shock 20 kDa like-protein)	0.42	-0.42
Crystallin aB	Pan- specific	Crystallin alpha B (heat-shock 20 kDa like-protein)	0.73	0.46
Crystallin aB	Pan- specific	Crystallin alpha B (heat-shock 20 kDa like-protein)	0.79	-0.07
Crystallin aB	Pan- specific	Crystallin alpha B (heat-shock 20 kDa like-protein)	0.12	0.19
Crystallin aB	S19	Crystallin alpha B (heat-shock 20 kDa like-protein)	-0.31	-0.80
Crystallin aB	S45	Crystallin alpha B (heat-shock 20 kDa like-protein)	-0.08	-1.18
Csk	Pan- specific	C-terminus of Src tyrosine kinase	-0.36	-0.85
Csk	Pan- specific	C-terminus of Src tyrosine kinase	1.16	-9.53
Cyclin A	Pan- specific	Cyclin A1	0.01	-0.71
Cyclin B1	Pan- specific	Cyclin B1	1.17	0.46
Cyclin D1	Pan- specific	Cyclin D1 (PRAD1)	0.10	-0.79
Cyclin D1	Pan- specific	Cyclin D1 (PRAD1)	-0.27	-0.13
Cyclin E	Pan- specific	Cyclin E1	-0.53	0.40
Cyclin G1	Pan- specific	Cyclin G1	-1.61	-2.84
CytoC	Pan- specific	Cytochrome C	0.78	-1.76
Dab1	Y198	Disabled homolog 1	0.11	-0.48
DAPK1	Pan- specific	Death-associated protein kinase 1	-0.64	-0.39
DAPK2	Pan- specific	Death-associated protein kinase 2	-1.70	-0.53
DAXX	Pan- specific	Death-associated protein 6 (BING2)	-1.15	-1.56
DFF35, DFF45	Pan- specific	DNA fragmentation factor alpha (ICAD) 35-kDa, 45-kDa subunit	-0.73	-0.35
DGKz	Pan- specific	Diacylglycerol kinase zeta	-0.43	-0.34
DNAPK	Pan- specific	DNA-activated protein-serine kinase	-1.14	-0.66
DNAPK	Pan- specific	DNA-dependent protein kinase catalytic subunit	-1.65	-2.16
Dok2	Y142	Docking protein 2 (mouse)	0.40	-0.42
Dok2	Y142	Docking protein 2	0.28	-0.27
DRAK2	Pan- specific	DAP kinase-related apoptosis- inducing protein-serine kinase 2 (STK17B)	-0.23	0.29
eEF2K	Pan- specific	Elongation factor-2 protein- serine kinase	-0.41	-0.90
EGFR	Pan- specific	Epidermal growth factor receptor-tyrosine kinase	-0.10	-0.47
EGFR	Y1092	Epidermal growth factor receptor-tyrosine kinase	-1.75	-0.61
EGFR	Y1172	Epidermal growth factor	-0.06	-0.19

		receptor-tyrosine kinase		
EGFR	Y1172	Epidermal growth factor receptor-tyrosine kinase	0.09	-1.43
EGFR	Y1197	Epidermal growth factor receptor-tyrosine kinase	-0.67	-0.12
EGFR	T693	Epidermal growth factor receptor-tyrosine kinase	-0.29	-0.64
eIF2a	S51	Eukaryotic translation initiation factor 2 alpha	-0.49	-0.01
eIF2a	S51	Eukaryotic translation initiation factor 2 alpha	0.12	-0.40
eIF4E	Pan-specific	Eukaryotic translation initiation factor 4 (mRNA cap binding protein)	0.47	-0.11
eIF4E	S209	Eukaryotic translation initiation factor 4 (mRNA cap binding protein)	-0.19	-0.43
eIF4E	S209	Eukaryotic translation initiation factor 4 (mRNA cap binding protein)	-0.27	-1.02
eIF4G	S1107	Eukaryotic translation initiation factor 4 gamma 1	-0.33	0.97
EphA1	Pan-specific	Ephrin type-A receptor 1 protein-tyrosine kinase	-0.33	-0.14
ErbB2 (HER2)	Pan-specific	ErbB2 (Neu) receptor-tyrosine kinase	-0.88	-1.16
ErbB2 (HER2)	Pan-specific	ErbB2 (Neu) receptor-tyrosine kinase	0.29	-0.11
ErbB2 (HER2)	Y1248	ErbB2 (Neu) receptor-tyrosine kinase	-0.10	0.00
ErbB2 (HER2)	Y1248	ErbB2 (Neu) receptor-tyrosine kinase	0.36	0.04
ErbB2 (HER2)	T686	ErbB2 (Neu) receptor-tyrosine kinase	-0.12	-1.42
ErbB2 (HER2)	Y1112	ErbB2 (Neu) receptor-tyrosine kinase	0.06	0.00
Erk1/2	Pan-specific	Extracellular regulated protein-serine kinase 1 (p44 MAP kinase), 2 (p42MAP kinase)	-1.07	-0.42
Erk1/2	Pan-specific	Extracellular regulated protein-serine kinase 1 (p44 MAP kinase), 2 (p42MAP kinase)	0.14	-0.58
Erk1/2	Pan-specific	Extracellular regulated protein-serine kinase 1 (p44 MAP kinase), 2 (p42MAP kinase)	-0.78	-0.42
Erk1/2	Pan-specific	Extracellular regulated protein-serine kinase 1 (p44 MAP kinase), 2 (p42MAP kinase)	-0.76	0.07
Erk1/2	Pan-specific	Extracellular regulated protein-serine kinase 1 (p44 MAP kinase), 2 (p42MAP kinase)	-0.25	-0.01
Erk1/2	Pan-specific	Extracellular regulated protein-serine kinase 1 (p44 MAP kinase), 2 (p42MAP kinase)	-0.39	-0.47
Erk2	Pan-specific	Extracellular regulated protein-serine kinase 2 (p42 MAP kinase)	-0.48	-0.13
Erk1/2	T202+Y204; T184/Y186	Extracellular regulated protein-serine kinase 1 (p44 MAP kinase), 2 (p42MAP kinase)	-0.88	-0.89
Erk1/2	T202+Y204; T184/Y186	Extracellular regulated protein-serine kinase 1 (p44 MAP kinase), 2 (p42MAP kinase)	-0.15	-0.50
Erk1/2	T202+Y204; T184/Y186	Extracellular regulated protein-serine kinase 1 (p44 MAP kinase), 2 (p42MAP kinase)	-0.46	-0.57

Erk3	Pan-specific	Extracellular regulated protein-serine kinase 3	-0.90	-1.33
Erk4	Pan-specific	Extracellular regulated protein-serine kinase 4	-0.02	0.05
Erk5	Pan-specific	Extracellular regulated protein-serine kinase 5 (Big MAP kinase 1 (BMK1))	-3.78	-0.44
Erk5	Pan-specific	Extracellular regulated protein-serine kinase 5 (Big MAP kinase 1 (BMK1))	-0.09	-0.14
Erk5	Pan-specific	Extracellular regulated protein-serine kinase 5 (Big MAP kinase 1 (BMK1))	1.13	2.13
Erk5	T218+Y220	Extracellular regulated protein-serine kinase 5 (Big MAP kinase 1 (BMK1))	-0.41	-0.29
Erk5	T218+Y220	Extracellular regulated protein-serine kinase 5 (Big MAP kinase 1 (BMK1))	0.02	-0.11
ERP57	Pan-specific	ER protein 57 kDa (protein disulfide isomerase-associated 3; 58 kDa glucose regulated protein)	-3.54	-0.59
ERP72	Pan-specific	ER protein 72 kDa (protein disulfide isomerase-associated 4)	0.03	-0.03
FAK	Pan-specific	Focal adhesion protein-tyrosine kinase	0.17	0.44
FAK	Y397	Focal adhesion protein-tyrosine kinase	0.11	0.81
FAK	Y576	Focal adhesion protein-tyrosine kinase	-0.24	-0.13
FAK	Y576	Focal adhesion protein-tyrosine kinase	-0.83	0.49
FAK	S722	Focal adhesion protein-tyrosine kinase	-0.29	0.79
FAK	S732	Focal adhesion protein-tyrosine kinase	0.40	-0.08
FAK	S843	Focal adhesion protein-tyrosine kinase	1.23	1.10
FAK	S910	Focal adhesion protein-tyrosine kinase	0.05	-1.21
FAS	Pan-specific	Tumor necrosis factor superfamily member 6 (Apo1, CD95)	-2.98	1.43
FasL	Pan-specific	Tumor necrosis factor ligand, member 6	-0.48	-0.37
Fes	Pan-specific	Fes/Fps protein-tyrosine kinase	1.07	0.28
FGFR1	Pan-specific	Fibroblast growth factor receptor-tyrosine kinase 1	0.03	0.09
FGFR2	Pan-specific	Fibroblast growth factor receptor-tyrosine kinase 2 (BEK)	0.23	0.06
FKBP52	Pan-specific	FK506-binding protein 4	-1.41	-0.49
FKHRL1	T32	Forkhead-like transcription factor 1 (FOXO3A)	-1.68	-0.44
FLT4	Pan-specific	Vascular endothelial growth factor receptor-protein-tyrosine kinase 3 (VEGFR3)	0.72	0.69
Fos	Pan-specific	Fos-c FBJ murine osteosarcoma oncoprotein-related transcription factor	-0.69	2.18
Fos	T232	Fos-c FBJ murine osteosarcoma oncoprotein-related transcription factor	0.31	0.65

Fyn	Pan-specific	Fyn proto-oncogene-encoded protein-tyrosine kinase	-1.93	1.40
GAP-43	S41	Growth associated protein 43 (Neuromodulin)	-0.84	-0.43
GCK	Pan-specific	Germinal centre protein-serine kinase	-0.57	0.16
GFAP	S8	Glial fibrillary acidic protein	-0.49	-1.08
GNB2L1	Pan-specific	Guanine nucleotide-binding protein beta (receptor for activated C kinase 1 (RACK1))	-2.20	0.09
GRK2 (BARK1)	Pan-specific	G protein-coupled receptor-serine kinase 2	-1.35	-0.02
GRK2 (BARK1)	S670	G protein-coupled receptor-serine kinase 2	-0.15	0.17
GRK3 (BARK2)	Pan-specific	G protein-coupled receptor-serine kinase 3	-0.55	-0.21
GroEL	Pan-specific	GroEL homolog (may correspond to Hsp60)	0.08	0.58
Grp75	Pan-specific	Glucose regulated protein 75	-1.22	-0.23
Grp78	Pan-specific	Glucose regulated protein 78	0.23	0.96
Grp78	Pan-specific	Glucose regulated protein 78	-0.27	0.55
Grp94	Pan-specific	Glucose regulated protein 94 (endoplasmic)	-0.19	0.01
Grp94	Pan-specific	Glucose regulated protein 94 (endoplasmic)	-0.07	0.53
GSK3ab	Pan-specific	Glycogen synthase-serine kinase 3 alpha/beta	-0.35	0.03
GSK3ab	Pan-specific	Glycogen synthase-serine kinase 3 alpha/beta	0.32	-0.45
GSK3ab	S21/S9	Glycogen synthase-serine kinase 3 alpha/beta	0.24	0.15
GSK3ab	Y279/Y216	Glycogen synthase-serine kinase 3 alpha/beta	-0.44	0.18
GSK3ab	Pan-specific	Glycogen synthase-serine kinase 3 alpha/beta	0.09	0.35
GSK3ab	Pan-specific	Glycogen synthase-serine kinase 3 alpha/beta	-0.20	0.16
GSK3ab	Pan-specific	Glycogen synthase-serine kinase 3 alpha/beta	-0.16	-0.02
Haspin	Pan-specific	Haploid germ cell-specific nuclear protein-serine kinase	0.16	-0.03
hHR23B	Pan-specific	UV excision repair protein RAD23 homolog B	-0.11	-0.52
Hip	Pan-specific	Hsp70/Hsc70 interacting protein (ST13)	-0.01	0.40
Histone H1	phospho CDK1 sites	Histone H1 phosphorylated	1.64	0.17
Histone H2A.X	S139	Histone H2A variant X	-0.20	-0.35
Histone H2B	S14	Histone H2B	-0.86	-0.11
Histone H3	S10	Histone H3.3	0.26	-0.40
Histone H3	S28	Histone H3.3	1.06	1.67
Histone H3	T11	Histone H3.3	0.07	-0.07
Histone H3	T3	Histone H3.3	0.05	0.73
Histone H3	T3	Histone H3.3	-1.56	0.52
HO1	Pan-specific	Heme oxygenase 1	-0.67	1.17
HO1	Pan-specific	Heme oxygenase 1	-0.24	2.51
HO2	Pan-specific	Heme oxygenase 2	-0.30	-0.15

Hpk1	Pan-specific	Hematopoietic progenitor protein-serine kinase 1	0.70	-0.78
Hsc70	Pan-specific	Heat shock 70 kDa protein 8	-2.11	3.06
Hsc70	Pan-specific	Heat shock 70 kDa protein 8	-0.26	0.29
Hsc70	Pan-specific	Heat shock 70 kDa protein 8	0.72	1.09
HSF4	Pan-specific	Heat shock transcription factor 4	-0.14	-0.91
Hsp105	Pan-specific	Heat shock 105 kDa protein	1.31	0.92
Hsp27	Pan-specific	Heat shock 27 kDa protein beta 1 (HspB1)	-0.84	-0.09
Hsp27	Pan-specific	Heat shock 27 kDa protein beta 1 (HspB1)	0.16	0.29
Hsp27	S15	Heat shock 27 kDa protein beta 1 (HspB1)	3.48	0.14
Hsp27	S15	Heat shock 27 kDa protein beta 1 (HspB1)	0.37	0.33
Hsp27	S78	Heat shock 27 kDa protein beta 1 (HspB1)	0.55	-1.04
Hsp27	S82	Heat shock 27 kDa protein beta 1 (HspB1)	-0.22	0.54
Hsp27	S82	Heat shock 27 kDa protein beta 1 (HspB1)	-0.81	-0.28
Hsp27	S82	Heat shock 27 kDa protein beta 1 (HspB1)	2.23	-0.37
Hsp40	Pan-specific	DnaJ homolog, subfamily B member 1	0.11	0.06
Hsp40	Pan-specific	DnaJ homolog, subfamily B member 1	0.21	-0.10
Hsp40	Pan-specific	DnaJ homolog, subfamily B member 1	-0.12	0.65
Hsp47	Pan-specific	Heat shock 47 kDa protein (collagen-binding protein 1, colligin 1)	0.80	0.20
Hsp60	Pan-specific	Heat shock 60 kDa protein 1 (chaperonin, CPN60)	1.21	-0.91
Hsp60	Pan-specific	Heat shock 60 kDa protein 1 (chaperonin, CPN60)	-0.10	-0.28
Hsp60	Pan-specific	Heat shock 60 kDa protein 1 (chaperonin, CPN60)	0.02	-0.21
Hsp70	Pan-specific	Heat shock 70 kDa protein 1	-0.07	-0.03
Hsp70	Pan-specific	Heat shock 70 kDa protein 1	-0.48	-0.14
Hsp70	Pan-specific	Heat shock 70 kDa protein 1	0.23	-0.02
Hsp90	Pan-specific	Heat shock 90 kDa protein alpha/beta	1.30	1.53
Hsp90	Pan-specific	Heat shock 90 kDa protein alpha/beta	-0.10	-0.27
Hsp90	Pan-specific	Heat shock 90 kDa protein alpha/beta	-1.14	0.25
Hsp90	Pan-specific	Heat shock 90 kDa protein alpha/beta	0.05	-0.07
Hsp90	Pan-specific	Heat shock 90 kDa protein alpha/beta	0.06	0.06
Hsp90	Pan-specific	Heat shock 90 kDa protein alpha/beta	1.05	0.11
Hsp90	Pan-specific	Heat shock 90 kDa protein alpha/beta	-0.22	-0.65
Hsp90	Pan-specific	Heat shock 90 kDa protein alpha/beta	0.04	-0.86
Hsp90	Pan-	Heat shock 90 kDa protein	-0.82	-1.20

	specific	alpha/beta		
Hsp90	Pan-specific	Heat shock 90 kDa protein alpha/beta	0.39	0.38
Hsp90a	Pan-specific	Heat shock 90 kDa protein alpha	1.85	0.06
Hsp90a	Pan-specific	Heat shock 90 kDa protein alpha	0.32	-0.36
Hsp90a	Pan-specific	Heat shock 90 kDa protein alpha	0.64	-0.76
Hsp90a	Pan-specific	Heat shock 90 kDa protein alpha	0.71	-1.27
Hsp90a	Pan-specific	Heat shock 90 kDa protein alpha	-0.72	1.10
Hsp90a	Pan-specific	Heat shock 90 kDa protein alpha	0.11	0.35
Hsp90a	Pan-specific	Heat shock 90 kDa protein alpha	-0.12	-0.07
Hsp90b	Pan-specific	Heat shock 90 kDa protein beta	-1.90	0.53
HspBP1	Pan-specific	Hsp70 binding protein 1	0.32	-0.51
Huntingtin	S421	Huntington's disease protein	-0.25	0.22
I1PP2A	Pan-specific	Acidic leucine-rich nuclear phosphoprotein 32 family member A	0.16	-0.11
I2PP2A	Pan-specific	Protein SET	-0.36	-0.12
ICK	Pan-specific	Intestinal cell protein-serine kinase (MAK-related kinase (MRK)	0.22	-0.26
IGF1R	Pan-specific	Insulin-like growth factor receptor protein-tyrosine kinase	0.08	-0.01
IkBa	Pan-specific	Inhibitor of NF-kappa-B alpha (MAD3)	-0.35	-0.98
IkBa	Pan-specific	Inhibitor of NF-kappa-B alpha (MAD3)	0.30	-1.84
IkBa	Pan-specific	Inhibitor of NF-kappa-B alpha (MAD3)	1.04	-0.06
IkBa	Pan-specific	Inhibitor of NF-kappa-B alpha (MAD3)	0.58	-0.80
IkBb	Pan-specific	Inhibitor of NF-kappa-B beta (thyroid receptor interacting protein 9)	0.15	-1.14
IkBb	Pan-specific	Inhibitor of NF-kappa-B beta (thyroid receptor interacting protein 9)	-0.07	-0.32
IKKa	Pan-specific	Inhibitor of NF-kappa-B protein-serine kinase alpha (CHUK)	0.03	0.06
IKKa	Pan-specific	Inhibitor of NF-kappa-B protein-serine kinase alpha (CHUK)	1.76	-1.32
IKKa	Pan-specific	Inhibitor of NF-kappa-B protein-serine kinase alpha (CHUK)	-0.80	0.26
IKKa	Pan-specific	Inhibitor of NF-kappa-B protein-serine kinase alpha (CHUK)	0.30	0.08
IKKa	Pan-specific	Inhibitor of NF-kappa-B protein-serine kinase alpha (CHUK)	0.36	-0.57
IKKa/b	S180/S181	Inhibitor of NF-kappa-B protein-serine kinase alpha/beta	1.84	-0.19
IKKb	Pan-specific	Inhibitor of NF-kappa-B protein-serine kinase beta	4.13	-4.33
IKKb	Pan-specific	Inhibitor of NF-kappa-B protein-serine kinase beta	-0.02	-0.41
IKKb	Pan-specific	Inhibitor of NF-kappa-B protein-serine kinase beta	1.47	0.92
IKKg	Pan-	I-kappa-B kinase gamma/NF-	0.22	-0.71

(NEMO)	specific	kappa-B essential modulator		
ILK1	Pan-specific	Integrin-linked protein-serine kinase 1	1.34	-0.24
ILK1	Pan-specific	Integrin-linked protein-serine kinase 1	3.54	-0.78
Integrin a4	S988	Integrin alpha 4 (VLA4)	-0.84	-0.28
Integrin b1	S785	Integrin beta 1 (fibronectin receptor beta subunit, CD29 antigen)	2.43	0.61
IR	Pan-specific	Insulin receptor beta chain	0.68	-0.97
IR (INSR)	Y999	Insulin receptor	0.26	-0.54
IR (INSR)	Y999	Insulin receptor	-0.14	-1.39
IR/IGF1R (INSR)	Y1189/Y1190	Insulin receptor / Insulin-like growth factor 1 receptor	1.62	1.60
IRAK1	Pan-specific	Interleukin 1 receptor-associated kinase 1 (Pelle-like protein kinase)	1.43	-0.82
IRAK1	Pan-specific	Interleukin 1 receptor-associated kinase 1 (Pelle-like protein kinase)	1.12	-1.01
IRAK2	Pan-specific	Interleukin 1 receptor-associated kinase 2	0.49	0.34
IRAK2	Pan-specific	Interleukin 1 receptor-associated kinase 2	1.91	0.01
IRAK3	Pan-specific	Interleukin 1 receptor-associated kinase 3	0.56	-0.09
IRAK4	Pan-specific	Interleukin 1 receptor-associated kinase 4	-0.47	-1.02
IRAK4	Pan-specific	Interleukin 1 receptor-associated kinase 4	-0.17	-0.18
IRb/IGF1R b	Y1131/Y1146	Insulin receptor / Insulin-like growth factor 1 receptor beta	1.05	-0.15
IRS1	Y612	Insulin receptor substrate 1	-0.23	-0.43
IRS1	Y1179	Insulin receptor substrate 1	2.23	1.95
IRS1	S312	Insulin receptor substrate 1	1.43	2.63
IRS1	S639	Insulin receptor substrate 1	1.08	-0.15
JAK1	Pan-specific	Janus protein-tyrosine kinase 1	0.74	0.59
JAK1	Pan-specific	Janus protein-tyrosine kinase 1	0.54	-0.45
JAK2	Pan-specific	Janus protein-tyrosine kinase 2	-0.45	-0.05
JAK3	Pan-specific	Janus protein-tyrosine kinase 3	1.32	-0.94
JIK (TAO3)	Pan-specific	STE20-like protein-serine kinase	0.11	-0.11
JNK	T183/Y185	Jun N-terminus protein-serine kinase (stress-activated protein kinase (SAPK))	0.10	-0.17
JNK	T183/Y185	Jun N-terminus protein-serine kinase (stress-activated protein kinase (SAPK))	-0.88	0.10
JNK	T183+Y185	Jun N-terminus protein-serine kinase (stress-activated protein kinase (SAPK))	0.18	-0.41
JNK1	Pan-specific	Jun N-terminus protein-serine kinase (stress-activated protein kinase (SAPK)) 1	0.09	-0.66
JNK1/2/3	Pan-specific	Jun N-terminus protein-serine kinases (stress-activated protein kinase (SAPK)) 1/2/3	-0.19	0.00
JNK1/2/3	Pan-specific	Jun N-terminus protein-serine kinases (stress-activated protein kinase (SAPK)) 1/2/3	3.61	-0.02

JNK1/2/3	Pan-specific	Jun N-terminus protein-serine kinases (stress-activated protein kinase (SAPK)) 1/2/3	0.01	-0.34
JNK2	Pan-specific	Jun N-terminus protein-serine kinases (stress-activated protein kinase (SAPK)) 2	0.34	0.66
JNK2/3	Pan-specific	Jun N-terminus protein-serine kinase (stress-activated protein kinase (SAPKa/b)) 2/3	-1.86	0.16
JNK3	Pan-specific	Jun N-terminus protein-serine kinase (stress-activated protein kinase (SAPKb)) 3	0.12	-0.03
Jun	Pan-specific	Jun proto-oncogene-encoded AP1 transcription factor	0.04	-0.88
Jun	S63	Jun proto-oncogene-encoded AP1 transcription factor	-0.19	-0.03
Jun	S73	Jun proto-oncogene-encoded AP1 transcription factor	0.15	-0.19
Jun	S73	Jun proto-oncogene-encoded AP1 transcription factor	0.61	0.69
Jun	S73	Jun proto-oncogene-encoded AP1 transcription factor	-0.29	-0.08
KAP	Pan-specific	Cyclin-dependent kinase associated phosphatase (CDK inhibitor 3, CIP2)	0.89	0.87
KDEL receptor 1	Pan-specific	ER lumen protein retaining receptor 1	0.40	-0.07
KHS	Pan-specific	Kinase homologous to SPS1/STE20 (MAP kinase kinase kinase protein-serine kinase 5 (MEKKK5))	-0.41	0.43
Kit	Y703	Kit/Steel factor receptor-tyrosine kinase	-0.34	-0.02
Kit	Y730	Kit/Steel factor receptor-tyrosine kinase	-0.06	0.33
Kit	Y936	Kit/Steel factor receptor-tyrosine kinase	0.06	-0.51
Ksr1	Pan-specific	Protein-serine kinase suppressor of Ras 1	-0.28	-0.04
Ksr-1	Pan-specific	Protein-serine kinase suppressor of Ras 1	-0.99	-0.30
LAR	Pan-specific	LCA antigen-related (LAR) receptor tyrosine phosphatase	-0.28	-0.46
LATS1	Pan-specific	Large tumor suppressor 1 protein-serine kinase (WARTS)	0.12	0.19
Lck	Pan-specific	Lymphocyte-specific protein-tyrosine kinase	-1.42	0.46
Lck	Pan-specific	Lymphocyte-specific protein-tyrosine kinase	-0.34	-0.60
Lck	S158	Lymphocyte-specific protein-tyrosine kinase	0.04	0.13
Lck	Y192	Lymphocyte-specific protein-tyrosine kinase	-0.41	-0.11
Lck	Y505	Lymphocyte-specific protein-tyrosine kinase	-0.15	-0.04
LIMK1	Pan-specific	LIM domain kinase 1	-0.19	-0.81
LIMK1/2	Y507+T508, Y504+T505	LIM domain kinase 1/2	-0.39	-0.19
LOK	Pan-specific	Lymphocyte-oriented protein-serine kinase	-0.07	-0.34
Lyn	Pan-specific	Yes-related protein-tyrosine kinase	-1.02	0.19
Lyn	Y507	Yes-related protein-tyrosine	0.09	-1.10

		kinase		
MAK	Pan-specific	Male germ cell-associated protein-serine kinase	0.36	-0.16
MAPKAPK 2	Pan-specific	Mitogen-activated protein kinase-activated protein kinase 2	-0.70	0.13
MAPKAPK 2	T222	Mitogen-activated protein kinase-activated protein kinase 2	-0.23	0.00
MAPKAPK 2ab	T334	Mitogen-activated protein kinase-activated protein kinase 2 alpha/beta	0.06	-0.33
MAPKAPK 2ab	T334	Mitogen-activated protein kinase-activated protein kinase 2 alpha/beta	0.04	0.26
MARCKS	S158+S162	Myristoylated alanine-rich protein kinase C substrate	-0.59	-0.13
MARK	Pan-specific	MAP/microtubule affinity-regulating protein-serine kinase 1	0.57	0.05
Mcl1	Pan-specific	Myeloid cell leukemia differentiation protein 1	-0.30	0.06
MEF-2	Pan-specific	Myelin expression factor 2 (MYEF2)	-6.42	-2.35
MEK1 (MAP2K1)	Pan-specific	MAPK/ERK protein-serine kinase 1 (MKK1)	-0.06	-0.17
MEK1 (MAP2K1)	Pan-specific	MAPK/ERK protein-serine kinase 1 (MKK1)	0.04	-0.37
MEK1 (MAP2K1)	Pan-specific	MAPK/ERK protein-serine kinase 1 (MKK1)	-0.03	0.09
MEK1 (MAP2K1)	Pan-specific	MAPK/ERK protein-serine kinase 1 (MKK1)	0.20	-0.07
MEK1 (MAP2K1)	Pan-specific	MAPK/ERK protein-serine kinase 1 (MKK1)	0.20	-0.45
MEK1 (MAP2K1)	T291	MAPK/ERK protein-serine kinase 1 (MKK1)	0.06	0.03
MEK1 (MAP2K1)	T291	MAPK/ERK protein-serine kinase 1 (MKK1)	-0.33	-0.46
MEK1 (MAP2K1)	T291	MAPK/ERK protein-serine kinase 1 (MKK1)	-0.36	-1.28
MEK1 (MAP2K1)	S297	MAPK/ERK protein-serine kinase 1 (MKK1)	-0.30	-0.32
MEK1 (MAP2K1)	T385	MAPK/ERK protein-serine kinase 1 (MKK1)	-0.07	-0.27
MEK1 (MAP2K1)	T385	MAPK/ERK protein-serine kinase 1 (MKK1)	-0.03	-0.29
MEK1 (MAP2K1)	T385	MAPK/ERK protein-serine kinase 1 (MKK1)	-0.60	-1.14
MEK1/2	Pan-specific	MAPK/ERK protein-serine kinase 1/2 (MKK1/2)	-0.20	-0.26
MEK1/2+B23 (NPM)	S217+S221, S4	MAPK/ERK protein-serine kinase 1/2 (MKK1/2) + B23 (nucleophosmin, numatrin, nucleolar protein NO38)	-0.06	-0.88
MEK2 (MAP2K2)	Pan-specific	MAPK/ERK protein-serine kinase 2 (MKK2)	-0.25	0.03
MEK2 (MAP2K2)	Pan-specific	MAPK/ERK protein-serine kinase 2 (MKK2)	-0.13	0.14
MEK2 (MAP2K2)	Pan-specific	MAPK/ERK protein-serine kinase 2 (MKK2)	-0.20	-0.49
MEK2 (MAP2K2)	T394	MAPK/ERK protein-serine kinase 2 (MKK2) (human)	-0.15	-0.35
MEK2 (MAP2K2)	T394	MAPK/ERK protein-serine kinase 2 (MKK2)	-0.05	-0.23
MEK2 (MAP2K2)	T394	MAPK/ERK protein-serine kinase 2 (MKK2) (mouse)	-0.29	-0.24

MEK3 (MAP2K3)	Pan-specific	MAPK/ERK protein-serine kinase 3 (MKK3)	-0.54	1.75
MEK3 (MAP2K3)	Pan-specific	MAPK/ERK protein-serine kinase 3 (MKK3)	-0.47	-0.38
MEK3 (MAP2K3)	Pan-specific	MAPK/ERK protein-serine kinase 3 (MKK3)	1.28	1.01
MEK3 (MAP2K3)	S218	MAPK/ERK protein-serine kinase 3 (MKK3)	0.92	0.06
MEK3/6 (MAP2K3/6)	S218/S207	MAPK/ERK protein-serine kinase 3/6 (MKK3/6)	-0.05	-0.43
MEK3/6 (MAP2K3/6)	S218/S207	MAPK/ERK protein-serine kinase 3/6 (MKK3/6)	-0.21	-0.16
MEK3/6 (MAP2K3/6)	S218/S207	MAPK/ERK protein-serine kinase 3/6 (MKK3/6)	-0.68	-0.42
MEK3b (MAP2K3)	Pan-specific	MAPK/ERK protein-serine kinase 3 beta isoform (MKK3 beta)	-0.29	-0.45
MEK4 (MAP2K4)	Pan-specific	MAPK/ERK protein-serine kinase 4 (MKK4)	-1.39	5.74
MEK4 (MAP2K4)	Pan-specific	MAPK/ERK protein-serine kinase 4 (MKK4)	-0.33	-0.09
MEK4 (MAP2K4)	Pan-specific	MAPK/ERK protein-serine kinase 4 (MKK4)	-0.27	0.94
MEK4 (MAP2K4)	S257+T261	MAPK/ERK protein-serine kinase 4 (MKK4)	0.00	-0.68
MEK5 (MAP2K5)	Pan-specific	MAPK/ERK protein-serine kinase 5 (MKK5)	-0.90	-0.39
MEK5 (MAP2K5)	Pan-specific	MAPK/ERK protein-serine kinase 5 (MKK5)	-0.78	-0.08
MEK6 (MAP2K6)	Pan-specific	MAPK/ERK protein-serine kinase 6 (MKK6)	-0.01	0.04
MEK6 (MAP2K6)	Pan-specific	MAPK/ERK protein-serine kinase 6 (MKK6)	-0.23	-0.27
MEK6 (MAP2K6)	S207	MAPK/ERK protein-serine kinase 6 (MKK6)	-0.10	-0.22
MEK7 (MAP2K7)	Pan-specific	MAPK/ERK protein-serine kinase 7 (MKK7)	-0.42	0.06
MEKK1 (MAP3K1)	Pan-specific	MAPK/ERK kinase kinase 1	-0.07	-0.75
MEKK1 (MAP3K1)	Pan-specific	MAPK/ERK kinase kinase 1	-0.22	-0.03
MEKK1 (MAP3K1)	Pan-specific	MAPK/ERK kinase kinase 1	-0.07	-0.12
MEKK1 (MAP3K1)	Pan-specific	MAPK/ERK kinase kinase 1	-1.11	0.59
MEKK2 (MAP3K2)	Pan-specific	MAPK/ERK kinase kinase 2	0.07	0.25
MEKK2 (MAP3K2)	Pan-specific	MAPK/ERK kinase kinase 2	-1.05	-0.77
MEKK4 (MAP3K4)	Pan-specific	MAPK/ERK kinase kinase 4	0.07	0.17
Met	Pan-specific	Hepatocyte growth factor (HGF) receptor-tyrosine kinase	-0.37	-0.26
Met	Y1003	Hepatocyte growth factor (HGF) receptor-tyrosine kinase	-0.22	0.25
MKP1	Pan-specific	MAP kinase phosphatase 1 (CL100, VH1)	-0.24	-0.23
MKP2	Pan-specific	MAP kinase phosphatase 2 (VH2)	-0.45	-0.72
MLC(MLR C2)	S19	Myosin regulatory light chain 2, smooth muscle isoform	-0.73	-0.68
MLC(MLR C2)	S19	Myosin regulatory light chain 2, smooth muscle isoform	-1.45	-0.12

MLK3	Pan-specific	Mixed-lineage protein-serine kinase 3	-1.42	0.94
MLK3	T277+S281	Mixed-lineage protein-serine kinase 3	-0.14	0.13
mMOB1	Pan-specific	Preimplantation protein 3	0.02	0.37
Mn SOD	Pan-specific	Manganese superoxide dismutase (SOD2)	-0.10	-0.50
Mnk1	T209+T214	MAP kinase-interacting protein-serine kinase 1 (calmodulin-activated)	-0.36	-0.38
Mnk2	Pan-specific	MAP kinase-interacting protein-serine kinase 2 (calmodulin-activated)	0.93	1.03
Mos	Pan-specific	Moloney sarcoma oncogene-encoded protein-serine kinase	-0.77	-0.39
MSH2	Pan-specific	DNA mismatch repair protein mutS homolog2, colon cancer, nonpolyposis type 1	-0.51	-0.13
Msk1	S376	Mitogen & stress-activated protein-serine kinase 1	-0.17	-0.74
MST1	Pan-specific	Mammalian STE20-like protein-serine kinase 1 (KRS2)	-0.11	-0.14
MST1	Pan-specific	Mammalian STE20-like protein-serine kinase 1 (KRS2)	-0.48	0.05
MST1	Pan-specific	Mammalian STE20-like protein-serine kinase 1 (KRS2)	-0.65	-0.11
MST1	Pan-specific	Mammalian STE20-like protein-serine kinase 1 (KRS2)	0.08	-0.39
MST2	Pan-specific	Mammalian STE20-like protein-serine kinase 2 (KRS1)	0.10	-1.10
MST3	Pan-specific	Mammalian STE20-like protein-serine kinase 3	-0.55	-0.78
mTOR (FRAP)	Pan-specific	Mammalian target of rapamycin (FRAP)	-1.08	-1.05
mTOR (FRAP)	S2448	Mammalian target of rapamycin (FRAP)	-0.80	-0.92
MYPT1	T696	Myosin phosphatase target 1	-0.52	-0.93
Nek2	Pan-specific	NIMA (never-in-mitosis)-related protein-serine kinase 2	-0.34	-0.88
Nek2	Pan-specific	NIMA (never-in-mitosis)-related protein-serine kinase 2	0.07	0.08
Nek2	Pan-specific	NIMA (never-in-mitosis)-related protein-serine kinase 2	0.26	1.00
Nek2	Pan-specific	NIMA (never-in-mitosis)-related protein-serine kinase 2	0.73	0.00
Nek2	Pan-specific	NIMA (never-in-mitosis)-related protein-serine kinase 2	0.54	0.32
Nek4	Pan-specific	NIMA (never-in-mitosis)-related protein-serine kinase 4	0.01	-0.34
Nek7	Pan-specific	NIMA (never-in-mitosis)-related protein-serine kinase 7	-0.16	-0.04
NFkappaB p50	Pan-specific	NF-kappa-B p50 nuclear transcription factor	-0.60	-0.38
NFkappaB p65	Pan-specific	NF-kappa-B p65 nuclear transcription factor	-0.32	-0.68
NIK	Pan-specific	NF-kappa beta-inducing kinase	-0.74	-2.46
Nlk	Pan-specific	Serine/threonine protein kinase NLK	-0.39	0.45
NMDAR2B	Y1474	N-methyl-D-aspartate (NMDA) glutamate receptor 2B subunit	-2.84	0.06
NME7	Pan-specific	Nucleotide diphosphate kinase 7 (nm23-H7)	-0.24	-0.40
NR1	S896	N-methyl-D-aspartate (NMDA) glutamate receptor 1 subunit	0.57	0.04

		zeta		
Nrf2	Pan-specific	Nuclear factor erythroid 2-related factor 2	0.59	-0.16
NT5E	Pan-specific	Ecto-5'-nucleotidase (CD73 antigen)	0.43	0.61
p107	Pan-specific	Retinoblastoma (Rb) protein-related p107 (PRB1)	0.27	-0.57
p18 INK4c	Pan-specific	p18 INK4c cyclin-dependent kinase inhibitor	-0.36	-0.12
p21 CDK1	Pan-specific	cyclin-dependent kinase inhibitor 1 (MDA6)	0.86	0.14
p27 Kip1	Pan-specific	p27 cyclin-dependent kinase inhibitor 1B	0.73	-2.47
p27 Kip1	T187	p27 cyclin-dependent kinase inhibitor 1B	-0.34	-0.31
p35, p25	Pan-specific	CDK5 regulatory subunit 1, p35, p25	-0.85	-2.31
p38a MAPK	T180+Y182	Mitogen-activated protein-serine kinase p38 alpha	-2.59	-0.49
p38a MAPK	T180+Y182	Mitogen-activated protein-serine kinase p38 alpha	1.56	-0.16
p38a MAPK	T180+Y182	Mitogen-activated protein-serine kinase p38 alpha	-0.06	-0.73
p38a MAPK	T180+Y182	Mitogen-activated protein-serine kinase p38 alpha	-0.39	-1.67
p38a MAPK	T180+Y182	Mitogen-activated protein-serine kinase p38 alpha	1.25	0.10
p38a MAPK	Pan-specific	Mitogen-activated protein-serine kinase p38 alpha	-1.36	-0.07
p38a MAPK	Pan-specific	Mitogen-activated protein-serine kinase p38 alpha	0.09	-0.21
p38a MAPK	Pan-specific	Mitogen-activated protein-serine kinase p38 alpha	0.11	0.18
p38a MAPK	Pan-specific	Mitogen-activated protein-serine kinase p38 alpha	0.10	-0.99
p38a MAPK	Pan-specific	Mitogen-activated protein-serine kinase p38 alpha	0.07	-0.27
p38a MAPK	Pan-specific	Mitogen-activated protein-serine kinase p38 alpha	-0.51	-0.03
p38a MAPK	Pan-specific	Mitogen-activated protein-serine kinase p38 alpha	-0.43	-0.13
p38a MAPK	Pan-specific	Mitogen-activated protein-serine kinase p38 alpha	-0.14	-0.30
p38d MAPK	Pan-specific	Mitogen-activated protein-serine kinase p38 delta (MAPK13)	-0.20	0.28
p38g MAPK (Erk6)	Pan-specific	Mitogen-activated protein-serine kinase p38 gamma (MAPK12)	-0.29	0.09
p38g MAPK (Erk6)	Pan-specific	Mitogen-activated protein-serine kinase p38 gamma (MAPK12)	-0.19	-0.30
p53	Pan-specific	Tumor suppressor protein p53 (antigenNY-CO-13)	-1.18	-0.60
p53	S392	Tumor suppressor protein p53 (antigenNY-CO-13)	-1.06	-0.19
p53	S392	Tumor suppressor protein p53 (antigenNY-CO-13)	-0.37	-0.58
p53	S392	Tumor suppressor protein p53 (antigenNY-CO-13)	-0.05	-1.39
p73	Pan-specific	Tumor suppressor protein p73	-0.02	0.23
PAC1	Pan-specific	Dual specificity MAP kinase protein phosphatase	-0.68	6.84
PACSIN1	Pan-specific	Protein kinase C + casein kinase substrate in neurons protein 1	0.48	-0.28

PAK1	Pan-specific	p21-activated kinase 1 (alpha) (serine/threonine-protein kinase PAK 1)	-0.23	-1.23
PAK1	Pan-specific	p21-activated kinase 1 (alpha) (serine/threonine-protein kinase PAK 1)	-0.02	-0.09
PAK1	Pan-specific	p21-activated kinase 1 (alpha) (serine/threonine-protein kinase PAK 1)	0.40	0.85
PAK1/2/3	S144/S141 /S154	p21-activated kinase 1/2/3 (serine/threonine-protein kinase PAK 1/2/3)	0.27	-0.09
PAK1/2/3	T423/402/4 21	p21-activated kinase 1/2/3 (serine/threonine-protein kinase PAK 1/2/3)	0.26	-0.75
PAK2	Pan-specific	p21-activated kinase 2 (gamma) (serine/threonine-protein kinase PAK 2)	-0.28	-0.10
PAK2	Pan-specific	p21-activated kinase 2(gamma) (serine/threonine-protein kinase PAK 2)	-0.14	-0.30
PAK3	Pan-specific	p21-activated kinase 3 (beta) (serine/threonine-protein kinase PAK 3)	0.73	0.27
PAK5	Pan-specific	p21-activated kinase 5 (serine/threonine-protein kinase PAK 7)	1.34	0.28
PAK6	Pan-specific	p21-activated kinase 6 (serine/threonine-protein kinase PAK 6)	0.47	-0.19
PARP1	Pan-specific	Poly [ADP-ribose] polymerase 1 (ADPRT)	0.54	-0.01
PARP1	Pan-specific	Poly [ADP-ribose] polymerase 1 (ADPRT)	-0.07	-0.09
Pax2	S394	Paired box protein 2	-0.47	-0.26
Paxillin	Pan-specific	Paxillin 1	-0.19	-0.99
Paxillin 1	Y31	Paxillin 1	0.24	-0.56
Paxillin 1	Y118	Paxillin 1	-1.65	-1.90
Paxillin 1	Y118	Paxillin 1	-0.58	-0.62
PCNA	Pan-specific	Proliferating cell nuclear antigen	3.87	1.70
PCK1 (PCTAIRE 1)	Pan-specific	PCTAIRE-1 protein-serine kinase	-0.01	-0.20
PDGFRa	Y754	Platelet-derived growth factor receptor kinase alpha	-0.29	-0.61
PDGFRa/b	Y572+Y57 4/Y579+Y5 81	Platelet-derived growth factor receptor kinase alpha/beta	-1.13	-0.73
PDGFRb	Y716	Platelet-derived growth factor receptor kinase beta	-0.63	-1.31
PDI	Pan-specific	Protein disulfide-isomerase	0.01	-0.41
PDK1	Pan-specific	3-phosphoinositide-dependent protein-serine kinase 1	-0.66	-0.38
PDK1	Pan-specific	3-phosphoinositide-dependent protein-serine kinase 1	-2.01	-0.95
PDK1	S244	3-Phosphoinositide-dependent protein-serine kinase 1	-0.05	-0.01
PED15 (PEA15)	S116	Phosphoprotein-enriched in diabetes/astrocytes 15	0.78	-0.80
PERP	Pan-specific	p53-induced protein PIGPC1	1.69	-1.45
PI3K	Pan-	Phosphatidylinositol 3-kinase	-0.17	-0.66

	specific	regulatory subunit alpha		
PI3K p110 delta	Pan-specific	Phosphatidylinositol-4,5-biphosphate 3-kinase catalytic subunit delta isoform	0.46	-0.09
PI3K p85/p55	Y467/Y199	Phosphatidylinositol 3-kinase regulatory subunit alpha	0.14	-0.35
PI3KR4	Pan-specific	Phosphoinositide-3-kinase, regulatory subunit 4	0.70	-0.37
PI4KCB	Pan-specific	phosphatidylinositol 4-kinase, catalytic, beta polypeptide	0.70	0.20
PIP5K2a	Pan-specific	Phosphatidylinositol 4-phosphatase 5-kinase type 2 alpha	-0.16	-0.69
PITSLRE	Pan-specific	PITSLRE serine/threonine-protein kinase CDC2L1	2.73	-4.08
PKA Ca/b	Pan-specific	cAMP-dependent protein-serine kinase catalytic subunit alpha/beta	-0.18	-0.63
PKA Ca/b	Pan-specific	cAMP-dependent protein-serine kinase catalytic subunit alpha/beta	0.65	0.83
PKA Ca/b	T197	cAMP-dependent protein-serine kinase catalytic subunit alpha/beta	0.00	-0.52
PKA Cb	S338	cAMP-dependent protein-serine kinase catalytic subunit beta	-0.27	-0.69
PKA R1a	Pan-specific	cAMP-dependent protein-serine kinase type I-alpha regulatory chain	-0.01	-1.37
PKA R2a	Pan-specific	cAMP-dependent protein-serine kinase regulatory type 2 subunit alpha	0.26	0.29
PKA R2a	S98	cAMP-dependent protein-serine kinase regulatory type 2 subunit alpha	-1.12	-0.72
PKBa (Akt1)	Pan-specific	Protein-serine kinase B alpha	0.09	-0.47
PKBa (Akt1)	Pan-specific	Protein-serine kinase B alpha	-0.01	-0.54
PKBa (Akt1)	T308	Protein-serine kinase B alpha	-0.22	-0.71
PKBa (Akt1)	T308	Protein-serine kinase B alpha	0.25	-0.25
PKBa (Akt1)	S473	Protein-serine kinase B alpha	0.12	-0.19
PKBa (Akt1)	S473	Protein-serine kinase B alpha	0.29	-0.54
PKBb (Akt2)	Pan-specific	Protein-serine kinase B beta	0.60	-0.23
PKBb (Akt2)	Pan-specific	Protein-serine kinase B beta	1.19	-0.35
PKBb (Akt2)	Pan-specific	Protein-serine kinase B beta	-0.75	-0.36
PKBb (Akt2)	Pan-specific	Protein-serine kinase B beta	0.77	-0.06
PKBb (Akt2)	Pan-specific	Protein-serine kinase B beta	-0.20	-0.80
PKBb (Akt2)	Pan-specific	Protein-serine kinase B beta	0.47	-0.38
PKBg (Akt3)	Pan-specific	Protein-serine kinase B gamma	0.42	0.30
PKBg (Akt3)	Pan-specific	Protein-serine kinase B gamma	0.12	-0.33
PKC	Pan-specific	Protein-serine kinase C alpha	0.57	-0.87
PKC h	Pan-	Protein kinase C eta type	-0.44	0.40

	specific			
PKCa	Pan-specific	Protein-serine kinase C alpha	-0.60	-0.43
PKCa	S657	Protein-serine kinase C alpha	-0.45	-0.85
PKCa/b2	T638/T641	Protein-serine kinase C alpha, beta 2	-1.76	-0.44
PKCb1	Pan-specific	Protein-serine kinase C beta 1	-2.03	0.66
PKCb1	Pan-specific	Protein-serine kinase C beta 1	0.19	0.03
PKCb1/2	T500	Protein-serine kinase C beta 1/2	-0.02	0.02
PKCb2	Pan-specific	Protein-serine kinase C beta 2	-0.18	0.58
PKCb2	Pan-specific	Protein-serine kinase C beta 2	0.87	0.63
PKCb2	T641	Protein-serine kinase C beta 2	0.17	0.02
PKCd	Pan-specific	Protein-serine kinase C delta	-0.74	0.38
PKCd	Y313	Protein-serine kinase C delta	-0.21	-0.14
PKCd	Y313	Protein-serine kinase C delta	-0.02	-0.06
PKCd	T507	Protein-serine kinase C delta	-0.21	0.13
PKCd	S664	Protein-serine kinase C delta	-0.68	-0.14
PKCe	Pan-specific	Protein-serine kinase C epsilon	-1.28	0.69
PKCe	Pan-specific	Protein-serine kinase C epsilon	-1.76	1.80
PKCe	S729	Protein-serine kinase C epsilon	0.09	0.31
PKCg	Pan-specific	Protein-serine kinase C gamma	0.35	-2.28
PKCg	T514	Protein-serine kinase C gamma	-0.05	-0.08
PKCg	T514	Protein-serine kinase C gamma	0.02	0.41
PKCg	T655	Protein-serine kinase C gamma	0.55	1.16
PKCg	T674	Protein-serine kinase C gamma	0.08	1.31
PKCh	S674	Protein-serine kinase C eta	0.20	0.21
PKCl/i	Pan-specific	Protein-serine kinase C lambda/iota	1.11	0.85
PKCl/i	T555	Protein-serine kinase C lambda/iota	0.85	0.44
PKCm (PKD)	Pan-specific	Protein-serine kinase C mu (Protein kinase D)	-2.52	0.46
PKCm (PKD)	S738+S742	Protein-serine kinase C mu (Protein kinase D)	-0.35	0.17
PKCm (PKD)	S910	Protein-serine kinase C mu (Protein kinase D)	-0.29	0.38
PKCm (PKD)	S910	Protein-serine kinase C mu (Protein kinase D)	-0.11	-0.42
PKN3	Pan-specific	Protein-serine kinase C nu	0.56	1.40
PKCq	Pan-specific	Protein-serine kinase C theta	-0.10	-0.28
PKCq	T538	Protein-serine kinase C theta	-0.56	0.48
PKCz	Pan-specific	Protein-serine kinase C zeta	-0.47	0.04
PKCz/l	T410/T403	Protein-serine kinase C zeta/lambda	0.30	-0.04
PKG1	Pan-specific	Protein-serine kinase G1 (cGMP-dependent protein kinase)	0.87	0.74
PKG1a	Pan-specific	cGMP-dependent protein kinase 1, alpha isozyme	-0.26	-0.38
PKG1b	Pan-specific	cGMP-dependent protein kinase 1, beta isozyme	-0.20	-0.03
PKM2	Pan-	Pyruvate kinase, isozymes	0.25	0.51

	specific	M1/M2		
PKR1	Pan-specific	Double stranded RNA dependent protein-serine kinase	1.12	0.38
PKR1	Pan-specific	Double stranded RNA dependent protein-serine kinase	0.05	-0.17
PKR1	T451	Double-stranded RNA-dependent protein-serine kinase	-0.26	0.03
PKR1	T446	Double-stranded RNA-dependent protein-serine kinase	1.34	0.44
PLC R(PLCg2)	Pan-specific	1-phosphatidylinositol-4,5-bisphosphate phosphodiesterase gamma-2	-0.36	2.71
Plk1	Pan-specific	Polo-like protein-serine kinase 1	0.50	0.10
Plk1	T210	Polo-like protein-serine kinase 1	-0.05	0.53
Plk2	Pan-specific	Polo-like protein kinase 2 (serum -inducible kinase (SNK))	0.51	0.35
Plk2	Pan-specific	Polo-like protein kinase 2 (serum -inducible kinase (SNK))	1.69	1.45
Plk3	Pan-specific	Polo-like protein kinase 3 (cytokine- inducible kinase (CNK))	0.08	0.39
PP1/Ca	Pan-specific	Protein-serine phosphatase 1 - catalytic subunit - alpha isoform	0.07	0.59
PP1/Ca	Pan-specific	Protein-serine phosphatase 1 - catalytic subunit - alpha isoform	0.55	0.67
PP1/Ca	T320	Protein-serine phosphatase 1 - catalytic subunit - alpha isoform	0.04	0.22
PP1/Cb	Pan-specific	Protein-serine phosphatase 1 - catalytic subunit - beta isoform	0.41	0.61
PP1/Cb	Pan-specific	Protein-serine phosphatase 1 - catalytic subunit - beta isoform	-0.18	0.02
PP1/Cg	Pan-specific	Protein-serine phosphatase 1 - catalytic subunit - gamma isoform	0.44	0.23
PP2A B' (B56)	Pan-specific	Protein-serine phosphatase 2A - B regulatory subunit - B56 alpha isoform	0.09	0.99
PP2A/Aa/b	Pan-specific	Protein-serine phosphatase 2A - A regulatory subunit - alpha and beta isoforms	-0.42	1.07
PP2A/Aa/b	Pan-specific	Protein-serine phosphatase 2A - A regulatory subunit - alpha and beta isoforms	0.11	-0.74
PP2A/Bb	Pan-specific	Protein-serine phosphatase 2A - B regulatory subunit - beta isoform	-0.64	-0.91
PP2A/Bg2	Pan-specific	Protein-serine phosphatase 2A - B regulatory subunit - gamma isoform	-0.62	2.32
PP2A/Ca	Pan-specific	Protein-serine phosphatase 2A - catalytic subunit alpha isoform	-0.59	-0.27
PP2B/Aa	Pan-specific	Protein-serine phosphatase 2B - catalytic subunit - alpha isoform	0.39	0.46
PP2Ca	Pan-specific	Protein-serine phosphatase 2C - catalytic subunit - alpha/beta	-0.43	0.67
PP2Cd	Pan-specific	Protein-serine phosphatase 2C - catalytic subunit - delta isoform	-0.36	-1.00
PP4/A'2	Pan-specific	Protein-serine phosphatase 4 - regulatory subunit (PPX/A'2)	-1.53	0.75
PP4C	Pan-specific	Protein-serine phosphatase X - catalytic subunit (PPX/C)	-2.44	-0.21
PP4C	Pan-specific	Protein-serine phosphatase X - catalytic subunit (PPX/C)	-0.86	0.14
PP5C	Pan-specific	Protein-serine phosphatase 5 - catalytic subunit (PPT)	-0.26	0.04

PP5C	Pan-specific	Protein-serine phosphatase 5 - catalytic subunit (PPT)	-0.07	-0.39
PP6C	Pan-specific	Protein-serine phosphatase 6 - catalytic subunit (PPVC)	0.29	-0.18
PP6C	Pan-specific	Protein-serine phosphatase 6 - catalytic subunit (PPVC)	-1.43	1.22
PRAS40	T246	Proline-rich Akt substrate 40 kDa (Akt1S1)	-0.74	0.02
PRK1 (PKN1)	Pan-specific	Protein kinase C-related protein-serine kinase 1	-2.00	1.97
PRK1/2 (PKN1/2)	T774, T816	Protein kinase C-related protein-serine kinase 1/2	0.42	0.28
PRK2 (PKN2)	Pan-specific	Protein kinase C-related protein-serine kinase 2	-0.24	-0.24
PRK2 (PKN2)	Pan-specific	Protein kinase C-related protein-serine kinase 2	-0.25	0.23
PRKAB1	Pan-specific	5'-AMP-activated protein kinase (AMPK), beta-1 regulatory subunit	-0.07	0.55
PRKWINK4	Pan-specific	Putative protein-serine kinase WNK4	-0.24	0.11
Progesterone Receptor	S294	Progesterone receptor	-0.73	-0.34
PRP4K	Pan-specific	Protein-serine kinase PRP4 homolog	0.10	0.19
PSD-95	Pan-specific	Disks large homolog 4	0.09	-0.11
PSTAIR	Pan-specific	PSTAIR	-0.72	-0.11
PTEN	Pan-specific	Phosphatidylinositol-3,4,5-trisphosphate 3-phosphatase and protein phosphatase and tensin homolog deleted on chromosome 10	0.07	0.69
PTEN	Pan-specific	Phosphatidylinositol-3,4,5-trisphosphate 3-phosphatase and protein phosphatase and tensin homolog deleted on chromosome 10	-0.45	-0.13
PTEN	S380+T382+S385	Phosphatidylinositol-3,4,5-trisphosphate 3-phosphatase and protein phosphatase and tensin homolog deleted on chromosome 10	0.09	0.20
PTP1B	Pan-specific	Protein-tyrosine phosphatase 1B	0.00	-0.26
PTP1C	Pan-specific	Protein-tyrosine phosphatase 1C (SHP1, SHPTP1)	-0.33	-0.11
PTP1D	Pan-specific	Protein-tyrosine phosphatase 1D (SHP2, SHPTP2, Syp, PTP2C)	-0.17	0.34
PTP1D	Pan-specific	Protein-tyrosine phosphatase 1D (SHP2, SHPTP2, Syp, PTP2C)	-0.51	0.29
PTPD1	Pan-specific	Protein-tyrosine phosphatase non-receptor type 21	0.00	-0.16
PyDK2 (PDHK2)	Pan-specific	Pyruvate dehydrogenase kinase isoform 2	0.07	-0.31
Pyk2	Pan-specific	Protein-tyrosine kinase 2	0.46	0.39
Pyk2	Pan-specific	Protein-tyrosine kinase 2	-0.11	0.35
Pyk2	Y579	Protein-tyrosine kinase 2	-0.33	0.35
Rab5	Pan-specific	Ras-related protein Rab-5A	1.14	0.10

Rab5	Pan-specific	Ras-related protein Rab-5A	0.67	0.44
Rac1	Pan-specific	Ras-related C3 botulinum toxin substrate 1	-0.05	-0.19
Rac1	S71	Ras-related C3 botulinum toxin substrate 1	0.40	0.24
Rad17	S645	Rad17 homolog	0.27	0.57
Raf1	Pan-specific	Raf1 proto-oncogene-encoded protein-serine kinase	-0.45	-0.18
Raf1	Pan-specific	Raf1 proto-oncogene-encoded protein-serine kinase	0.37	0.30
Raf1	Pan-specific	Raf1 proto-oncogene-encoded protein-serine kinase	2.09	2.31
Raf1	S259	Raf1 proto-oncogene-encoded protein-serine kinase	0.37	0.84
RafA (Araf)	Pan-specific	A-Raf proto-oncogene serine/threonine-protein kinase	0.09	-0.23
RafA (Araf)	Pan-specific	A-Raf proto-oncogene serine/threonine-protein kinase	1.83	0.60
RafB (Braf)	Pan-specific	RafB proto-oncogene-encoded protein-serine kinase	-0.92	0.64
RafB (Braf)	Pan-specific	RafB proto-oncogene-encoded protein-serine kinase	0.21	0.33
Rb	Pan-specific	Retinoblastoma-associated protein 1	-0.61	-0.14
Rb	T356	Retinoblastoma-associated protein 1	0.71	0.01
Rb	S612	Retinoblastoma-associated protein 1	-0.47	0.06
Rb	S780	Retinoblastoma-associated protein 1	0.23	-0.27
Rb	S807	Retinoblastoma-associated protein 1	0.36	0.00
Rb	S807+S811	Retinoblastoma-associated protein 1	0.58	0.34
Rb	T821	Retinoblastoma-associated protein 1	-0.10	0.09
Rb	T826	Retinoblastoma-associated protein 1	-0.22	0.09
Rb	S608	Retinoblastoma-associated protein 1	-0.43	-0.60
Rb	S795	Retinoblastoma-associated protein 1	0.60	0.59
RIP2/RICK	Pan-specific	Receptor-interacting serine/threonine-protein kinase 2 (RIPK2)	-0.37	-0.21
RIPK1	Pan-specific	Receptor-interacting protein-serine kinase 1	0.00	-0.27
ROKα (ROCK2)	Pan-specific	RhoA protein-serine kinase alpha	-0.21	0.26
ROKα (ROCK2)	Pan-specific	RhoA protein-serine kinase alpha	0.15	0.12
ROKβ (ROCK1)	Pan-specific	RhoA protein-serine kinase beta	-0.45	-0.19
RONα	Pan-specific	Macrophage-stimulating protein receptor alpha chain	-0.23	-0.32
ROR2	Pan-specific	ROR2 neurotrophic receptor-tyrosine kinase	0.00	0.13
ROS	Pan-specific	Orosomucoid 1 receptor-tyrosine kinase	0.09	0.19
RSK1	Pan-specific	Ribosomal S6 protein-serine kinase 1	0.68	2.05
RSK1	Pan-specific	Ribosomal S6 protein-serine kinase 1	0.89	0.16
RSK1	S363	Ribosomal S6 protein-serine kinase 1	0.84	-0.33

RSK1/2	S221/S227	Ribosomal S6 protein-serine kinase 1/2	0.22	0.12
RSK1/2	S363/S369	Ribosomal S6 protein-serine kinase 1/2	-0.18	0.12
RSK1/2	S380/S386	Ribosomal S6 protein-serine kinase 1/2	-0.08	-0.07
RSK1/2	S380/S386	Ribosomal S6 protein-serine kinase 1/2	0.23	0.39
RSK1/2/3	T573/T577/T570	Ribosomal S6 protein-serine kinase 1/2/3	1.24	1.27
RSK1/3	T359+S363/T356+S360	Ribosomal S6 protein-serine kinase 1/3	0.41	-0.14
RSK2	Pan-specific	Ribosomal S6 protein-serine kinase 2	-1.22	0.21
RSK4	Pan-specific	Ribosomal S6 protein-serine kinase 4 (alpha 6)	0.02	-0.66
RYK	Pan-specific	RYK tyrosine-protein kinase	0.35	0.97
S6	S235	40S ribosomal protein S6	0.97	-0.55
S6Ka (p70 S6Ka, p85 S6Ka)	Pan-specific	p70/p85 ribosomal protein-serine S6 kinase alpha	3.50	0.30
S6Ka (p70 S6Ka, p85 S6Ka)	Pan-specific	p70/p85 ribosomal protein-serine S6 kinase alpha	-0.29	0.09
S6Ka (p70 S6Ka, p85 S6Ka)	Pan-specific	p70/p85 ribosomal protein-serine S6 kinase alpha	0.12	0.09
S6Ka (p70 S6Ka, p85 S6Ka)	T229, T252	p70/p85 ribosomal protein-serine S6 kinase alpha	-0.98	0.72
S6Ka (p70 S6Ka, p85 S6Ka)	T444+S447, T421+S424	p70/p85 ribosomal protein-serine S6 kinase alpha	1.17	0.18
S6Ka (p70 S6Ka, p85 S6Ka)	T412, T389	p70/p85 ribosomal protein-serine S6 kinase alpha	1.54	-0.66
S6Kb (p70 S6Kb)	Pan-specific	p70 ribosomal protein-serine S6 kinase beta	0.09	0.80
SG2NA	Pan-specific	Striatin-3	0.14	0.15
SGK3	Pan-specific	Serum/glucocorticoid regulated kinase 3	0.69	2.69
Shc1	Y349+Y350	SH2 domain-containing transforming protein 1	-0.04	0.21
Shc1	Y349+Y350	SH2 domain-containing transforming protein 1	0.06	0.04
SHP2	S576	Protein-tyrosine phosphatase 1D (SHPTP2, Syp, PTP2C)	0.40	0.80
SLK	Pan-specific	STE20-like protein-serine kinase	0.44	-0.82
Smac/DIABLO	Pan-specific	Second mitochondria-derived activator of caspase	0.21	0.28
SMAD1/5/9	S463+S465/S463+S465/S465+S467	Mothers against decapentaplegic homologs 1/5/9	0.96	0.14
SMAD2	S465+S467	Mothers against decapentaplegic homolog 2	0.58	0.10
SMAD2/3	Pan-specific	SMA- and mothers against decapentaplegic homolog 2/3	0.70	-0.03
SMC1	S957	Structural maintenance of chromosomes protein 1A	0.55	0.31

SOCS2	Pan-specific	Suppressor of cytokine signaling 2	0.94	1.99
SOCS4	Pan-specific	Suppressor of cytokine signalling 4 (SOCS7)	0.81	-0.39
SOD (Cu/Zn)	Pan-specific	Superoxide dismutase 1	0.40	0.34
SOD (Mn)	Pan-specific	Superoxide dismutase [Mn], mitochondrial [Precursor]	0.29	0.84
SODD	Pan-specific	Silencer of death domains (Bcl2 associated athanogene 4 (BAG4))	-0.53	-0.19
SOX9	S181	SRY (sex determining region Y)-box 9 (campomelic dysplasia, autosomal sex-reversal)	-0.22	0.14
SPHK1	Pan-specific	Sphingosine kinase 1	0.41	-0.49
SPHK2	Pan-specific	Sphingosine kinase 2	-0.05	-0.67
Src	Pan-specific	Src proto-oncogene-encoded protein-tyrosine kinase	-0.07	0.00
Src	Pan-specific	Src proto-oncogene-encoded protein-tyrosine kinase	-0.21	0.18
Src	Pan-specific	Src proto-oncogene-encoded protein-tyrosine kinase	-1.41	-0.12
Src	Pan-specific	Src proto-oncogene-encoded protein-tyrosine kinase	1.50	-1.28
Src	Y418	Src proto-oncogene-encoded protein-tyrosine kinase	-0.38	-0.31
Src	Y529	Src proto-oncogene-encoded protein-tyrosine kinase	-0.21	-0.20
STAT1a/b	S727	Signal transducer and activator of transcription 1 alpha/beta	-0.13	-0.31
STAT1a/b	Y701	Signal transducer and activator of transcription 1 alpha/beta	-0.15	-0.28
STAT1a/b	Pan-specific	Signal transducer and activator of transcription 1 alpha/beta	0.77	0.00
STAT1a/b	Pan-specific	Signal transducer and activator of transcription 1 alpha/beta	-0.46	-0.49
STAT1a	Pan-specific	Signal transducer and activator of transcription 1 alpha	0.30	-0.61
STAT2	Pan-specific	Signal transducer and activator of transcription 2	0.35	-0.19
STAT2	Y690	Signal transducer and activator of transcription 2	-0.13	-0.65
STAT3	Pan-specific	Signal transducer and activator of transcription 3	0.30	0.80
STAT3	Pan-specific	Signal transducer and activator of transcription 3	-0.73	-0.51
STAT3	S727	Signal transducer and activator of transcription 3	0.20	-0.09
STAT3	Y705	Signal transducer and activator of transcription 3	-1.09	0.10
STAT4	Pan-specific	Signal transducer and activator of transcription 4	0.35	-0.39
STAT5A	Pan-specific	Signal transducer and activator of transcription 5A	0.66	0.23
STAT5A	Y694	Signal transducer and activator of transcription 5A	-0.37	0.29
STAT5B	Pan-specific	Signal transducer and activator of transcription 5B	0.91	-1.78
STAT6	Pan-specific	Signal transducer and activator of transcription 6	1.07	0.01
STI1	Pan-specific	Stress induced phosphoprotein 1 (Hsc70/Hsp90 organizing protein (Hop))	0.13	-0.37
STK33	Pan-	FLJ35932 protein-serine kinase	0.60	1.58

	specific			
Striatin	Pan-specific	Striatin	0.11	0.09
Syk	Pan-specific	Spleen protein-tyrosine kinase	0.39	-0.10
Synapsin 1	S9	Synapsin 1 isoform Ia	0.25	0.61
Synapsin 1	S603	Synapsin 1 isoform Ia	-0.23	-1.08
TAK1	Pan-specific	TGF-beta-activated protein-serine kinase 1	0.12	0.90
TAK1	Pan-specific	TGF-beta-activated protein-serine kinase 1	0.03	0.06
TAK1	Pan-specific	TGF-beta-activated protein-serine kinase 1	-0.23	-0.52
TAK1	Pan-specific	TGF-beta-activated protein-serine kinase 1	-0.36	0.58
TAK1	Pan-specific	TGF-beta-activated protein-serine kinase 1	1.15	0.72
Tau	S515	Microtubule-associated protein tau	0.21	-0.15
Tau	S515+S518	Microtubule-associated protein tau	0.02	0.02
Tau	S712	Microtubule-associated protein tau	1.02	-0.20
Tau	S712	Microtubule-associated protein tau	0.06	-0.65
Tau	S716	Microtubule-associated protein tau	-1.03	1.09
Tau	S720	Microtubule-associated protein tau	-0.02	-0.30
Tau	S518	Microtubule-associated protein tau	0.32	0.34
Tau	S738	Microtubule-associated protein tau	0.10	-0.27
Tau	T547	Microtubule-associated protein tau	1.01	0.52
TBK1	Pan-specific	Serine/threonine-protein kinase TBK1	-0.23	0.66
TBK1	Pan-specific	Serine/threonine-protein kinase TBK1	-0.21	2.23
TEK (TIE2)	Pan-specific	Angiopoietin-1 receptor-tyrosine kinase	-0.32	-0.14
Tik1	Pan-specific	Tousled-like protein-serine kinase 1	0.06	0.02
TPIPb	Pan-specific	Phosphatidylinositol-3,4,5-trisphosphate 3-phosphatase TPTP2	-0.55	-0.13
TRADD	Pan-specific	Tumor necrosis factor receptor type 1 associated DEATH domain protein	0.08	-0.23
Trail	Pan-specific	Tumor necrosis factor-related apoptosis-inducing ligand	-0.25	-0.48
TrkA	Pan-specific	Nerve growth factor (NGF) receptor-tyrosine kinase	-0.05	-0.16
TrkB	Pan-specific	BDNF/NT3/4/5 receptor-tyrosine kinase	0.09	-1.35
TTK	Pan-specific	Dual specificity protein kinase	-0.44	0.25
Tyk2	Pan-specific	Protein-tyrosine kinase 2 (Jak-related)	-0.43	-1.34
Tyk2	Pan-specific	Protein-tyrosine kinase 2 (Jak-related)	-9.07	1.69
Tyro10 (DDR2)	Pan-specific	Neurotrophic receptor-tyrosine kinase of discoidin domain receptor family, member 2 precursor	-0.63	-0.37

Tyro10 (DDR2)	Pan-specific	Neurotrophic receptor-tyrosine kinase of discoidin domain receptor family, member 2 precursor	-0.05	0.07
Tyrosine Hydroxylase	S71	Tyrosine hydroxylase isoform a	-0.08	0.29
Tyrosine Hydroxylase	S19	Tyrosine hydroxylase isoform a	-0.16	0.11
Ubiquitin	Pan-specific	Ubiquitin	-0.24	0.17
VEGFR2 (KDR)	Y1054	Vascular endothelial growth factor receptor-tyrosine kinase 2 (Flk1)	-0.58	-0.33
VEGFR2 (KDR)	Y1214	Vascular endothelial growth factor receptor-tyrosine kinase 2 (Flk1)	0.05	0.31
VHR	Pan-specific	Dual specificity protein phosphatase 3	-0.11	-0.14
Vimentin	S33	Vimentin	-0.43	0.28
Vrk1	Pan-specific	Vaccinia related protein-serine kinase 1	0.06	0.40
Wee1	Pan-specific	Wee1 protein-tyrosine kinase	-1.04	-0.50
WIP1	Pan-specific	Protein phosphatase 1D	-0.85	-0.09
Yes	Pan-specific	Yamaguchi sarcoma proto-oncogene-encoded tyrosine kinase	-2.01	0.10
Yes	Pan-specific	Yamaguchi sarcoma proto-oncogene-encoded tyrosine kinase	-0.25	-0.32
YSK1	Pan-specific	Serine/threonine-protein kinase 25	-0.10	-0.67
ZAP70	Pan-specific	Zeta-chain (TCR) associated protein-tyrosine kinase, 70 kDa	-0.29	-0.35
ZAP70	Pan-specific	Zeta-chain (TCR) associated protein-tyrosine kinase, 70 kDa	-0.21	1.04
ZAP70	Y292	Zeta-chain (TCR) associated protein-tyrosine kinase, 70 kDa	0.04	-0.13
ZAP70	Y315+Y319	Zeta-chain (TCR) associated protein-tyrosine kinase, 70 kDa	-0.13	-0.43
ZAP70/Syk	Y319/Y352	Zeta-chain (TCR) associated protein-tyrosine kinase, 70 kDa/Spleen protein-tyrosine kinase	0.77	0.15
ZIPK	Pan-specific	ZIP kinase (death associated protein-serine kinase 3 (DAPK3))	-1.20	0.03
ZIPK	Pan-specific	ZIP kinase (death associated protein-serine kinase 3 (DAPK3))	0.19	-0.21

7.4 Bioanalyser Results

Table 7.2- RNA Integrity Numbers (RIN) following Bioanalyser analysis of RNA extracted from unstimulated and OPG-stimulated HPA-SMC lysates.

3 pooled samples were used for each subarray of the Agilent RNA microarray.

Subarray Sample (pooled)	RIN
hPASMCMC No Stim hPASMCMC No Stim hPASMCMC No Stim	8.90
hPASMCMC No Stim hPASMCMC No Stim hPASMCMC No Stim	8.90
hPASMCMC No Stim hPASMCMC No Stim hPASMCMC No Stim	8.80
hPASMCMC OPG hPASMCMC OPG hPASMCMC OPG	9.20
hPASMCMC OPG hPASMCMC OPG hPASMCMC OPG	9.40
hPASMCMC OPG hPASMCMC OPG hPASMCMC OPG	9.30

7.5 PAH-associated genes

Table 7.3 - List of PAH-associated genes used to focus the results of the RNA microarray in Chapter 4.

Name	Gene	References
Apelin	APLN	(Alastalo et al. 2011; Jongmin Kim et al. 2013)
Caveolin 1	CAV1	(Achcar et al. 2006)
Activin A Receptor type II-like 1	ACVRL1	(Richter et al. 2004)
Arachidonate 5-lipoxygenase	ALOX5	(Song et al. 2008)
Angiopoietin-1	ANGPT1	(Kugathasan et al. 2005)
Angiopoietin-2	ANGPT2	(Gill & Brindle 2005)
Angiopoietin-3	ANGPT3	(Gill & Brindle 2005)
Angiopoietin-4	ANGPT4	(Gill & Brindle 2005)
Apelin Receptor	APLNR	(Alastalo et al. 2011; Jongmin Kim et al. 2013)
Apolipoprotein E	APOE	(Hansmann et al. 2008)
Rho Guanine Nucleotide Exchange Factor 12	ARHGEF12	(McMurtry et al. 2010)
B-cell Lymphoma 2	BCL2	(Archer et al. 2010)
Bone Morphogenetic Protein-10	BMP10	(Archer et al. 2010)

Bone Morphogenetic Protein-2	BMP2	(Humbert et al. 2004; Archer et al. 2010)
Bone Morphogenetic Protein-4	BMP4	(Humbert et al. 2004; Archer et al. 2010)
Bone Morphogenetic Protein-6	BMP6	(Archer et al. 2010)
Bone Morphogenetic Protein-7	BMP7	(Archer et al. 2010)
Bone Morphogenetic Protein-9	BMP9	(Archer et al. 2010)
Bone Morphogenetic Protein Receptor, type IA	BMPR1A	(Richter et al. 2004)
Bone Morphogenetic Protein Receptor, type 1B	BMPR1B	(Richter et al. 2004; Simonneau et al. 2009)
Bone Morphogenetic Protein Receptor, type II	BMPR2	(Deng et al. 2000; Perkett et al. 1990; Machado et al. 2001)
CACNA1C calcium channel, voltage-dependent, L type, alpha 1C subunit	CACNA1c	(Sitbon et al. 2005)
Chemokine (C-C motif) Ligand 2	CCL2	(Ikeda et al. 2002)
Chemokine (C-C motif) Ligand 3	CCL3	(Hassoun et al. 2009)
Chemokine (C-C motif) Ligand 5 (RANTES)	CCL5	(Dorfmueller et al. 2002)
Cyclin-Dependent Kinase Inhibitor-1B	CDKN1B	(Yu et al. 2005)
Cofilin-1 (non-muscle)	CFL1	(Foletta et al. 2003)
Cofilin-2 (muscle)	CFL2	(Foletta et al. 2003)

Chemokine (C-X3-C motif) Ligand 1	CX3CL1	(Perros, Dorfmueller, Souza, Durand-Gasselín, Godot, et al. 2007)
Chemokine (C-X3-C motif) Receptor 1	CX3CR1	(Perros, Dorfmueller, Souza, Durand-Gasselín, Godot, et al. 2007)
Stromal Cell Derived Factor -1	CXCL12	(Nemenoff et al. 2008)
Dynein, Light Chain, Tctex-type 1 (TCTEX)	DYNLT1	(Machado et al. 2003)
Endothelin-1	EDN1	(Stelzner et al. 1992)
Endothelin-2	EDN2	(Stelzner et al. 1992)
Endothelin-3	EDN3	(Stelzner et al. 1992)
Endothelin Receptor A	EDNRA	(Trow & Taichman 2009)
Epidermal Growth Factor	EGF	(Dahal et al. 2010)
Epidermal Growth Factor Receptor	EGFR	(Dahal et al. 2010)
Endothelin Receptor B	ENDRB	(Trow & Taichman 2009)
Endoglin	ENG	(Simonneau et al. 2009; Chaouat et al. 2004)
HIF-2alpha	EPAS1	(Brusselmans et al. 2003)
FK506 binding protein 12	FKBP12	(Spiekerkoetter et al. 2013)
FK506 binding protein 1A	FKBP1A	(Kwapiszewska et al. 2005)

FK506 binding protein 1B	FKBP1B	(Spiekerkoetter et al. 2013)
FK506 binding protein 2	FKBP2	(Spiekerkoetter et al. 2013)
Guanosine triphosphate cyclohydrolyase 1	GCH1	(Fagan et al. 2000)
Guanine Nucleotide Binding Protein (G protein), beta Polypeptide 2-Like 1 (RACK1)	GNB2L1	(Zakrzewicz et al. 2007)
Gremlin	GREM1	(Cahill et al. 2012)
Soluble Guanylate Cyclase 1, alpha 2 subunit	GUCY1A2	(Schermuly et al. 2008)
Soluble Guanylate Cyclase 1, alpha 3 subunit	GUCY1A3	(Schermuly et al. 2008)
Soluble Guanylate Cyclase 1, beta 2 subunit	GUCY1B2	(Schermuly et al. 2008)
Soluble Guanylate Cyclase 1, beta 3 subunit	GUCY1B3	(Schermuly et al. 2008)
Hepatitis C Virus	HCV	(Cool et al. 2011)
Human Herpes Virus-8	HHV8	(Cool et al. 2011)
HIF-1alpha	HIF1A	(Fijalkowska et al. 2010)
Major Histocompatibility Complex, class I, B Major	HLA-B	(Johnson et al. 2008)
Histocompatibility Complex, class II, DRβ5	HLA-DRB5	(Johnson et al. 2008)
3-Hydroxy-3-Methylglutaryl-Coa Reductase	HMGCR	(Girgis et al. 2007)

Heme Oxygenase (decycling) 1	HMOX1	(Achcar et al. 2006)
Serotonin Receptor 1B	HTR1B	(Keegan et al. 2001)
Serotonin Receptor 2B	HTR2B	(Launay et al. 2002)
Intracellular Adhesion Molecule 1	ICAM1	(Pendergrass et al. 2010)
Interleukin-13	IL13	(Hecker et al. 2010)
Interleukin-18	IL18	(Soon et al. 2010)
Interleukin-1α	IL1A	(Beasley & Cooper 1999)
Interleukin-1β ⁵⁶	IL1B	(Itoh et al. 2003)
Interleukin-6	IL6	(Furuya et al. 2010)
Potassium Voltage-Gated Channel, Shaker-related Subfamily, member 2 (Kv1.5)	KCNA5	(Bonnet et al. 2006)
Kv Channel Interacting Protein 2	KCNIP2	(Archer et al. 2010)
Potassium Channel, Subfamily K, Member 3	KCNK3	(Ma et al. 2013)
Kinase Insert Domain Receptor	KDR	(Mata-Greenwood et al. 2003)
Microtubule-associated protein-1 light chain-3B	LC3B	(Lee et al. 2011)
LIM motif containing Protein Kinase 1	LIMK1	(Foletta et al. 2003)

PTGIR Low Density Lipoprotein Receptor-related Protein 1	LRP1	(Hansmann et al. 2008)
Leukotriene B4	LTB4	(Tian et al. 2013)
Matrix Metallopeptidase 1	MMP1	(Hassoun 2005)
Matrix Metallopeptidase 2	MMP2	(Hassoun 2005)
Matrix Metallopeptidase 3	MMP3	(Hassoun 2005)
Matrix Metallopeptidase 9	MMP9	(Hassoun 2005)
Negative Regulatory Factor (HIV)	Nef	(Cool et al. 2011)
Nuclear Factor of Activated T-cells, Cytoplasmic, Calcineurin-Dependent 2	NFATC2	(Bonnet et al. 2006)
Nuclear Factor of Activated T-cells, Cytoplasmic, Calcineurin-Dependent 3	NFATc3	(de Frutos et al. 2007)
Nuclear factor-kappa B	NFKB	(Sawada et al. 2007)
Nitric Oxide Synthase 1	NOS1	(Giaid & Saleh 1995)
Nitric Oxide Synthase 2	NOS2	(Kawaguchi et al. 2006)
Nitric Oxide Synthase 3	NOS3	(Giaid & Saleh 1995)
Osteopontin	OPN	(Lorenzen et al. 2011)
Phosphodiesterase 1A	PDE1A	(Schermuly et al. 2007)

Phosphodiesterase 1C	PDE1C	(Schermuly et al. 2007)
Phosphodiesterase 3A	PDE3A	(Murray et al. 2002)
Phosphodiesterase 5A	PDE5A	(Murray et al. 2002)
Platelet-derived Growth Factor alpha	PDGFA	(Grimminger & Schermuly 2010)
Platelet-derived Growth Factor beta	PDGFB	(Grimminger & Schermuly 2010)
Platelet-derived Growth Factor Receptor, alpha	PDGFRA	(Grimminger & Schermuly 2010)
Platelet-derived Growth Factor Receptor, beta	PDGFRB	(Grimminger & Schermuly 2010)
Pyruvate Dehydrogenate Kinase 1	PDK1	(Archer et al. 2010)
Pyruvate Dehydrogenate Kinase 2	PDK2	(Archer et al. 2010)
Pyruvate Dehydrogenate Kinase 3	PDK3	(Archer et al. 2010)
Pyruvate Dehydrogenate Kinase 4	PDK4	(Archer et al. 2010)
Peroxisome Proliferator-activated Receptor-γ	PPARG	(Hansmann et al. 2008; Sutliff et al. 2010)
Prostacyclin Receptor	PRGIR	(Christman et al. 1992)
Phosphatase and Tensin Homolog	PTEN	(Nemenoff et al. 2008)
Prostacyclin Synthase	PTGIS	(Christman et al. 1992)

Resistin-like beta	RETNLB	(Angelini et al. 2009)
Ras Homologue Gene Family member A	RHOA	(McMurtry et al. 2010)
Ras Homologue Gene Family member B	RHOB	(McMurtry et al. 2010)
Rho-associated, Coiled-Coil containing Protein Kinase 1	ROCK1	(McMurtry et al. 2010)
Rho-associated, Coiled-Coil containing Protein Kinase 2	ROCK2	(McMurtry et al. 2010)
Selectin P	SELP	(Sakamaki et al. 2000)
Serotonin Transporter 4	SLC6A4	(MacLean 2007)
SMAD 1	SMAD1	(Morrell 2010)
SMAD 2	SMAD2	(Morrell 2010)
SMAD 3	SMAD3	(Morrell 2010)
SMAD 4	SMAD4	(Morrell 2010)
SMAD 5	SMAD5	(Morrell 2010)
SMAD 6	SMAD6	(Morrell 2010)
SMAD 7	SMAD7	(Morrell 2010)
SMAD 8	SMAD8	(Morrell 2010)
SMAD 9	SMAD9	(Morrell 2010)
SMAD specific E3 ubiquitin protein ligase 1	SMURF1	

		(Murakami et al. 2010)
Superoxide Dismutase 2	SOD2	(Archer et al. 2010)
Src	SRC	(Tuder et al. 2001)
Signal Transducer and Activator of Transcription	STAT1	(Cool et al. 2011)
Trans-activator of Transcription (HIV)	Tat	(Cool et al. 2011)
Thromboxane A2 Receptor	TBXA2R	(Christman et al. 1992)
Endothelium-Specific Receptor Tyrosine Kinase, type 2	TEK/TIE2	(Yamamoto et al. 2008)
Transforming Growth Factor-β, type 1	TGFB1	(Deng et al. 2000; Perkett et al. 1990; Machado et al. 2001)
Transforming Growth Factor-β, induced	TGFBI	(Richter et al. 2004)
Transforming Growth Factor-β Receptor type 1	TGFBR1	(Deng et al. 2000; Perkett et al. 1990; Machado et al. 2001)
Transforming Growth Factor-β Receptor type 2	TGFBR2	(Perkett et al. 1990)
Tenascin-C	TNC	(Jones et al. 1997)
Tumor necrosis factor receptor superfamily, member 11A	TNFRSF11A	(Lawrie et al. 2008)
Tumor necrosis factor receptor superfamily, member 11B	TNFRSF11B	(Lawrie et al. 2008)
Tumor necrosis factor (ligand) superfamily, member 10	TNFSF10	(Hameed et al. 2012)

Tumor necrosis factor superfamily, member 11	TNFSF11	(Lawrie et al. 2008)
Transient Receptor Potential Cation Channel, Subfamily C, member 1	TRPC1	(Zhang et al. 2007)
Transient Receptor Potential Cation Channel, Subfamily C, member 3	TRPC3	(Zhang et al. 2007)
Transient Receptor Potential Cation Channel, Subfamily C, member 6	TRPC6	(Hamid & Newman 2009)
Vascular Cell Adhesion Molecule 1	VCAM1	(Pendergrass et al. 2010)
Vascular Endothelial Growth Factor A	VEGFA	(Schermuly et al. 2008; Tuder et al. 2001; Mata-Greenwood et al. 2003)
Von Hippel Lindau	VHL	(Hickey et al. 2010)
Vasoactive Intestinal Peptide	VIP	(Said 2008)
Vasoactive Intestinal Peptide Receptor 1	VPAC1	(Said 2008)
Vasoactive Intestinal Peptide Receptor 2	VPAC2	(Said 2008)
Integrin alphaVbeta3 (Vitronectin Receptor)	VTNR	(Hassoun 2005)
X-linked Inhibitor of Apoptosis	XIAP	(Liu et al. 2009)

8. BIBLIOGRAPHY

- Achcar, R.O.D. et al., 2006. Loss of caveolin and heme oxygenase expression in severe pulmonary hypertension. *Chest*, 129(3), pp.696–705. Available at: <http://www.ncbi.nlm.nih.gov/pubmed/16537870>.
- Aggarwal, B.B. et al., 1995. Fas antigen signals proliferation of normal human diploid fibroblast and its mechanism is different from tumor necrosis factor receptor. *FEBS letters*, 364(1), pp.5–8. Available at: <http://www.ncbi.nlm.nih.gov/pubmed/7538467>.
- Alastalo, T.-P. et al., 2011. Disruption of PPAR γ / β -catenin-mediated regulation of apelin impairs BMP-induced mouse and human pulmonary arterial EC survival. *The Journal of clinical investigation*, 121(9), pp.3735–46. Available at: <http://www.pubmedcentral.nih.gov/articlerender.fcgi?artid=3163943&tool=pmcentrez&rendertype=abstract> [Accessed October 10, 2014].
- Alderson, M.R. et al., 1993. Fas transduces activation signals in normal human T lymphocytes. *The Journal of experimental medicine*, 178(6), pp.2231–5. Available at: <http://www.pubmedcentral.nih.gov/articlerender.fcgi?artid=2191272&tool=pmcentrez&rendertype=abstract> [Accessed July 28, 2014].
- Angelini, D.J. et al., 2009. Resistin-like molecule-beta in scleroderma-associated pulmonary hypertension. *American journal of respiratory cell and molecular biology*, 41(5), pp.553–61. Available at: <http://www.pubmedcentral.nih.gov/articlerender.fcgi?artid=2778162&tool=pmcentrez&rendertype=abstract> [Accessed October 10, 2014].
- Archer, S.L., Weir, E.K. & Wilkins, M.R., 2010. Basic science of pulmonary arterial hypertension for clinicians: new concepts and experimental therapies. *Circulation*, 121(18), pp.2045–66. Available at: <http://www.pubmedcentral.nih.gov/articlerender.fcgi?artid=2869481&tool=pmcentrez&rendertype=abstract> [Accessed October 10, 2014].
- Arcot, S.S. et al., 1993. Alterations of growth factor transcripts in rat lungs during development of monocrotaline-induced pulmonary hypertension. *Biochemical pharmacology*, 46(6), pp.1086–91. Available at: <http://www.ncbi.nlm.nih.gov/pubmed/8216353>.
- Arcot, S.S. et al., 1995. Basic fibroblast growth factor alterations during development of monocrotaline-induced pulmonary hypertension in rats. *Growth factors (Chur, Switzerland)*, 12(2), pp.121–30. Available at: <http://www.ncbi.nlm.nih.gov/pubmed/8679246> [Accessed September 22, 2014].
- Arif, A., 2012. Extraneuronal activities and regulatory mechanisms of the atypical cyclin-dependent kinase Cdk5. *Biochemical pharmacology*, 84(8), pp.985–93.

- Arita, Y. et al., 2010. The efficacy of tocilizumab in a patient with pulmonary arterial hypertension associated with Castleman's disease. *Heart and vessels*, 25(5), pp.444–7. Available at: <http://www.ncbi.nlm.nih.gov/pubmed/20676969> [Accessed August 28, 2014].
- Ashkenazi, A. & Dixit, V.M., 1998. Death Receptors: Signaling and Modulation. *Science*, 281(5381), pp.1305–1308. Available at: <http://www.sciencemag.org/cgi/doi/10.1126/science.281.5381.1305> [Accessed January 25, 2014].
- Atkinson, C. et al., 2002. Primary Pulmonary Hypertension Is Associated With Reduced Pulmonary Vascular Expression of Type II Bone Morphogenetic Protein Receptor. *Circulation*, 105(14), pp.1672–1678. Available at: <http://circ.ahajournals.org/cgi/doi/10.1161/01.CIR.0000012754.72951.3D> [Accessed June 9, 2014].
- Austin, E.D. et al., 2012. Whole exome sequencing to identify a novel gene (caveolin-1) associated with human pulmonary arterial hypertension. *Circulation. Cardiovascular genetics*, 5(3), pp.336–43. Available at: <http://www.pubmedcentral.nih.gov/articlerender.fcgi?artid=3380156&tool=pmcentrez&rendertype=abstract> [Accessed August 7, 2014].
- Avignon, A. et al., 2005. Osteoprotegerin is associated with silent coronary artery disease in high-risk but asymptomatic type 2 diabetic patients. *Diabetes care*, 28(9), pp.2176–80. Available at: <http://www.ncbi.nlm.nih.gov/pubmed/16123486> [Accessed August 11, 2014].
- Bauer, P.M. et al., 2012. Activated CD47 promotes pulmonary arterial hypertension through targeting caveolin-1. *Cardiovascular research*, 93(4), pp.682–93. Available at: <http://www.pubmedcentral.nih.gov/articlerender.fcgi?artid=3291089&tool=pmcentrez&rendertype=abstract> [Accessed June 9, 2014].
- Beasley, D. & Cooper, A.L., 1999. Constitutive expression of interleukin-1alpha precursor promotes human vascular smooth muscle cell proliferation. *The American journal of physiology*, 276(3 Pt 2), pp.H901–12. Available at: <http://www.ncbi.nlm.nih.gov/pubmed/10070073> [Accessed October 10, 2014].
- Benisty, J.I. et al., 2004. Elevated basic fibroblast growth factor levels in patients with pulmonary arterial hypertension. *Chest*, 126(4), pp.1255–61. Available at: <http://www.ncbi.nlm.nih.gov/pubmed/15486390> [Accessed September 22, 2014].
- Bennett, B.J. et al., 2006. Osteoprotegerin inactivation accelerates advanced atherosclerotic lesion progression and calcification in older ApoE^{-/-} mice. *Arteriosclerosis, thrombosis, and vascular biology*, 26(9), pp.2117–24. Available at: <http://www.ncbi.nlm.nih.gov/pubmed/16840715> [Accessed August 11, 2014].
- Benslimane-Ahmim, Z. et al., 2011. Osteoprotegerin, a new actor in vasculogenesis, stimulates endothelial colony-forming cells properties. *Journal of thrombosis and*

- haemostasis* : *JTH*, 9(4), pp.834–43. Available at:
<http://www.ncbi.nlm.nih.gov/pubmed/21255246> [Accessed February 12, 2014].
- Bhargava, A. et al., 1999. Monocrotaline induces interleukin-6 mRNA expression in rat lungs. *Heart disease (Hagerstown, Md.)*, 1(3), pp.126–32. Available at:
<http://www.ncbi.nlm.nih.gov/pubmed/11720614> [Accessed August 13, 2014].
- Bonnet, S. et al., 2006. An abnormal mitochondrial-hypoxia inducible factor-1alpha-Kv channel pathway disrupts oxygen sensing and triggers pulmonary arterial hypertension in fawn hooded rats: similarities to human pulmonary arterial hypertension. *Circulation*, 113(22), pp.2630–41. Available at:
<http://www.ncbi.nlm.nih.gov/pubmed/16735674> [Accessed October 10, 2014].
- Boraschi, D. & Tagliabue, A., 2013. The interleukin-1 receptor family. *Seminars in Immunology*, pp.394–407.
- Boron, W.F., 2005. Organization of the Respiratory System. In W. F. Boron et al., eds. *Medical Physiology*. Philadelphia: Elsevier Saunders, pp. 591–734.
- Bosman, M.C.J. et al., 2014. Decreased affinity of recombinant human tumor necrosis factor-related apoptosis-inducing ligand (rhTRAIL) D269H/E195R to osteoprotegerin (OPG) overcomes TRAIL resistance mediated by the bone microenvironment. *The Journal of biological chemistry*, 289(2), pp.1071–8. Available at: <http://www.ncbi.nlm.nih.gov/pubmed/24280212> [Accessed August 9, 2014].
- Boyce, B.F. & Xing, L., 2007. Biology of RANK, RANKL, and osteoprotegerin. *Arthritis research & therapy*, 9 Suppl 1, p.S1. Available at:
<http://www.pubmedcentral.nih.gov/articlerender.fcgi?artid=1924516&tool=pmcentrez&rendertype=abstract> [Accessed January 23, 2014].
- Brenner, O., 1957. The lungs in heart disease. *The British journal of tuberculosis and diseases of the chest*, 51(3), pp.209–22. Available at:
<http://www.ncbi.nlm.nih.gov/pubmed/13446408> [Accessed July 31, 2014].
- Brinkkoetter, P.T. et al., 2009. Cyclin I activates Cdk5 and regulates expression of Bcl-2 and Bcl-XL in postmitotic mouse cells. , 119(10), pp.3089–3101.
- Brint, E., O’Callaghan, G. & Houston, A., 2013. Life in the Fas lane: differential outcomes of Fas signaling. *Cellular and Molecular Life Sciences*, 70, pp.4085–4099. Available at: <http://www.ncbi.nlm.nih.gov/pubmed/23579628>.
- Brusselmans, K. et al., 2003. Heterozygous deficiency of hypoxia-inducible factor-2alpha protects mice against pulmonary hypertension and right ventricular dysfunction during prolonged hypoxia. *The Journal of clinical investigation*, 111(10), pp.1519–27. Available at:
<http://www.pubmedcentral.nih.gov/articlerender.fcgi?artid=155039&tool=pmcentrez&rendertype=abstract> [Accessed October 10, 2014].

- Bucay, N. et al., 1998. Osteoprotegerin-Deficient Mice Develop Early Onset Osteoporosis and Arterial Calcification. *Genes & development*, 12(9), pp.1260–8. Available at: <http://www.pubmedcentral.nih.gov/articlerender.fcgi?artid=316769&tool=pmcentrez&rendertype=abstract>.
- Budhiraja, R., Tuder, R.M. & Hassoun, P.M., 2004. Endothelial dysfunction in pulmonary hypertension. *Circulation*, 109(2), pp.159–65. Available at: <http://www.ncbi.nlm.nih.gov/pubmed/14734504> [Accessed September 17, 2014].
- Cahill, E. et al., 2012. Gremlin plays a key role in the pathogenesis of pulmonary hypertension. *Circulation*, 125(7), pp.920–30. Available at: <http://www.ncbi.nlm.nih.gov/pubmed/22247494> [Accessed October 10, 2014].
- Callegari, a et al., 2013. Bone marrow- or vessel wall-derived osteoprotegerin is sufficient to reduce atherosclerotic lesion size and vascular calcification. *Arteriosclerosis, thrombosis, and vascular biology*, 33(11), pp.2491–500. Available at: <http://www.ncbi.nlm.nih.gov/pubmed/23990207> [Accessed January 30, 2014].
- Carlomagno, G. et al., 2013. Serum soluble ST2 and interleukin-33 levels in patients with pulmonary arterial hypertension. *International journal of cardiology*, 168(2), pp.1545–7. Available at: <http://www.ncbi.nlm.nih.gov/pubmed/23290950> [Accessed September 1, 2014].
- Carragher, D.M., Rangel-Moreno, J. & Randall, T.D., 2008. Ectopic lymphoid tissues and local immunity. *Seminars in immunology*, 20(1), pp.26–42. Available at: <http://www.pubmedcentral.nih.gov/articlerender.fcgi?artid=2276727&tool=pmcentrez&rendertype=abstract> [Accessed August 29, 2014].
- Chaouat, A. et al., 2004. Endoglin germline mutation in a patient with hereditary haemorrhagic telangiectasia and dexfenfluramine associated pulmonary arterial hypertension. *Thorax*, 59(5), pp.446–8. Available at: <http://www.pubmedcentral.nih.gov/articlerender.fcgi?artid=1746994&tool=pmcentrez&rendertype=abstract> [Accessed October 10, 2014].
- Charette, S.J. et al., 2000. Inhibition of Daxx-mediated apoptosis by heat shock protein 27. *Molecular and cellular biology*, 20(20), pp.7602–12. Available at: <http://www.pubmedcentral.nih.gov/articlerender.fcgi?artid=86317&tool=pmcentrez&rendertype=abstract> [Accessed August 20, 2014].
- Charette, S.J. & Landry, J., 2000. The interaction of HSP27 with Daxx identifies a potential regulatory role of HSP27 in Fas-induced apoptosis. *Annals of the New York Academy of Sciences*, 926, pp.126–31. Available at: <http://www.ncbi.nlm.nih.gov/pubmed/11193028> [Accessed August 22, 2014].
- Chazova, I. et al., 1995. Pulmonary artery adventitial changes and venous involvement in primary pulmonary hypertension. *The American journal of pathology*, 146(2), pp.389–97. Available at:

<http://www.pubmedcentral.nih.gov/articlerender.fcgi?artid=1869854&tool=pmcentrez&rendertype=abstract> [Accessed August 5, 2014].

- Chen, Y.-J. et al., 2013. Clinical and genetic characteristics of Chinese patients with hereditary haemorrhagic telangiectasia-associated pulmonary hypertension. *European journal of clinical investigation*, 43(10), pp.1016–24. Available at: <http://www.ncbi.nlm.nih.gov/pubmed/23919827> [Accessed June 16, 2014].
- Chen, Z. et al., 2010. Autophagy protein microtubule-associated protein 1 light chain-3B (LC3B) activates extrinsic apoptosis during cigarette smoke-induced emphysema. *PNAS*, 107(44), pp.18880–18885.
- Chertov, A.O. et al., 2011. Roles of glucose in photoreceptor survival. *The Journal of biological chemistry*, 286(40), pp.34700–11. Available at: <http://www.pubmedcentral.nih.gov/articlerender.fcgi?artid=3186402&tool=pmcentrez&rendertype=abstract> [Accessed September 30, 2014].
- Cheung, Z.H., Gong, K. & Ip, N.Y., 2008. Cyclin-dependent kinase 5 supports neuronal survival through phosphorylation of Bcl-2. *The Journal of neuroscience : the official journal of the Society for Neuroscience*, 28(19), pp.4872–7. Available at: <http://www.jneurosci.org/content/28/19/4872.abstract> [Accessed July 25, 2014].
- Chokki, M. et al., 2004. Human airway trypsin-like protease increases mucin gene expression in airway epithelial cells. *American journal of respiratory cell and molecular biology*, 30, pp.470–478.
- Christman, B.W. et al., 1992. An imbalance between the excretion of thromboxane and prostacyclin metabolites in pulmonary hypertension. *The New England journal of medicine*, 327(2), pp.70–5. Available at: <http://www.ncbi.nlm.nih.gov/pubmed/1603138> [Accessed August 6, 2014].
- Ciarcia, R. et al., 2012. Imatinib treatment inhibit IL-6, IL-8, NF-KB ... [J Cell Physiol. 2012] - PubMed - NCBI. *Journal of cellular biochemistry*, 227, pp.2798–2803. Available at: <http://www.ncbi.nlm.nih.gov/pubmed/?term=Imatinib+Treatment+Inhibit+IL-6,+IL-8,+NF-KB+and+AP-1+Production+and+Modulate+Intracellular+Calcium+in+CML+Patients> [Accessed September 2, 2014].
- Codogno, P., Mehrpour, M. & Proikas-Cezanne, T., 2012. Canonical and non-canonical autophagy: variations on a common theme of self-eating? *Nature reviews. Molecular cell biology*, 13(1), pp.7–12.
- Collin-Osdoby, P. et al., 2001. Receptor activator of NF-kappa B and osteoprotegerin expression by human microvascular endothelial cells, regulation by inflammatory cytokines, and role in human osteoclastogenesis. *The Journal of biological chemistry*, 276(23), pp.20659–72. Available at: <http://www.ncbi.nlm.nih.gov/pubmed/11274143> [Accessed February 12, 2014].

- Condliffe, R. et al., 2012. Serum osteoprotegerin is increased and predicts survival in idiopathic pulmonary arterial hypertension. *Pulmonary Circulation*, 2, p.21.
- Cool, C.D., Voelkel, N.F. & Bull, T., 2011. Viral infection and pulmonary hypertension: is there an association? *Expert review of respiratory medicine*, 5(2), pp.207–16. Available at: <http://www.ncbi.nlm.nih.gov/pubmed/21510731> [Accessed October 10, 2014].
- Cross, S.S. et al., 2006. Osteoprotegerin (OPG)--a potential new role in the regulation of endothelial cell phenotype and tumour angiogenesis? *International journal of cancer. Journal international du cancer*, 118(8), pp.1901–8. Available at: <http://www.ncbi.nlm.nih.gov/pubmed/16287088> [Accessed February 12, 2014].
- D'Alonzo, G.E. et al., 1991. Survival in patients with primary pulmonary hypertension. Results from a national prospective registry. *Annals of internal medicine*, 115(5), pp.343–9. Available at: <http://www.ncbi.nlm.nih.gov/pubmed/1863023> [Accessed August 4, 2014].
- Dahal, B.K. et al., 2010. Role of epidermal growth factor inhibition in experimental pulmonary hypertension. *American journal of respiratory and critical care medicine*, 181(2), pp.158–67. Available at: <http://www.ncbi.nlm.nih.gov/pubmed/19850946> [Accessed October 10, 2014].
- Das, M. et al., 2008. Hypoxia exposure induces the emergence of fibroblasts lacking replication repressor signals of PKCzeta in the pulmonary artery adventitia. *Cardiovascular research*, 78(3), pp.440–8. Available at: <http://www.ncbi.nlm.nih.gov/pubmed/18218684> [Accessed September 1, 2014].
- Davie, N. et al., 2002. ET A and ET B Receptors Modulate the Proliferation of Human Pulmonary Artery Smooth Muscle Cells. *American Journal of Critical Care Medicine*, 165(27), pp.398–405.
- Davies, R.J. & Morrell, N.W., 2008. Molecular mechanisms of pulmonary arterial hypertension: role of mutations in the bone morphogenetic protein type II receptor. *Chest*, 134(1931-3543 (Electronic)), pp.1271–1277. Available at: <http://www.ncbi.nlm.nih.gov/pubmed/19059957> [Accessed February 12, 2014].
- Dawson, S. et al., 2014. TRAIL Deficient Mice Are Protected from Sugen/Hypoxia Induced Pulmonary Arterial Hypertension. *Diseases*, 2(3), pp.260–273. Available at: <http://www.mdpi.com/2079-9721/2/3/260/html> [Accessed August 9, 2014].
- Deng, Z. et al., 2000. Familial primary pulmonary hypertension (gene PPH1) is caused by mutations in the bone morphogenetic protein receptor-II gene. *American journal of human genetics*, 67(3), pp.737–44. Available at: <http://www.pubmedcentral.nih.gov/articlerender.fcgi?artid=1287532&tool=pmcentrez&rendertype=abstract>.

- Denny, J.B., 2006. Molecular mechanisms, biological actions, and neuropharmacology of the growth-associated protein GAP-43. *Current neuropharmacology*, 4, pp.293–304.
- Van Dijk, M. et al., 2013. Resistance to TRAIL in non-transformed cells is due to multiple redundant pathways. *Cell death & disease*, 4, p.e702. Available at: <http://www.pubmedcentral.nih.gov/articlerender.fcgi?artid=3730397&tool=pmcentrez&rendertype=abstract> [Accessed September 22, 2014].
- Dorfmüller, P. et al., 2002. Chemokine RANTES in Severe Pulmonary.
- Du, L. et al., 2003. Signaling molecules in nonfamilial pulmonary hypertension. *The New England Journal of Medicine*, 348(6), pp.500–509. Available at: <http://www.ncbi.nlm.nih.gov/pubmed/12571257>.
- Eddahibi, S. et al., 2006. Cross talk between endothelial and smooth muscle cells in pulmonary hypertension: critical role for serotonin-induced smooth muscle hyperplasia. *Circulation*, 113(15), pp.1857–64. Available at: <http://www.ncbi.nlm.nih.gov/pubmed/16606791> [Accessed August 13, 2014].
- Eddahibi, S. et al., 2002. Pathobiology of pulmonary arterial hypertension. *European Respiratory Journal*, 20(6), pp.1559–1572. Available at: <http://erj.ersjournals.com/cgi/doi/10.1183/09031936.02.00081302> [Accessed February 12, 2014].
- Elliot, C.A. & Kiely, D.G., 2006. Pulmonary hypertension. *Continuing Education in Anaesthesia, Critical Care & Pain*, 6(1), pp.17–22. Available at: <http://bjarev.oxfordjournals.org/cgi/doi/10.1093/bjaceaccp/mki061> [Accessed January 25, 2014].
- Emery, J.G. et al., 1998. Osteoprotegerin is a receptor for the cytotoxic ligand TRAIL. *The Journal of biological chemistry*, 273(23), pp.14363–7. Available at: <http://www.ncbi.nlm.nih.gov/pubmed/9603945>.
- Eyries, M. et al., 2012. ACVRL1 germinal mosaic with two mutant alleles in hereditary hemorrhagic telangiectasia associated with pulmonary arterial hypertension. *Clinical genetics*, 82(2), pp.173–9. Available at: <http://www.ncbi.nlm.nih.gov/pubmed/21651515> [Accessed June 9, 2014].
- Fagan, K.A., McMurtry, I. & Rodman, D.M., 2000. Nitric oxide synthase in pulmonary hypertension: lessons from knockout mice. *Physiological research / Academia Scientiarum Bohemoslovaca*, 49(5), pp.539–48. Available at: <http://www.ncbi.nlm.nih.gov/pubmed/11191358> [Accessed October 10, 2014].
- Farber, H.W. & Loscalzo, J., 2007. Pulmonary Arterial Hypertension. *The New England journal of medicine*, 351(16), pp.1655–1665.
- Feinberg, L. et al., 1999. Soluble immune mediators in POEMS syndrome with pulmonary hypertension: case report and review of the literature. *Critical reviews*

in oncogenesis, 10(4), pp.293–302. Available at:
<http://www.ncbi.nlm.nih.gov/pubmed/10654928> [Accessed July 28, 2014].

Fijalkowska, I. et al., 2010. Hypoxia inducible-factor1alpha regulates the metabolic shift of pulmonary hypertensive endothelial cells. *The American journal of pathology*, 176(3), pp.1130–8. Available at:
<http://www.pubmedcentral.nih.gov/articlerender.fcgi?artid=2832136&tool=pmc.ncbi.nlm.nih.gov/articles/PMC2832136/abstract> [Accessed October 10, 2014].

Foletta, V.C. et al., 2003. Direct signaling by the BMP type II receptor via the cytoskeletal regulator LIMK1. *The Journal of cell biology*, 162(6), pp.1089–98. Available at:
<http://www.pubmedcentral.nih.gov/articlerender.fcgi?artid=2172847&tool=pmc.ncbi.nlm.nih.gov/articles/PMC2172847/abstract> [Accessed July 15, 2014].

Frid, M.G. et al., 2006. Hypoxia-induced pulmonary vascular remodeling requires recruitment of circulating mesenchymal precursors of a monocyte/macrophage lineage. *The American journal of pathology*, 168(2), pp.659–69. Available at:
<http://www.pubmedcentral.nih.gov/articlerender.fcgi?artid=1606508&tool=pmc.ncbi.nlm.nih.gov/articles/PMC1606508/abstract> [Accessed August 21, 2014].

Frid, M.G. et al., 1997. Smooth muscle cells isolated from discrete compartments of the mature vascular media exhibit unique phenotypes and distinct growth capabilities. *Circulation research*, 81(6), pp.940–52. Available at:
<http://www.ncbi.nlm.nih.gov/pubmed/9400374> [Accessed August 6, 2014].

Frid, M.G., Moiseeva, E.P. & Stenmark, K.R., 1994. Multiple phenotypically distinct smooth muscle cell populations exist in the adult and developing bovine pulmonary arterial media in vivo. *Circulation Research*, 75(4), pp.669–681. Available at:
http://circres.ahajournals.org/content/75/4/669.abstract?ijkey=2f4f888175e6ea75c471c9d50e4afedc1266be0&keytype=tf_ipsecsha [Accessed August 6, 2014].

Fritze, L.M., Reilly, C.F. & Rosenberg, R.D., 1985. An antiproliferative heparan sulfate species produced by postconfluent smooth muscle cells. *The Journal of cell biology*, 100(4), pp.1041–9. Available at:
<http://www.pubmedcentral.nih.gov/articlerender.fcgi?artid=2113750&tool=pmc.ncbi.nlm.nih.gov/articles/PMC2113750/abstract> [Accessed August 6, 2014].

De Frutos, S. et al., 2007. NFATc3 mediates chronic hypoxia-induced pulmonary arterial remodeling with alpha-actin up-regulation. *The Journal of biological chemistry*, 282(20), pp.15081–9. Available at:
<http://www.pubmedcentral.nih.gov/articlerender.fcgi?artid=2754407&tool=pmc.ncbi.nlm.nih.gov/articles/PMC2754407/abstract> [Accessed October 10, 2014].

Fujiwara, M. et al., 2008. Implications of mutations of activin receptor-like kinase 1 gene (ALK1) in addition to bone morphogenetic protein receptor II gene (BMP2) in children with pulmonary arterial hypertension. *Circulation journal : official journal of the Japanese Circulation Society*, 72(1), pp.127–33. Available at: <http://www.ncbi.nlm.nih.gov/pubmed/18159113> [Accessed August 7, 2014].

- Furuya, Y., Satoh, T. & Kuwana, M., 2010. Interleukin-6 as a potential therapeutic target for pulmonary arterial hypertension. *International journal of rheumatology*, 2010, p.720305. Available at: <http://www.pubmedcentral.nih.gov/articlerender.fcgi?artid=2958514&tool=pmcentrez&rendertype=abstract> [Accessed October 10, 2014].
- Galiè, N. et al., 2013. Updated treatment algorithm of pulmonary arterial hypertension. *Journal of the American College of Cardiology*, 62(25 Suppl), pp.D60–72. Available at: <http://www.ncbi.nlm.nih.gov/pubmed/24355643> [Accessed January 24, 2014].
- Gao, D. et al., 2011. mTOR drives its own activation via SCF(β TrCP)-dependent degradation of the mTOR inhibitor DEPTOR. *Molecular cell*, 44(2), pp.290–303. Available at: <http://www.pubmedcentral.nih.gov/articlerender.fcgi?artid=3229299&tool=pmcentrez&rendertype=abstract> [Accessed September 17, 2014].
- Geeleher, P. et al., 2011. BioconductorBuntu Users Manual. *BioconductorBuntu Users Manual*, pp.7–34. Available at: <http://www3.it.nuigalway.ie/agolden/bioconductor/version1/handbook.pdf>.
- Geiger, R. et al., 2009. Pulmonary vascular remodeling in congenital heart disease: enhanced expression of heat shock proteins. *Indian journal of biochemistry & biophysics*, 46(6), pp.482–90. Available at: <http://www.ncbi.nlm.nih.gov/pubmed/20361711>.
- Geng, Y.J. et al., 1997. Fas is expressed in human atherosclerotic intima and promotes apoptosis of cytokine-primed human vascular smooth muscle cells. *Arteriosclerosis, thrombosis, and vascular biology*, 17, pp.2200–2208.
- George, P.M. et al., 2014. Evidence for the involvement of type I interferon in pulmonary arterial hypertension. *Circulation research*, 114(4), pp.677–88. Available at: <http://circres.ahajournals.org/content/114/4/677.long> [Accessed July 24, 2014].
- Geraci, M.W., Bull, T.M. & Tuder, R.M., 2010. Genomics of pulmonary arterial hypertension: implications for therapy. *Heart failure clinics*, 6(1), pp.101–14. Available at: <http://www.pubmedcentral.nih.gov/articlerender.fcgi?artid=2786817&tool=pmcentrez&rendertype=abstract> [Accessed September 2, 2014].
- Ghayour-Mobarhan, M., Saber, H. & Ferns, G.A.A., 2012. The potential role of heat shock protein 27 in cardiovascular disease. *Clinica chimica acta; international journal of clinical chemistry*, 413(1-2), pp.15–24. Available at: <http://www.ncbi.nlm.nih.gov/pubmed/21514288> [Accessed September 26, 2014].
- Giaid, A. et al., 1993. Expression of endothelin-1 in the lungs of patients with pulmonary hypertension. *The New England journal of medicine*, 328(24), pp.1732–9. Available at: <http://www.ncbi.nlm.nih.gov/pubmed/8497283> [Accessed August 6, 2014].

- Giaid, A. & Saleh, D., 1995. Reduced expression of endothelial nitric oxide synthase in the lungs of patients with pulmonary hypertension. *The New England journal of medicine*, 333(4), pp.214–21. Available at: <http://www.ncbi.nlm.nih.gov/pubmed/7540722> [Accessed August 6, 2014].
- Gill, K.A. & Brindle, N.P.J., 2005. Angiopoietin-2 stimulates migration of endothelial progenitors and their interaction with endothelium. *Biochemical and biophysical research communications*, 336(2), pp.392–6. Available at: <http://www.ncbi.nlm.nih.gov/pubmed/16129411> [Accessed October 10, 2014].
- Girgis, R.E. et al., 2007. Regression of chronic hypoxic pulmonary hypertension by simvastatin. *American journal of physiology. Lung cellular and molecular physiology*, 292(5), pp.L1105–10. Available at: <http://www.ncbi.nlm.nih.gov/pubmed/17277047> [Accessed October 10, 2014].
- Goel, H.L. & Mercurio, A.M., 2013. VEGF targets the tumour cell. *Nature reviews. Cancer*, 13(12), pp.871–82. Available at: <http://dx.doi.org/10.1038/nrc3627> [Accessed July 22, 2014].
- Gore, B. et al., 2014. Key Role of the Endothelial TGF- β /ALK1/Endoglin Signaling Pathway in Humans and Rodents Pulmonary Hypertension. *PloS one*, 9(6), p.e100310. Available at: <http://www.ncbi.nlm.nih.gov/pubmed/24956016> [Accessed June 26, 2014].
- Greenberg, B., Rhoden, K. & Barnes, P.J., 1987. Relaxant effects of vasoactive intestinal peptide and peptide histidine isoleucine in human and bovine pulmonary arteries. *Blood vessels*, 24(1-2), pp.45–50. Available at: <http://www.ncbi.nlm.nih.gov/pubmed/3567364> [Accessed October 9, 2014].
- Grimminger, F. & Schermuly, R.T., 2010. PDGF receptor and its antagonists: role in treatment of PAH. *Advances in experimental medicine and biology*, 661, pp.435–46. Available at: <http://www.ncbi.nlm.nih.gov/pubmed/20204747> [Accessed October 10, 2014].
- Guignabert, C. et al., 2013. Pathogenesis of pulmonary arterial hypertension: lessons from cancer. *European respiratory review : an official journal of the European Respiratory Society*, 22(130), pp.543–51. Available at: <http://www.ncbi.nlm.nih.gov/pubmed/24293470> [Accessed September 23, 2014].
- Hamann, K.J. et al., 2000. Fas cross-linking induces apoptosis in human airway smooth muscle cells. *American journal of physiology. Lung cellular and molecular physiology*, 278(3), pp.L618–24. Available at: <http://www.ncbi.nlm.nih.gov/pubmed/10710535>.
- Hameed, A.G. et al., 2012. Inhibition of tumor necrosis factor-related apoptosis-inducing ligand (TRAIL) reverses experimental pulmonary hypertension. *The Journal of experimental medicine*, 209(11), pp.1919–35. Available at: <http://www.pubmedcentral.nih.gov/articlerender.fcgi?artid=3478928&tool=pmcentrez&rendertype=abstract> [Accessed February 11, 2014].

- Hamid, R. & Newman, J.H., 2009. Evidence for inflammatory signaling in idiopathic pulmonary artery hypertension: TRPC6 and nuclear factor-kappaB. *Circulation*, 119(17), pp.2297–8. Available at: <http://www.ncbi.nlm.nih.gov/pubmed/19414653> [Accessed October 10, 2014].
- Hansmann, G. et al., 2008. An antiproliferative BMP-2 / PPAR γ / apoE axis in human and murine SMCs and its role in pulmonary hypertension. , 118(5).
- Harrison, R.E. et al., 2003. Molecular and functional analysis identifies ALK-1 as the predominant cause of pulmonary hypertension related to hereditary haemorrhagic telangiectasia. *Journal of medical genetics*, 40(12), pp.865–71. Available at: <http://www.pubmedcentral.nih.gov/articlerender.fcgi?artid=1735342&tool=pmcentrez&rendertype=abstract>.
- Hassoun, P.M., 2005. Deciphering the “matrix” in pulmonary vascular remodelling. *The European respiratory journal*, 25(5), pp.778–9. Available at: <http://www.ncbi.nlm.nih.gov/pubmed/15863631> [Accessed October 10, 2014].
- Hassoun, P.M. et al., 1992. Endothelin 1: mitogenic activity on pulmonary artery smooth muscle cells and release from hypoxic endothelial cells. *Proceedings of the Society for Experimental Biology and Medicine. Society for Experimental Biology and Medicine (New York, N.Y.)*, 199(2), pp.165–70. Available at: <http://www.ncbi.nlm.nih.gov/pubmed/1741408> [Accessed August 6, 2014].
- Hassoun, P.M. et al., 2009. Inflammation, growth factors, and pulmonary vascular remodeling. *Journal of the American College of Cardiology*, 54(1 Suppl), pp.S10–9. Available at: <http://www.ncbi.nlm.nih.gov/pubmed/19555853> [Accessed January 29, 2014].
- Hatano, S., Strasser, T. & Organization, W.H., 1975. Primary pulmonary hypertension : report on a WHO meeting, Geneva, 15-17 October 1973 / edited by Shuichi Hatano and Toma Strasser. Available at: <http://apps.who.int/iris/handle/10665/39094> [Accessed July 31, 2014].
- He, C. & Klionsky, D.J., 2009. Regulation Mechanisms and Signaling Pathways of Autophagy. *NIH Public Access*, (68), pp.67–93.
- Health and Social Care Information Centre, 2013. National Audit of Pulmonary Hypertension, 2013. , pp.1–55. Available at: <http://www.hscic.gov.uk/catalogue/PUB13318/nati-pulm-hype-audi-2013-rep.pdf> [Accessed August 1, 2014].
- Heath, D. & Whitaker, W., 1956. Hypertensive Pulmonary Vascular Disease. *Circulation*, 14(3), pp.323–343. Available at: <http://circ.ahajournals.org/content/14/3/323> [Accessed July 31, 2014].
- Hecker, M. et al., 2010. Dysregulation of the IL-13 receptor system: a novel pathomechanism in pulmonary arterial hypertension. *American journal of respiratory and critical care medicine*, 182(6), pp.805–18. Available at: <http://www.ncbi.nlm.nih.gov/pubmed/20522789> [Accessed October 10, 2014].

- Hervé, P. et al., 1995. Increased plasma serotonin in primary pulmonary hypertension. *The American journal of medicine*, 99(3), pp.249–54. Available at: <http://www.ncbi.nlm.nih.gov/pubmed/7653484>.
- Hickey, M.M. et al., 2010. The von Hippel-Lindau Chuvash mutation promotes pulmonary hypertension and fibrosis in mice. *The Journal of clinical investigation*, 120(3), pp.827–39. Available at: <http://www.pubmedcentral.nih.gov/articlerender.fcgi?artid=2827942&tool=pmcentrez&rendertype=abstract> [Accessed October 10, 2014].
- Hirai, H. et al., 1995. Novel INK4 proteins, p19 and p18, are specific inhibitors of the cyclin D-dependent kinases CDK4 and CDK6. *Molecular and cellular biology*, 15(5), pp.2672–81. Available at: <http://www.pubmedcentral.nih.gov/articlerender.fcgi?artid=230497&tool=pmcentrez&rendertype=abstract> [Accessed July 16, 2014].
- Hirose, S. et al., 2000. Expression of vascular endothelial growth factor and its receptors correlates closely with formation of the plexiform lesion in human pulmonary hypertension. *Pathology international*, 50(6), pp.472–9. Available at: <http://www.ncbi.nlm.nih.gov/pubmed/10886723>.
- Hooper, M.M., Bogaard, H.J., et al., 2013. Definitions and diagnosis of pulmonary hypertension. *Journal of the American College of Cardiology*, 62(25 Suppl), pp.D42–50. Available at: <http://www.ncbi.nlm.nih.gov/pubmed/24355641> [Accessed January 23, 2014].
- Hooper, M.M., Barst, R.J., et al., 2013. Imatinib mesylate as add-on therapy for pulmonary arterial hypertension: results of the randomized IMPRES study. *Circulation*, 127(10), pp.1128–38. Available at: <http://www.ncbi.nlm.nih.gov/pubmed/23403476> [Accessed August 18, 2014].
- Hofbauer, L.C. & Schoppet, M., 2004. Clinical Implications of the Osteoprotegerin / RANKL / RANK System for Bone. *The journal of the American Medical Association*, 292(4), pp.490–495.
- Hosbond, S.E. et al., 2012. Osteoprotegerin as a marker of atherosclerosis: a systematic update. *Scandinavian cardiovascular journal : SCJ*, 46(4), pp.203–11. Available at: <http://www.ncbi.nlm.nih.gov/pubmed/22506827> [Accessed August 12, 2014].
- Hsu, H. et al., 1999. Tumor necrosis factor receptor family member RANK mediates osteoclast differentiation and activation induced by osteoprotegerin ligand. *Proceedings of the National Academy of Sciences*, 96(7), pp.3540–3545. Available at: <http://www.pnas.org/content/96/7/3540.long> [Accessed July 23, 2014].
- Humbert, M. et al., 2004. Cellular and molecular pathobiology of pulmonary arterial hypertension. *Journal of the American College of Cardiology*, 43(12 Suppl S), p.13S–24S. Available at:

<http://www.sciencedirect.com/science/article/pii/S0735109704004383> [Accessed August 5, 2014].

- Humbert, M. et al., 2008. Endothelial cell dysfunction and cross talk between endothelium and smooth muscle cells in pulmonary arterial hypertension. *Vascular pharmacology*, 49(4-6), pp.113–8. Available at: <http://www.ncbi.nlm.nih.gov/pubmed/18606248> [Accessed February 12, 2014].
- Humbert, M. et al., 1995. Increased interleukin-1 and interleukin-6 serum concentrations in severe primary pulmonary hypertension. *American journal of respiratory and critical care medicine*, 151, pp.1628–1631.
- Hurdman, J. et al., 2012. ASPIRE registry: assessing the Spectrum of Pulmonary hypertension Identified at a REferral centre. *The European respiratory journal*, 39(4), pp.945–55. Available at: <http://www.ncbi.nlm.nih.gov/pubmed/21885399> [Accessed July 17, 2014].
- Ibe, B.O. et al., 2008. Platelet-activating factor stimulates ovine foetal pulmonary vascular smooth muscle cell proliferation: role of nuclear factor-kappa B and cyclin-dependent kinases. *Cell proliferation*, 41(2), pp.208–29. Available at: <http://www.ncbi.nlm.nih.gov/pubmed/18336468> [Accessed July 16, 2014].
- Ihida-Stansbury, K. et al., 2006. Tenascin-C is induced by mutated BMP type II receptors in familial forms of pulmonary arterial hypertension. *American journal of physiology. Lung cellular and molecular physiology*, 296, pp.L694–L702. Available at: <http://ajplung.physiology.org.eresources.shef.ac.uk/content/ajplung/291/4/L694.full.pdf> [Accessed June 24, 2014].
- Ikeda, Y. et al., 2002. Anti-monocyte chemoattractant protein-1 gene therapy attenuates pulmonary hypertension in rats. *American journal of physiology. Heart and circulatory physiology*, 283(5), pp.H2021–8. Available at: <http://www.ncbi.nlm.nih.gov/pubmed/12384481> [Accessed October 10, 2014].
- Itoh, A. et al., 2003. Effects of IL-1beta, TNF-alpha, and macrophage migration inhibitory factor on prostacyclin synthesis in rat pulmonary artery smooth muscle cells. *Respirology (Carlton, Vic.)*, 8(4), pp.467–72. Available at: <http://www.ncbi.nlm.nih.gov/pubmed/14629650> [Accessed October 10, 2014].
- Ivy, D.D. et al., 2005. Development of occlusive neointimal lesions in distal pulmonary arteries of endothelin B receptor-deficient rats: a new model of severe pulmonary arterial hypertension. *Circulation*, 111(22), pp.2988–96. Available at: <http://circ.ahajournals.org/content/111/22/2988.long> [Accessed June 24, 2014].
- Jia, L., Wang, R. & Tang, D.D., 2012. Abl regulates smooth muscle cell proliferation by modulating actin dynamics and ERK1/2 activation. *American journal of physiology. Cell physiology*, 302(7), pp.C1026–34. Available at: http://apps.webofknowledge.com.eresources.shef.ac.uk/full_record.do?product=UA&search_mode=GeneralSearch&qid=16&SID=T2uX7uDM7ZXDpHz7M3w&page=1&doc=8 [Accessed July 16, 2014].

- Johnson, D. et al., 1996. Mutations in the activin receptor-like kinase 1 gene in hereditary haemorrhagic telangiectasia type 2. *Nature genetics*, 13, pp.189–195.
- Johnson, S.R. et al., 2008. Prognostic factors for survival in scleroderma associated pulmonary arterial hypertension. *The Journal of rheumatology*, 35(8), pp.1584–90. Available at: <http://www.ncbi.nlm.nih.gov/pubmed/18597400> [Accessed October 10, 2014].
- Jones, P.L. et al., 2002. Altered hemodynamics controls matrix metalloproteinase activity and tenascin-C expression in neonatal pig lung. *American journal of physiology. Lung cellular and molecular physiology*, 282(1), pp.L26–35. Available at: <http://ajplung.physiology.org/content/282/1/L26> [Accessed June 24, 2014].
- Jones, P.L., Cowan, K.N. & Rabinovitch, M., 1997. Tenascin-C, proliferation and subendothelial fibronectin in progressive pulmonary vascular disease. *The American journal of pathology*, 150(4), pp.1349–60. Available at: <http://www.pubmedcentral.nih.gov/articlerender.fcgi?artid=1858188&tool=pmcentrez&rendertype=abstract> [Accessed June 24, 2014].
- Jones, P.L. & Rabinovitch, M., 1996. Tenascin-C Is Induced With Progressive Pulmonary Vascular Disease in Rats and Is Functionally Related to Increased Smooth Muscle Cell Proliferation. *Circulation Research*, 79(6), pp.1131–1142. Available at: <http://circres.ahajournals.org.eresources.shef.ac.uk/content/79/6/1131> [Accessed June 24, 2014].
- Kadavath, S. et al., 2014. A novel therapeutic approach in pulmonary arterial hypertension as a complication of adult-onset Still's disease: targeting IL-6. *International journal of rheumatic diseases*, 17(3), pp.336–40. Available at: <http://www.ncbi.nlm.nih.gov/pubmed/24581387> [Accessed August 28, 2014].
- Karatolios, K. et al., 2012. Osteoprotegerin (OPG) and TNF-related apoptosis-inducing ligand (TRAIL) levels in malignant and benign pericardial effusions. *Clinical biochemistry*, 45(3), pp.237–42. Available at: <http://www.ncbi.nlm.nih.gov/pubmed/22202560> [Accessed February 12, 2014].
- El Kasmi, K.C. et al., 2014. Adventitial fibroblasts induce a distinct proinflammatory/profibrotic macrophage phenotype in pulmonary hypertension. *Journal of immunology (Baltimore, Md. : 1950)*, 193(2), pp.597–609. Available at: <http://www.jimmunol.org/content/193/2/597.full> [Accessed August 17, 2014].
- Kawaguchi, Y. et al., 2006. NOS2 polymorphisms associated with the susceptibility to pulmonary arterial hypertension with systemic sclerosis: contribution to the transcriptional activity. *Arthritis research & therapy*, 8(4), p.R104. Available at: <http://www.pubmedcentral.nih.gov/articlerender.fcgi?artid=1779390&tool=pmcentrez&rendertype=abstract> [Accessed October 10, 2014].
- Kay, J.M., Smith, P. & Heath, D., 1971. Aminorex and the pulmonary circulation. *Thorax*, 26(3), pp.262–70. Available at:

<http://www.pubmedcentral.nih.gov/articlerender.fcgi?artid=1019080&tool=pmcentrez&rendertype=abstract> [Accessed August 1, 2014].

Keegan, A. et al., 2001. Contribution of the 5-HT(1B) receptor to hypoxia-induced pulmonary hypertension: converging evidence using 5-HT(1B)-receptor knockout mice and the 5-HT(1B/1D)-receptor antagonist GR127935. *Circulation research*, 89(12), pp.1231–9. Available at: <http://www.ncbi.nlm.nih.gov/pubmed/11739290> [Accessed October 10, 2014].

Kiely, D.G. et al., 2013. Pulmonary hypertension: diagnosis and management. *BMJ (Clinical research ed.)*, 346(April), p.f2028. Available at: <http://www.ncbi.nlm.nih.gov/pubmed/23592451> [Accessed January 22, 2014].

Kim, D.-H. et al., 2003. GbetaL, a positive regulator of the rapamycin-sensitive pathway required for the nutrient-sensitive interaction between raptor and mTOR. *Molecular cell*, 11(4), pp.895–904. Available at: <http://www.ncbi.nlm.nih.gov/pubmed/12718876> [Accessed September 30, 2014].

Kim, J. et al., 2013. An endothelial apelin-FGF link mediated by miR-424 and miR-503 is disrupted in pulmonary arterial hypertension. *Nature medicine*, 19(1), pp.74–82. Available at: <http://www.pubmedcentral.nih.gov/articlerender.fcgi?artid=3540168&tool=pmcentrez&rendertype=abstract> [Accessed January 21, 2014].

Kim, J. et al., 2013. Plasma osteoprotegerin levels increase with the severity of cerebral artery atherosclerosis. *Clinical biochemistry*, 46(12), pp.1036–40. Available at: <http://www.ncbi.nlm.nih.gov/pubmed/23726804> [Accessed August 12, 2014].

Kingsley, K. et al., 2002. ERK1/2 mediates PDGF-BB stimulated vascular smooth muscle cell proliferation and migration on laminin-5. *Biochemical and biophysical research communications*, 293(3), pp.1000–6. Available at: http://apps.webofknowledge.com.eresources.shef.ac.uk/full_record.do?product=UA&search_mode=GeneralSearch&qid=25&SID=T2uX7uDM7ZXDpHz7M3w&page=1&doc=1 [Accessed July 16, 2014].

Kiss, T. et al., 2014. Novel Mechanisms of Sildenafil in Pulmonary Hypertension Involving Cytokines/Chemokines, MAP Kinases and Akt. *PLoS one*, 9(8), p.e104890. Available at: <http://www.pubmedcentral.nih.gov/articlerender.fcgi?artid=4136836&tool=pmcentrez&rendertype=abstract> [Accessed August 26, 2014].

Kobayashi-Sakamoto, M. et al., 2008. Role of alpha5 integrin in osteoprotegerin-induced endothelial cell migration and proliferation. *Microvascular research*, 76(3), pp.139–44. Available at: <http://www.ncbi.nlm.nih.gov/pubmed/18656492> [Accessed February 12, 2014].

Koyama, H. et al., 1996. Fibrillar collagen inhibits arterial smooth muscle proliferation through regulation of Cdk2 inhibitors. *Cell*, 87(6), pp.1069–78.

Available at: <http://www.ncbi.nlm.nih.gov/pubmed/8978611> [Accessed August 6, 2014].

- Kugathasan, L. et al., 2005. Role of angiopoietin-1 in experimental and human pulmonary arterial hypertension. *Chest*, 128(6 Suppl), p.633S–642S. Available at: <http://www.ncbi.nlm.nih.gov/pubmed/16373885> [Accessed October 10, 2014].
- Kwapiszewska, G. et al., 2005. Expression profiling of laser-microdissected intrapulmonary arteries in hypoxia-induced pulmonary hypertension. *Respiratory research*, 6, p.109. Available at: <http://www.pubmedcentral.nih.gov/articlerender.fcgi?artid=1261535&tool=pmcentrez&rendertype=abstract> [Accessed October 10, 2014].
- Lamoureux, F. et al., 2014. Suppression of heat shock protein 27 using OGX-427 induces endoplasmic reticulum stress and potentiates heat shock protein 90 inhibitors to delay castrate-resistant prostate cancer. *European urology*, 66(1), pp.145–55. Available at: <http://www.ncbi.nlm.nih.gov/pubmed/24411988> [Accessed September 2, 2014].
- Lane, D. et al., 2013. Osteoprotegerin (OPG) activates integrin, focal adhesion kinase (FAK), and Akt signaling in ovarian cancer cells to attenuate TRAIL-induced apoptosis. *Journal of ovarian research*, 6(1), p.82. Available at: <http://www.pubmedcentral.nih.gov/articlerender.fcgi?artid=3874685&tool=pmcentrez&rendertype=abstract> [Accessed August 11, 2014].
- Lane, D. et al., 2012. Osteoprotegerin (OPG) protects ovarian cancer cells from TRAIL-induced apoptosis but does not contribute to malignant ascites-mediated attenuation of TRAIL-induced apoptosis. *Journal of ovarian research*, 5(1), p.34. Available at: <http://www.pubmedcentral.nih.gov/articlerender.fcgi?artid=3507713&tool=pmcentrez&rendertype=abstract> [Accessed August 11, 2014].
- Lane, K.B. et al., 2000. Heterozygous germline mutations in BMPR2, encoding a TGF-beta receptor, cause familial primary pulmonary hypertension. *Nature genetics*, 26(1), pp.81–4. Available at: <http://www.ncbi.nlm.nih.gov/pubmed/10973254>.
- Launay, J.-M. et al., 2002. Function of the serotonin 5-hydroxytryptamine 2B receptor in pulmonary hypertension. *Nature medicine*, 8(10), pp.1129–35. Available at: <http://www.ncbi.nlm.nih.gov/pubmed/12244304> [Accessed October 10, 2014].
- Lavoie, J.N. et al., 1996. Cyclin D1 Expression Is Regulated Positively by the p42/p44MAPK and Negatively by the p38/HOGMAPK Pathway. *Journal of Biological Chemistry*, 271(34), pp.20608–20616. Available at: <http://www.jbc.org.eresources.shef.ac.uk/content/271/34/20608> [Accessed July 16, 2014].
- Lawrie, A. et al., 2008. Evidence of a role for osteoprotegerin in the pathogenesis of pulmonary arterial hypertension. *The American journal of pathology*, 172(1),

pp.256–64. Available at:
<http://www.pubmedcentral.nih.gov/articlerender.fcgi?artid=2189625&tool=pmcentrez&rendertype=abstract> [Accessed February 12, 2014].

Lawrie, A. et al., 2011. Paigen diet-fed apolipoprotein E knockout mice develop severe pulmonary hypertension in an interleukin-1-dependent manner. *The American journal of pathology*, 179(4), pp.1693–705. Available at:
<http://www.pubmedcentral.nih.gov/articlerender.fcgi?artid=3181351&tool=pmcentrez&rendertype=abstract> [Accessed February 12, 2014].

Lee, S.-J. et al., 2011. Autophagic protein LC3B confers resistance against hypoxia-induced pulmonary hypertension. *American journal of respiratory and critical care medicine*, 183(5), pp.649–58. Available at:
<http://www.pubmedcentral.nih.gov/articlerender.fcgi?artid=3081281&tool=pmcentrez&rendertype=abstract> [Accessed July 16, 2014].

Lee, S.D. et al., 1998. Monoclonal endothelial cell proliferation is present in primary but not secondary pulmonary hypertension. *The Journal of clinical investigation*, 101(5), pp.927–34. Available at:
<http://www.pubmedcentral.nih.gov/articlerender.fcgi?artid=508641&tool=pmcentrez&rendertype=abstract>.

Lee, S.L. et al., 1994. Serotonin produces both hyperplasia and hypertrophy of bovine pulmonary artery smooth muscle cells in culture. *The American journal of physiology*, 266(1 Pt 1), pp.L46–52. Available at:
<http://www.ncbi.nlm.nih.gov/pubmed/8304469>.

Leithäuser, F. et al., 1993. Constitutive and induced expression of APO-1, a new member of the nerve growth factor/tumor necrosis factor receptor superfamily, in normal and neoplastic cells. *Laboratory investigation; a journal of technical methods and pathology*, 69(4), pp.415–29. Available at:
<http://www.ncbi.nlm.nih.gov/pubmed/7693996> [Accessed July 28, 2014].

Leuchte, H.H. et al., 2008. Inhalation of vasoactive intestinal peptide in pulmonary hypertension. *The European respiratory journal*, 32(5), pp.1289–94. Available at: <http://www.ncbi.nlm.nih.gov/pubmed/18978135> [Accessed June 30, 2014].

Li, G.-W. et al., 2011. The calcium-sensing receptor mediates hypoxia-induced proliferation of rat pulmonary artery smooth muscle cells through MEK1/ERK1,2 and PI3K pathways. *Basic & clinical pharmacology & toxicology*, 108(3), pp.185–93. Available at:
<http://www.ncbi.nlm.nih.gov/pubmed/21073657> [Accessed July 16, 2014].

Li, M. et al., 2011. Emergence of fibroblasts with a proinflammatory epigenetically altered phenotype in severe hypoxic pulmonary hypertension. *Journal of immunology (Baltimore, Md. : 1950)*, 187(5), pp.2711–22. Available at:
<http://www.pubmedcentral.nih.gov/articlerender.fcgi?artid=3159707&tool=pmcentrez&rendertype=abstract> [Accessed August 17, 2014].

- Li, Y. et al., 2007. B cells and T cells are critical for the preservation of bone homeostasis and attainment of peak bone mass in vivo. *Blood*, 109(9), pp.3839–48. Available at: <http://www.pubmedcentral.nih.gov/articlerender.fcgi?artid=1874582&tool=pmcentrez&rendertype=abstract> [Accessed August 12, 2014].
- Liu, C. et al., 2013. Human airway trypsin-like protease induces mucin5AC hypersecretion via a protease-activated receptor 2-mediated pathway in human airway epithelial cells. *Archives of Biochemistry and Biophysics*, 535, pp.234–240.
- Liu, G. et al., 2013. PPAR δ agonist GW501516 inhibits PDGF-stimulated pulmonary arterial smooth muscle cell function related to pathological vascular remodeling. *BioMed research international*, 2013, p.903947. Available at: <http://www.pubmedcentral.nih.gov/articlerender.fcgi?artid=3625582&tool=pmcentrez&rendertype=abstract> [Accessed July 16, 2014].
- Liu, Z. et al., 2009. GDF5 and BMP2 inhibit apoptosis via activation of BMP2 and subsequent stabilization of XIAP. *Biochimica et biophysica acta*, 1793(12), pp.1819–27. Available at: <http://www.ncbi.nlm.nih.gov/pubmed/19782107> [Accessed October 10, 2014].
- Long, L. et al., 2013. Chloroquine prevents progression of experimental pulmonary hypertension via inhibition of autophagy and lysosomal bone morphogenetic protein type II receptor degradation. *Circulation research*, 112(8), pp.1159–70. Available at: <http://circres.ahajournals.org/content/112/8/1159.abstract> [Accessed July 16, 2014].
- Lorenzen, J.M. et al., 2011. Osteopontin in patients with idiopathic pulmonary hypertension. *Chest*, 139(5), pp.1010–7. Available at: <http://www.ncbi.nlm.nih.gov/pubmed/20947652> [Accessed August 9, 2014].
- Lu, B. et al., 2002. Regulation of Fas (CD95)-induced apoptosis by nuclear factor-kappaB and tumor necrosis factor-alpha in macrophages. *American journal of physiology. Cell physiology*, 283(3), pp.C831–8. Available at: <http://www.ncbi.nlm.nih.gov/pubmed/12176740>.
- Lukas, J., Bartkova, J. & Bartek, J., 1996. Convergence of mitogenic signalling cascades from diverse classes of receptors at the cyclin D-cyclin-dependent kinase-pRb-controlled G1 checkpoint. *Molecular and cellular biology*, 16(12), pp.6917–25. Available at: <http://www.pubmedcentral.nih.gov/articlerender.fcgi?artid=231695&tool=pmcentrez&rendertype=abstract> [Accessed July 16, 2014].
- Ma, L. et al., 2013. A novel channelopathy in pulmonary arterial hypertension. *The New England journal of medicine*, 369(4), pp.351–61. Available at: <http://www.pubmedcentral.nih.gov/articlerender.fcgi?artid=3792227&tool=pmcentrez&rendertype=abstract> [Accessed July 9, 2014].

- Machado, R.D. et al., 2001. BMPR2 haploinsufficiency as the inherited molecular mechanism for primary pulmonary hypertension. *American journal of human genetics*, 68(1), pp.92–102. Available at: <http://www.pubmedcentral.nih.gov/articlerender.fcgi?artid=1234937&tool=pmcentrez&rendertype=abstract> [Accessed October 10, 2014].
- Machado, R.D. et al., 2003. Functional interaction between BMPR-II and Tctex-1, a light chain of Dynein, is isoform-specific and disrupted by mutations underlying primary pulmonary hypertension. *Human molecular genetics*, 12(24), pp.3277–86. Available at: <http://www.ncbi.nlm.nih.gov/pubmed/14583445> [Accessed October 10, 2014].
- MacLean, M.R., 2007. Pulmonary hypertension and the serotonin hypothesis: where are we now? *International journal of clinical practice. Supplement*, 61(156), pp.27–31. Available at: <http://www.ncbi.nlm.nih.gov/pubmed/17663674> [Accessed February 12, 2014].
- Maeyama, T. et al., 2001. Upregulation of Fas-signalling molecules in lung epithelial cells from patients with idiopathic pulmonary fibrosis. *The European respiratory journal*, 17(2), pp.180–9. Available at: <http://www.ncbi.nlm.nih.gov/pubmed/11334117>.
- Mahmood, A. et al., 2010. S155 The role of ST2 in a model of pulmonary hypertension. *Thorax*, 65, pp.A70–A71.
- Majka, S. et al., 2011. Physiologic and molecular consequences of endothelial Bmpr2 mutation. *Respiratory research*, 12, p.84. Available at: <http://www.pubmedcentral.nih.gov/articlerender.fcgi?artid=3141420&tool=pmcentrez&rendertype=abstract> [Accessed August 7, 2014].
- Malyankar, U.M. et al., 2000. Osteoprotegerin is an alpha vbeta 3-induced, NF-kappa B-dependent survival factor for endothelial cells. *The Journal of biological chemistry*, 275(28), pp.20959–62. Available at: <http://www.ncbi.nlm.nih.gov/pubmed/10811631> [Accessed February 12, 2014].
- Maruno, K., Absood, A. & Said, S.I., 1995. VIP inhibits basal and histamine-stimulated proliferation of human airway smooth muscle cells. *Am J Physiol Lung Cell Mol Physiol*, 268(6), pp.L1047–1051. Available at: <http://ajplung.physiology.org/content/268/6/L1047> [Accessed June 29, 2014].
- Mata-Greenwood, E. et al., 2003. Expression of VEGF and its receptors Flt-1 and Flk-1/KDR is altered in lambs with increased pulmonary blood flow and pulmonary hypertension. *American journal of physiology. Lung cellular and molecular physiology*, 285(1), pp.L222–31. Available at: <http://www.ncbi.nlm.nih.gov/pubmed/12665467> [Accessed October 10, 2014].
- Mathew, R., 2011. Cell-specific dual role of caveolin-1 in pulmonary hypertension. *Pulmonary medicine*, 2011, p.573432. Available at: <http://www.pubmedcentral.nih.gov/articlerender.fcgi?artid=3109422&tool=pmcentrez&rendertype=abstract> [Accessed June 21, 2014].

- Mathew, R. et al., 2004. Disruption of endothelial-cell caveolin-1alpha/raft scaffolding during development of monocrotaline-induced pulmonary hypertension. *Circulation*, 110(11), pp.1499–506. Available at: <http://www.ncbi.nlm.nih.gov/pubmed/15353500> [Accessed June 21, 2014].
- Matsushima, R. et al., 2006. Human airway trypsin-like protease stimulates human bronchial fibroblast proliferation in a protease-activated receptor-2-dependent pathway. *American journal of physiology. Lung cellular and molecular physiology*, 290(2), pp.L385–95. Available at: <http://www.ncbi.nlm.nih.gov/pubmed/16199437> [Accessed September 26, 2014].
- Matute-Bello, G. et al., 2001. Recombinant human Fas ligand induces alveolar epithelial cell apoptosis and lung injury in rabbits. *American journal of physiology. Lung cellular and molecular physiology*, 281(2), pp.L328–35. Available at: <http://www.ncbi.nlm.nih.gov/pubmed/11435207>.
- McAllister, K.A. et al., 1994. Endoglin, a TGF-beta binding protein of endothelial cells, is the gene for hereditary haemorrhagic telangiectasia type 1. *Nature genetics*, 8(4), pp.345–51. Available at: <http://www.ncbi.nlm.nih.gov/pubmed/7894484> [Accessed October 11, 2014].
- McGonigle, J.S. et al., 2008. Heparin-regulated delivery of osteoprotegerin promotes vascularization of implanted hydrogels. *Journal of biomaterials science. Polymer edition*, 19(8), pp.1021–34. Available at: <http://www.ncbi.nlm.nih.gov/pubmed/18644228> [Accessed August 12, 2014].
- McGoon, M.D. et al., 2013. Pulmonary arterial hypertension: epidemiology and registries. *Journal of the American College of Cardiology*, 62(25 Suppl), pp.D51–9. Available at: <http://www.ncbi.nlm.nih.gov/pubmed/24355642> [Accessed January 21, 2014].
- McLaughlin, V. V & McGoon, M.D., 2006. Pulmonary arterial hypertension. *Circulation*, 114(13), pp.1417–31. Available at: <http://www.ncbi.nlm.nih.gov/pubmed/17000921> [Accessed February 12, 2014].
- McMurtry, I.F. et al., 2010. Rho kinase-mediated vasoconstriction in pulmonary hypertension. *Advances in experimental medicine and biology*, 661, pp.299–308. Available at: <http://www.ncbi.nlm.nih.gov/pubmed/20204738> [Accessed October 10, 2014].
- Meloche, S. & Pouyssegur, J., 2007. The ERK1/2 mitogen-activated protein kinase pathway as a master regulator of the G1- to S-phase transition. *Oncogene*, 26(22), pp.3227–39. Available at: <http://dx.doi.org/10.1038/sj.onc.1210414> [Accessed July 16, 2014].
- Meoli, D.F. & White, R.J., 2010. Endothelin-1 induces pulmonary but not aortic smooth muscle cell migration by activating ERK1/2 MAP kinase. *Canadian journal of physiology and pharmacology*, 88(8), pp.830–9. Available at: <http://www.ncbi.nlm.nih.gov/pubmed/20725141> [Accessed May 12, 2014].

- Meyrick, B. et al., 1974. Primary pulmonary hypertension a case report including electronmicroscopic study. *British Journal of Diseases of the Chest*, 68, pp.11–20. Available at: <http://www.sciencedirect.com/science/article/pii/0007097174900035> [Accessed August 5, 2014].
- Michelakis, E.D., Wilkins, M.R. & Rabinovitch, M., 2008. Emerging concepts and translational priorities in pulmonary arterial hypertension. *Circulation*, 118(14), pp.1486–95. Available at: <http://www.ncbi.nlm.nih.gov/pubmed/18824655> [Accessed February 12, 2014].
- Mollinedo, F. & Gajate, C., 2006. Fas/CD95 death receptor and lipid rafts: new targets for apoptosis-directed cancer therapy. *Drug resistance updates : reviews and commentaries in antimicrobial and anticancer chemotherapy*, 9(1-2), pp.51–73. Available at: <http://www.ncbi.nlm.nih.gov/pubmed/16687251> [Accessed March 11, 2014].
- Morony, S. et al., 2008. Osteoprotegerin inhibits vascular calcification without affecting atherosclerosis in ldlr(-/-) mice. *Circulation*, 117(3), pp.411–20. Available at: <http://www.pubmedcentral.nih.gov/articlerender.fcgi?artid=2680735&tool=pmcentrez&rendertype=abstract> [Accessed August 12, 2014].
- Morrell, N.W. et al., 2001. Altered Growth Responses of Pulmonary Artery Smooth Muscle Cells From Patients With Primary Pulmonary Hypertension to Transforming Growth Factor- 1 and Bone Morphogenetic Proteins. *Circulation*, 104(7), pp.790–795. Available at: <http://circ.ahajournals.org/cgi/doi/10.1161/hc3201.094152> [Accessed June 27, 2014].
- Morrell, N.W., 2010. Role of bone morphogenetic protein receptors in the development of pulmonary arterial hypertension. *Advances in experimental medicine and biology*, 661, pp.251–64. Available at: <http://www.ncbi.nlm.nih.gov/pubmed/20204735> [Accessed October 10, 2014].
- Mosheimer, B. a et al., 2005. Syndecan-1 is involved in osteoprotegerin-induced chemotaxis in human peripheral blood monocytes. *The Journal of clinical endocrinology and metabolism*, 90(5), pp.2964–71. Available at: <http://www.ncbi.nlm.nih.gov/pubmed/15728209> [Accessed February 12, 2014].
- Murakami, K. et al., 2010. Smurf1 ubiquitin ligase causes downregulation of BMP receptors and is induced in monocrotaline and hypoxia models of pulmonary arterial hypertension. *Experimental biology and medicine (Maywood, N.J.)*, 235(7), pp.805–13. Available at: <http://www.ncbi.nlm.nih.gov/pubmed/20558834> [Accessed October 10, 2014].
- Murray, F., MacLean, M.R. & Pyne, N.J., 2002. Increased expression of the cGMP-inhibited cAMP-specific (PDE3) and cGMP binding cGMP-specific (PDE5) phosphodiesterases in models of pulmonary hypertension. *British journal of pharmacology*, 137(8), pp.1187–94. Available at:

<http://www.pubmedcentral.nih.gov/articlerender.fcgi?artid=1573609&tool=pmcentrez&rendertype=abstract> [Accessed October 10, 2014].

Naeije, R., 2013. Physiology of the pulmonary circulation and the right heart. *Current hypertension reports*, 15(6), pp.623–31. Available at: <http://www.ncbi.nlm.nih.gov/pubmed/24097187> [Accessed September 11, 2014].

Naeije, R. & Westerhof, N., 2011. Pulmonary Vascular Function. In J. X.-J. Yuan et al., eds. *Textbook of Pulmonary Vascular Disease*. New York: Springer, pp. 61–72.

Nakai, A. et al., 2007. The role of autophagy in cardiomyocytes in the basal state and in response to hemodynamic stress. *Nature medicine*, 13(5), pp.619–24. Available at: <http://dx.doi.org/10.1038/nm1574> [Accessed July 16, 2014].

Nakamura, K. et al., 2012. Pro-apoptotic effects of imatinib on PDGF-stimulated pulmonary artery smooth muscle cells from patients with idiopathic pulmonary arterial hypertension. *International journal of cardiology*, 159(2), pp.100–6. Available at: <http://www.ncbi.nlm.nih.gov/pubmed/21376411> [Accessed September 5, 2014].

Nasim, M.T. et al., 2011. Molecular genetic characterization of SMAD signaling molecules in pulmonary arterial hypertension. *Human mutation*, 32(12), pp.1385–9. Available at: <http://www.ncbi.nlm.nih.gov/pubmed/21898662> [Accessed August 7, 2014].

Nemenoff, R.A. et al., 2008. Targeted deletion of PTEN in smooth muscle cells results in vascular remodeling and recruitment of progenitor cells through induction of stromal cell-derived factor-1 alpha. *Circulation research*, 102(9), pp.1036–45. Available at: <http://www.ncbi.nlm.nih.gov/pubmed/18340011> [Accessed October 10, 2014].

Newman, J.H. et al., 2004. Genetic basis of pulmonary arterial hypertension: current understanding and future directions. *Journal of the American College of Cardiology*, 43(12 Suppl S), p.33S–39S. Available at: <http://www.sciencedirect.com/science/article/pii/S0735109704004371> [Accessed August 5, 2014].

Nishihara, A. et al., 2002. Functional Heterogeneity of Bone Morphogenetic Protein Receptor-II Mutants Found in Patients with Primary Pulmonary Hypertension. , 13(September), pp.3055–3063.

Olesen, M. et al., 2012. No influence of OPG and its ligands, RANKL and TRAIL, on proliferation and regulation of the calcification process in primary human vascular smooth muscle cells. *Molecular and cellular endocrinology*, 362(1-2), pp.149–56. Available at: <http://www.sciencedirect.com/science/article/pii/S0303720712003188> [Accessed July 9, 2014].

- Olesen, P., Ledet, T. & Rasmussen, L.M., 2005. Arterial osteoprotegerin: increased amounts in diabetes and modifiable synthesis from vascular smooth muscle cells by insulin and TNF-alpha. *Diabetologia*, 48(3), pp.561–8. Available at: <http://www.ncbi.nlm.nih.gov/pubmed/15700136> [Accessed August 12, 2014].
- Olschewski, A. et al., 2006. Impact of TASK-1 in human pulmonary artery smooth muscle cells. *Circulation research*, 98(8), pp.1072–80. Available at: <http://www.ncbi.nlm.nih.gov/pubmed/16574908> [Accessed August 7, 2014].
- Orikawa, H. et al., 2012. Activation of macrophage-stimulating protein by human airway trypsin-like protease. *FEBS letters*, 586(3), pp.217–21. Available at: <http://www.ncbi.nlm.nih.gov/pubmed/22245154> [Accessed September 26, 2014].
- Ormiston, M.L. et al., 2012. Impaired natural killer cell phenotype and function in idiopathic and heritable pulmonary arterial hypertension. *Circulation*, 126(9), pp.1099–109. Available at: <http://www.ncbi.nlm.nih.gov/pubmed/22832786> [Accessed September 18, 2014].
- Ouyang, L. et al., 2012. Programmed cell death pathways in cancer: a review of apoptosis, autophagy and programmed necrosis. *Cell proliferation*, 45(6), pp.487–98. Available at: <http://www.ncbi.nlm.nih.gov/pubmed/23030059> [Accessed January 27, 2014].
- Palmer, G. et al., 2008. The IL-1 receptor accessory protein (AcP) is required for IL-33 signaling and soluble AcP enhances the ability of soluble ST2 to inhibit IL-33. *Cytokine*, 42(3), pp.358–64. Available at: <http://www.ncbi.nlm.nih.gov/pubmed/18450470> [Accessed July 28, 2014].
- Pankey, E.A. et al., 2013. Imatinib attenuates monocrotaline pulmonary hypertension and has potent vasodilator activity in pulmonary and systemic vascular beds in the rat. *American journal of physiology. Heart and circulatory physiology*, 305(9), pp.H1288–96. Available at: <http://ajpheart.physiology.org/content/305/9/H1288.long> [Accessed June 24, 2014].
- Patel, H.H. et al., 2007. Increased smooth muscle cell expression of caveolin-1 and caveolae contribute to the pathophysiology of idiopathic pulmonary arterial hypertension. *FASEB journal : official publication of the Federation of American Societies for Experimental Biology*, 21(11), pp.2970–9. Available at: <http://www.ncbi.nlm.nih.gov/pubmed/17470567> [Accessed June 20, 2014].
- Pendergrass, S.A. et al., 2010. Limited systemic sclerosis patients with pulmonary arterial hypertension show biomarkers of inflammation and vascular injury. *PloS one*, 5(8), p.e12106. Available at: <http://www.pubmedcentral.nih.gov/articlerender.fcgi?artid=2923145&tool=pmcentrez&rendertype=abstract> [Accessed October 9, 2014].
- Perkett, E.A. et al., 1990. Transforming growth factor-beta activity in sheep lung lymph during the development of pulmonary hypertension. *The Journal of clinical investigation*, 86(5), pp.1459–64. Available at:

<http://www.pubmedcentral.nih.gov/articlerender.fcgi?artid=296890&tool=pmcentrez&rendertype=abstract> [Accessed October 10, 2014].

- Perros, F., Dorfmueller, P., Souza, R., Durand-Gasselien, I., Mussot, S., et al., 2007. Dendritic cell recruitment in lesions of human and experimental pulmonary hypertension. *The European respiratory journal*, 29(3), pp.462–8. Available at: <http://www.ncbi.nlm.nih.gov/pubmed/17107989> [Accessed August 29, 2014].
- Perros, F., Dorfmueller, P., Souza, R., Durand-Gasselien, I., Godot, V., et al., 2007. Fractalkine-induced smooth muscle cell proliferation in pulmonary hypertension. *The European respiratory journal : official journal of the European Society for Clinical Respiratory Physiology*, 29, pp.937–943.
- Perros, F. et al., 2008. Platelet-derived growth factor expression and function in idiopathic pulmonary arterial hypertension. *American journal of respiratory and critical care medicine*, 178(1), pp.81–8. Available at: <http://www.ncbi.nlm.nih.gov/pubmed/18420966> [Accessed February 12, 2014].
- Petkov, V. et al., 2003. Vasoactive intestinal peptide as a new drug for treatment of primary pulmonary hypertension. , 111(9), pp.1339–1346.
- Pietra, G.G. et al., 2004. Pathologic assessment of vasculopathies in pulmonary hypertension. *Journal of the American College of Cardiology*, 43(12 Suppl S), p.25S–32S. Available at: <http://www.ncbi.nlm.nih.gov/pubmed/15194175> [Accessed February 12, 2014].
- Pokreisz, P., Marsboom, G. & Janssens, S., 2007. Pressure overload-induced right ventricular dysfunction and remodelling in experimental pulmonary hypertension: the right heart revisited. *European Heart Journal Supplements*, 9(Suppl H), pp.H75–H84. Available at: <http://eurheartjsupp.oxfordjournals.org/cgi/doi/10.1093/eurheartj/sum021> [Accessed February 12, 2014].
- Pritzker, L.B., Scatena, M. & Giachelli, C.M., 2004. The Role of Osteoprotegerin and Tumor Necrosis Factor-related Apoptosis-inducing Ligand in Human Microvascular Endothelial Cell Survival. *Molecular biology of the cell*, 15(June), pp.2834–2841.
- Rabinovitch, M. et al., 2014. Inflammation and immunity in the pathogenesis of pulmonary arterial hypertension. *Circulation research*, 115(1), pp.165–75. Available at: <http://www.ncbi.nlm.nih.gov/pubmed/24951765> [Accessed July 22, 2014].
- Rabinovitch, M., 2008. Molecular pathogenesis of pulmonary arterial hypertension. *The Journal of clinical investigation*, 118(7).
- Radstake, T.R.D.J. et al., 2009. Increased frequency and compromised function of T regulatory cells in systemic sclerosis (SSc) is related to a diminished CD69 and TGFbeta expression. *PloS one*, 4(6), p.e5981. Available at:

<http://www.pubmedcentral.nih.gov/articlerender.fcgi?artid=2695559&tool=pmcentrez&rendertype=abstract> [Accessed August 29, 2014].

Rai, P.R. et al., 2008. The cancer paradigm of severe pulmonary arterial hypertension. *American journal of respiratory and critical care medicine*, 178(6), pp.558–64. Available at:

<http://www.pubmedcentral.nih.gov/articlerender.fcgi?artid=2542431&tool=pmcentrez&rendertype=abstract> [Accessed September 22, 2014].

Rasmussen, L.M. et al., 2006. Plasma osteoprotegerin levels are associated with glycaemic status, systolic blood pressure, kidney function and cardiovascular morbidity in type 1 diabetic patients. *European journal of endocrinology / European Federation of Endocrine Societies*, 154(1), pp.75–81. Available at:

<http://www.ncbi.nlm.nih.gov/pubmed/16381994> [Accessed August 11, 2014].

Reyes, R. et al., 1998. Cloning and expression of a novel pH-sensitive two pore domain K⁺ channel from human kidney. *The Journal of biological chemistry*, 273(47), pp.30863–9. Available at:

<http://www.ncbi.nlm.nih.gov/pubmed/9812978> [Accessed August 7, 2014].

Rich, S. et al., 1987. Primary pulmonary hypertension. A national prospective study. *Annals of internal medicine*, 107(2), pp.216–23. Available at:

<http://www.ncbi.nlm.nih.gov/pubmed/3605900> [Accessed August 1, 2014].

Richter, A. et al., 2004. Impaired transforming growth factor-beta signaling in idiopathic pulmonary arterial hypertension. *American journal of respiratory and critical care medicine*, 170(12), pp.1340–8. Available at:

<http://www.ncbi.nlm.nih.gov/pubmed/15361368> [Accessed June 26, 2014].

Rudarakanchana, N. et al., 2002. Functional analysis of bone morphogenetic protein type II receptor mutations underlying primary pulmonary hypertension. *Human molecular genetics*, 11(13), pp.1517–25. Available at:

<http://www.ncbi.nlm.nih.gov/pubmed/12045205>.

Said, S.I., 2008. The vasoactive intestinal peptide gene is a key modulator of pulmonary vascular remodeling and inflammation. *Annals of the New York Academy of Sciences*, 1144, pp.148–53. Available at:

<http://www.ncbi.nlm.nih.gov/pubmed/19076374> [Accessed October 10, 2014].

Sakamaki, F. et al., 2000. Increased plasma P-selectin and decreased thrombomodulin in pulmonary arterial hypertension were improved by continuous prostacyclin therapy. *Circulation*, 102(22), pp.2720–5. Available at:

<http://www.ncbi.nlm.nih.gov/pubmed/11094038> [Accessed October 10, 2014].

Sale, M.J. & Cook, S.J., 2013. That which does not kill me makes me stronger; combining ERK1/2 pathway inhibitors and BH3 mimetics to kill tumour cells and prevent acquired resistance. *British journal of pharmacology*, 169(8), pp.1708–22. Available at:

<http://www.pubmedcentral.nih.gov/articlerender.fcgi?artid=3753831&tool=pmcentrez&rendertype=abstract> [Accessed August 28, 2014].

- Samali, A. & Cotter, T.G., 1996. Heat shock proteins increase resistance to apoptosis. *Experimental cell research*, 223(1), pp.163–70. Available at: <http://www.ncbi.nlm.nih.gov/pubmed/8635489> [Accessed October 11, 2014].
- Sanchez, O. et al., 2007. Role of endothelium-derived CC chemokine ligand 2 in idiopathic pulmonary arterial hypertension. *American journal of respiratory and critical care medicine*, 176(10), pp.1041–7. Available at: <http://www.ncbi.nlm.nih.gov/pubmed/17823354> [Accessed February 12, 2014].
- Sata, M., Suhara, T. & Walsh, K., 2000. Vascular Endothelial Cells and Smooth Muscle Cells Differ in Expression of Fas and Fas Ligand and in Sensitivity to Fas Ligand-Induced Cell Death : Implications for Vascular Disease and Therapy. *Arteriosclerosis, Thrombosis, and Vascular Biology*, 20(2), pp.309–316. Available at: <http://atvb.ahajournals.org/cgi/doi/10.1161/01.ATV.20.2.309> [Accessed March 13, 2014].
- Savai, R. et al., 2012. Immune and inflammatory cell involvement in the pathology of idiopathic pulmonary arterial hypertension. *American journal of respiratory and critical care medicine*, 186(9), pp.897–908. Available at: <http://www.ncbi.nlm.nih.gov/pubmed/22955318> [Accessed August 21, 2014].
- Savale, L. et al., 2009. Impact of interleukin-6 on hypoxia-induced pulmonary hypertension and lung inflammation in mice. *Respiratory research*, 10, p.6. Available at: <http://www.pubmedcentral.nih.gov/articlerender.fcgi?artid=2644669&tool=pmcentrez&rendertype=abstract> [Accessed February 12, 2014].
- Sawada, H. et al., 2007. A nuclear factor-kappaB inhibitor pyrrolidine dithiocarbamate ameliorates pulmonary hypertension in rats. *Chest*, 132(4), pp.1265–74. Available at: <http://www.ncbi.nlm.nih.gov/pubmed/17934115> [Accessed October 9, 2014].
- Scaffidi, C. et al., 1998. Two CD95 (APO-1/Fas) signaling pathways. *The EMBO journal*, 17(6), pp.1675–87. Available at: <http://www.pubmedcentral.nih.gov/articlerender.fcgi?artid=1170515&tool=pmcentrez&rendertype=abstract> [Accessed July 11, 2014].
- Schermuly, R.T. et al., 2008. Expression and function of soluble guanylate cyclase in pulmonary arterial hypertension. *The European respiratory journal*, 32(4), pp.881–91. Available at: <http://www.ncbi.nlm.nih.gov/pubmed/18550612> [Accessed October 10, 2014].
- Schermuly, R.T. et al., 2011. Mechanisms of disease: pulmonary arterial hypertension. *Nature reviews. Cardiology*, 8(8), pp.443–455. Available at: <http://www.ncbi.nlm.nih.gov/pubmed/21691314> [Accessed January 31, 2014].
- Schermuly, R.T. et al., 2007. Phosphodiesterase 1 upregulation in pulmonary arterial hypertension: target for reverse-remodeling therapy. *Circulation*, 115(17), pp.2331–9. Available at: <http://www.ncbi.nlm.nih.gov/pubmed/17438150> [Accessed October 10, 2014].

- Schermuly, R.T. et al., 2005. Reversal of experimental pulmonary hypertension by PDGF inhibition. *The Journal of clinical investigation*, 115(10), pp.2811–21. Available at: <http://www.pubmedcentral.nih.gov/articlerender.fcgi?artid=1236676&tool=pmcentrez&rendertype=abstract>.
- Schneeweis, L.A., Willard, D. & Milla, M.E., 2005. Functional dissection of osteoprotegerin and its interaction with receptor activator of NF-kappaB ligand. *The Journal of biological chemistry*, 280(50), pp.41155–64. Available at: <http://www.jbc.org/content/280/50/41155.full> [Accessed October 9, 2014].
- Schoppet, M. et al., 2011. Crystallizing nanoparticles derived from vascular smooth muscle cells contain the calcification inhibitor osteoprotegerin. *Biochemical and biophysical research communications*, 407(1), pp.103–7. Available at: <http://www.ncbi.nlm.nih.gov/pubmed/21371424> [Accessed February 12, 2014].
- Secchiero, P. et al., 2003. TRAIL promotes the survival and proliferation of primary human vascular endothelial cells by activating the Akt and ERK pathways. *Circulation*, 107(17), pp.2250–6. Available at: <http://www.ncbi.nlm.nih.gov/pubmed/12668516> [Accessed February 12, 2014].
- Secchiero, P. et al., 2004. TRAIL promotes the survival, migration and proliferation of vascular smooth muscle cells. *Cellular and molecular life sciences : CMLS*, 61(15), pp.1965–74. Available at: <http://www.ncbi.nlm.nih.gov/pubmed/15289937> [Accessed February 12, 2014].
- Selimovic, N. et al., 2009. Growth factors and interleukin-6 across the lung circulation in pulmonary hypertension. *The European respiratory journal*, 34(3), pp.662–8. Available at: <http://erj.ersjournals.com/content/34/3/662.long> [Accessed June 27, 2014].
- Serrao, K.L. et al., 2001. Neutrophils induce apoptosis of lung epithelial cells via release of soluble Fas ligand. *American journal of physiology. Lung cellular and molecular physiology*, 280(2), pp.L298–305. Available at: <http://www.ncbi.nlm.nih.gov/pubmed/11159009>.
- Shao, D. et al., 2014. Nuclear IL-33 regulates soluble ST2 receptor and IL-6 expression in primary human arterial endothelial cells and is decreased in idiopathic pulmonary arterial hypertension. *Biochemical and biophysical research communications*, 451(1), pp.8–14. Available at: <http://www.ncbi.nlm.nih.gov/pubmed/25003325> [Accessed September 1, 2014].
- Sharma, M.R., Tuszynski, G.P. & Sharma, M.C., 2004. Angiostatin-induced inhibition of endothelial cell proliferation/apoptosis is associated with the down-regulation of cell cycle regulatory protein cdk5. *Journal of cellular biochemistry*, 91(2), pp.398–409. Available at: <http://www.ncbi.nlm.nih.gov/pubmed/14743398> [Accessed July 25, 2014].
- Sharony, R. et al., 2010. Protein targets of inflammatory serine proteases and cardiovascular disease. *Journal of inflammation (London, England)*, 7, p.45.

- Shintani, M. et al., 2009. A new nonsense mutation of SMAD8 associated with pulmonary arterial hypertension. *Journal of medical genetics*, 46(5), pp.331–7. Available at: <http://www.ncbi.nlm.nih.gov/pubmed/19211612> [Accessed August 7, 2014].
- Siemeister, G. et al., 2012. BAY 1000394, a novel cyclin-dependent kinase inhibitor, with potent antitumor activity in mono- and in combination treatment upon oral application. *Molecular cancer therapeutics*, 11(10), pp.2265–73. Available at: <http://www.ncbi.nlm.nih.gov/pubmed/22821149> [Accessed October 9, 2014].
- Simonet, W.S. et al., 1997. Osteoprotegerin: a novel secreted protein involved in the regulation of bone density. *Cell*, 89(2), pp.309–19. Available at: <http://www.ncbi.nlm.nih.gov/pubmed/9108485>.
- Simonneau, G. et al., 2004. Clinical classification of pulmonary hypertension. *Journal of the American College of Cardiology*, 43(12 Suppl S), p.S5–12S. Available at: <http://www.ncbi.nlm.nih.gov/pubmed/15194173> [Accessed July 29, 2014].
- Simonneau, G. et al., 2009. Updated clinical classification of pulmonary hypertension. *Journal of the American College of Cardiology*, 54(1 Suppl), pp.S43–54. Available at: <http://www.ncbi.nlm.nih.gov/pubmed/19555858> [Accessed July 10, 2014].
- Simonneau, G. et al., 2013. Updated clinical classification of pulmonary hypertension. *Journal of the American College of Cardiology*, 62(25 Suppl), pp.D34–41. Available at: <http://www.ncbi.nlm.nih.gov/pubmed/24355639> [Accessed July 9, 2014].
- Sitbon, O. et al., 2005. Long-term response to calcium channel blockers in idiopathic pulmonary arterial hypertension. *Circulation*, 111(23), pp.3105–11. Available at: <http://www.ncbi.nlm.nih.gov/pubmed/15939821> [Accessed October 10, 2014].
- Song, S. et al., 2013. Biliverdin reductase/bilirubin mediates the anti-apoptotic effect of hypoxia in pulmonary arterial smooth muscle cells through ERK1/2 pathway. *Experimental cell research*, 319(13), pp.1973–87. Available at: http://apps.webofknowledge.com.eresources.shef.ac.uk/full_record.do?product=UA&search_mode=GeneralSearch&qid=13&SID=T2uX7uDM7ZXDpHz7M3w&page=1&doc=1 [Accessed July 16, 2014].
- Song, Y. et al., 2008. Inflammation, endothelial injury, and persistent pulmonary hypertension in heterozygous BMPR2-mutant mice. *American journal of physiology. Heart and circulatory physiology*, 295(2), pp.H677–90. Available at: <http://www.pubmedcentral.nih.gov/articlerender.fcgi?artid=2519229&tool=pmcentrez&rendertype=abstract> [Accessed October 10, 2014].
- Soon, E. et al., 2010. Elevated levels of inflammatory cytokines predict survival in idiopathic and familial pulmonary arterial hypertension. *Circulation*, 122(9), pp.920–7. Available at: <http://www.ncbi.nlm.nih.gov/pubmed/20713898> [Accessed February 12, 2014].

- Soubrier, F. et al., 2013. Genetics and genomics of pulmonary arterial hypertension. *Journal of the American College of Cardiology*, 62(25 Suppl), pp.D13–21. Available at: <http://www.ncbi.nlm.nih.gov/pubmed/24355637> [Accessed February 10, 2014].
- Speich, R. et al., 1991. Primary pulmonary hypertension in HIV infection. *Chest*, 100(5), pp.1268–71. Available at: <http://www.ncbi.nlm.nih.gov/pubmed/1935280> [Accessed August 29, 2014].
- Spiekerkoetter, E. et al., 2013. FK506 activates BMPR2, rescues endothelial dysfunction, and reverses pulmonary hypertension. *The Journal of clinical investigation*, 123(8), pp.3600–13. Available at: <http://www.pubmedcentral.nih.gov/articlerender.fcgi?artid=3726153&tool=pmcentrez&rendertype=abstract> [Accessed September 24, 2014].
- Spierings, D.C., 2004. Tissue Distribution of the Death Ligand TRAIL and Its Receptors. *Journal of Histochemistry and Cytochemistry*, 52(6), pp.821–831. Available at: <http://jhc.sagepub.com/lookup/doi/10.1369/jhc.3A6112.2004> [Accessed January 24, 2014].
- Standal, T. et al., 2002. Osteoprotegerin is bound, internalized, and degraded by multiple myeloma cells. *Blood*, 100, pp.3002–3007.
- Steiner, M.K. et al., 2009. Interleukin-6 overexpression induces pulmonary hypertension. *Circulation research*, 104(2), pp.236–44, 28p following 244. Available at: <http://www.ncbi.nlm.nih.gov/pubmed/19074475> [Accessed August 13, 2014].
- Stelzner, T.J. et al., 1992. Increased lung endothelin-1 production in rats with idiopathic pulmonary hypertension. *The American journal of physiology*, 262(5 Pt 1), pp.L614–20. Available at: <http://www.ncbi.nlm.nih.gov/pubmed/1534203> [Accessed October 10, 2014].
- Stenmark, K.R. et al., 2012. Targeting the adventitial microenvironment in pulmonary hypertension: A potential approach to therapy that considers epigenetic change. *Pulmonary circulation*, 2(1), pp.3–14. Available at: <http://www.pubmedcentral.nih.gov/articlerender.fcgi?artid=3342746&tool=pmcentrez&rendertype=abstract> [Accessed August 12, 2014].
- Stenmark, K.R. & Frid, M.G., 2011. Pulmonary Vascular Remodeling: Cellular and Molecular Mechanisms. In J. X.-J. Yuan et al., eds. *Textbook of Pulmonary Vascular Disease*. Springer, pp. 759–777.
- Stępień, E. et al., 2011. Increased levels of bone remodeling biomarkers (osteoprotegerin and osteopontin) in hypertensive individuals. *Clinical biochemistry*, 44(10-11), pp.826–31. Available at: <http://www.ncbi.nlm.nih.gov/pubmed/21539822> [Accessed February 12, 2014].

- Strittmatter, S.M. et al., 1991. An intracellular guanine nucleotide release protein for G0. GAP-43 stimulates isolated alpha subunits by a novel mechanism. *The Journal of biological chemistry*, 266, pp.22465–22471.
- Sutliff, R.L., Kang, B.-Y. & Hart, C.M., 2010. PPARgamma as a potential therapeutic target in pulmonary hypertension. *Therapeutic advances in respiratory disease*, 4(3), pp.143–60. Available at: <http://www.pubmedcentral.nih.gov/articlerender.fcgi?artid=3978142&tool=pmcentrez&rendertype=abstract> [Accessed October 10, 2014].
- Tajsic, T. & Morrell, N.W., 2011. Cellular and Molecular Mechanisms of Pulmonary Vascular Smooth Muscle Cell Proliferation. In J. X.-J. Yuan et al., eds. *Textbook of Pulmonary Vascular Disease*. Springer, pp. 323–334.
- Takahashi, M. et al., 2001. Localization of human airway trypsin-like protease in the airway: an immunohistochemical study. *Histochemistry and cell biology*, 115, pp.181–187.
- Tamosiuniene, R. et al., 2011. Regulatory T cells limit vascular endothelial injury and prevent pulmonary hypertension. *Circulation research*, 109(8), pp.867–79. Available at: <http://www.pubmedcentral.nih.gov/articlerender.fcgi?artid=3204361&tool=pmcentrez&rendertype=abstract> [Accessed August 23, 2014].
- Tanaka, A. et al., 2012. Hyperoxia-induced LC3B interacts with the Fas apoptotic pathway in epithelial cell death. *American journal of respiratory cell and molecular biology*, 46(4), pp.507–14. Available at: <http://www.pubmedcentral.nih.gov/articlerender.fcgi?artid=3359946&tool=pmcentrez&rendertype=abstract> [Accessed February 18, 2014].
- Tanaka, H. et al., 2011. Expression of RANKL/OPG during bone remodeling in vivo. *Biochemical and biophysical research communications*, 411(4), pp.690–4. Available at: <http://www.ncbi.nlm.nih.gov/pubmed/21771583> [Accessed February 12, 2014].
- Taraseviciene-Stewart, L. et al., 2001. Inhibition of the VEGF receptor 2 combined with chronic hypoxia causes cell death-dependent pulmonary endothelial cell proliferation and severe pulmonary hypertension. *The FASEB journal : official publication of the Federation of American Societies for Experimental Biology*, 15, pp.427–438.
- Teichert-Kuliszewska, K., 2006. Bone Morphogenetic Protein Receptor-2 Signaling Promotes Pulmonary Arterial Endothelial Cell Survival: Implications for Loss-of-Function Mutations in the Pathogenesis of Pulmonary Hypertension. *Circulation Research*, 98(2), pp.209–217. Available at: <http://circres.ahajournals.org/content/98/2/209.long> [Accessed August 5, 2014].
- Thomson, J.R. et al., 2000. Sporadic primary pulmonary hypertension is associated with germline mutations of the gene encoding BMPR-II, a receptor member of the TGF-beta family. *Journal of medical genetics*, 37(10), pp.741–5. Available

at:

<http://www.pubmedcentral.nih.gov/articlerender.fcgi?artid=1757155&tool=pmcentrez&rendertype=abstract>.

Tian, W. et al., 2013. Blocking macrophage leukotriene b4 prevents endothelial injury and reverses pulmonary hypertension. *Science translational medicine*, 5(200), p.200ra117. Available at:

<http://www.pubmedcentral.nih.gov/articlerender.fcgi?artid=4016764&tool=pmcentrez&rendertype=abstract> [Accessed August 29, 2014].

To, M. et al., 2011. Osteoprotegerin in sputum is a potential biomarker in COPD. *Chest*, 140(1), pp.76–83. Available at:

<http://www.ncbi.nlm.nih.gov/pubmed/21127170> [Accessed March 10, 2014].

Trauth, B.C. et al., 1989. Monoclonal antibody-mediated tumor regression by induction of apoptosis. *Science (New York, N.Y.)*, 245(4915), pp.301–5.

Available at: <http://www.ncbi.nlm.nih.gov/pubmed/2787530> [Accessed July 27, 2014].

Trow, T.K. & Taichman, D.B., 2009. Endothelin receptor blockade in the management of pulmonary arterial hypertension: selective and dual antagonism. *Respiratory medicine*, 103(7), pp.951–62. Available at:

<http://www.ncbi.nlm.nih.gov/pubmed/19304472> [Accessed October 10, 2014].

Tsuda, E. et al., 1997. Isolation of a novel cytokine from human fibroblasts that specifically inhibits osteoclastogenesis. *Biochemical and biophysical research communications*, 234(1), pp.137–42. Available at:

<http://www.ncbi.nlm.nih.gov/pubmed/9168977>.

Tuder, R. & Graham, B., 2010. The diseased endothelium: Would it explain it all? *PVRI Review*, 2(1), p.5. Available at:

<http://www.pvrireview.org/text.asp?2010/2/1/5/58622> [Accessed February 12, 2014].

Tuder, R.M. et al., 2001. Expression of angiogenesis-related molecules in plexiform lesions in severe pulmonary hypertension: evidence for a process of disordered angiogenesis. *The Journal of pathology*, 195(3), pp.367–74. Available at:

<http://www.ncbi.nlm.nih.gov/pubmed/11673836> [Accessed September 5, 2014].

Tuder, R.M. et al., 1994a. Exuberant endothelial cell growth and elements of inflammation are present in plexiform lesions of pulmonary hypertension. *The American journal of pathology*, 144(2), pp.275–85. Available at:

<http://www.pubmedcentral.nih.gov/articlerender.fcgi?artid=1887146&tool=pmcentrez&rendertype=abstract>.

Tuder, R.M. et al., 1994b. Exuberant endothelial cell growth and elements of inflammation are present in plexiform lesions of pulmonary hypertension. *The American journal of pathology*, 144, pp.275–285.

- Tuder, R.M., Flook, B.E. & Voelkel, N.F., 1995. Increased gene expression for VEGF and the VEGF receptors KDR/Flk and Flt in lungs exposed to acute or to chronic hypoxia. Modulation of gene expression by nitric oxide. *The Journal of clinical investigation*, 95(4), pp.1798–807. Available at: <http://www.pubmedcentral.nih.gov/articlerender.fcgi?artid=295709&tool=pmcentrez&rendertype=abstract> [Accessed June 27, 2014].
- Ueland, T. et al., 2012. TNF revisited: osteoprotegerin and TNF-related molecules in heart failure. *Current heart failure reports*, 9(2), pp.92–100. Available at: <http://www.ncbi.nlm.nih.gov/pubmed/22453763> [Accessed February 12, 2014].
- Vergadi, E. et al., 2011. Early macrophage recruitment and alternative activation are critical for the later development of hypoxia-induced pulmonary hypertension. *Circulation*, 123(18), pp.1986–95. Available at: <http://www.pubmedcentral.nih.gov/articlerender.fcgi?artid=3125055&tool=pmcentrez&rendertype=abstract> [Accessed August 28, 2014].
- Vicenová, B. et al., 2009. Emerging role of interleukin-1 in cardiovascular diseases. *Physiological research / Academia Scientiarum Bohemoslovaca*, 58, pp.481–498.
- Vitovski, S. et al., 2007. Investigating the interaction between osteoprotegerin and receptor activator of NF-kappaB or tumor necrosis factor-related apoptosis-inducing ligand: evidence for a pivotal role for osteoprotegerin in regulating two distinct pathways. *The Journal of biological chemistry*, 282(43), pp.31601–9. Available at: <http://www.ncbi.nlm.nih.gov/pubmed/17702740> [Accessed February 12, 2014].
- Voelkel, N.F. et al., 1994. Interleukin-1 receptor antagonist treatment reduces pulmonary hypertension generated in rats by monocrotaline. *Am J Respir. Cell Mol. Biol.*, 11, pp.664–675. Available at: PM:7946395.
- Voelkel, N.F. et al., 2012. Pathobiology of pulmonary arterial hypertension and right ventricular failure. *The European respiratory journal*, 40(6), pp.1555–65. Available at: <http://www.pubmedcentral.nih.gov/articlerender.fcgi?artid=4019748&tool=pmcentrez&rendertype=abstract> [Accessed September 17, 2014].
- Vuckovic, A. et al., 2009. Expression of vasoactive intestinal peptide and related receptors in overcirculation-induced pulmonary hypertension in piglets. *Pediatric research*, 66(4), pp.395–9. Available at: <http://dx.doi.org/10.1203/PDR.0b013e3181b33804> [Accessed June 29, 2014].
- Wesche, H. et al., 1997. The interleukin-1 receptor accessory protein (IL-1RAcP) is essential for IL-1-induced activation of interleukin-1 receptor-associated kinase (IRAK) and stress-activated protein kinases (SAP kinases). *The Journal of biological chemistry*, 272(12), pp.7727–31. Available at: <http://www.ncbi.nlm.nih.gov/pubmed/9065432> [Accessed July 28, 2014].

- Whyte, M.P. et al., 2002. Osteoprotegerin deficiency and juvenile Paget's disease. *The New England journal of medicine*, 347(3), pp.175–84. Available at: <http://www.ncbi.nlm.nih.gov/pubmed/12124406> [Accessed August 12, 2014].
- Wilden, P. et al., 1998. ATP-stimulated smooth muscle cell proliferation requires independent Erk1/2 and PI3K signaling pathways. *DIABETES*, 47, pp.A364–A364. Available at: http://apps.webofknowledge.com.eresources.shef.ac.uk/full_record.do?product=UA&search_mode=GeneralSearch&qid=20&SID=T2uX7uDM7ZXDpHz7M3w&page=1&doc=5 [Accessed July 16, 2014].
- Van Wolferen, S. a, Grünberg, K. & Vonk Noordegraaf, a, 2007. Diagnosis and management of pulmonary hypertension over the past 100 years. *Respiratory medicine*, 101(3), pp.389–98. Available at: <http://www.ncbi.nlm.nih.gov/pubmed/17222544> [Accessed February 12, 2014].
- Xie, Z. & Tsai, L., 2004. Cdk5 Phosphorylation of FAK Regulates Centrosome-Associated Microtubules and Neuronal Migration. *Cell Cycle*, 3(2), pp.108–110.
- Yamaguchi, K. et al., 1998. Characterization of structural domains of human osteoclastogenesis inhibitory factor. *The Journal of biological chemistry*, 273(9), pp.5117–23. Available at: <http://www.ncbi.nlm.nih.gov/pubmed/9478964> [Accessed July 23, 2014].
- Yamamoto, A. et al., 2008. Downregulation of angiotensin-1 and Tie2 in chronic hypoxic pulmonary hypertension. *Respiration; international review of thoracic diseases*, 75(3), pp.328–38. Available at: <http://www.ncbi.nlm.nih.gov/pubmed/18073453> [Accessed October 10, 2014].
- Yasuda, H. et al., 1998. Osteoclast differentiation factor is a ligand for osteoprotegerin/osteoclastogenesis-inhibitory factor and is identical to TRANCE/RANKL. *Proceedings of the National Academy of Sciences*, 95(7), pp.3597–3602. Available at: <http://www.pnas.org/content/95/7/3597.long> [Accessed July 23, 2014].
- Yasuoka, S. et al., 1997. Purification, characterization, and localization of a novel trypsin-like protease found in the human airway. *American journal of respiratory cell and molecular biology*, 16, pp.300–308.
- Yeager, M.E. et al., 2001. Microsatellite instability of endothelial cell growth and apoptosis genes within plexiform lesions in primary pulmonary hypertension. *Circulation research*, 88(1), pp.E2–E11. Available at: <http://www.ncbi.nlm.nih.gov/pubmed/11139485> [Accessed September 2, 2014].
- Yonehara, S., Ishii, A. & Yonehara, M., 1989. A cell-killing monoclonal antibody (anti-Fas) to a cell surface antigen co-downregulated with the receptor of tumor necrosis factor. *The Journal of experimental medicine*, 169(5), pp.1747–56. Available at: <http://www.pubmedcentral.nih.gov/articlerender.fcgi?artid=2189304&tool=pmcentrez&rendertype=abstract> [Accessed July 28, 2014].

- Yoshizumi, M. et al., 1998. Effect of endothelin-1 (1-31) on extracellular signal-regulated kinase and proliferation of human coronary artery smooth muscle cells. *British journal of pharmacology*, 125(5), pp.1019–27. Available at: http://apps.webofknowledge.com.eresources.shef.ac.uk/full_record.do?product=UA&search_mode=GeneralSearch&qid=22&SID=T2uX7uDM7ZXDpHz7M3w&page=1&doc=7 [Accessed July 16, 2014].
- Yu, L. et al., 2005. Cyclin-dependent kinase inhibitor p27Kip1, but not p21WAF1/Cip1, is required for inhibition of hypoxia-induced pulmonary hypertension and remodeling by heparin in mice. *Circulation research*, 97(9), pp.937–45. Available at: <http://www.ncbi.nlm.nih.gov/pubmed/16195480> [Accessed October 10, 2014].
- Yu, Y. et al., 2003. PDGF stimulates pulmonary vascular smooth muscle cell proliferation by upregulating TRPC6 expression. *American journal of physiology. Cell physiology*, 284(2), pp.C316–30. Available at: <http://ajpcell.physiology.org/content/284/2/C316.long> [Accessed June 24, 2014].
- Yuan, J.X.-J. & Rubin, L.J., 2005. Pathogenesis of pulmonary arterial hypertension: the need for multiple hits. *Circulation*, 111(5), pp.534–8. Available at: <http://www.ncbi.nlm.nih.gov/pubmed/15699271> [Accessed February 8, 2014].
- Zakrzewicz, A. et al., 2007. Receptor for activated C-kinase 1, a novel interaction partner of type II bone morphogenetic protein receptor, regulates smooth muscle cell proliferation in pulmonary arterial hypertension. *Circulation*, 115(23), pp.2957–68. Available at: <http://www.ncbi.nlm.nih.gov/pubmed/17515463> [Accessed October 10, 2014].
- Zannettino, a C.W. et al., 2005. Osteoprotegerin (OPG) is localized to the Weibel-Palade bodies of human vascular endothelial cells and is physically associated with von Willebrand factor. *Journal of cellular physiology*, 204(2), pp.714–23. Available at: <http://www.ncbi.nlm.nih.gov/pubmed/15799029> [Accessed February 12, 2014].
- Zauli, G. et al., 2009. Role of full-length osteoprotegerin in tumor cell biology. *Cellular and molecular life sciences : CMLS*, 66(5), pp.841–51. Available at: <http://www.ncbi.nlm.nih.gov/pubmed/19011755> [Accessed August 12, 2014].
- Zhang, J. et al., 2002. PDGF induces osteoprotegerin expression in vascular smooth muscle cells by multiple signal pathways. *FEBS letters*, 521(1-3), pp.180–4. Available at: <http://www.ncbi.nlm.nih.gov/pubmed/12067713>.
- Zhang, M. et al., 2011. Caveolin-1 mediates Fas-BID signaling in hyperoxia-induced apoptosis. *Free radical biology & medicine*, 50(10), pp.1252–62. Available at: <http://www.ncbi.nlm.nih.gov/pubmed/21382479> [Accessed April 10, 2014].
- Zhang, S. et al., 2003. Bone morphogenetic proteins induce apoptosis in human pulmonary vascular smooth muscle cells. *American journal of physiology. Lung cellular and molecular physiology*, 285(3), pp.L740–54. Available at: <http://www.ncbi.nlm.nih.gov/pubmed/12740218> [Accessed August 7, 2014].

- Zhang, S. et al., 2007. Pulmonary artery smooth muscle cells from normal subjects and IPAH patients show divergent cAMP-mediated effects on TRPC expression and capacitative Ca²⁺ entry. *American journal of physiology. Lung cellular and molecular physiology*, 292(5), pp.L1202–10. Available at: <http://www.ncbi.nlm.nih.gov/pubmed/17189322> [Accessed October 10, 2014].
- Zhao, Y. et al., 2009. Persistent eNOS activation secondary to caveolin-1 deficiency induces pulmonary hypertension in mice and humans through PKG nitration. , 119(7), pp.2009–2018.
- Zhao, Y.-Y. et al., 2002. Defects in caveolin-1 cause dilated cardiomyopathy and pulmonary hypertension in knockout mice. *Proceedings of the National Academy of Sciences of the United States of America*, 99(17), pp.11375–80. Available at: <http://www.pubmedcentral.nih.gov/articlerender.fcgi?artid=123264&tool=pmcentrez&rendertype=abstract>.
- Zhao, Y.D. et al., 2005. Rescue of monocrotaline-induced pulmonary arterial hypertension using bone marrow-derived endothelial-like progenitor cells: efficacy of combined cell and eNOS gene therapy in established disease. *Circulation research*, 96(4), pp.442–50. Available at: <http://www.ncbi.nlm.nih.gov/pubmed/15692087> [Accessed February 11, 2014].
- Zheng, Y.-G. et al., 2014. Plasma Soluble ST2 Levels Correlate With Disease Severity and Predict Clinical Worsening in Patients With Pulmonary Arterial Hypertension. *Clinical Cardiology*, p.n/a–n/a. Available at: <http://doi.wiley.com/10.1002/clc.22262> [Accessed March 12, 2014].
- Zhou, S. et al., 2013. Osteoprotegerin inhibits calcification of vascular smooth muscle cell via down regulation of the Notch1-RBP-J κ /Msx2 signaling pathway. *PLoS one*, 8(7), p.e68987. Available at: <http://www.pubmedcentral.nih.gov/articlerender.fcgi?artid=3711585&tool=pmcentrez&rendertype=abstract> [Accessed August 9, 2014].
- Ziegler, S. et al., 2005. Osteoprotegerin plasma concentrations correlate with severity of peripheral artery disease. *Atherosclerosis*, 182(1), pp.175–80. Available at: <http://www.ncbi.nlm.nih.gov/pubmed/16115489> [Accessed February 12, 2014].
- Zoubeydi, A. & Gleave, M., 2012. Small heat shock proteins in cancer therapy and prognosis. *The international journal of biochemistry & cell biology*, 44(10), pp.1646–56. Available at: <http://www.ncbi.nlm.nih.gov/pubmed/22571949> [Accessed August 26, 2014].